Volume 95 Number 4 April 2014

BAMS

Bulletin of the American Meteorological Society

OCEAN WIND CLIMATOLOGY

CHANGING EXTREMES IN U.S.

WINDCHILL ON MARS

GLOBAL WIND PROFILES

A SPACE-BASED LIDAR SOLUTION

BAMS

Bulletin of the American Meteorological Society

VOLUME 95, NUMBER 4, APRIL 2014

ON THE COVER

Hurricane Felix captured on 3 September 2007 at 11:38:46 UTC with a digital camera on the International Space Station and provided by the NASA Johnson Space Center. Even when far from land-based observing sites, hurricanes would not escape the coverage of a global wind profiling system using space-based lidar. See Baker et al., p. 543.

CONTENTS

Supplements (S) and online content are available online at http://journals.ametsoc.org/toc/bams/95/4.

The *Bulletin of the American Meteorological Society* is the official organ of the Society, devoted to editorials, articles of interest to a large segment of the membership, professional and membership news, announcements, and Society activities. Editing and publishing are under the direction of Keith L. Seitter, executive director. Contributors are encouraged to send proposals to be considered for publication. For guidance on preparation and style, see the Authors' Resource Center online at www.ametsoc.org/pubs/arcindex.html.

The *Bulletin of the American Meteorological Society* (ISSN 0003-0007) is published monthly by the American Meteorological Society, 45 Beacon St., Boston, MA 02108-3693. Periodical postage paid at Boston, MA, and at additional mailing offices. Subscription price to members is included in annual dues. Subscription price to nonmembers is available on request; single issues are $12.50 each for members, $20 for nonmembers (prices incl. shipping and handling). Address all business communications to the Executive Director, AMS, 45 Beacon St., Boston, MA 02108-3693 (617-227-2425). POSTMASTER: Send address changes to *Bulletin of the American Meteorological Society*, 45 Beacon St., Boston, MA 02108-3693.

LETTER FROM THE EDITOR: WHEN A TREE FALLS…

If a tree falls in a forest, and no one is there to hear it…wait. Does a meteorologist care about this metaphysical conundrum?

Certainly, fallen trees have an honored place in meteorological history. William Redfield walked through New England's woods after a hurricane in 1821 and came to the realization, based on the varying direction of the fallen trees, that the winds of the storm must have blown in a circular pattern. More recently, thanks to Ted Fujita, fallen trees have been rigorous clues to assessing tornado strength and understanding microbursts.

Again and again, meteorology is, at its core, a thorough explanation of unseen events; a sturdy tree is a peerless indicator of ephemeral movement. The tree sways, bends, and—ultimately—falls. But scientists must study things that are not only invisible but also far from any observer, where trees fall unheard, or where there are, in fact, no trees at all.

While philosophers have the luxury of puzzling over the existence of things that cannot be sensed, meteorologists must forge ahead and make observations where none exist. This issue's cover article (p. 543) by Wayman Baker and colleagues shows how helpful it would be to have wind profiles through the depth of the atmosphere, from all around the globe. It is not enough to rely on weather stations that are most densely situated in developed countries. The article points to space-based lidar as a solution to getting global profiles. Such a virtual network of stations must fill the gap left by tangible observing.

The development of clever algorithms is another approach to apprehending the world beyond our senses, as we see in the article by Frank Monaldo and colleagues (p. 565). They take advantage of advancing software to reexamine a decade's worth of synthetic aperture radar data from satellites and thereby construct a high-resolution database of winds over the oceans—winds that usually blow far from any person or instruments.

Few things, however, are further from our senses than the winds of Mars. Weather in the rest of the solar system is so alien that we are hardly aware of the possibilities. Astronomers can impress us with unfathomable facts like winter low temperatures of –120°C and global dust storms with winds exceeding 100 km h^{-1}. Randall Oszevski (p. 533) walks us through the imagined dangers of Mars and makes the unsensible quite sensible, pointing out that the air is so thin there, even the worst winds and temperatures don't create fearsome wind chills.

The wind chill on Mars seems like a perfectly natural preoccupation for meteorologists. Here's a science that takes into account the invisible and puts it in terms of how it feels. Remember the tale of two monks watching a flag on a breezy day? One remarked, "The flag is moving." The other countered, "The wind is moving." An elder finally settled their debate: "Not the wind, not the flag: the mind is moving."

I don't know about today's metaphysicians, but the ancient Zen masters surely would have been good meteorologists.

—*Jeff Rosenfeld,* Editor-in-Chief

ABSTRACTS

UNDERSTANDING THE METEOROLOGICAL DRIVERS OF U.S. PARTICULATE MATTER CONCENTRATIONS IN A CHANGING CLIMATE

Particulate matter (PM) air pollution is a serious public health issue for the United States. While there is a growing body of evidence that climate change will partially counter the effectiveness of future precursor emission reductions to reduce ozone (O_3) air pollution, the links between PM and climate change are more complex and less understood. This paper discusses what we currently understand about the potential sensitivity of PM episodes to climate-change-related shifts in air pollution meteorology, in the broader context of the emissions and atmospheric chemistry drivers of PM. For example, initial studies have focused largely on annual average concentrations of inorganic aerosol species. However, the potential for future changes in the occurrence of PM episodes, and their underlying meteorological drivers, are likely more important to understand and remain highly uncertain. In addition, a number of other poorly understood factors interact with these likely critical meteorological changes. These include changes in emissions from wildfires, as well as atmospheric processing of organic aerosol precursor chemicals. More work is needed to support the management of the health and environmental risks of climate-induced changes in PM. We suggest five priorities for the research community to address based on the current state of the literature. *(Page 521)*

MARTIAN WINDCHILL IN TERRESTRIAL TERMS

With an average temperature of –63°C and winter lows of –120°C,

Mars sounds far too cold for humans. However, thermometer readings from Mars are highly misleading to terrestrials who base their expectations of thermal comfort on their experience in Earth's much thicker atmosphere. The two-planet model of windchill described here suggests that Martian weather is much less dangerous than it sounds because in the meager atmosphere of Mars, convection is a comparatively feeble heat transfer mechanism. The windchill on Mars is expressed as the air temperature on Earth that produces the same cooling rate in still air, in Earth's much denser atmosphere. Because Earth equivalent temperature (EET) is identical to the familiar wind chill equivalent temperature (WCET) that is broadcast across much of North America in winter, it provides a familiar context for gauging the rigors of weather on another planet. On Earth, WCET is always lower than the air temperature, but on Mars the equivalent temperature can be 100°C higher than the thermometer reading. Mars is much colder for thermometers than for people. Some frontier areas of Earth are at least as cold as midlatitude Mars is, year round. Summer afternoons in the tropics of Mars might even feel as comfortable as an average winter day in the south of England. Sunshine on Mars should be about as warm as it is on Earth. Heat balance and clothing emissivity are also briefly discussed. *(Page 533)*

LIDAR-MEASURED WIND PROFILES—THE MISSING LINK IN THE GLOBAL OBSERVING SYSTEM

The three-dimensional global wind field is the most important remaining measurement needed to accurately assess the dynamics of the atmosphere. Wind information in the tropics, high latitudes, and stratosphere is particularly deficient. Furthermore, only a small fraction of the atmosphere is sampled in terms of wind profiles. This limits our ability to optimally specify initial conditions for numerical weather prediction (NWP) models and our understanding of several key climate change issues.

Because of its extensive wind measurement heritage (since 1968) and especially the rapid recent technology advances, Doppler lidar has reached a level of maturity required for a space-based mission. The European Space Agency (ESA)'s Atmospheric Dynamics Mission Aeolus (ADM-Aeolus) Doppler wind lidar (DWL), now scheduled for launch in 2015, will be a major milestone.

This paper reviews the expected impact of DWL measurements on NWP and climate research, measurement concepts, and the recent advances in technology that will set the stage for space-based deployment. Forecast impact experiments with actual airborne DWL measurements collected over the North Atlantic in 2003 and assimilated into the European Centre for Medium-Range Weather Forecasts (ECMWF) operational model are a clear indication of the value of lidar-measured wind profiles. Airborne DWL measurements collected over the western Pacific in 2008 and assimilated into both the ECMWF and U.S. Navy operational models support the earlier findings.

These forecast impact experiments confirm observing system simulation experiments (OSSEs) conducted over the past 25–30 years. The addition of simulated DWL wind observations in recent OSSEs performed at the Joint Center for Satellite Data Assimilation (JCSDA) leads to a statistically significant increase in forecast skill. *(Page 543)*

OCEAN WIND SPEED CLIMATOLOGY FROM SPACEBORNE SAR IMAGERY

Spaceborne synthetic aperture radar (SAR) imagery can make high-resolution (≤500 m) ocean wind speed measurements. The authors anticipate reprocessing the full decade and a half of *Radarsat-1* SAR imagery and generating a SAR wind speed archive. These data will be of use for studies of coastal atmospheric phenomena and assessment of offshore wind power potential. To illustrate the potential of this latter application, they review the ability of SARs to measure wind speed, discuss an approach for using SARs to create wind speed climatologies useful for wind power resource assessments, and consider issues concerning the applicably of such data for these assessments. *(Page 565)*

CMIP5 CLIMATE MODEL ANALYSES: CLIMATE EXTREMES IN THE UNITED STATES

This is the fourth in a series of four articles on historical and projected climate extremes in the United States. Here, we examine the results of historical and future climate model experiments from the phase 5 of the Coupled Model Intercomparison Project (CMIP5) based on work presented at the World Climate Research Programme (WCRP) Workshop on CMIP5 Climate Model Analyses held in March 2012. Our analyses assess the ability of CMIP5 models to capture observed trends, and we also evaluate the projected future changes in extreme events over the contiguous Unites States. Consistent with the previous articles, here we focus on model-simulated historical trends and projections for temperature extremes, heavy precipitation, large-scale drivers of precipitation variability and drought, and extratropical storms. Comparing new CMIP5 model results with earlier CMIP3 simulations shows that in general CMIP5 simulations give similar patterns and magnitudes of future temperature and precipitation extremes in the United States relative to the projections from the earlier phase 3 of the Coupled Model Intercomparison Project (CMIP3) models. Specifically, projections presented here show significant changes in hot and cold temperature extremes, heavy precipitation, droughts, atmospheric patterns such as the North American monsoon and the North Atlantic subtropical high that affect interannual precipitation, and in extratropical storms over the twenty-first century. Most of these trends are consistent with, although in some cases (such as heavy precipitation) underestimate, observed trends. *(Page 571)*

THE NORTH AMERICAN MULTIMODEL ENSEMBLE (NMME): PHASE-1 SEASONAL-TO-INTERANNUAL PREDICTION, PHASE-2 TOWARD DEVELOPING INTRASEASONAL PREDICTION

The recent U.S. National Academies report, *Assessment of Intraseasonal to Interannual Climate Prediction and Predictability,* was unequivocal in recommending the need for the development of a North American Multimodel Ensemble (NMME) operational predictive capability. Indeed, this effort is required to meet the specific tailored regional prediction and decision support needs of a large community of climate information users.

The multimodel ensemble approach has proven extremely effective at quantifying prediction uncertainty due to uncertainty in model formulation and has proven to produce better prediction quality (on average) than any single model ensemble. This multimodel approach is the basis for several international collaborative prediction research efforts and an operational European system, and there are numerous examples of how this multimodel ensemble approach yields superior forecasts compared to any single model.

Based on two NOAA Climate Test bed (CTB) NMME workshops (18 February and 8 April 2011), a collaborative and coordinated implementation strategy for a NMME prediction system has been developed and is currently delivering real-time seasonal-to-interannual predictions on the NOAA Climate Prediction Center (CPC) operational schedule. The hindcast and real-time prediction data are readily available (e.g., http://iridl.ldeo.columbia.edu/SOURCES/.Models/.NMME/) and in graphical format from CPC (www.cpc.ncep.noaa.gov/products/NMME/). Moreover, the NMME forecast is already currently being used as guidance for operational forecasters. This paper describes the new NMME effort, and presents an overview of the multimodel forecast quality and the complementary skill associated with individual models. *(Page 585)*

ABSTRACTS

THE SAARC STORM: A COORDINATED FIELD EXPERIMENT ON SEVERE THUNDERSTORM OBSERVATIONS AND REGIONAL MODELING OVER THE SOUTH ASIAN REGION

This article describes a unique field experiment on Severe Thunderstorm Observations and Regional Modeling (STORM) jointly undertaken by eight South Asian countries. Several pilot field experiments have been conducted so far, and the results are analyzed. The field experiments will continue through 2016.

The STORM program was originally conceived for understanding the severe thunderstorms known as nor'westers that affect West Bengal and the northeastern parts of India during the premonsoon season. The nor'westers cause loss of human lives and damage to properties worth millions of dollars annually. Since the neighboring South Asian countries are also affected by thunderstorms, the STORM program is expanded to cover the South Asian countries under the South Asian Association for Regional Cooperation (SAARC). It covers all the SAARC countries (Afghanistan, Bangladesh, Bhutan, India, Maldives, Nepal, Pakistan, and Sri Lanka) in three phases. Some of the science plans (monitoring the life cycle of nor'westers/severe thunderstorms and their three-dimensional structure) designed to understand the interrelationship among dynamics, cloud microphysics, and electrical properties in the thunderstorm environment are new to severe weather research. This paper describes the general setting of the field experiment and discusses preliminary results based on the pilot field data. Typical lengths and the intensity of squall lines, the speed of movements, and cloud-top temperatures and their heights are discussed based on the pilot field data. The SAARC STORM program will complement the Severe Weather Forecast Demonstration Project (SWFDP) of the WMO. It should also generate large-scale interest for fueling research among the scientific community and broaden the perspectives of operational meteorologists and researchers. *(Page 603)*

NOWCAST

NEWS AND NOTES

Seafloor Replica Provides Clues to Internal Wave Dynamics

Despite their often awesome size, internal waves have long been difficult to monitor because they are almost entirely under the surface of the ocean. But new research has overcome their elusiveness with the help of a miniature reproduction of the seafloor, and in the process has made valuable discoveries on the formation of these important waves that can play a key role in ocean circulation and global climate.

Researchers first studied satellite records to find the huge submerged waves, detecting the telltale slow and subtle rise and fall of the ocean across the Luzon Strait, which is in the South China Sea between Taiwan and the Philippines. There, beneath the surface, internal waves can reach "skyscraper-scale" heights of 550 feet, according to the study's lead author, Thomas Peacock of MIT, who also calls them "the lumbering giants of the ocean" because the waves commonly move at speeds of just a few centimeters per second. Then, using a rotating wave tank 50 feet in diameter, the team built a model that replicated in detail the seafloor topography of the strait. They studied the wave dynamics in the tank, using water stratified by layers of different salt content to reproduce internal wave movement among different ocean layers—deep, colder, saltier water and warmer, less salty water closer to the surface. They observed the internal waves originate when tidal currents propelled the cold, deep waters over the complex, double-ridge system of the Luzon seafloor; notably, they found that the ridge system as a whole—and not a specific feature such as a higher peak in the ridge—caused the formation of the internal waves.

The finding is "an important missing piece of the puzzle in climate modeling," Peacock says. "Right now, global climate models are not able to capture these processes," and internal waves could be "the key mechanism for transferring heat from the upper ocean to the depths."

The study, which the researchers call the largest laboratory experiment ever to study internal waves, was recently published in *Geophysical Research Letters*. (Source: Phys.org)

How Bubbles Could Help Measure Hurricane Intensity

While hurricane forecasting has made significant progress in recent years, scientists continue to pursue methods to more accurately predict the movement and variations in intensity of tropical storms. Now, a team of researchers has discovered a novel way to help understand these dynamics: by observing soap bubbles.

Several years ago the scientists noticed that when they heated hand-sized soap bubbles, colored vortices that resembled hurricanes moved across the bubbles' surface. In their original work, they were able to create a mathematical model from these vortices that could essentially project the trajectory of actual tropical cyclones—the movement wasn't smooth but the storms eventually ended up in same place, the researchers found. In more

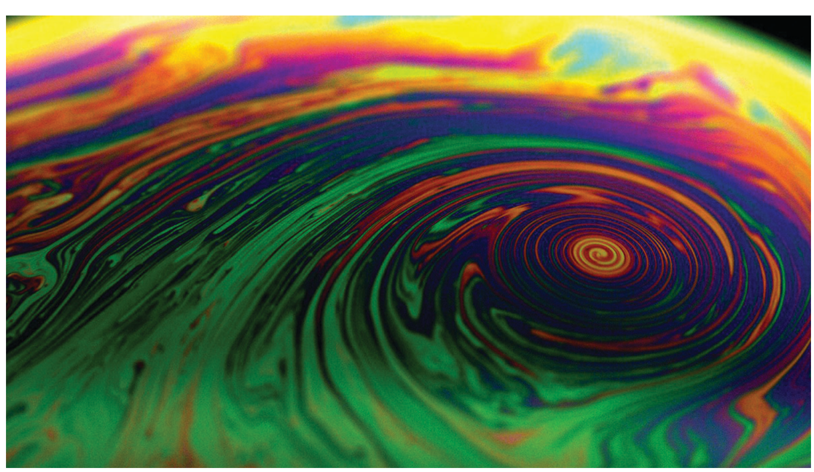

Closeup of a vortex in a soap bubble. (Figure: H. Kellay, U. Bordeaux)

STORM NAMES NOT FREE AT FREE UNIVERSITY

If you've ever considered what it would be like to have your name attached to a storm, there's a program in Europe that provides the service. Since 2002, the Institute of Meteorology at Berlin's Free University has been giving people the opportunity to name a storm for 199 euros ($275). Add another 100 euros and you can label periods of fine weather, otherwise known as anticyclones. According to university meteorologist Thomas Duemmel, the steeper price attached to anticyclones is due to their infrequency compared to low-pressure storms; anticyclones occur approximately 50 times a years compared to 150–160 storms anually. Adding up those numbers, the Institute of Meteorology collects about 25,000–30,000 euros each year through the program. The majority of the sponsors are German, but some live in other parts of Europe and even Japan, according to Duemmel. This year, anticyclones will take on female names, and male names will be used for the low-pressure storms. Until recently, storms consistently had feminine names and anticyclones had masculine, but complaints from a number of feminist organizations inspired the university to alternate years by gender. (Source: ZeeNews)

recent research, published in *Scientific Reports*, the team used the bubbles to create a model of a storm's intensity. They were able to reproduce the curvature of the atmosphere and emulate a primitive model of atmospheric flow on the bubbles, from which they recreated vortices dynamically comparable to tropical cyclones. They then closely analyzed the bubble vortices—focusing on their rotation rate—and developed a relational model that simulated the variations in the vortices' intensity from formation to expiration. The scientists tested their model against data taken from 150 Pacific and Atlantic Ocean tropical cyclones and found that it accurately—albeit simply—recreated the storms, including their general intensification and demise. Despite the complexity of real-world tropical cyclones, their results suggest that the new model could be a useful tool in helping to predict tropical storm intensity.

Antarctic Glacier Melt Linked to La Niña Winds

Glacial melting in Antarctica has for some time been connected to long-term global climate change, but a recent study published in *Science* has found that shorter-term weather and climate events such as La Niña have influenced the melting of Pine Island Glacier, which constitutes about 10% of the West Antarctic Ice Sheet (WAIS) and is one of the primary conduits for ice shedding from Antarctica. As the WAIS is a potential significant contributor to rising global sea levels, the finding could have important implications for sea level projections.

Pine Island Glacier's ice shelf—the part of the glacier that's over water—has been thinning since at least the 1970s, when such measurements were first taken there. An inflow of circumpolar deep water (CDW) from the Pacific and Indian Oceans collects in a gap underneath the ice shelf, with warmer water sliding over an underwater ridge and melting the ice shelf from below, causing the tip of the glacier to discharge more ice. But in observations taken in 2012, scientists noticed that cold water had accumulated around the underside of the shelf, resulting in a 50% decrease in melting of the shelf compared to measurements

Reading Algae to Determine Historical Sea Ice Cover

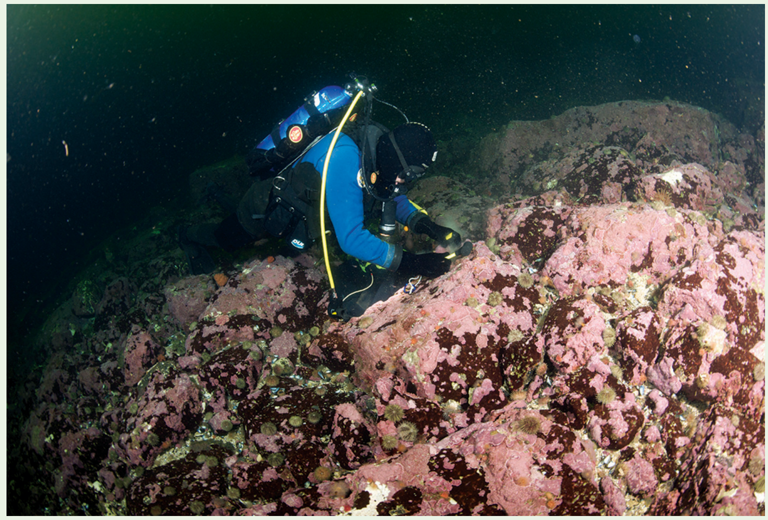

PHOTO: NICK CALOYIANUS

Trees aren't the only objects in nature that can provide clues to historical climatic conditions. Recent research in sub-Arctic waters has shown that calcified algae on underwater rocks have layers similar to tree rings that reveal past changes in sea ice cover. Researchers working in the Labrador Sea studied samples of the alga *Clathromorphum compactum*, a type of coralline algae also found in Arctic waters. The algae grow in warm and bright conditions each year during the ice-free season and stop growing when ice covers the sea surface. This cycle of dormancy and growth generates layering in the calcite algal crust that can be studied to determine how long sea ice covered the water and limited algal growth. The layering reveals a historical record of ice cover using "the same principle as using rings to determine a tree's age and the levels of precipitation," according to University of Toronto Mississauga's Jochen Halfar, lead author of a recent paper on the research published in the *Proceedings of the National Academy of Sciences*. The research team also used radiocarbon dating to pinpoint the age of the algal layers, and they found that since the end of the Little Ice Age in the mid-1850s the thickness of the algae's growth layers has more than doubled, indicating a "dramatic decrease in ice cover over the last 150 years," according to Halfar, who also noted that the study was "the first time coralline algae have been used to track changes in Arctic sea ice." The photo above shows a diver removing coralline red algal crust from the surface of a rock in the Labrador Sea. (Source: University of Toronto)

taken two years earlier; in fact, the melting was the lowest ever recorded at the location.

To understand this change, the scientists combined water temperature measurements with an ocean circulation model. They found that the top of the thermocline—which around the ice sheet actually divides cold surface water from deeper warm waters (the opposite of typical water layering)—had sunk about 250 meters compared to prior measurements, which pushed the warm water to depths where it was largely unable to rise above the ridge and reach the bottom of the ice shelf. The unusually thick layer of cold surface water instead seeped under the ice, leading to the decrease in melting.

The scientists partly attributed the cooler waters around the ice shelf and the subsequent melting slowdown to an escalation of easterly winds pushed by a strong La Niña in January of 2012—the opposite of the westerly winds that normally prevail in the region.

"We had thought that the wind variability played an interesting, but relatively small role, but the new data supports our idea and shows that it has a strong effect," explains the University of Washington's Eric Steig, a coauthor of the study. "The wind field in late 2011 and early 2012 had changed dramatically compared to previous years—the dominant westerly winds in the surrounding area were easterly almost all through late 2011 and early 2012, and those changes were related to the very large 2011 La Niña event."

The decrease in melting was especially surprising given that the oceanic response to this climatic event was relatively small.

"It is not so much the ocean variability, which is modest by comparison with many parts of the ocean, but the extreme sensitivity of the ice shelf to such modest changes in ocean properties that took us by surprise," notes the British Antarctic Survey (BAR)'s Adrian Jenkins, another coauthor.

The finding "contradicts the widespread view that a simple and steady ocean warming in the region is eroding the West Antarctic Ice Sheet," says coauthor Pierre Dutrieux of BAR, and also reveals that "the sea level contribution of the ice sheet is influenced by climatic variability over a wide range of time scales." (SOURCES: University of Washington; LiveScience.com; *International Business Times*)

ON THE WEB

DISASTER DATA STORAGE MADE EASIER

A new system developed at Purdue University provides researchers studying the impacts of natural disasters with a convenient and free way to store and share their data. Known as DataStore, the system is able to convert spreadsheets into databases that can be accessed and searched by researchers worldwide.

DataStore is part of NEEShub, a web portal for civil engineering research. Purdue's Network for Earthquake Engineering Simulation, or NEES, comprises 14 laboratories that study earthquakes and tsunamis. All NEEShub users can search, download, and analyze the information in DataStore databases, which are composed specifically of data on hurricanes, tornadoes, floods, and earthquakes. They include clickable links to documents, photos, video, audio, maps, and other information, and 14 customizable databases established by research groups, professional communities, and government agencies are featured on NEEShub's website (http://nees.org/databases).

"Data kept in spreadsheets is easily lost," says Ann Christine Catlin of Purdues Rosen Center for Advanced Computing. "Now you can go to the NEEShub and use DataStore to store—and share—your data."

A database can be created in just a few minutes, and once it is in the system, Catlin notes, it's "a living, breathing" catalogue of information that can be augmented and revised.

"Until now, the study of specific subjects in engineering required each investigator to collect data on

the subject manually, from journal to journal and from report to report, through hundreds or thousands of sources," says Santiago Pujol, a Purdue civil engineering professor. "Without the generalized use of tools like DataStore, we [were] losing data, time, and effort." (SOURCE: Purdue University)

PAPERS OF NOTE

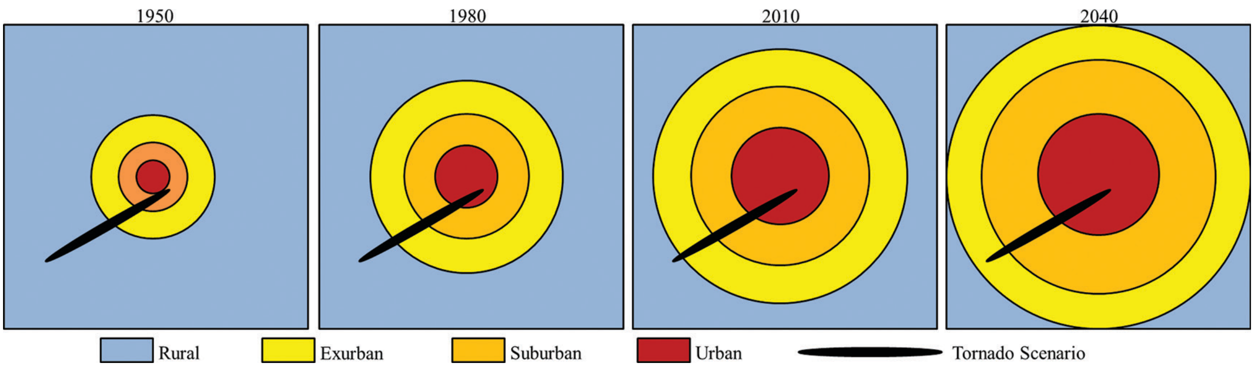

A conceptual model of the "expanding bull's-eye effect" for a hypothetical metropolitan region that is characterized by increasing development spreading from an urban core over time. A sample tornado scenario is overlaid to show how expanding development creates larger areas of potential impacts from hazards.

IS THE EXPANDING BULL'S-EYE EFFECT LEADING TO GREATER AND MORE FREQUENT WEATHER DISASTERS?

Despite decades of improvement in activities aimed at reducing impacts from extreme events, the rapid increase in disaster losses and people affected suggests that swelling populations, development trends, and vulnerabilities are outpacing mitigation, leading to greater event frequencies and amplified impacts. Due to data, computational, and methodological restrictions, research quantifying changes in human exposure to hazards has been relatively limited. Our research attempts to rectify this deficiency, advancing a framework for future work exploring how exposure and vulnerability contribute to disasters.

Our investigation employs historical exposure data on a uniform grid to appraise how transformations in Chicago's land use have led to greater potential for tornado disasters. Chicago is an ideal example of the enormous growth that metropolitan regions have witnessed during the last century. The area is characterized by a dense urban core and has experienced extensive, spatially fragmented suburban growth, or sprawl. We argue that this development pattern leads to an "expanding bull's-eye effect"—that is, people, their possessions, and infrastructure are increasingly exposed to geophysical hazards as populations grow and spread. Accordingly, it is not solely the population magnitude that is important in creating disaster potential; it is how the population is distributed across the landscape that determines how the underlying disaster components of risk and vulnerability are realized.

We couple synthetic tornado events and event-derived (Joplin,

ECHOES

"Novel and optimistic though these submissions are, they are unconvincing and must fail."

—New Zealand High Court Judge JOHN PRIESTLEY, in his ruling against a Pacific islander who was attempting to become the first climate change refugee. A native of Kiribati, Ioane Teitiota had sought to remain in New Zealand after his visa expired because his island home was threatened by rising water levels. His lawyers claimed he was being "persecuted passively" by the environment and that the Kiribati government was unable to rectify the situation. While the judge agreed that Kiribati and its residents suffered environmental hardships, he rejected Teitiota's claim of persecution, also noting that millions of other residents of low-lying countries face similar environmental threats to their homes. (SOURCES: Agence France-Presse; Phys.org)

Missouri EF5) damage context with a spatial modeling approach to evaluate the expanding bull's-eye effect using the superposition of hypothetical tornado events atop varying development morphologies. Results show that the number of people and their housing continue to geographically expand, confirming that more people and their possessions are potential targets for tornadoes. We illustrate how differing development types lead to varying exposure rates that contribute to the unevenness of potential weather-related disasters across the region. For instance, a sprawl type of suburban development has led to the greatest change in hazard exposure setting. Conversely, while population loss along the periphery of the urban core has decreased the number of people potentially affected, those that remain may be highly vulnerable due to enhanced sensitivity/susceptibility and reduced adaptive capacity caused by poverty. More recently, inward migration to the central business district has promoted a very dense exposure in the urban core with concentrated catastrophic disaster potential that could potentially overwhelm critical infrastructure.

While climate change may amplify the risk of certain hazards, the root cause of escalating disasters is not necessarily event frequency, or risk, related. Rather, our research confirms that the upward trend in disasters is predicated on increasing exposure and vulnerability of populations. We recommend a worst-case hazard scenario approach using representative hazard models on high spatial resolution datasets of vulnerability as the basis for mitigation planning and action. Communities need to understand how local exposure landscapes have transformed spatiotemporally and how those changes may influence the tasks of warning, rescue, and recovery should a catastrophic scenario come to fruition.—Walker S. Ashley (Northern Illinois University), S. Strader, T. Rosencrants, and A. Krmenec. "Spatiotemporal Changes in Tornado Hazard Exposure: The Case Of the Expanding Bull's Eye Effect in Chicago, IL," in a forthcoming issue of *Weather, Climate, and Society*.

The Explosive Layman (Australia) Fire: Dynamics in a Fire Environment

The Layman fuel-reduction burn, in scenic southwest Western Australia, produced fire behavior that was never anticipated in the prevailing weather conditions. The prescribed burn was ignited in mid-October 2010. Late morning on the day following ignition, fire activity escalated rapidly and a deep convection column developed. The ensuing intense fire with tall flames caused extensive crown scorch and defoliation, and resulted in concerns about the safety of rural communities adjoining the planned burn. Traditional measures of severe fire weather assess high temperatures, low relative humidity, and strong winds. None of these factors were present at the Layman fire.

The observations and meteorological model data indicate that the intense fire activity was driven by a combination of meteorological processes not routinely assessed in fire environments. Meteorological features that were present included low-level sea breeze convergence in the wind field, a potentially unstable atmosphere, entrainment of dry air from aloft desiccating already climatologically dry fuels, and vertical circulation on a frontal change. The dramatic development of the Layman burn shows that meteorological features not currently embedded in fire science may be conducive to intense fire activity.

Recent followup research has involved simulating the event with the Weather Research and Forecasting (WRF) coupled fire–atmosphere model WRF-Fire. The advantage of WRF-Fire over other fire models is that the coupled model captures dynamical interactions between the fire and atmosphere. Simulation results show WRF-Fire has done a remarkable job of reproducing the timing and vertical development of the fire plume.

The WRF-Fire simulations show that light environmental winds and a subtle wind shift, in combination with fire-modified winds, created local convergence over the fire area. In the early morning, the fire plume was constrained by a shallow, cool, stable, near-surface layer that had developed overnight. The wind convergence coincided with rapid fire plume growth through the deepening boundary layer into the mixed layer from the previous day. In the simulations, the fire plume developed rapidly between 10 and 11 a.m., a remarkable match to the time fire activity began in the real world.

The question is: Could the plume development have been anticipated in advance? Results from the coupled model would have provided a useful warning. However, due to initialization time and computation costs, WRF-Fire is unlikely to be run in real time for similar events in the near future. However, operational nu-

PEACE

NASA MODIS (Moderate Resolution Imaging Spectroradiometer) *Terra* and *Aqua* satellite images of the Layman burn reveal the explosive growth in the fire. Left panel (*Terra*) is from 17 Oct 2010 at 10:00 a.m. local time (0200 UTC); right panel (*Aqua*) is a little more than 4 hours later, 2:20 p.m. local time (0620 UTC).

merical weather prediction output is at one-hour intervals, so vertical growth of the plume through the boundary layer may be predictable in future events.—Mika Peace (University of Adelaide). "Meteorological Dynamics in a Fire Environment: A Case Study of the Layman Prescribed Burn in Western Australia," presented at the 10th Symposium on Fire and Forest Meteorology, 14–18 October 2013, Bowling Green, Kentucky.

Wind Speed Thresholds for Vorticity-Driven Lateral Fire Spread

Under conditions of extreme fire weather, bushfires burning in rugged terrain can exhibit highly atypical patterns of propagation, which can have dramatic effects on subsequent fire development. In particular, wildfires have been observed to spread laterally across steep, lee-facing slopes in a process that has been termed "fire channeling." Such erratic fire behavior is extremely dangerous for firefighting operations. Coupled fire-atmosphere modeling using large eddy simulation has indicated that the fire channeling phenomenon occurs in response to fire-induced vorticity on the fire's flanks in the immediate lee of a ridge line. Our research extends previous modeling, using the Weather Research and Forecasting (WRF) coupled fire-atmosphere model, WRF-Fire, to specifically consider the effect of wind speed in generating the fire-induced vorticity necessary to drive the lateral spread associated with fire channeling.

We simulated fires on leeward slopes under different wind speed regimes, with wind speeds characterised in terms of a reference wind speed U_0. The topography in the model was an idealized triangular mountain with a north-south oriented ridge line and windward and leeward slopes of 20° and 35°, respectively. The reference wind speed U_0 was prescribed values of 0, 2.5, 5, 7.5, 10, and 15 m s^{-1}.

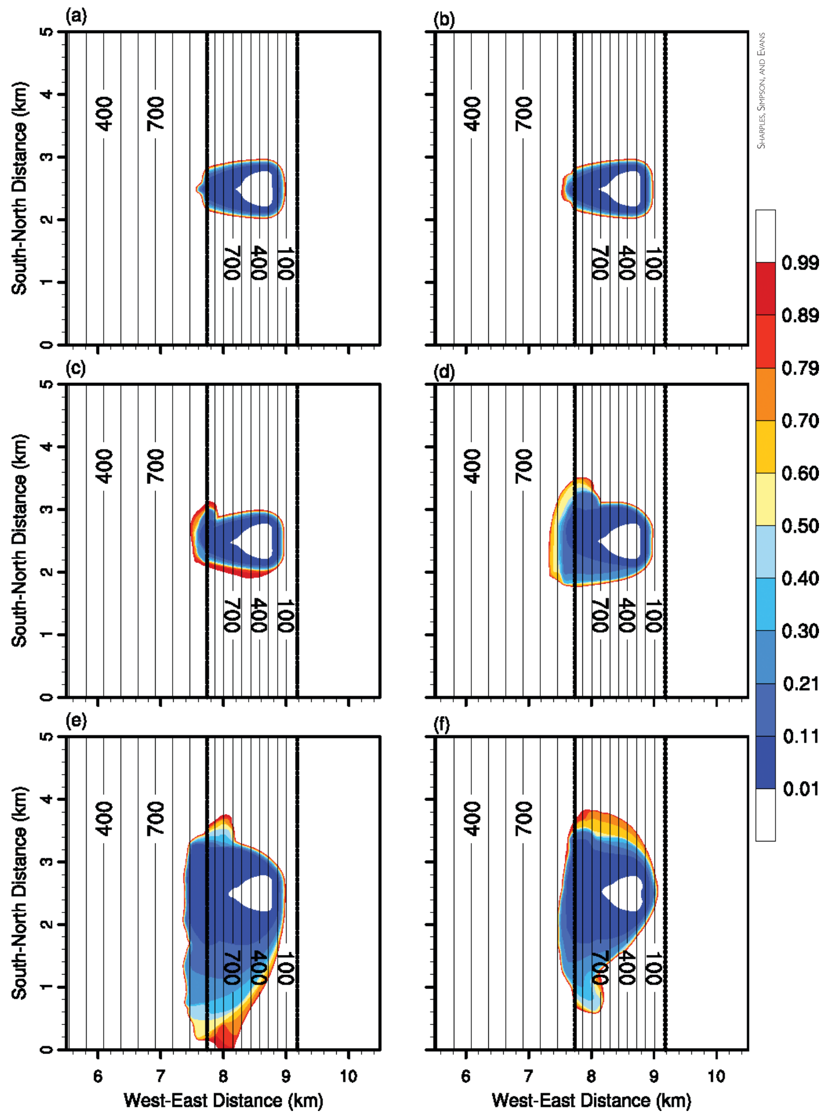

***Growing with the wind.* Fuel fraction after 120 minutes of elapsed time, simulated using different reference wind speeds: (a) 0; (b) 2.5; (c) 5; (d) 7.5; (e) 10; and (f) 15 m s^{-1} on an idealized 1000-m mountain slope. The ridgeline is the vertical black line near the middle of each panel; parallel lines on either side indicate terrain changes in 100-m increments. Note that lateral fire spread begins with a wind of 5 m s^{-1} [panel (c)].**

Under the two lowest wind-speed regimes the fire did not exhibit any atypical lateral spread, in stark contrast to the two highest wind speed regimes, in which the simulated fires readily exhibited significantly faster lateral spread. The results suggest the existence of a threshold wind speed, below which the prevailing winds are too weak to drive the vorticity-generating interaction between the wind, the terrain, and the fire's plume, so that no atypical lateral spread occurs. The model simulations further suggest that this

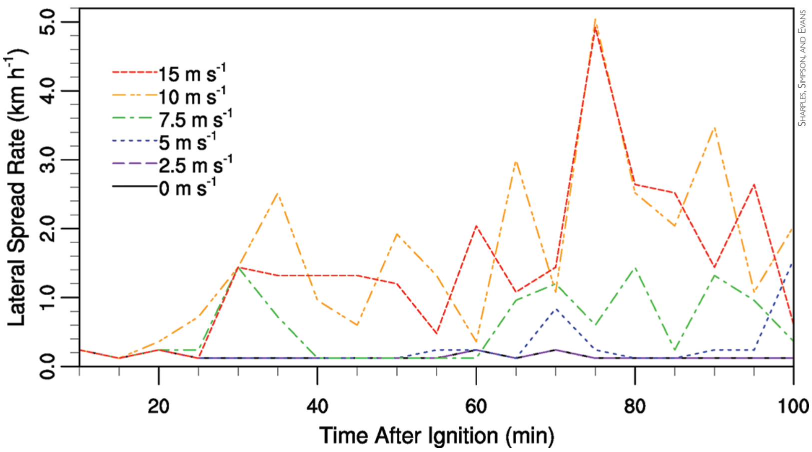

Spreading fire. **Lateral fire spread rates for different reference wind speeds.**

threshold occurs for wind regimes characterized by $U_0 \approx 5$ m s^{-1}.

The simulated behavior of fires on leeward slopes, and the transition in fire propagation that can occur when prevailing winds are sufficiently strong, highlight the inherent dangers associated with firefighting in rugged terrain. The propensity for dynamic interactions to produce erratic and dangerous fire behavior in such environments has strong implications for firefighter and community safety. At the very least our findings provide additional support for the use of well-briefed observers in firefighting operations in complex topography.—Jason J. Sharples (University of New South Wales, Canberra), C. C. Simpson, and J. P. Evans. "Examination of Wind Speed Thresholds for Vorticity-Driven Lateral Fire Spread," presented at the 10th Symposium on Fire and Forest Meteorology, 14–18 October 2013, Bowling Green, Kentucky.

Meteorology for Coastal/Offshore Wind Energy in the United States

Recommendations and Research Needs for the Next 10 Years

BY CRISTINA L. ARCHER, BRIAN A. COLLE, LUCA DELLE MONACHE, MICHAEL J. DVORAK, JULIE LUNDQUIST, BRUCE H. BAILEY, PHILIPPE BEAUCAGE, MATTHEW J. CHURCHFIELD, ANNA C. FITCH, BRANKO KOSOVIC, SANG LEE, PATRICK J. MORIARTY, HUGO SIMAO, RICHARD J. A. M. STEVENS, DANA VERON, AND JOHN ZACK

Offshore wind energy harvesting is just starting in the United States, with imminent offshore wind farms in Massachusetts, Maryland, and Rhode Island waters, and with an ambitious goal of 10 GW of installed offshore capacity by 2020 set by the U.S. Department of Energy (DOE), which has recently funded seven "Advanced Technology Demonstration" offshore wind projects to help achieve that goal. Although new in the United States, offshore wind energy harvesting began more than 20 years ago in Europe and has now reached more than 5.5 GW of installed capacity worldwide, predominantly in Denmark and the United Kingdom. Given the unfortunate coincidence of introducing a new industry during challenging economic times, it is essential that public and private financial resources be effectively and optimally directed toward those meteorological research needs that are emerging today and that will be critical in the next decade. Identifying these research needs for wind energy along the U.S. East Coast, both coastal and offshore, was the goal of a two-day symposium held at the University of Delaware on 27–28 February 2013. More than 40 participants gathered from academia, national laboratories, wind industry, and funding agencies.

AFFILIATIONS: ARCHER AND VERON—University of Delaware, College of Earth, Ocean, and Environment, Newark, Delaware; COLLE—Stony Brook University/SUNY, Stony Brook, New York; DELLE MONACHE, FITCH, AND KOSOVIC—National Center for Atmospheric Research, Boulder, Colorado; DVORAK—Sailor's Energy, Berkeley, California; LUNDQUIST—University of Colorado at Boulder, Boulder, Colorado, and National Renewable Energy Laboratory, Golden, Colorado; BAILEY, BEAUCAGE, AND ZACK—AWS Truepower, LLC, Albany, New York; CHURCHFIELD, LEE, AND MORIARTY—National Renewable Energy Laboratory, Golden, Colorado; SIMAO—Princeton University, Princeton, New Jersey; STEVENS—Johns Hopkins University, Baltimore, Maryland, and University of Twente, Enschede, The Netherlands
CORRESPONDING AUTHOR: Cristina L. Archer, University of Delaware, College of Earth, Ocean, and Environment, Newark, DE 19716
E-mail: carcher@udel.edu

DOI:10.1175/BAMS-D-13-00108.1

A supplement to this article is available online (10.1175/BAMS-D-13-00108.2).

During the symposium, three main topics were explored: 1) wind resource assessment; 2) wind power forecasting; and 3) turbulent wake losses. Overviews of the latest findings in the three topics were given on the first day in the form of presentations, which were open to students and the general public. On the second day, the experts gathered in a workshop to identify research needs and provide recommendations for urgent action items. Whereas specific research needs were identified for each of the three main topics, two emerged as crosscutting and urgent: 1) continuous, publicly available, multilevel measurements of winds and temperature over U.S. offshore waters; and 2) quantification and reduction of uncertainty. These two research needs and relevant recommendations (in italics) are described first.

RESEARCH NEED #1: MORE OFFSHORE OBSERVATIONS. Offshore meteorological measurements are challenging and expensive. Ideal measurements would quantify the wind resource at several vertical levels spanning the height of the turbine rotor disk to understand the rotor equivalent wind speed and possible impacts on turbine power production. In European waters, designated research platforms (e.g., FINO1 in Germany) have been established for characterization of offshore flow as well as validation of new measurement technologies such as light detection and ranging (lidar) and modeling approaches. The few long-term meteorological observations off the East Coast are typically buoy-based, thereby restricting the altitude of wind measurements to a few meters above the surface. A sparse network of nine towers, with an elevation of ~50 m, extends along the coast from Florida to Maine, but fails to provide multilevel information and measurements at turbine hub height or above.

Periodically, detailed measurements of wind and temperature have been conducted offshore in short-term field campaigns, but the consistent long-term measurements required for resource assessment are generally not available off the East Coast (with the only exception being the Cape Wind tower in Nantucket Sound, Massachusetts). The standard approach considered buoy measurements and then extrapolated them to higher altitudes with assumptions of the shape of the wind profile (log-law or power-law). By extrapolating surface or near-surface measurements with such smooth profiles, important wind structures such as low-level jets are ignored.

The first recommendation is the deployment of a more dense network of meteorological towers, which will enable traditional resource assessment measurements such as wind speed, wind direction, and turbulence at several levels from the surface to the rotor disk top, and temperature profiles for quantifying atmospheric stratification and stability. Ideally, such towers could also provide a platform for validating remote-sensing measurements. The U.S. DOE has proposed the Reference Facility for Offshore Renewable Energy (RFORE) to be located at the Chesapeake Light Tower, approximately 13 miles off the Virginia Coast. The facility provides a first step toward addressing the shortage of offshore wind data.

Beyond meteorological towers, *remote-sensing technology mounted either on fixed towers or on floating platforms could provide data over broader regions.* Scanning Doppler lidar, wind-profiling lidar, and sodar can provide valuable wind speed and direction measurements throughout the turbine rotor disk and beyond. Radiometers can quantify temperature and humidity profiles to determine atmospheric stability.

In addition to long-term measurements of winds, temperature, and moisture profiles, *short-term intensive measurement campaigns with a broader deployment of instruments would also be of value,* especially for model validation.

These recommendations for more intensive observations extend a prior call for more onshore meteorological observations and focused field campaigns made by DOE in 2008. Since then, new types of remote-sensing instruments have become more widely available and more accepted in the wind energy industry for wind resource characterization.

RESEARCH NEED #2: UNCERTAINTY CHARACTERIZATION. Deterministic wind power forecasts based on numerical weather prediction (NWP) can provide useful information for decision making. However, by design, a single plausible future state of the atmosphere starting from a single initial state is generated. Imperfect initial and boundary conditions and model deficiencies inevitably lead to nonlinear error growth during model integration. Accurate knowledge of the continuum of plausible future states [the forecast probability density function (PDF)] is considerably more useful for decision making because it allows for a quantification of the uncertainty associated with a forecast.

"Ensembles" are used today to generate a set of plausible future atmospheric states and to estimate the forecast PDF of atmospheric variables relevant to wind power. Ensembles are created from the outputs of NWP models using any of the following: various initial conditions, different parameterizations within a single model, stochastic approaches with diverse numerical schemes, different models, and coupled ocean–atmosphere schemes. For wind energy, one important additional source of uncertainty comes from the challenging step of wind-to-power conversion.

Ensembles are affected by biases in the ensemble mean and by lack of diversity among the ensemble members, particularly in the planetary boundary layer (PBL). Therefore, *postprocessing is an important component of the wind forecasting process and should be explored further,* preferably including methods and techniques developed by the wind industry. Since the wind industry benefits from the findings published by the research community and the public sector, *it is recommended that a regular two-way exchange of know-how between academia, the public sector, and industry be established* to help advance the science and prevent duplication of efforts. A promising postprocessing technique is the analog approach, in which past observations that correspond to past predictions that best match selected features of the current forecast, such as time series of wind speed and direction, are used to correct the current forecast. Other promising techniques are advanced model output statistics (e.g., neural networks, support vector machines, and random forests).

Recently, operational centers have generated multiyear reforecast datasets to support successful calibration of both deterministic and probabilistic forecasts. It is expected that in the next few years new calibration techniques, possibly combining statistical and dynamical approaches, will lead to large improvements in the accuracy of wind power predictions and in the reliable characterization of their uncertainty.

Next, the three main topics and their associated specific research needs are described.

TOPIC #1: RESOURCE ASSESSMENT. Initial maps of the U.S. offshore wind resource from the National Renewable Energy Laboratory (NREL) and others by Stanford University have identified gross characteristics of the hub-height offshore wind resource, which have been generally useful to policymakers and researchers and for early-stage project development. Using mesoscale modeling techniques, these maps provide estimates of wind speed and direction, diurnal and seasonal patterns, wind shear, and air density at horizontal grid scales of approximately 1–5 km. This information, although essentially unverified due to the lack of hub-height measurements described in Research Need #1, has enabled numerous project siting studies, wind farm layout and energy production simulations, and estimates of development potential as a factor of water depth, distance from shore, wind resource, and other factors. However, *there is a need to accurately capture dynamic coastal processes,* such as sea breezes, low-level jets, and other land–air–ocean interactions, as they represent a significant source of variability in the available wind.

Data representing assessment periods of 20–25 years (i.e., project lifetimes) are typically required for bankable offshore projects; interannual speed variability of 4%–6% is not uncommon. The probability and magnitude of extreme events—particularly peak winds and waves and hurricanes—and the effects of more common events—such as winter storms, icing from sea spray, and salt corrosion—need to be better known to properly design turbines and foundations and meet industry standards. *In a changing climate, more studies are needed to reduce the uncertainty of a changing wind resource* as ocean, offshore, and coastal temperatures change. Changes in the local wind environment over time may also be caused by the increasing presence of other wind farms within a given region, as described in Topic #3.

Recent studies have explored strategic temporal, climatological, and spatial aspects of the offshore resource, including large-scale wind farm interconnection scenarios. U.S. East Coast offshore wind has been found to be particularly coincident with peak-electricity demand. Similar studies should be performed to identify resource attributes that can add value to generally higher offshore costs and evaluate the sensitivity of project location, including distance from the shore, to load coincidence.

Significant offshore resource assessment uncertainties exist. Most of the aforementioned studies relied on mesoscale modeling that was validated with generally sparse in situ data. Perhaps the largest uncertainty is extrapolating surface observations—generally 5-m buoy anemometer measurements to heights across the turbine rotor. As such, *there is an urgent need for multilevel wind and temperature observations at platforms offshore (as in Research Need #1),* equipped with either meteorological towers that are as tall or taller than hub height, or lidars. In the coastal region, transport processes (advection of either maritime air inland or continental air offshore) during sea- and land-breeze events often cause the PBL to deviate from classic well-mixed, neutrally stable conditions. Existing PBL parameterizations struggle to perform well in these conditions. *Research effort is needed to improve such PBL parameterizations in coastal regions.*

Long-term wind climatologies require publicly available historic reanalysis data and future climate data generated by models forced under different anthropogenic emission scenarios. Most of the existing publicly available data are at a relatively coarse spatial scale (> 20 km) compared to the size of a typical wind farm. Dynamical downscaling methods typically employ a regional climate model to generate higher spatiotemporal wind climatologies but at a high computational expense for long climate records. Stochastic downscaling methods are computationally cheaper and have been shown to accurately downscale low-resolution reanalysis data with acceptable accuracy, as compared to in situ validation data.

TOPIC #2: WIND POWER FORECASTING. Wind power forecasting is challenging because the relationship between wind speed and power production for a single wind turbine or a wind farm is nonlinear;

for some wind speed ranges, the sensitivity of power production forecasts to wind speed forecast error is quite high. For example, a modest 1.5 m s^{-1} error in a wind speed forecast can, in some cases, result in a power production forecast error of over 20% of a wind farm's capacity.

A diverse set of prediction tools and input data has been applied to the wind power forecast problem for a range of time scales. Intrahour forecasts (0–60 min ahead) are needed for regulation and real-time dispatch decisions. At this scale, the effects of small eddies and turbulent mixing are important but cannot be resolved by operational models. Therefore, mainly statistical methods are used, which are based on near-real-time observations. This has driven the deployment of meteorological sensors and lidars for intrahour forecasting.

The forecast 1–6 h ahead for load-following and next-operating-hour commitment has to account for various mesoscale weather phenomena (e.g., sea breezes, convective systems, and local topography). The rapid-update NWP approach most likely offers the best potential for improvement in this time frame. This is a tool with increasing capability, largely because of improvements in data assimilation techniques (e.g., the hybrid ensemble Kalman filter approach), the formulations of physics-based submodels, and the amount and quality of data available for assimilation. The state of the art in rapid-update systems is the High-Resolution Rapid Refresh (HRRR) model, currently undergoing experimental operation at NOAA, which assimilates the latest data and generates a 15-h forecast on a 3-km grid every hour.

The day-ahead forecast is important for unit commitment, scheduling, and market trading, which require knowledge of the evolving synoptic storm systems using NWP models and ensembles. The seasonal predictions for resource planning and contingency analysis require knowledge of global teleconnections (such as El Niño). These predictions are based largely on the analysis of cyclical patterns and climate forecast system models.

It is also recommended that more offshore observations be collected using towers, lidars, and buoys, to better validate models, help with data assimilation and uncertainty characterization, and improve the model physics, because many of the PBL schemes were originally developed over land. These efforts will require a close collaboration between operational forecast centers, industry, and academia.

Finally, *future efforts should focus on improving the models' ability to represent the PBL* and the interactions of finescale processes with larger scale flows, both inland and offshore. Such improvements will be possible only with investments that focus on improving our understanding of these key processes using real observations. Several workshops over the past 20 years have noted the need for improved PBL modeling, but no concerted effort at making such improvements has been made.

TOPIC #3: TURBULENT WAKE LOSSES. Wind turbines generate wakes downstream, which are generally characterized by a wind speed deficit and higher turbulence than the upwind environment. Because wakes can reduce power production and increase structural fatigue in downstream turbines, understanding wake properties, quantifying resulting power losses, and optimizing wind turbine layouts to minimize such losses is especially important to the wind energy industry. Accurately modeling turbine wakes is also important for other atmospheric applications that span a wide range of spatial scales, such as the impacts of wind energy deployment on the global climate, local meteorology, crop production, and the wind resource itself.

Because atmospheric flows are characterized by high Reynolds numbers (~10^7–10^8), the number of grid points required to explicitly resolve such flows with operating wind turbines via direct numerical simulation is ~10^{18}, which is prohibitive in the foreseeable future. As such, the wind industry has traditionally relied on computationally efficient wake models to simulate wind turbine wakes. In order of increasing complexities, these earlier wake models include: analytical representations of the wake deficit (e.g., the PARK model); parabolized forms of the Reynolds-Averaged Navier-Stokes (RANS) equations (e.g., the Ainslie model, also called the eddy viscosity model; UPMPARK, which uses a k-ε turbulence closure); hybrid models based on an internal boundary layer growth parameterization and coupled with a parabolized RANS or an analytical model (e.g., Deep-Array Wake Model and Large Array Wind Farm model); and nonlinear RANS models (e.g., WindModeller, Ellipsys, and FUGA). Although these models are attractive for their quick runtime, they have limited ability to capture the detailed wake characteristics because they are not suitable for simulations of unsteady, anisotropic turbulent flows.

To overcome these limitations, the research community has been using large-eddy simulation (LES), in which large-scale flow structures are resolved while the effects of smaller eddies are represented with a subgrid model (Smagorinsky or dynamical). In addition, the wind turbine is represented by either an actuator disk (with or without rotation features) or by actuator lines (one per blade) that exert a force on the flow and act as a momentum sink, or by the vortex method. Arrays of multiple wind turbines, in which multiple wakes interact with one another, have also been successfully simulated with LES. However, because of the high CPU-hours required, LES can be conducted for only a few hours or at equilibrium-state using periodic boundary conditions.

Because LES models for turbine wakes were traditionally developed in-house by research centers or universities without any funds for distributing, maintaining, or testing the codes, they are generally not available to the public. The only exception is the open-source Simulator for Offshore/Onshore Wind Farm Applications (SOWFA) from NREL, which includes a finite-volume scheme, actuator disks/lines, and options for periodic or nonperiodic boundary conditions. Although developing numerous in-house LES codes is of value because researchers can obtain independent verification of results, *it is recommended that more effort and funds be devoted to maintaining LES codes for turbine wakes and making them available to the public.*

To avoid the steep computational costs of simulating real wind farms with high numbers of turbines via LES, parameterizations of the effects of large wind farms on regional meteorology and global climate have been developed for mesoscale NWP and large-scale climate models, which are less computationally demanding. These parameterizations represent wind farms as either an elevated momentum sink [often with an added source of turbulent kinetic energy (TKE)], increased surface roughness, or an increased surface drag coefficient. *Because surface-based parameterizations incorrectly extract momentum near the surface, as opposed to around hub height, they are not recommended for turbine wake impact studies.* Although the global-scale impacts of even high penetrations of wind energy have proven to be negligible, local wakes extending tens of kilometers downwind of individual large wind farms have been generated by some wind farm parameterizations. However, to date, few observations are available to verify these model results.

Comparing model results with wind tunnel experiments, with either a single turbine or multiple turbines, is useful because the constant and controllable environment in a wind tunnel can be reproduced well. However, wind tunnel conditions are different from real atmospheric conditions and therefore *field measurements are also recommended both at individual turbines and at offshore wind farms.* Short-term field campaigns, as well as routine measurements (especially offshore) are needed to validate results under a large umbrella of atmospheric conditions. *It is recommended that inflow, near-wake, and far-wake vertical wind profiles and atmospheric stability be measured, as well as wake properties, such as TKE and turbulent fluxes* (preferably with scanning lidars or arrays of sonic anemometers).

An extensive list of references for all the topics described above is available online as supplemental material (http://dx.doi.org/10.1175/BAMS-D-13–00108.2).

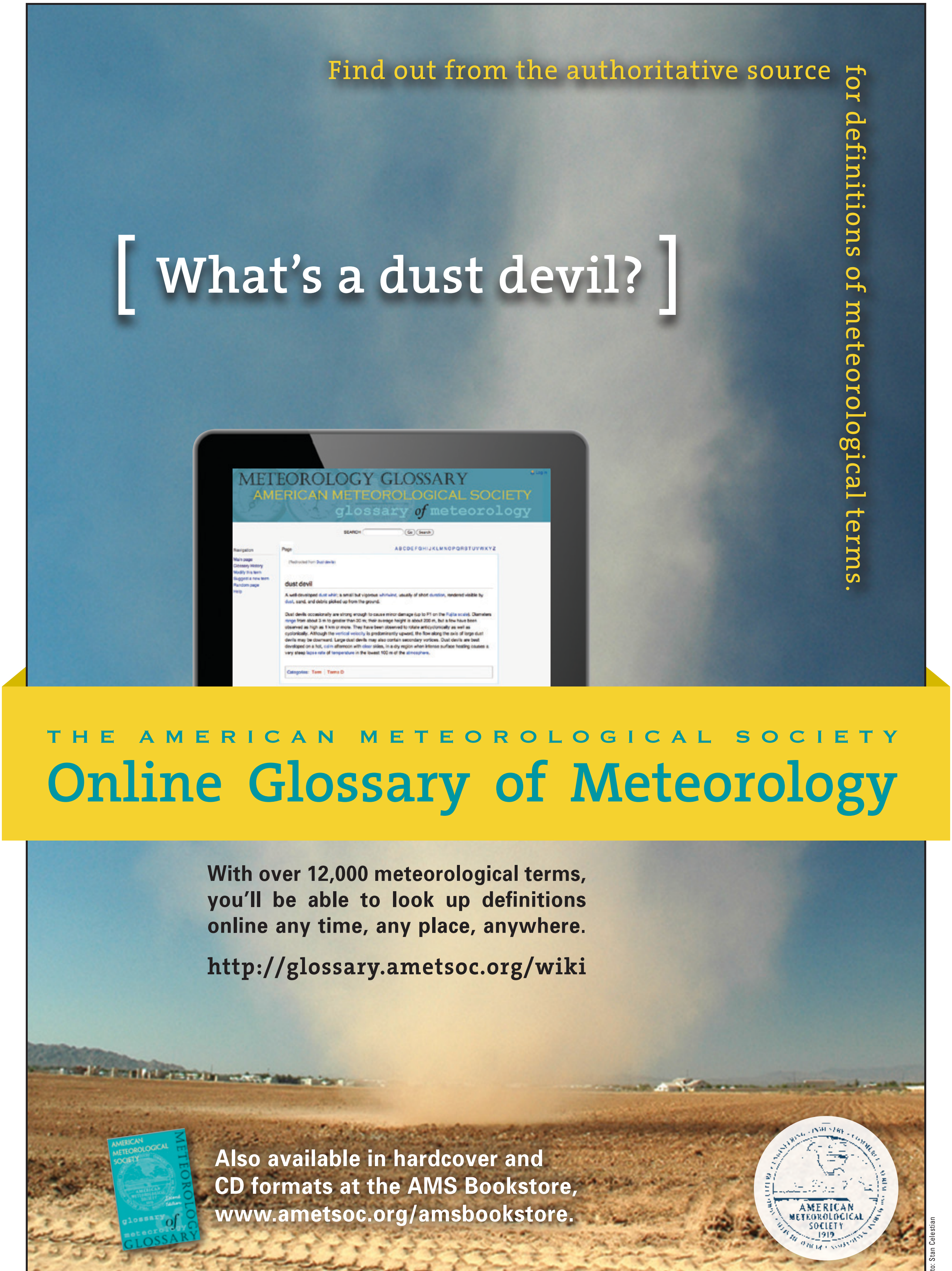

Photo: Stan Celestian

UNDERSTANDING THE METEOROLOGICAL DRIVERS OF U.S. PARTICULATE MATTER CONCENTRATIONS IN A CHANGING CLIMATE

BY JOHN P. DAWSON, BRYAN J. BLOOMER, DARRELL A. WINNER, AND CHRISTOPHER P. WEAVER

Research priorities for understanding the impacts of climate change on particulate matter air pollution due to shifts in weather patterns, emissions, and chemistry.

Particulate matter (PM) is one of the most pervasive air quality problems facing the United States, posing a major challenge for public health. PM is a complex mixture of anthropogenic, biogenic, and natural materials, suspended as aerosol particles in the atmosphere. Major components of PM include sulfate, nitrate, ammonium, organic carbon, elemental carbon, sea salt, and dust. The aerosols that make up PM may be emitted directly, in which case they are known as primary aerosols, or they may be formed as secondary aerosols from gas-phase precursors. Major aerosol precursors include SO_2, NO_x ($\equiv NO + NO_2$), NH_3, and volatile organic compounds (VOCs). Primary aerosols and precursors of secondary aerosols are emitted by a variety of processes and sources, including combustion, evaporation, agricultural activities, and natural processes. When inhaled, PM can lead to significant health problems, including asthma, chronic bronchitis, reduced lung function, irregular heartbeat, heart attack, and premature death (e.g., see U.S. EPA 2009c; Lave and Seskin 1973; Dockery et al. 1993; Pope et al. 2002; Sacks et al. 2011). In addition to its effects on health, PM has several other types of impacts. For example, PM reduces visibility in cities and national parks. In addition, certain PM species are extremely important climate forcers (Charlson et al. 1992; Forster et al. 2007; Bond et al. 2013).

In recent decades, U.S. environmental legislation, such as the Clean Air Act, has been highly successful in reducing the atmospheric burden of PM nationally, with corresponding positive effects on public health. Pope et al. (2009) attributed nearly five months of the 2.72-yr increase in U.S. life expectancy between 1980 and 2000 to reductions in average $PM_{2.5}$ levels

AFFILIATIONS: DAWSON, BLOOMER, WINNER, AND WEAVER—Office of Research and Development, U.S. Environmental Protection Agency, Arlington, Virginia
CORRESPONDING AUTHOR: Christopher Weaver, Office of Research and Development, U.S. Environmental Protection Agency, 1200 Pennsylvania Ave. NW, Mail Stop 8601-P, Washington, DC 20460
E-mail: weaver.chris@epa.gov

The abstract for this article can be found in this issue, following the table of contents.
DOI:10.1175/BAMS-D-12-00181.1

In final form 25 July 2013

by 6.52 $\mu g\ m^{-3}$ across the United States. While emissions of pollutants and precursors are the main determinant of ambient pollution concentrations, there has emerged a growing understanding that global climate change has the potential to make it more difficult to continue to achieve such air quality improvements (NRC 2001, 2004; Forster et al. 2007). In response to this challenge, the U.S. Environmental Protection Agency (EPA) has been leading a major effort to improve our fundamental understanding of the multiple, complex links between global climate change and regional U.S. air quality. This growing knowledge base provides a foundation for adapting the U.S. air quality management system to the long-term challenge of climate change. While anthropogenic emissions of PM and its precursors are expected to continue to decrease in the United States over the coming decades, understanding the extent to which the changing climate will affect strategies to improve air quality is an important aspect of this adaptation.

One of the most important aspects of air quality management is the mitigation of air pollution episodes. The potential for climate change to significantly impact PM concentrations during air pollution episodes, with corresponding negative implications for public health, is situated within the broader context of the dominant role that environmental extremes play in conversations about climate change adaptation and mitigation (e.g., see Field et al. 2012). For example, evidence suggests that extremes, such as very hot temperatures, are becoming much more frequent as a result of the changing climate (Hansen et al. 2012). Beyond hydroclimatic extremes, such as hurricanes, tornadoes, torrential downpours, heat waves, and droughts, Earth system extremes like harmful algal blooms, wildfires, air pollution episodes, and disease outbreaks also affect important sectors of the economy and the environment, impacting people where they live and work. Critical research questions for the scientific community relate to whether such extremes are changing, or may in the future change, in intensity, duration, frequency, timing, and spatial extent as a result of climate change, as well as the potential for the occurrence of unprecedented extremes.

This paper discusses what we currently understand about the potential sensitivity of PM episodes to climate-change-related changes in air pollution meteorology, in the broader context of the emissions and atmospheric chemistry drivers of PM. We reiterate the recommendations of Ravishankara et al. (2012) in proposing a research agenda to improve scientific understanding of PM in a changing climate, as a foundation for an improved ability to adapt to the impacts and to manage the risks of climate-induced changes in air quality.

BACKGROUND: CURRENT UNDERSTANDING OF CLIMATE CHANGE AND PM. An important part of our background knowledge base for understanding the potential implications of climate change on PM is recently improved understanding of the links between climate change and ground-level ozone (O_3) concentrations. A number of recent studies of the effects of climate change on ground-level O_3 have shown that the changing climate could have significant impacts on O_3 air quality, as synthesized in recent efforts (U.S. EPA 2009a; Weaver et al. 2009; Jacob and Winner, 2009). For example, the sensitivity of O_3 to temperature has been explored in several modeling studies (e.g., Sillman and Samson 1995; Dawson et al. 2007; Rasmussen et al. 2012). Collectively, this work suggests that, all else being equal, climate-induced changes in temperature, cloud cover, biogenic emissions, and synoptic-scale circulation patterns pose a significant risk for increased O_3 concentrations over large portions of the United States, with corresponding risks for human health (Post et al. 2012). This impact, as well as the additional precursor emissions decreases that may be needed as a result, was termed the "climate penalty" by Wu et al. (2008). It is likely that the United States is already experiencing this climate penalty, as shown in a study of 21 years of O_3 and temperature observations across the rural eastern United States (Bloomer et al. 2009). This body of research was an important consideration in the EPA administrator's 2009 finding that current and projected greenhouse gas concentrations pose a threat to human health and welfare (U.S. EPA 2009b).

Some of this work also considered PM. Most notably, the review of the impacts of climate change on air quality by Jacob and Winner (2009), while focusing more on O_3, did also examine initial results regarding the effects of climate change on PM. The studies summarized therein pointed to several of the same meteorological variables as the main drivers behind climate-induced changes in PM. For example, Racherla and Adams (2006) and Tagaris et al. (2007) considered the effect of changing precipitation on sulfate to be especially important, while the latter study also discussed boundary layer height and wind speed changes. Tsigaridis and Kanakidou (2007) suggested that temperature- and precipitation-induced changes in biogenic emissions of VOCs could increase organic aerosol concentrations appreciably over the United States, while Heald et al. (2008) pointed to changes in both biogenic emissions and direct effects of precipitation as potentially important drivers of changes in organic aerosol concentrations.

Additional analysis (see Fig. 1) shows links between meteorology and observed $PM_{2.5}$ episodes at one monitoring site in Chicago, Illinois (in the U.S. upper Midwest), and one in Birmingham, Alabama (in the U.S. Southeast), from 2007 to 2011. For this analysis, a modified version of the Wang and Angell (1999) definition of stagnation was used with National Centers for Environmental Prediction–National Center for Atmospheric Research (NCEP–NCAR) Reanalysis 1 data (Kalnay et al. 1996) to classify days as "stagnant" or "nonstagnant." In Chicago, PM episodes are largely a cold-weather phenomenon, resulting from stagnant days with low mixing heights and temperature inversions, while PM episodes in Birmingham are generally associated with stagnation, regardless of temperature bin (Fig. 1). In Fig. 1, the presence of stagnant conditions appears to have caused consistently greater PM concentrations in Birmingham, regardless of temperature, while stagnant conditions appear to have had the most impact on Chicago PM concentrations on cold days. While only about a one-quarter of days during this 5-yr period were classified as stagnant in this analysis, two-thirds of the episode days (with $PM_{2.5}$ concentrations greater than 35 $\mu g\ m^{-3}$) in Fig. 1 met the criteria for being considered stagnant. Climate change has the potential to strongly affect these driving factors, with corresponding implications for the occurrence of PM episodes. Horton et al. (2012) examined how the changing climate may affect stagnation frequency. Using an ensemble of the phase 3 of the Coupled Model Intercomparison

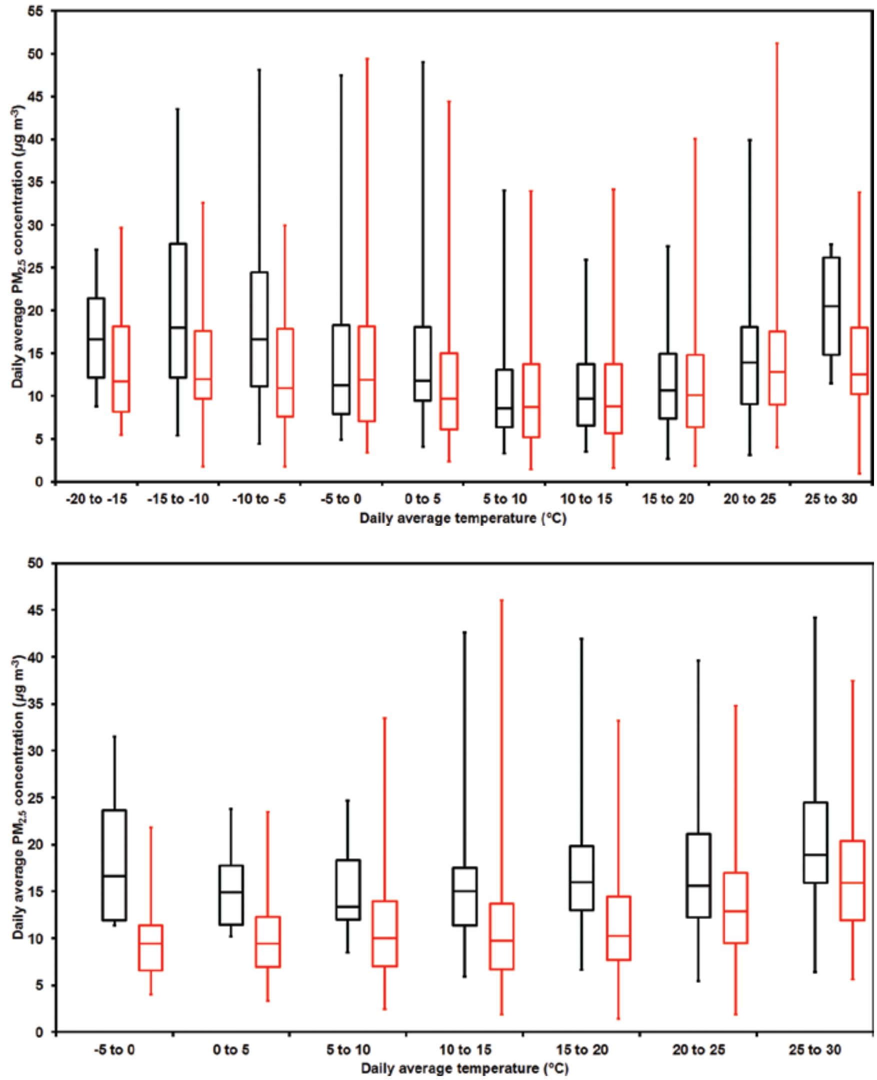

Fig. 1. Box plots of daily average $PM_{2.5}$ concentrations in 5°C bins in (top) Chicago and (bottom) Birmingham for the 2007–11 period. Black boxes and whiskers represent days classified as stagnant, while red boxes and whiskers represent days classified as nonstagnant. Boxes and whiskers represent the minimum, 25th percentile, median, 75th percentile, and maximum $PM_{2.5}$ concentrations in each bin. Chicago PM data are from the Mayfair Pumping Station monitoring site (17-031-0052), while Birmingham PM data are from the Wylam monitoring site (01-073-2003). Temperature and other meteorological data in the stagnation determination were from the NCEP–NCAR reanalysis. Measurements from dates surrounding the 4 Jul holiday have been removed due to the PM contribution from fireworks. The 500-mb wind speed criterion was not used in Chicago for determining stagnant days, since this criterion is more relevant for multiday warm weather stagnation episodes, and the precipitation threshold was raised to 10 mm in Birmingham due to the wet bias in the reanalysis in the Southeast in summer; both of these are departures from the Wang and Angell (1999) definition of stagnation.

Project (CMIP3) models and the A1B scenario for the late twenty-first century, they calculated that the eastern United States would experience an increase in stagnant days in all four seasons. Both the average summer and the average autumn were calculated to have two more stagnant days per season than under late twentieth-century conditions.

These initial study findings, and the above-mentioned simple analysis, thus tend to paint a complex picture of the range and types of potential impacts of climate change on PM in the United States, in part because changes in the most relevant meteorological factors for PM (temperature, precipitation, and mixing) will often have competing impacts—and these impacts and interactions are difficult to diagnose by focusing on longer-term monthly, seasonal, and annual averages or by grouping various regions or PM species together. For example, Pye et al. (2009) simulated large seasonal and regional effects (on the order of several μg m^{-3}) that mostly negated one another when averaged over the entire year and summed to account for total PM. Nevertheless, some common general conclusions emerged from these initial studies:

- Very broadly, for sulfate, these earlier modeling studies consistently found that simulated multidecadal climate change led to concentration increases in the U.S. Northeast and decreases in the Southeast, assuming no changes to SO_2 emissions, with less agreement for other regions. Climate-induced increases in sulfate could most often be associated with changes in oxidation due to warmer temperatures, whereas climate-induced decreases resulted from increases in wet deposition due to increases in precipitation.
- By contrast, simulated climate change resulted in decreases in annual average nitrate concentrations over most of the country due to the effect of higher temperatures on nitrate partitioning, though precipitation and transport added significant second-order complexity to this simple temperature–nitrate relationship.
- For carbonaceous aerosols, changes in temperature-driven partitioning, biogenic emissions, wet deposition, and synoptic-scale cyclones were all important.

As a whole, the studies summarized by Jacob and Winner (2009) suggested that climate-change-induced differences in model-simulated annual average total PM concentrations between the present day and the 2050s would be less than 1.0 μg m^{-3} in average PM concentration as a result of these competing changes in individual aerosol species. As indicated earlier, however, average values may not be a good metric for evaluating policy relevant impacts of climate change on PM, and episode analysis may be better. Additionally, these conclusions are subject to major gaps in our understanding of several critical factors with the potential to overwhelm these simulated changes. In particular, the influence of climate change on synoptic- and event-scale mixing and precipitation, the impacts of temperature changes on partitioning of primary and secondary organic aerosols, and the links between climate change and PM emissions from wildfires and dust events are not yet well captured in such studies. These gaps are also heavily intertwined with complicated anthropogenic factors related to development or farming, such as land use and land cover, and emissions of both greenhouse gases and traditional pollutants. We discuss these gaps and put forward an integrated climate and PM research agenda to address them.

RESEARCH OPPORTUNITIES FOR UNDERSTANDING CLIMATE IMPACTS ON PM. The research summarized above suggests that there are several understudied links between climate and aerosol research that, if pursued, could significantly increase our understanding of the implications of climate change for PM in the United States, portrayed schematically in Fig. 2. Major elements include the meteorology of pollution episodes; natural emissions from wildfires, vegetation, and dust events; and organic aerosol modeling. These elements are heavily intertwined, and thus understanding the linkages between them and their links to anthropogenic emissions and human activities is also critical. For example, the meteorology of air pollution episodes is related to the meteorology that is most conducive to wildfires. Similarly, the emissions of biogenic VOCs are strongly related to meteorology (Guenther et al. 2006). Here we summarize current understanding in these areas to suggest a set of high-priority foci for future climate and PM research.

Meteorological drivers of PM episodes. ***Recommendation 1:*** *Understand the links among climate change, synoptic phenomena, local stagnation, and frequency of precipitation.* Figures 1 and 2 suggest that studies of the impacts of a changing climate on PM episodes should consider changes in both winter and summer stagnation, in particular, on a regional basis. Such stagnation events, in turn, result from distinct synoptic-scale conditions that have strong, but as yet uncertain, links to climate change. While they did not simulate air quality, Bengtsson et al. (2006) projected decreased frequency of storm tracks under a late twenty-first-century A1B climate as compared to a twentieth-century climate in the upper Midwest in winter and in both the Midwest and Northeast in summer. The analyses by Lambert and Fyfe (2006) and Pinto et al. (2007) also showed decreases in cyclone frequency over the Northern Hemisphere in general, while the latter study also suggested that this is true over North America in particular. In their analysis of the CMIP5 GCMs, Chang et al. (2012) showed that these models generally predict a decrease in cyclone frequency over North America in winter and over much of the continent in summer, and that CMIP5 models show a stronger decrease in cyclone frequency than CMIP3 models.

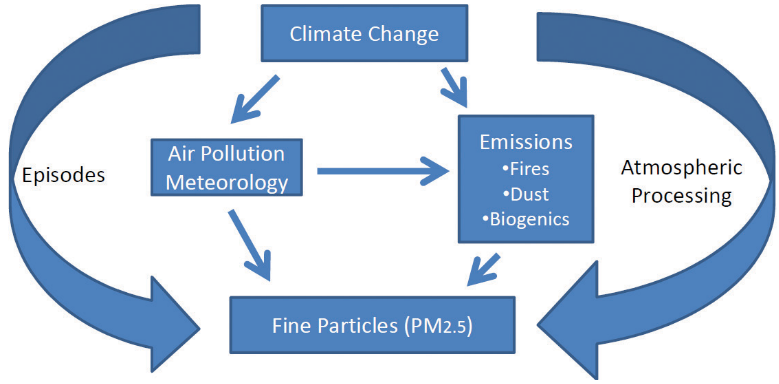

Fig. 2. Conceptual model of the climate change impact on the PM problem. Several of the arrows could point in both directions to signify feedback; however, this figure is intended only to illustrate the impact of the changing climate on PM.

Indeed, climate-induced changes in synoptic-scale weather patterns, such as midlatitude cyclones, frontal passages, and location and frequency of high pressure systems, have been suggested as major drivers of future changes in PM episodes (see, e.g., Leung and Gustafson 2005). The interannual variability in the frequency of cyclones has been shown by Tai et al. (2012) to be a strong driver of the interannual variability in $PM_{2.5}$ concentrations in the Midwest. In their study, regional annual average $PM_{2.5}$ concentrations were compared to the average amount of time between cyclones in a given year; years with less frequent cyclones had higher annual average $PM_{2.5}$ concentrations, which has implications for the concentrations during and frequency of individual episodes. In their study focused on ozone, Zhu and Liang (2013) showed a strong link between the Bermuda high and the pattern of ozone concentrations over the eastern half of the United States. These studies would suggest that changes in synoptic phenomena could have major implications for pollution episodes.

However, the potential for changes in short-term and episodic PM concentrations as a result of climate change has only been considered by a small number of studies. Though few, these results suggest the potential for appreciable changes in short-term PM concentrations and episodes of PM under a future climate, as a result of the potential for climate change to impact synoptic meteorology. For example, Mickley et al. (2004) performed a modeling study in which an inert black carbon (BC) tracer was used to represent PM in a global-scale simulation of the time period from 1950 to 2052 in the Goddard Institute for Space Studies (GISS) GCM II. Emissions of BC were held at present-day levels throughout the simulation so that the effects of meteorologically driven transport could be isolated. The authors highlighted the importance of changes in pollution episodes, rather than seasonal mean concentrations, which changed little between the present and the 2050s. The simulation results showed an increase in the severity of summertime pollution episodes in the Northeast and Midwest by 2050, which occurred despite simulated increases in mixing depth over these regions, due to a decreasing trend in cyclones. As fewer cold fronts with clean air traveled across the Midwest and Northeast, episode severity increased accordingly.

In addition, the number of simulated PM episodes increased considerably from the present day to the 2050s in the study of January and July PM concentrations by Dawson et al. (2009), who held emissions at present-day levels and compared air quality under simulated present-day and future meteorology. The average area experiencing a 24-h-average $PM_{2.5}$ concentration greater than 35 $\mu g\ m^{-3}$ on any day in a given July increased by a factor of 6.4, indicating a major increase in episode extent, with the largest increases occurring in the Midwest and Ohio River valley, where sulfate is the dominant summertime PM component. These changes in simulated short-term PM concentrations also reflected an increase in stagnation over the Midwest. Additionally, in some areas, such as the Southeast, simulated PM concentrations increased despite increases in precipitation, indicating that other factors outweighed precipitation changes (or, alternatively, that total precipitation may not be the best metric for assessing potential impacts on PM and that other metrics, such as the number of days with precipitation, might be more appropriate). Changes in episodes under a 2050s "business as usual" scenario in California were examined by Mahmud et al. (2012); their simulations indicated that extreme events would be exacerbated in the future in the Central Valley, though changes in extremes in the Los Angeles area and changes in annual average concentrations were small.

Furthermore, we have Leibensperger et al. (2008), whose conclusions, while focused on O_3, are likely applicable to PM as well. This study showed that the frequency of midlatitude cyclones has been decreasing across the Midwest and Northeast, thereby increasing the number of stagnation days each year, and the authors concluded that this has in large part countered the benefits of decreasing emissions of O_3 precursors. Similarly, slowly migrating anticyclones and stagnating high pressure conditions, such as those associated with the Bermuda high, have been strongly linked with O_3 episodes in the eastern United States (Comrie and Yarnal 1992), and evidence suggests that the Bermuda high is strengthening due to anthropogenic climate change (Li et al. 2011). If these links between stagnant conditions and O_3 are considered in light of the observation by Tai et al. (2010) that concentrations of $PM_{2.5}$ in the United States are on average 2.6 μg m^{-3} (compared to a 24-h $PM_{2.5}$ air quality standard of 35 μg m^{-3}) higher on stagnant days versus nonstagnant days, then the implication is that anticipated future changes in stagnation and synoptic-scale meteorology could have a large impact on episodic PM concentrations in the United States. Additionally, given the relationships between weather types, air pollution episodes, and associated health impacts (Hanna et al. 2011; Winner and Cass 2001), it would likely follow that changes in synoptic-scale meteorology and weather type would affect air pollution episodes and pollution-related health impacts.

Finally, while precipitation has frequently been examined in studies of the changing climate and its impacts on pollution concentrations, explorations of future climate scenarios' impacts on PM have generally reported changes in total precipitation in units such as millimeters per year (mm yr^{-1}), rather than as a frequency. Changes in how often precipitation occurs, however, is likely to be an important driver of changes in PM episodes (Dawson et al. 2009). In addition, the frequency of precipitation is linked to wildfires, which in turn are a potentially important driver of climate-change-related changes in PM, especially PM episodes, as discussed in more detail in the "Emissions" section below.

Addressing this recommendation will also require addressing several methodological challenges presented by the modeling required to support such investigations. For example, Tai et al. (2012) showed that even the same general circulation model can predict quite different changes in cyclone frequency for different realizations of a given future emissions scenario, which would suggest that one realization of a particular scenario may not be adequate for estimating changes in cyclones and stagnation. Similarly, Manders et al. (2012) showed that different GCMs simulating the same future scenario can produce different impacts on regional O_3 and PM.

The modeling of precipitation, even for the present day, is a difficult undertaking. And the downscaling of GCM output to the regional scale requires a careful consideration of technical issues, such as meteorological and chemical boundary conditions, and nudging approaches. However, progress (e.g., Bowden et al. 2012) has been made recently in determining how best to link these scales to capture the global-scale dynamics of the GCM (or reanalysis) while still making use of the finer spatial scale of the regional model.

Emissions. WILDFIRES. ***RECOMMENDATION 2:** REFINE ESTIMATES OF CLIMATE-CHANGE-RELATED WILDFIRE ACTIVITY CHANGES AND THEIR IMPACTS ON PM AND PM PRECURSOR EMISSIONS.* In addition to synoptic-scale meteorology, wildfires are also a major contributor to PM episodes, particularly carbonaceous aerosol concentrations in the western United States during summer (Park et al. 2003). As was summarized in the review by Keywood et al. (2013), the area burned by wildfires in North America is expected to increase dramatically over the twenty-first century, primarily due to warmer temperatures and precipitation changes. The changing climate has already led to higher large-wildfire frequency, longer wildfire durations, and longer wildfire seasons in the western United States (Westerling et al. 2006). The consequence for this on area burned could be dramatic; for example, Flannigan et al. (2005) estimated a doubling (from +74% to +118%) of area burned in Canada under a 3 × CO_2 climate.

The links between the changing climate and changing PM emissions from wildfires show a rather consistent increase in wildfire-related PM under a changed climate for seasonal or annual averages of PM. For example, Spracklen et al. (2007) estimated that changes in wildfires have caused a 30% increase in summertime organic carbon aerosol concentrations in the western United States over the last 30 years. In subsequent work, Spracklen et al. (2009) simulated increases in May–October average concentrations of organic carbon aerosols of 40% and elemental carbon aerosol concentrations of 20% over the western United States due to changes in wildfires in a changing climate [between 2000 and the 2050s, using the Intergovernmental Panel on Climate Change (IPCC) A1B scenario]. Yue et al. (2013) suggest that the effect of wildfires will be most consequential for PM episodes, with a smaller effect on longer-term average concentrations. However, only a small number of studies have considered the changes in PM concentrations and PM episodes (frequency, severity, and duration) that might result from climate-induced changes in wildfires. Research on better quantifying the emissions and subsequent impacts on ambient PM concentrations from changing wildfires is necessary to improve adaptation planning for air quality. Such research would likely build on the foundational work linking wildfires to specific meteorological phenomena, such as the work of Lafon and Quiring (2012), who most strongly related wildfire activity and area burned to daily variability of precipitation. This research would suggest that the changing frequency of precipitation (discussed in the "Meteorological drivers of PM episodes" section), not just the changing amount of precipitation, could affect PM concentrations via wildfires. Another example is the research of Hessl et al. (2004), who linked wildfires in the Pacific Northwest to the Pacific decadal oscillation and the drought severity index, which shows the varying temporal scales of important meteorological drivers of fires.

Biogenic VOC emissions. ***Recommendation 3: Better quantify how changing climatic conditions and CO_2 concentrations will affect emissions of the biogenic VOC species that are PM precursors. Also, incorporate recent advances in the understanding of the chemistry of biogenic VOCs into studies of how the changing climate will affect PM concentrations.*** One of the ways climate change is expected to impact O_3 concentrations is through changes in biogenic VOC emissions, especially increased emissions of the O_3 precursor isoprene (Weaver et al. 2009). While isoprene has been thought to be a relatively minor precursor of PM, recent advances in the understanding of the oxidation of isoprene (and its oxidation products) in the aqueous phase (Ervens et al. 2008), suggest that the role of isoprene in forming organic aerosols may generally be underestimated in chemical transport models. In addition to isoprene, other biogenic VOCs are also important PM precursors. For example, monoterpenes and sesquiterpenes can be oxidized to form organic aerosols. How climate change will impact emissions of biogenic VOCs, such as α-pinene and β-pinene, which are also PM precursors, has not been well studied. Similarly, recent research (Horváth et al. 2012) has suggested that soils may be a source of terpene emissions, though this generally has not been taken into account in chemical transport models.

A link between increased temperature and increased biogenic VOC emissions has been included in representations such as the Model of Emissions of Gases and Aerosols from Nature (MEGAN; Guenther et al. 2006) and used in many studies to estimate increases in biogenic emissions resulting from climate change. However, substantial uncertainties remain. For example, isoprene emissions are affected in very complex ways by ambient CO_2 concentrations (Rosenstiel et al. 2003; Monson et al. 2007; Possell and Hewitt, 2011; Sun et al. 2012), creating an unclear net effect of elevated CO_2 on isoprene emissions. One recent study (Pacifico et al. 2012) of these competing effects suggests that the temperature-driven increase and CO_2-driven suppression of isoprene emissions may essentially negate one another. The ambient CO_2 concentration may also affect the sensitivity of isoprene emissions to temperature (Way et al. 2011). However, the effect on the changing climate on nonisoprene biogenic VOCs, which are thought to form aerosols more readily than does isoprene, has not been a major focus of research to date.

In addition, land cover will also change in the coming decades, driven by both climatic and human factors, but in ways that may be hard to anticipate; some plantation tree species, such as poplar, are high isoprene emitters (Wiedinmyer et al. 2006), so increases in their production may lead to increased biogenic VOC emissions that should be accounted for in studies of climate-related impacts on air quality (e.g., see Avise et al. 2009). Similarly, Berg et al. (2013) showed that invasive species, such as bark beetles, which are affected by climate change, can, in turn, affect biogenic emissions and the aerosols that form from them. As the flux and spatial pattern of biogenic emissions change, there will be effects on the concentrations of organic aerosol concentrations.

In the few modeling studies to date to address some of these questions, future changes in biogenic emissions, induced by both the changing climate and the changing land use and land cover, had significant impacts on biogenic aerosol concentrations (Heald et al. 2008; Chen et al. 2009; Lam et al. 2011). For example, Wu et al. (2012) projected that climate- and CO_2-driven changes in land cover would result in a 10% increase in global secondary organic aerosol (SOA) burden between 2000 and 2050, and a 20% increase in SOA burden between 2000 and 2100 (following the IPCC A1B scenario), including increases in SOA concentration of several tenths of a microgram per cubic meter ($\mu g\ m^{-3}$) over much of the southwestern and northeastern United States. However, these studies do not yet paint a consistent picture of the magnitude of this impact. Additionally, recent advances in isoprene modeling, such as improved aqueous chemistry treatments, have not yet been incorporated into these studies of the impacts of climate change on organic PM.

Drought and dust. ***Recommendation 4:*** *Estimate the effects of evolving precipitation patterns, especially changes in droughts, on the emissions and transport of the dust component of PM.* Dust is an important constituent of PM, especially in the coarse fraction between 2.5 and 10 μm. Dust from Asia (Duce et al. 1980; Prospero 1979) and Africa (Prospero et al. 1970) can be transported over very long distances to the United States, though only a small fraction of the PM in the United States is attributed to long-range transport from other continents. However, the Task Force on Hemispheric Transport of Air Pollution mentioned changing source-to-receptor relationships for long-range transport as one aspect of climate change that needs further study (TF HTAP 2011). For example, the transport of African dust to southern Europe appears to be linked to synoptic-scale meteorological phenomena such as the North Atlantic Oscillation (NAO) (Cusack et al. 2012; Pey et al. 2012), so changes in the NAO could result in changing dust transport. Similarly, domestically generated dust is also related to meteorology; for example, Okin and Reheis (2002) related the strength of the ENSO anomaly to dust events in the southwestern United States. Given the expected changes in droughts over the coming decades, there could potentially be an appreciable impact on dust concentrations; for example, the transition to a more arid climate in the U.S. Southwest has been rather well established (Seager et al. 2007), though the consequences for airborne dust have not been quantified. Numerous basic scientific questions surround all of these potential pathways for altered dust contributions to PM concentrations in an altered climate.

Modeling of organic aerosol processing. ***Recommendation 5:*** *Incorporate recent advances in the modeling of organic aerosols, including those formed from biogenic VOC emissions, into studies of the effects of the changing climate on these aerosols.* Changing biogenic VOCs emissions are linked to another uncertain aspect of the impacts of climate change on PM: atmospheric processing of organic aerosols. Similarly, advances in the modeling of aqueous chemistry (Carlton et al. 2008) suggest that there is an important link between cloud water and organic aerosol production, though the question of how climate change will affect this production pathway remains an open one. While recent advances in the understanding of the oxidation of organic aerosol precursors and the partitioning of organic aerosols between the condensed and vapor phases (Robinson et al. 2007; Jimenez et al. 2009) have led to more complete modeling of how temperature affects organic aerosols, these improvements have not fully been incorporated into studies of the impacts of climate change. The study by Day and Pandis (2011), which included the organic aerosol model improvements by Murphy and Pandis (2009), represents an important step in incorporating these developments into studies of climate change impacts on PM; Day and Pandis (2011) compared the effects of changing organic aerosol partitioning at higher temperatures and increased biogenic emissions (see also the "Biogenic VOC emissions" section) and found that increased aerosol concentrations due to increased biogenic emissions could greatly outweigh partitioning effects. While this study suggests that advances in the modeling of aerosol partitioning are less consequential for understanding climatic impacts than are advances in the understanding of biogenic emissions, this cannot yet be stated with a high degree of confidence.

CONCLUSIONS. Research to date on the impacts of climate change on policy relevant to concentrations of ambient PM air pollution suggest that there are several critical but understudied links between climate and aerosol research that, if pursued, could significantly increase our understanding of the implications of climate change for PM in the United States. While emissions of aerosols and precursors will likely remain the biggest determinant of ambient PM concentrations, climatic changes can have important impacts on PM. Changes in land use and land cover, from farming or development, for example, will affect emissions important to both ambient PM concentrations and to climate change. The initial studies of climate change and PM examined here have largely excluded some of the key processes that could result in large climate-induced PM changes, including changing emissions from wildfires and dust, and atmospheric processing of organic aerosol precursors. In addition, original analysis presented here indicates that regional and seasonal consideration of meteorological episodes, rather than simply shifts in mean climate, is critically important for understanding climate change impacts on PM. The few studies that have examined how climate change is expected to impact PM pollution episodes and short-term concentrations of PM have provided preliminary evidence that climate change may exacerbate high PM episodes, but the meteorological variables to which these studies point as driving changes in pollution episodes require more attention in modeling studies of future climate. Potentially important aspects of this issue include stagnation, synoptic-scale meteorology, weather-type classification, and precipitation frequency.

In this paper we have summarized the current understanding in these areas to suggest a set of high-priority foci for future climate and PM research. These science needs are encapsulated in the following set of recommendations:

Recommendation 1: *Understand the links among climate change, synoptic phenomena, local stagnation, and frequency of precipitation.*

Recommendation 2: *Refine estimates of climate-change-related wildfire activity changes and their impacts on PM and PM precursor emissions.*

Recommendation 3: *Better quantify how changing climatic conditions and CO_2 concentrations will affect emissions of the biogenic VOC species that are PM precursors. Also, incorporate recent advances in the understanding of the chemistry of biogenic VOCs into studies of how the changing climate will affect PM concentrations.*

Recommendation 4: *Estimate the effects of evolving precipitation patterns, especially changes in droughts, on the emissions and transport of the dust component of PM.*

Recommendation 5: *Incorporate recent advances in the modeling of organic aerosols into studies of the effects of the changing climate on these aerosols.*

We propose this set of recommendations as a research framework for organizing future investments in climate change–PM science, to build fundamental understanding of critical Earth system processes in an area of first-order societal importance.

ACKNOWLEDGMENTS. The authors thank Chris Nolte for his assistance with reanalysis data and comments on a previous draft, as well as Marcus Sarofim for his comments on a previous draft. The views expressed in this paper are those of the authors and do not necessarily represent the views or policies of the U.S. Environmental Protection Agency.

REFERENCES

Avise, J., J. Chen, B. Lamb, C. Wiedinmyer, A. Guenther, E. Salatheì, and C. Mass, 2009: Attribution of projected changes in summertime U.S. ozone and PM2.5 concentrations to global changes. *Atmos. Chem. Phys.,* **9,** 1111–1124.

Bengtsson, L., K. I. Hodges, and E. Roeckner, 2006: Storm tracks and climate change. *J. Climate,* **19,** 3518–3543.

Berg, A. R., C. L. Heald, K. E. Huff Hartz, A. G. Hallar, A. J. H. Meddens, J. A. Hicke, J.-F. Lamarque, and S. Tilmes, 2013: The impact of bark beetle infestation on monoterpene emissions and secondary organic aerosol formation in western North America. *Atmos. Chem. Phys.,* **13,** 3149–3161.

Bloomer, B. J., J. W. Stehr, C. A. Piety, R. J. Salawitch, and R. R. Dickerson, 2009: Observed relationships of ozone air pollution with temperature and emissions. *Geophys. Res. Lett.,* **36,** L09803, doi:10.1029/2009GL037308.

Bond, T. C., and Coauthors, 2013: Bounding the role of black carbon in the climate system: A scientific assessment. *J. Geophys. Res.,* **118,** 5380–5552, doi:10.1002/jgrd.50171.

Bowden, J. H., T. L. Otte, C. G. Nolte, and M. J. Otte, 2012: Examining interior grid nudging techniques using two-way nesting in the WRF model for regional climate modeling. *J. Climate,* **25,** 2805–2823.

Carlton, A. G., B. J. Turpin, K. E. Altieri, S. P. Seitzinger, R. Mathur, S. J. Roselle, and R. J. Weber, 2008: CMAQ model performance enhanced when in-cloud secondary organic aerosol is included: comparisons of organic carbon predictions with measurements. *Environ. Sci. Technol.,* **42,** 8798–8802.

Chang, E. K. M., Y. Guo, and X. Xia, 2012: CMIP5 multimodel ensemble projection of storm track change under global warming. *J. Geophys. Res.,* **117,** D23118, doi:10.1029/2012JD018578.

Charlson, R. J., S. E. Schwartz, J. M. Hales, R. D. Cess, J. A. Coakley Jr., J. E. Hansen, and D. J. Hofmann, 1992: Climate forcing by anthropogenic aerosols. *Science,* **255,** 423–430.

Chen, J., J. Avise, A. Guenther, C. Wiedinmyer, E. Salathe, R. B. Jackson, and B. Lamb, 2009: Future land use and land cover influences in regional biogenic emissions and air quality in the United States. *Atmos. Environ.,* **43,** 5771–5780.

Comrie, A. C., and B. Yarnal, 1992: Relationships between synoptic-scale atmospheric circulation and ozone concentrations in metropolitan Pittsburgh, Pennsylvania. *Atmos. Environ.,* **26B,** 301–312.

Cusack, M., A. Alastuey, N. Pérez, J. Pey, and X. Querol, 2012: Trends of particulate matter ($PM_{2.5}$) and chemical composition at a regional background site in the western Mediterranean over the last nine years (2002–2010). *Atmos. Chem. Phys.,* **12,** 8341–8357, doi:10.5194/acp-12-8341-2012.

Dawson, J. P., P. J. Adams, and S. N. Pandis, 2007: Sensitivity of ozone to summertime climate in the eastern USA: A modeling case study. *Atmos. Environ.,* **41,** 1494–1511.

——, P. N. Racherla, B. H. Lynn, P. J. Adams, and S. N. Pandis, 2009: Impacts of climate change on regional and urban air quality in the eastern United States: Role of meteorology. *J. Geophys. Res.,* **114,** D05308, doi:10.1029/2008JD009849.

Day, M. C., and S. N. Pandis, 2011: Predicted changes in summertime organic aerosols concentrations due to increased temperatures. *Atmos. Environ.,* **45,** 6546–6556.

Dockery, D. W., C. A. Pope III, X. Xu, J. D. Spengler, J. H. Ware, M. E. Fay, B. G. Ferris Jr., and F. E. Speizer, 1993: An association between air pollution and mortality in six U.S. cities. *N. Engl. J. Med.,* **329,** 1753–1759.

Duce, R. A., C. K. Unni, B. J. Ray, J. M. Prospero, and J. T. Merrill, 1980: Long-range atmospheric transport of soil dust from Asia to the tropical North Pacific: Temporal variability. *Science,* **209,** 1522–1524.

Ervens, B. E., A. G. Carlton, B. J. Turpin, K. E. Altieri, S. M. Kreidenweis, and G. Feingold, 2008: Secondary organic aerosol yields from cloud-processing of isoprene oxidation products. *Geophys. Res. Lett.,* **35,** L02816, doi:10.1029/2007GL031828.

Field, C. B., and Coauthors, 2012: Managing the risks of extreme events and disasters to advance climate change adaptation; Special report of the Intergovernmental Panel on Climate Change. Cambridge University Press, 582 pp.

Flannigan, M. D., K. A. Logan, B. D. Amiro, W. R. Skinner, and B. J. Stocks, 2005: Future area burned in Canada. *Climatic Change,* **72,** 1–16.

Forster, P., and Coauthors, 2007: Changes in atmospheric constituents and in radiative forcing. *Climate Change 2007: The Physical Science Basis,* S. Solomon et al., Eds., Cambridge University Press, 129–234.

Guenther, A., T. Karl, P. Harley, C. Wiedinmyer, P. I. Palmer, and C. Geron, 2006: Estimates of global terrestrial isoprene emissions using MEGAN (Model of Emissions of Gases and Aerosols from Nature). *Atmos. Chem. Phys.,* **6,** 3181–3210.

Hanna, A. F., and Coauthors, 2011: Associations between ozone and morbidity using the Spatial Synoptic Classification system. *Environ. Health,* **10,** 49, doi:10.1186/1476-069X-10-49.

Hansen, J., M. Sato, and R. Ruedy, 2012: Perception of climate change. *Proc. Natl. Acad. Sci. USA,* **109,** E2415–E2423, doi:10.1073/pnas.1205276109.

Heald, C. L., and Coauthors, 2008: Predicted change in global secondary organic aerosol concentrations in response to future climate, emissions, and land use change. *J. Geophys. Res.,* **113,** D05211, doi:10.1029/2007JD009092.

Hessl, A. E., D. McKenzie, and R. Schellhaas, 2004: Drought and the Pacific decadal oscillation linked to fire occurrence in the inland Pacific Northwest. *Ecol. Appl.,* **14,** 425–442.

Horton, D.E., Harshvardhan, and N. S. Diffenbaugh, 2012: Response of air stagnation frequency to anthropogenically enhanced radiative forcing. *Environ. Res. Lett.,* **7,** 044034, doi:10.1088/1748-9326/7/4/044034.

Horváth, E., A. Hoffer, F. Sebök, C. Dobolyi, S. Szoboszlay, B. Kriszt, and A. Gelencsér, 2012: Experimental evidence for direct sesquiterpene emission from soils. *J. Geophys. Res.,* **117,** D15304, doi:10.1029/2012JD017781.

Jacob, D. J., and D. A. Winner, 2009: Effect of climate change on air quality. *Atmos. Environ.,* **43,** 51–63.

Jimenez, J. L., and Coauthors, 2009: Evolution of organic aerosols in the atmosphere. *Science,* **326,** 1525–1529.

Kalnay, E., and Coauthors, 1996: The NCEP/NCAR 40-Year Reanalysis Project. *Bull. Amer. Meteor. Soc.,* **77,** 437–471.

Keywood, M., and Coauthors, 2013: Fire in the air: Biomass burning impacts in a changing climate. *Crit. Rev. Environ. Sci. Technol.,* **43,** 40–83.

Lafon, C. W., and S. M. Quiring, 2012: Relationships of fire and precipitation regimes in temperature forests of the eastern United States. *Earth Interact.,* **16,** doi:10.1175/2012EI000442.1.

Lam, Y. F., J. S. Fu, S. Wu, and L. J. Mickley, 2011: Impacts of future climate change and effects of biogenic emissions on surface ozone and particulate matter concentrations in the United States. *Atmos. Chem. Phys.,* **11,** 4789–4806, doi:10.5194/acp-11-4789-2011.

Lambert, S. J., and J. C. Fyfe, 2006: Changes in winter cyclone frequencies and strengths simulated in enhanced greenhouse warming experiments: Results from the models participating in the IPCC diagnostic exercise. *Climate Dyn.,* **26,** 713–728.

Lave, L. B., and E. P. Seskin, 1973: Air pollution and human health. *Science,* **169,** 723–733.

Leibensperger, E. M., L. J. Mickley, and D. J. Jacob, 2008: Sensitivity of US air quality to mid-latitude cyclone frequency and implications of 1980–2006 climate change. *Atmos. Chem. Phys.,* **8,** 7075–7086.

Leung, L. R., and W. I. Gustafson, 2005: Potential regional climate change and implications to U.S. air quality. *Geophys. Res. Lett.,* **32,** L16711, doi:10.1029/2005GL022911.

Li, W., L. Li, R. Fu, Y. Deng, and H. Wang, 2011: Changes to the North Atlantic subtropical high and its role in the intensification of summer rainfall variability in the southeastern United States. *J. Climate,* **24,** 1499–1506.

Mahmud, A., M. Hixson, and M. Kleeman, 2012: Quantifying population exposure to airborne particulate matter during extreme events in California due to climate change. *Atmos. Chem. Phys.,* **12,** 7453–7463.

Manders, A. M. M., E. van Meijgaard, A. C. Mues, R. Kranenburg, L. H. van Ulft, and M. Schaap, 2012: The impact of differences in large-scale circulation output from climate models on the regional modeling of ozone and PM. *Atmos. Chem. Phys.,* **12,** 9441–9458, doi:10.5194/acp-12-9441-2012.

Mickley, L. J., D. J. Jacob, B. D. Field, and D. Rind, 2004: Effects of future climate change on regional air pollution episodes in the United States. *Geophys. Res. Lett.,* **31,** L24013, doi:10.1029/2004GL021216.

Monson, R. K., and Coauthors, 2007: Isoprene emission from terrestrial ecosystems in response to global change: Minding the gap between models and observations. *Philos. Trans. Roy. Soc. London,* **A365,** 1677–1695.

Murphy, B., and S. N. Pandis, 2009: Simulating the formation of semivolatile primary and secondary organic aerosols in a regional chemical transport model. *Environ. Sci. Technol.,* **43,** 4722–4728.

NRC, 2001: *Global Air Quality: An Imperative for Long-Term Observational Strategies.* National Academy Press, 41 pp.

——, 2004: *Air Quality Management in the United States.* National Academies Press, 401 pp.

Okin, G. S., and M. C. Reheis, 2002: An ENSO predictor of dust emission in the southwestern United States. *Geophys. Res. Lett.,* **29** (9), doi:10.1029/2001GL014494.

Pacifico, F., G. A. Folberth, C. D. Jones, S. P. Harrison, and W. J. Collins, 2012: Sensitivity of biogenic isoprene emissions to past, present, and future environmental conditions and implications for atmospheric chemistry. *J. Geophys. Res.,* **117,** D22302, doi:10.1029/2012JD018276.

Park, R. J., D. J. Jacob, M. Chin, and R. V. Martin, 2003: Sources of carbonaceous aerosols over the United States and implications for natural visibility. *J. Geophys. Res.,* **108,** 4355, doi:10.1029/2002JD003190.

Pey, J., X. Querol, A. Alastuey, F. Forastiere, and M. Stafoggia, 2012: African dust outbreaks over the Mediterranean Basin during 2001–2011: PM_{10} concentrations, phenomenology and trends, and its relation with synoptic and mesoscale meteorology. *Atmos. Chem. Phys. Discuss.,* **12,** 28 195–28 235.

Pinto, J. G., U. Ulbrich, G. C. Leckebusch, T. Spangehl, M. Reyers, and S. Zacharias, 2007: Changes in storm track and cyclone activity in three SRES ensemble experiments with the ECHAM5/MPI-OM1 GCM. *Climate Dyn.,* **29,** 195–210.

Pope, C. A., III, and Coauthors, 2002: Lung Cancer, Cardiopulmonary Mortality, and Long-term Exposure to Fine Particulate Air Pollution. *J. Amer. Med. Assoc.,* **287,** 1132–1141.

——, M. Ezzati, and D. W. Dockery, 2009: Fine-particulate air pollution and life expectancy in the United States. *N. Engl. J. Med.,* **360,** 376–386.

Possell, M., and C. N. Hewitt, 2011: Isoprene emissions from plants are mediated by atmospheric CO_2 concentrations. *Global Change Biol.,* **17,** 1595–1610, doi:10.1111/j.1365-2486.2010.02306.x.

Post, E. S., and Coauthors, 2012: Variation in estimated ozone-related health impacts of climate change due to modeling choices and assumptions. *Environ. Health Perspect.,* **120,** 1559–1564, doi:10.1289/ehp.1104271.

Prospero, J. M., 1979: Mineral and sea-salt aerosol concentrations in various ocean regions. *J. Geophys. Res.,* **84** (C2), 725–731.

——, E. Bonatti, C. Schubert, and T. N. Carlson, 1970: Dust in the Caribbean atmosphere traced to an African dust storm. *Earth Planet. Sci. Lett.,* **9,** 287–293.

Pye, H. O. T., H. Liao, S. Wu, L. J. Mickley, D. J. Jacob, D. K. Henze, and J. H. Seinfeld, 2009: Effect of changes in climate and emissions on future sulfate-nitrate-ammonium aerosol levels in the United States. *J. Geophys. Res.,* **114,** D01205, doi:10.1029/2008JD010701.

Racherla, P. N., and P. J. Adams, 2006: Sensitivity of global tropospheric ozone and fine particulate matter concentrations to climate change. *J. Geophys. Res.,* **111,** D24103, doi:10.1029/2005JD006939.

Rasmussen, D. J., A. M. Fiore, V. Naik, L. W. Horowitz, S. J. McGinnis, and M. G. Schultz, 2012: Surface ozone-temperature relationships in the eastern US: A monthly climatology for evaluation chemistry-climate models. *Atmos. Environ.,* **47,** 142–153, doi:10.1016/j.atmosenv.2011.11.021.

Ravishankara, A. R., J. P. Dawson, and D. A. Winner, 2012: New directions: Adapting air quality management to climate change: A must for planning. *Atmos. Environ.,* **50,** 387–389.

Robinson, A. L., and Coauthors, 2007: Rethinking organic aerosols: Semivolatile emissions and photochemical aging. *Science,* **315,** 1259–1262.

Rosenstiel, T. N., M. J. Potosnak, K. L. Griffin, R. Fall, and R. K. Monson, 2003: Increased CO_2 uncouples growth from isoprene emission in an agriforest ecosystem. *Nature,* **421,** 256–259.

Sacks, J. D., L. W. Stanek, T. J. Luben, D. O. Johns, B. J. Buckley, J. S. Brown, and M. Ross, 2011: Particulate matter-induced health effects: Who is susceptible? *Environ. Health Perspect.,* **119,** 446–454.

Seager, R., and Coauthors, 2007: Model predictions of an imminent transition to a more arid climate in southwestern North America. *Science,* **316,** 1181–1184.

Spracklen, D. V., J. A. Logan, L. J. Mickley, R. J. Park, R. Yevich, A. L. Westerling, and D. A. Jaffe, 2007: Wildfires drive interannual variability of organic carbon aerosol in the western U.S. in summer. *Geophys. Res. Lett.,* **34,** L16816, doi:10.1029/2007GL030037.

——, L. J. Mickley, J. A. Logan, R. C. Hudman, R. Yevich, M. D. Flannigan, and A. L. Westerling, 2009: Impacts of climate change from 2000 to 2050 on wildfire activity and carbonaceous aerosol concentrations in the western United States. *J. Geophys. Res.,* **114,** D20301, doi:10.1029/2008JD010966.

Sillman, S., and P. J. Samson, 1995: Impact of temperature on oxidant photochemistry in urban, polluted rural, and remote environments. *J. Geophys. Res.,* **100** (D6), 11 497-11 508.

Sun, Z., Ü. Niinemets, K. Hüve, S. M. Noe, B. Rasulov, L. Copolovici, and V. Vislap, 2012: Enhanced isoprene emission capacity and altered light responsiveness in aspen grown under elevated atmospheric CO_2 concentration. *Global Change Biol.,* **18,** 3423–3440, doi:10.1111/j.1365-2486.2012.02789.x.

Tagaris, E., K. Manomaiphiboon, K.-J. Liao, L. R. Leung, J.-H. Woo, S. He, P. Amar, and A. G. Russell, 2007: Impacts of global climate change and emissions on regional ozone and fine particulate matter concentrations over the United States. *J. Geophys. Res.,* **112,** D14312, doi:10.1029/2006JD008262.

Tai, A. P. K., L. J. Mickley, and D. J. Jacob, 2010: Correlations between fine particulate matter ($PM_{2.5}$) and meteorological variables in the United States: Implications for the sensitivity of $PM_{2.5}$ to climate change. *Atmos. Environ.,* **44,** 3976–3984.

——, ——, ——, E. M. Leibensperger, L. Zhang, J. A. Fisher, and H. O. T. Pye, 2012: Meteorological modes of variability for fine particulate matter ($PM_{2.5}$) air quality in the United States: Implications for $PM_{2.5}$ sensitivity to climate change. *Atmos. Chem. Phys.,* **12,** 3131–3145, doi:10.5194/acp-12-3131-2012.

TF HTAP, 2011: Hemispheric transport of air pollution 2010. Part A: Ozone and particulate matter. F. Dententer, T. Keating, and H. Akimioto, Eds., Air Pollution Studies 17, United Nations Economic Commission for Europe, 304 pp.

Tsigaridis, K., and M. Kanakidou, 2007: Secondary organic aerosol importance in the future atmosphere. *Atmos. Environ.,* **41,** 4682–4692.

U.S. EPA, 2009a: Assessment of the impacts of global change on regional U.S. air quality: A synthesis of climate change impacts on ground-level ozone (an interim report of the U.S. EPA Global Change Research Program). U.S. Environmental Protection Agency Rep. EPA/600/R-07/094F, 131 pp.

——, 2009b: Endangerment and cause or contribute findings for greenhouse gases under section 202(a) of the Clean Air Act. Federal Register Docket ID EPA-HQ-OAR-2009-0171, 52 pp.

——, 2009c: Integrated science assessment for particulate matter (final report). U.S. Environmental Protection Agency EPA/600/R-08/139F, 2228 pp.

Wang, J. X. L., and J. K. Angell, 1999. Air stagnation climatology for the United States (1948–1998). NOAA/Air Resources Laboratory ATLAS 1, 73 pp.

Way, D. A., J.-P. Schnitzler, R. K. Monson, and R. B. Jackson, 2011: Enhanced isoprene-related tolerance of heat- and light-stressed photosynthesis at low, but not high, CO_2 concentrations. *Oecologia,* **166,** 273–282, doi:10.1007/s00442-011-1947-7.

Weaver, C. P., and Coauthors, 2009: A preliminary synthesis of modeled climate change impacts on U.S. regional ozone concentrations. *Bull. Amer. Meteor. Soc.,* **90,** 1843–1863.

Westerling, A. L., H. G. Hidalgo, D. R. Cayan, and T. W. Swetnam, 2006: Warming and earlier spring increase western U.S. forest wildfire activity. *Science,* **313,** 940–943.

Wiedinmyer, C., X. Tie, A. Guenther, R. Neilson, and C. Granier, 2006: Future changes in biogenic isoprene emissions: How might they affect regional and global atmospheric chemistry? *Earth Interact.,* **10,** doi:10.1175/EI174.1.

Winner, D. A., and G. R. Cass, 2001: Modeling the long-term frequency distribution of regional ozone concentrations using synthetic meteorology. *Environ. Sci. Technol.,* **35,** 3718–3726.

Wu, S., L. J. Mickley, E. M. Leibensperger, D. J. Jacob, D. Rind, and D. G. Streets, 2008: Effects of 2000–2050 global change on ozone air quality in the United States. *J. Geophys. Res.,* **113,** D06302, doi:10.1029/2007JD008917.

——, ——, J. O. Kaplan, and D. J. Jacob, 2012: Impacts of changes in land use and land cover on atmospheric chemistry and air quality over the 21st century. *Atmos. Chem. Phys.,* **12,** 1597–1609, doi:10.5194/acp-12-1597-2012.

Yue, X., L. J. Mickley, J. A. Logan, and J. O. Kaplan, 2013: Ensemble projections of wildfire activity and carbonaceous aerosol concentrations over the western United States in the mid-21st century. *Atmos. Environ.,* **77,** 767–780.

Zhu, J., and X.-Z. Liang, 2013: Impacts of the Bermuda high on regional climate and ozone over the United States. *J. Climate,* **26,** 1018–1032.

MARTIAN WINDCHILL IN TERRESTRIAL TERMS

Randall Osczevski

A two-planet model of windchill suggests that the weather on Mars is not nearly as cold as it sounds.

The groundbreaking book *The Case for Mars* (Zubrin 1996) advocates human exploration and colonization of the red planet. One of its themes is that Mars is beset by dragons of the sort that ancient mapmakers used to draw on maps in unexplored areas. The dragons of Mars are daunting logistical and safety challenges that deter human exploration. One such dragon must surely be its weather, for Mars sounds far too cold for human life.

No place on Earth experiences the low temperatures that occur every night on Mars, where even in the tropics in summer the thermometer often reads close to –90°C and, in midlatitudes in winter, as low as –120°C. The mean annual temperature of Mars is –63°C (Tillman 2009) compared to +14°C on Earth (NASA 2010). We can only try to imagine how cold the abysmally low temperatures of Mars might feel, especially when combined with high speed winds ▶

Left: The High Arctic feels at least as cold as Mars, year round (Photo by R. Osczevski 1989). Right: Twin Peaks of Mars. (Photo by NASA, Pathfinder Mission 1997)

that sometimes scour the planet. This intensely bone-chilling image of Mars could become a psychological barrier to potential colonists, as well as to public support for such ventures. Fortunately, it is an alien cold. Thermometer readings from Mars are highly misleading to terrestrials, who base their expectations of thermal comfort on their experience with low temperatures in Earth's much denser atmosphere.

A visitor to an educational National Aeronautics and Space Administration (NASA) website (NASA 1997) noted that because the atmosphere of the planet is so thin, "a –20°C temperature on Mars would not feel as cold as –20°C air on Earth." They went on to wonder what a person on Mars would feel the temperature to be and suggested that "It might be more relevant to many people to see the values shown on the website correlated to more human terms." This paper provides that missing perspective by expressing the windchill on Mars as an Earth equivalent temperature (EET). EET is the air temperature on Earth, in still air and without sunshine, that would result in the same heat transfer rate and surface temperature as the very cold but insubstantial winds of Mars.

The mathematical model used for this calculation was developed in 2001 to calculate the values in the wind chill equivalent temperature (WCET) chart for North America (Osczevski and Bluestein 2005). In terms of heat loss rate, surface temperature, and cold sensation, EET is identical to the familiar WCET that is reported each winter across much of North America. It therefore provides a familiar context for assessing the rigors of weather on another planet, in this case Mars.

While it is highly improbable that anyone would ever directly experience the weather on Mars by exposing bare skin to the virtual vacuum that passes as its atmosphere, it is also unlikely that anyone on Earth would choose to face a WCET of –60°C without proper protection. Both EET and WCET are indices of the potential cooling power of the weather, whether or not anyone actually experiences it directly. They refer to the steady state heat transfer from the upwind sides of internally heated vertical cylinders having the same diameter, internal thermal resistance, and core temperature as the human head.

AFFILIATIONS: Osczevski*—Defence Research and Development Canada, Toronto, Ontario, Canada
*Retired
CORRESPONDING AUTHOR: Randall Osczevski, 246 Plymouth Trail, Newmarket, ON L3Y 6G7, Canada
E-mail: randallo@hotmail.ca

The abstract for this article can be found in this issue, following the table of contents.
DOI:10.1175/BAMS-D-12-00158.1

In final form 7 July 2013

WINDCHILL. Air temperature alone is often a poor indicator of how cold the weather might feel. Wind, for example, makes a big difference to the thermal sensation at any temperature. The original "windchill index," invented by Siple and Passel (1946), combined the cooling effects of low temperatures and wind in a number that was proportional to the rate of heat transfer from a small plastic cylinder. (Except when referring to specific products, this paper will follow the originators, Siple and Passel, in spelling windchill as one word, much as "rainfall," "sunshine," and "frostbite" are each one word.)

The windchill index was used successfully for decades until it was "improved" by expressing the cooling power of the weather as an equivalent temperature (i.e., the air temperature that would cause the same heat transfer rate when there is no wind). Although very popular, WCET is a deceptive simplification that only seems to be easier to understand. Over the years, many authors have criticized the original WCET and the windchill index on which it was based (Molnar 1960; Eagan 1964; Steadman 1971; Kessler 1993; Osczevski 1995, 2000; Bluestein and Zecher 1999). In 2001, the calculation model was updated (Bluestein and Osczevski 2002; Osczevski and Bluestein 2005) and a new WCET chart was produced for use in weather reports in Canada and the United States.

How cold it feels outside also depends on the physical properties of the medium in which one is immersed. Many have experienced the shock of discovering that immersion in 20°C water feels much colder than being in air at the same temperature. Water carries the heat away from the body much faster than air does at the same temperature. We do not often experience this nuance of windchill on Earth because atmospheric properties do not vary greatly from place to place or from day to day, but they do from planet to planet. Earth's atmosphere, being much denser than that of Mars, is analogous to the water in the above example.

THE ATMOSPHERE OF MARS. *Composition and pressure.* The air we breathe on Earth is mostly nitrogen, with significant oxygen, a bit of argon, and trace amounts of other gases. The atmosphere of Mars is almost entirely carbon dioxide (95%). The pressure at the surface is typically less than 1% of the sea level air pressure on Earth. At the Viking 1 and 2 landing sites of the 1970s the pressure averaged 8.5 mb (Tillman 2009). At the Viking 2 site it varied with season, being about 10 mb in the Northern Hemisphere winter and 7.5 mb in the late summer. On Earth, where the mean atmospheric pressure is 1,013 mb, pressures as low as those on Mars are only encountered in the stratosphere at an altitude of 32 km (110,000 ft) (ICAO 1993). This is two-and-a-half times the altitude at which commercial airliners fly and more than three times the height of Mount Everest.

Ambient temperatures on Mars. Viking 2, which landed on Mars in 1976 at latitude 48°N, operated for over 1,000 sols (Martian days) and provided the longest and the most nearly complete record of weather conditions on Mars (Tillman 2009). Martian sols are 40 min longer than Earth days, and the solar year has 669 sols (Williams 2009). Wind and temperature data for the first 1,000 sols that Viking 2 operated are presented in Fig. 1. In summer, ambient temperatures, measured at 1.5 m above the surface, ranged from a low of –80°C at night to a comparatively balmy high of –30°C in during the day. In winter, they varied from roughly –120°C at night to –100°C during the daylight hours.

Winds on Mars. Because of the physical size of robot landers like Vikings 1 and 2, wind speeds on Mars have never been measured 10 m above the ground, as they are by convention on Earth. The Viking landers measured the wind at a height of 1.5 m, which is convenient for modeling windchill as 1.5 m is about the height of the average adult's nose.

Winds speeds can exceed 100 km h^{-1} in global dust storms and briefly in dust devils, but they are usually much lighter. Because the atmosphere of Mars is very thin, even a 100 km h^{-1} wind would hardly be noticed, no more than a breeze of 10 km h^{-1} would be noticed on Earth (Zubrin 1996). Winds stronger than 60 km h^{-1} occurred in less than 1% of the observations at the Viking 2 site (Matz et al. 1998). Over a full year, the average of the archived data (Tillman 2009) was 16 km h^{-1}. Winds stronger than 36 km h^{-1} occurred only during the fall, winter, and early spring at this site, when the average wind speed was 22 km h^{-1}. In summer, the average was 10 km h^{-1}.

HEAT TRANSFER CALCULATIONS.

Assumptions. The two-planet model assumes that the atmosphere of Mars is pure CO_2 at a constant pressure of 8.5 mb. The two hypothetical cylinders of the model are identical to those of Osczevski and Bluestein's (2005) windchill model, with the same diameter, constant internal temperature, internal thermal resistance, and emissivity. Both cylinders move into the wind at walking speed. Just what the walking speed on Mars might be (Hawkey 2005) has yet to be determined, so an average terrestrial walking speed of 1.34 m s^{-1} was used for both planets. Comparison of the Grashof number for free convection in still air or CO_2 with the Reynolds number for forced convection in the same gas confirms that on both planets, free convection at this minimum relative wind speed is only about a tenth of the forced convection and so may be neglected (Incropera and DeWitt 1996). On Mars, forced convection accounts for only about a quarter of the total heat transfer at low wind speeds. Radiation is the dominant heat transfer mechanism on Mars at low to moderate wind speeds. To calculate radiant heat transfer, the two-planet model assumes that the ground temperature on Mars is equal to the ambient temperature, which is approximately true when averaged over the whole sol. The reference condition for calculating equivalent temperature is not still "air" (CO_2) on Mars, but in still air on Earth, at night.

Physical properties of CO_2. The properties of CO_2 gas at 8.5 mb, at the extremely low temperatures found on Mars, were extracted from an online calculator (MegaWatSoft 2009) for a series of temperatures down to –55°C, which was the low temperature limit of the calculator. Trend lines were fitted to the data to develop regression equations for thermal conductivity, k; kinematic viscosity, n; and the Prandtl number, Pr (Table 1). Atmospheric properties used in the model were evaluated at the mean film

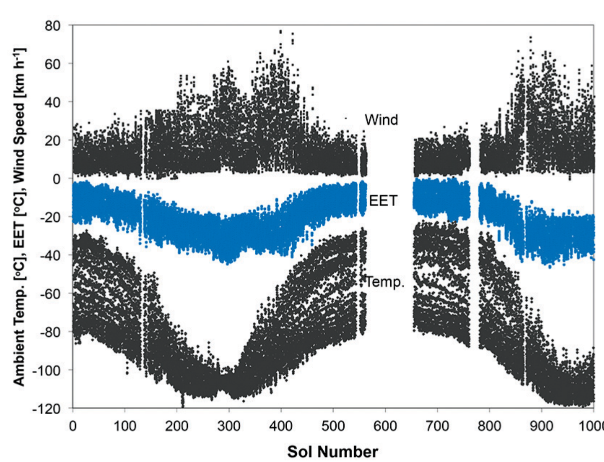

Fig. 1. Wind speeds and thermometer readings from the Viking 2 landing site on Mars (48°N), with the corresponding Earth equivalent temperatures.

temperature (i.e., the average of the cylinder surface temperature and the ambient temperature). As in 2001, an iterative method was used to find the heat transfer rate and the surface temperature of a vertical cylinder on Mars and the equivalent still air temperature on Earth.

THE COLDNESS OF MARS IN TERRESTRIAL TERMS. *A windchill chart for Mars.* Earth equivalent temperatures were calculated for a range of air temperatures and wind speeds on the planet Mars (Table 2). Note that the equivalent temperatures in each column are always higher than the thermometer reading at the head of the column—sometimes more than 100°C higher.

In Fig. 2, the windchill curves for the two planets are compared at –40°C, with winds measured at face level. At this temperature, chosen because it occurs regularly on both planets, the windchill on Mars is about 50°C warmer than the windchill calculated for the same wind speed and air temperature on Earth. According to the 2001 model of windchill on Earth, at –40°C with no wind other than the relative motion of the cylinder as it moves through still air at walking speed (WCET = –40°C), the surface temperature of the cylinder (or cheek skin temperature) would be –12°C. The risk of frostbite exceeds 5% whenever the skin temperature is below –4.8°C (Danielsson 1996). Thus, there is a significant risk of frostbite at –40°C on Earth even when there is no wind. On both planets, a cylinder surface temperature of –4.8°C is reached at an equivalent temperature of –27°C. On Mars at –40°C, the cylinder surface temperature will often be well above Danielsson's critical skin temperature. Even with a wind speed of 100 km h^{-1}, when EET is –20°C, the calculated cylinder surface temperature is just 0°C.

–20° on Mars. We can now answer the question of what an ambient temperature of –20°C might feel like on Mars. Without wind, it should feel much like +2°C does on Earth in still air. With a 100 km h^{-1} wind, –20°C should only feel as cold as it does on Earth when the WCET is –9°C.

Viking 2 weather. For convenience, an approximate equation was derived from the output of the model to calculate EET from wind speed and air temperature.

Table 1. Regression equations for physical properties of CO_2 at subzero temperatures and a pressure of 8.5 mb. Derived from data from MegaWatSoft (2009). Here, T is the mean film temperature.

Property	Regression equation
Thermal conductivity (W m^{-1} K^{-1})	$k = 1.1691 \times 10^{-7} T^2 + 1.3327 \times 10^{-5} T + 2.2469 \times 10^{-3}$ (T in °K)
Kinematic viscosity (m^2 s^{-1})	$\nu = 1.0486 \times 10^{-8} T^2 + 3.1687 \times 10^{-7} T - 3.6613 \times 10^{-5}$ (T in °K)
Prandtl number	$Pr = -3.344 \times 10^{-6} T^2 - 3.062 \times 10^{-4} T + 0.7665$ (T in °C)

Table 2. Earth equivalent temperatures for Mars (°C).

Mars wind speed (km h^{-1})	Mars wind speed (m s^{-1})	Mars ambient temperature (°C): 0	–10	–20	–30	–40	–50	–60	–80	–100	–120
0	0.0	8	5	2	–1	–3	–6	–8	–12	–15	–18
10	2.8	7	3	–1	–4	–7	–10	–13	–19	–23	–28
20	5.6	6	2	–2	–6	–10	–13	–17	–23	–29	–34
30	8.3	5	1	–3	–8	–12	–15	–19	–26	–33	–39
40	11	5	0	–4	–9	–13	–17	–21	–29	–36	–43
50	14	4	–1	–5	–10	–15	–19	–23	–31	–39	–46*
60	17	4	–1	–6	–11	–16	–20	–25	–33	–41	–49*
70	19	4	–2	–7	–12	–17	–22	–26	–35	–44	–52*
80	22	3	–2	–8	–13	–18	–23	–28	–37	–46*	–54*
90	25	3	–3	–8	–14	–19	–24	–29	–39	–48*	–56*
100	28	3	–3	–9	–14	–20	–25	–30	–40	–49*	–59*

* Extrapolated beyond the available data for the low temperature properties of CO_2 gas at 8.5 mb.

The equation and the model agree within 0.4°C over a very wide range. Twenty-five "hourly" EET values were calculated for each of the first 1,000 sols of Viking 2 data. These values constitute the middle curve of Fig. 1. The upper and lower curves are the measured wind speeds and ambient temperatures, respectively. The calculated equivalent temperatures are much higher than the thermometer readings—75°C higher during the coldest part of the year with average winds. EET minimums for the first 1,000 sols ranged from –20°C in midsummer to –45°C in midwinter; maximum values ranged from 0°C in midsummer to –20°C in midwinter. The mean daily EET in winter was approximately –30°C.

Typical Mars summer weather. Viking 2 sol 100 appears to have been an unremarkable summer sol. It had an average temperature of –60°C and average wind speed of 9.6 km h^{-1}. During the daylight hours, EET reached –7°C. The mean for the sol was –13°C. Most summer sols were unremarkable. At any hour the temperature was almost the same as it had been the day before at that same hour—slightly warmer as solstice approached and slightly cooler afterward.

Inland areas on Earth have an average wind speed of 14 km h^{-1} (NASA 2004). In order that the WCET be –13°C with an average wind, the air temperature need only be –7°C. That is, at –60°C, the tenuous winds of Mars should feel about as cold as winds usually do on Earth when the air temperature is –7°C (+19°F). Many people thrive on this planet in such conditions during winter.

A typical winter day on Mars. According to the two-planet model, at –100°C on Mars, with an average Viking 2 winter wind of 22 km h^{-1}, the EET is –29°C. On Earth, with an average terrestrial wind, a WCET of –29°C occurs when the air temperature is –20°C. This temperature is typical of winter lows in midlatitude areas of Earth with continental climates.

COMPARING THE WEATHER ON MARS AND EARTH. *Example 1: Minneapolis/St. Paul, United States, 45°N.* Three million people live in the metropolitan area of Minneapolis/St. Paul, a midlatitude urban area with a continental climate. The average winter (December, January, February) temperature is –8.1°C (14°F) and the average winter wind speed is 16.5 km h^{-1} (University of Minnesota 2005). These combine to produce an average WCET of –15°C. Mars, with a mean annual EET of –16°C, is only a degree colder on average than the "Twin Cities" in winter.

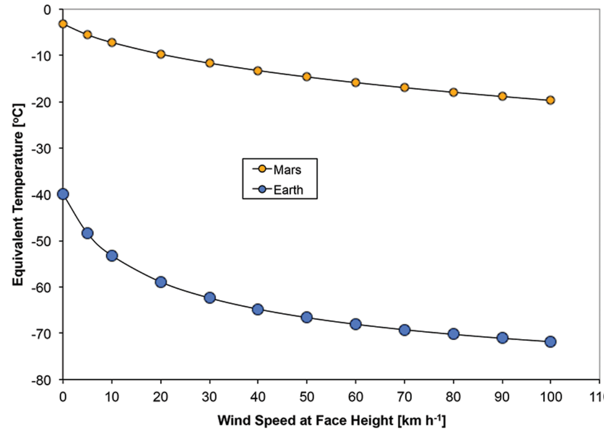

Fig. 2. Equivalent temperatures on Mars and on Earth at –40°C with winds at 1.5 m.

Example 2: Resolute, Canada, 75°N. Approximately 250 people live in the hamlet of Resolute, which is not far from the Haughton-Mars Project research station. The average annual temperature at Resolute is –16°C and the average wind speed is 20 km h^{-1} (Environment Canada 2012). The annual average WCET is therefore –25°C, which is 9°C colder than the mean annual EET of Mars. In summer, the average WCET at Resolute is –12°C, much like a typical summer day in the midlatitudes of Mars, except that the sun does not set.

During winter, the air temperature at Resolute averages –32°C, and the average WCET is –45°C. The latter is 15°C colder than the average EET during winter at the Viking 2 site on Mars and is close to the record low EET for this site. The lowest temperature ever recorded in Resolute was –52.2°C and the lowest WCET was –72°C (–98°F). For comparison, the lowest EET for the Viking 2 site on Mars is just –46°C, while the record low WCET for Minneapolis/St. Paul is a cool –55°C (–67°F).

In shade or heavy overcast, summer in the High Arctic probably feels much like a summer sol in the midlatitudes of the Northern Hemisphere of Mars. However, when the temperature drops after sunset on Mars, its weather probably feels colder than the High Arctic does in the continuous daylight of summer. In winter, the weather on Mars will generally feel more comfortable than the challenging, dark winter typical of Earth's High Arctic—more comfortable but, as Lowell (1908) put it, still having "a polar complexion to it not wholly pleasing to contemplate."

Example 3: The south of England. In 1907, American astronomer Percival Lowell calculated a mean global temperature for Mars of +8°C (Lowell 1907)—warm enough for liquid water to flow in the network of canals that he and other astronomers thought they could see on its surface. Wallace (1907) challenged Lowell's calculation and pointed out that an average temperature of +8°C was "almost exactly the same as that of mild and equable southern England," which he thought was impossible for a planet so far from the sun. He noted that in 1904 J. H. Poynting had calculated the average temperature of Mars to be –38°C (Wallace 1907).

To Lowell, the canals were evidence that a race of intelligent beings inhabited Mars and had probably constructed the canals to convey meltwater from the seasonally melting polar caps to arable land at lower latitudes in response to catastrophic global climate change (Lowell 1908). For ice to melt and water to flow, the temperatures on Mars had to be much higher than Poynting's estimate.

"Canals" continued to be observed, discussed, and drawn on authoritative maps of Mars for at least another half-century (e.g., NASA 1962). However, as we now know, they were an illusion. Wallace was correct; Mars is much colder than Lowell hoped, and colder still than Poynting thought.

Decades later, Carl Sagan (Sagan 1985) confused the issue when he commented that Lowell had imagined the Martian temperatures "a little on the chilly side, but still as comfortable as the 'South of England.'" Sagan did not say who he was quoting, but since Lowell does not seem to have mentioned either England or comfort in connection with the temperature of Mars, it could not have been him. Whatever its origins, the seemingly implausible notion that Mars might ever be as "comfortable" as the South of England can now be tested.

In December, January, and February, the mean temperature of a large area of southern England, one degree of longitude wide and one degree of latitude high, centered on 51.5°N, 1.5°W (approximately midway between London and Bristol) is +4.4°C, which is 67°C higher than the mean temperature of Mars. However, temperature is only one factor in thermal comfort. The average wind speed during this period is 23 km h^{-1} (NASA 2004). The average WCET in south England in winter is therefore 0°C, which is 16°C warmer than the average EET of Mars. On average then, south England is much more comfortable for humans than Mars—but perhaps not always.

If we compare the summer conditions on Mars to winter in south England, there is some similarity. At the Pathfinder landing site at 19°N latitude, the mean daily high temperature in early summer was –14°C (Tillman 2009). A typical wind speed at this location was 14 km h^{-1}. EET calculated for this combination of wind speed and temperature is +1°C, which is one degree warmer than the mean winter WCET of south England. Thus, in midafternoon in summer, the tropics of Mars were about as comfortable as an average winter day in south England. Even much farther north at the Viking 2 site, the EET in summer equaled the average winter WCET of south England on several occasions (Fig. 1).

Mars receives much less heat from the sun than Earth does because it is much farther away from it. The irradiance at the top of the atmosphere of Mars averages 590 W m^{-2}, which is 43% of the irradiance in Earth orbit (Matz et al. 1998). In the south of England, cloud cover in winter averages 70%, so bright sunshine is not the norm, but on Mars, it is.

In the area of south England defined earlier, the radiation incident on a horizontal surface at midday during December, January, and February averages just 150 W m^{-2} (NASA 2004). At the same latitude in the summer hemisphere of Mars, the solar load can exceed 500 W m^{-2} at midday, even when there is dust in the air (Justus Duvall and Johnson 2003). With the same geometry, the solar heat absorbed by the cylinder on Mars is likely to be about three times what it would be at midday in winter in cloudy south England. This difference in solar heating increases the likelihood that some regions of Mars might be as comfortable as the south of England in winter.

DISCUSSION. ***Radiant heat transfer to the sky and ground.*** The model assumes that the sky temperature on Mars is constant at –110°C and that ground temperature is equal to air temperature. On both planets, ground temperatures often differ significantly from the temperature of the atmosphere a meter or so above it, depending on the time of day, wind speed, and solar radiation. On Mars, ground temperature departures from ambient temperature are largest in the afternoon, when they can be 25°C warmer than ambient temperature (Matz et al. 1998). To see what effect this might have on calculated values of EET, the ground temperature in the Mars portion of the model was first set to 25°C above an ambient temperature of –60°C and then to 25°C below it. EET differed by less than 3°C from the value in Table 2 at any wind speed.

The constant sky temperature of –110°C is the average of the summer and winter daily maximum and minimum values of sky temperature taken from in Fig. 3 of Matz et al. (1998); thus, it is an estimate of the annual average sky temperature at 22°N latitude (Viking 1 landing site) in both clear and dusty skies. It is thought to vary by ±10°C during the daylight hours (Matz et al. 1998), and to be as high as –70°C during dust storms (Justus Duvall and Johnson 2003). When a sky temperature of –70°C was used in the model instead of –110°C, with an ambient temperature of –60°C, EET was less than 3°C warmer at any wind speed.

The radiant heat transfer to the sky (and ground) is proportional to the difference between the fourth powers of the cylinder surface temperature and the sky (or ground) temperature. At absolute zero there is no radiant heat from the sky. It increases slowly at first as sky temperature warms. Even at a sky temperature of –70°C, sky radiation received at the vertical surface of the cylinder is small compared to the total heat transferred from it when its temperature is around 0°C. Thus, on Mars, the net radiant heat transfer from the cylinder to the sky is relatively insensitive to errors in sky temperature. This is also why excursions in ground temperature do not have a large effect on radiant heat transfer and EET. The potential errors incurred by assuming that the ground temperature equals the ambient temperature, and that the sky temperature is a constant –110°C, seem acceptable for the limited purposes of this study.

Solar heating on Earth and on Mars. To see if solar heating might be more effective on Mars a small amount of external heat (10 W m^{-2}) was mathematically added to the vertical surfaces of the cylinders in both the 2001 terrestrial model and the new two-planet model. Air temperatures in this experiment were set at –40°C. No extra heat was added in either reference still air condition. The cylinders were mathematically exposed to the same wind speeds at cylinder level.

Over a wide range of wind speeds, the average increase in the calculated equivalent temperature due to the extra heating was 2.8 times as great on "Mars" as it was on "Earth" (Fig. 3). Thus, the lower irradiance at the orbit of Mars might be completely offset by the greater heating effectiveness of sunshine in the thin Martian atmosphere (i.e., 2.8 × 43% > 100%). On Earth, bright sunshine is thought to add about 10°C to the WCET in average winds (Environment Canada 2012). On Mars, sunshine should add at least that much, significantly enhancing the thermal comfort of individuals during daylight hours.

Internal thermal resistance. WCET and EET are not calculated for the average person, but for those most susceptible to facial cooling and frostbite. If windchill equivalent temperatures on both planets were calculated for the average person, the windchill on Mars might sound even less frightening.

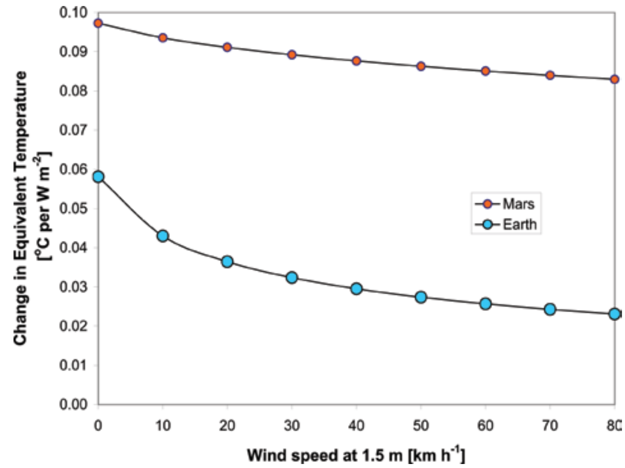

Fig. 3. The influence of absorbed solar radiation on equivalent temperatures at –40°C calculated with the two-planet model (Mars) and the 2001 WCET model (Earth).

Changing the internal thermal resistance of the cylinders used in the 2001 terrestrial WCET model from the 95th percentile value to the 50th percentile value (Ducharme et al. 2002) shifts the WCET for any given wind and temperature combination on Earth a few degrees lower (Osczevski and Bluestein 2005). That is, it makes Earth windchill sound colder, but any given WCET would now feel warmer to everyone than it did prior to that change.

Making the same changes to the internal resistances of the cylinders of the two-planet model shifts EET a degree or two higher, making Mars sound warmer than Table 2 now suggests. Not only would the number increase, but the WCET it equated to would feel warmer than it does now.

Cylinder emissivity, EET, and heat balance. Changing the surface emissivity of the model cylinder on Mars has an interesting effect on EET. The model assumes that its emissivity is 1, which is close to the emissivity of skin, many plastics, and most fabrics. An emissivity of 0.2 could be easily attained with a clean metal surface. Using an emissivity of 0.2 increases the calculated value of EET at –60°C by a whopping 27°C with no wind and by 17°C with a wind speed of 100 km h^{-1}.

On Earth, where convection dominates, the popular wisdom is to dress in layers so that clothing can be added or removed to maintain comfortable skin temperatures when activity level or ambient temperature changes. Because radiant heat transfer is the dominant heat transfer mechanism on Mars, significant adjustments to heat balance might be conveniently accomplished by varying the emissivity of the outer surface of the pressure suit or of some garment worn over it.

CONCLUSIONS. The tenuous winds of Mars are clearly far less challenging than those we face on Earth. Because of its thin atmosphere, Mars should prove to be much warmer for people than it is for thermometers. Those of us who live where the winter is colder than the winter in south England regularly experience weather that feels colder than the midlatitudes of Mars during the afternoon of an average summer sol. This includes much of Asia, North America, and northern Europe. Some sparsely populated frontier areas of Earth feel at least as cold as much of Mars does, year round.

Regardless of how one regards the thermal comfort of winter in England, or of summer in Resolute, they suggest a much improved prospect for summer on Mars than the one rendered up to now by raw temperature readings transmitted from its surface. The image of winter on Mars has also been enhanced, for it is not as fiercely cold as spacecraft weather reports have made it seem, but might actually seem warmer than the winter in some frontier areas of our home planet.

There may very well be good reasons why Mars is not suited for humans, but extremely cold air is not one of them. Mars simply does not have enough of it to be an insurmountable problem. Scratch one dragon.

ACKNOWLEDGMENTS. Defence Research and Development Canada provided financial support for the publication of this paper. Some solar and meteorological data were obtained from the NASA Langley Research Center Atmospheric Science Data Center. Also, my thanks go to David Phillips, Senior Climatologist at Environment Canada, for wondering if I could tell him what the windchill was on Mars.

REFERENCES

Bluestein, M., and J. Zecher, 1999: A new approach to an accurate wind chill factor. *Bull. Amer. Meteor. Soc.,* **80,** 1893–1899.

——, and R. Osczevski, 2002: The basis for the new wind chill temperature chart. Preprints, *15th Conf. on Biometeorology/Aerobiology and 16th Int. Congress of Biometeorology,* Kansas City, KS, Amer. Meteor. Soc., 6B.1. [Available online at https://ams.confex.com/ams/15BioAero/techprogram/paper_48428.htm.]

Danielsson, U., 1996: Windchill and the risk of tissue freezing. *J. Appl. Physiol.,* **81,** 2666–2673.

Ducharme, M., D. Brajkovic, R. Osczevski, and P. Tikuisis, cited 2002: Skin temperature, heat loss and thermal resistance of the cheek during exposure to cold winds. [Available online at https://ams.confex.com/ams/15BioAero/techprogram/paper_59025.htm.]

Eagan, C., 1964: The effect of air movement on atmospheric cooling power. Review of research on military problems in cold regions, Arctic Aeromedical Laboratory Tech. Doc. Rep. AAL-TDR-64-28, 147–156. [Available online at www.dtic.mil/dtic/tr/fulltext/u2/457733.pdf.]

Environment Canada, cited 2012: Climate normals and averages. [Available online at www.climate.weatheroffice.gc.ca/climate_normals/index_e.html.]

Hawkey, A., 2005: Physiological and biomechanical considerations for a human Mars mission. *J. Br. Interplanet. Soc.,* **58** (3–4), 117–130.

ICAO, 1993: *Manual of the ICAO Standard Atmosphere: Extended to 80 Kilometres (262 500 Feet).* 3rd ed. International Civil Aviation Organization, 304 pp.

Incropera, F., and D. DeWitt, 1996: *Fundamentals of Heat and Mass Transfer.* 4th ed. John Wiley and Sons, 487 pp.

Justus, C., A. Duvall, and D. Johnson, 2003: Mars Global Reference Atmospheric Model (Mars-GRAM) and database for mission design. *Extended Abstracts, Int. Workshop: Mars Atmosphere Modeling and Observations,* Granada, Spain. [Available online at www-mars.lmd.jussieu.fr/granada2003/abstract/justus.pdf.]

Kessler, E., 1993: Wind chill errors. *Bull. Amer. Meteor. Soc.,* **74,** 1743–1744.

Lowell, P., 1907: A general method for evaluating the surface-temperature of the planets; with special reference to the temperature of Mars. *Philos. Mag. Ser. 6,* **14,** 161–176.

——, 1908: *Mars as the Abode of Life.* The MacMillan Company, 322 pp.

Matz, E., J. Appelbaum, and Y. Taitel, 1998: Solar cell temperature on Mars. *J. Propul. Power,* **14,** 119–125.

MegaWatSoft, cited 2009: Carbon dioxide tables. [Available online at www.carbon-dioxide-properties.com/CO2TablesWeb.aspx.]

Molnar, G., 1960: An evaluation of wind chill. *Proc. Sixth Conf. of Cold Injury,* New York, NY, Josiah Macy Foundation, 175–221.

NASA 1962: Lunar and planetary sciences in space exploration. NASA SP-14, 84 pp.

——, cited 1997: Wind chill on Mars. [Available online at http://quest.arc.nasa.gov/mars/ask/weather/Wind_chill_on_Mars.txt.]

——, cited 2004: Surface meteorology and solar energy—Available tables. [Available online at http://eosweb.larc.nasa.gov/cgi-bin/sse/grid.cgi?uid=3030.]

——, cited 2010: NASA Earth Observatory. [Available online at www.earthobservatory.nasa.gov/Features/WorldOfChange/decadaltemp.php.]

Osczevski, R., 1995: The basis of wind chill. *Arctic,* **48,** 372–382. [Available online at http://pubs.aina.ucalgary.ca/arctic/Arctic48-4-372.pdf.]

——, 2000: Windward cooling: An overlooked factor in the calculation of wind chill. *Bull. Amer. Meteor. Soc.,* **81,** 2975–2978.

——, and M. Bluestein, 2005: The new wind chill equivalent temperature chart. *Bull. Amer. Meteor. Soc.,* **86,** 1453–1458.

Sagan, C., 1985: *Cosmos.* Random House, 324 pp.

Siple, P., and C. Passel, 1946: Measurements of dry atmospheric cooling in subfreezing temperatures. *Proc. Amer. Philos. Soc.,* **89,** 177–199.

Steadman, R., 1971: Indices of wind chill of clothed persons. *J. Appl. Meteor.,* **10,** 674–683.

Tillman, J., cited 2009: Mars temperature overview. [Available online at http://www-k12.atmos.washington.edu/k12/resources/mars_data-information/data.html.]

University of Minnesota, cited 2005: Normals, means, and extremes. [Available online at http://climate.umn.edu/pdf/normals_means_and_extremes/2005_Annual_LCD_MSP_page_3.pdf.]

Wallace, A. R., 1907: *Is Mars Habitable? A Critical Examination of Professor Percival Lowell's Book "Mars and Its Canals," with Alternative Explanation.* Macmillan & Co., 110 pp. [Available online at www.gutenberg.org/catalog/world/readfile?fk_files=46299&pageno=33.]

Williams, D., cited 2009: Mars fact sheet. [Available online http://nssdc.gsfc.nasa.gov/planetary/factsheet/marsfact.html.]

Zubrin, R., 1996: *The Case for Mars.* The Free Press, 352 pp.

LIDAR-MEASURED WIND PROFILES

The Missing Link in the Global Observing System

BY WAYMAN E. BAKER, ROBERT ATLAS, CARLA CARDINALI, AMY CLEMENT, GEORGE D. EMMITT, BRUCE M. GENTRY, R. MICHAEL HARDESTY, ERLAND KÄLLÉN, MICHAEL J. KAVAYA, ROLF LANGLAND, ZAIZHONG MA, MICHIKO MASUTANI, WILL MCCARTY, R. BRADLEY PIERCE, ZHAOXIA PU, LARS PETER RIISHOJGAARD, JAMES RYAN, SARA TUCKER, MARTIN WEISSMANN, AND JAMES G. YOE

Doppler lidar technology has advanced to the point where wind measurements can be made with confidence from space, thus filling a major gap in the global observing system.

The purpose of this paper is to document the advances in our understanding of the need for global wind measurements since our earlier paper (Baker et al. 1995), to summarize recent results from airborne wind measurement campaigns and OSSEs, and to discuss the technology advances that now make a space-based Doppler wind lidar (DWL) feasible.

Measurement of the three-dimensional global wind field is the final frontier that must be crossed to significantly improve the initial conditions for numerical weather forecasts. The World Meteorological Organization determined that global wind profiles are "essential for operational weather forecasting on all scales and at all latitudes." (WMO 1996, chapter 13, p. 295) This is because the wind field plays a unique dynamical role in forcing the mass field to adjust to it at all scales in the tropics, and at small scales in the extratropics (Baker et al. 1995). Wind profiles are also needed to depict vertical wind shear structures that are underrepresented in global NWP models (Houchi et al. 2010). Furthermore, the National Research Council (NRC) decadal survey

AFFILIATIONS: BAKER*—NOAA, McHenry, Maryland; ATLAS—NOAA/Atlantic Oceanographic and Meteorological Laboratory, Miami, Florida; CARDINALI AND KÄLLÉN—European Centre for Medium-Range Weather Forecasts, Reading, United Kingdom; CLEMENT—University of Miami, Miami, Florida; EMMITT—Simpson Weather Associates, Charlottesville, Virginia; GENTRY AND MCCARTY—NASA Goddard Space Flight Center, Greenbelt, Maryland; HARDESTY—Cooperative Institute for Research in Environmental Sciences, University of Colorado at Boulder, Boulder, Colorado; KAVAYA—NASA Langley Research Center, Hampton, Virginia; LANGLAND—Naval Research Laboratory, Monterey, California; RIISHOJGAARD—World Meteorological Organization, Geneva, Switzerland; MA AND YOE—Joint Center for Satellite Data Assimilation, College Park, Maryland; MASUTANI—NOAA/Environmental Modeling Center, College Park, Maryland; PIERCE—NOAA/National Environmental Satellite, Data, and Information Service, Madison, Wisconsin; PU—University of Utah, Salt Lake City, Utah; RYAN—University of New Hampshire, Durham, New Hampshire; TUCKER—Ball Aerospace and Technologies Corp., Boulder, Colorado; WEISSMANN—Hans-Ertel-Centre for Weather Research, Ludwig-Maximilians-Universität München, Munich, Germany
* Retired
CORRESPONDING AUTHOR: Dr. Wayman E. Baker, 253 Gleanings Drive, McHenry, MD 21541
E-mail: wayman.baker@gmail.com

The abstract for this article can be found in this issue, following the table of contents.
DOI:10.1175/BAMS-D-12-00164.1

A supplement to this article is available online (10.1175/BAMS-D-12-00164.2)

In final form 27 August 2013

report on *Earth Science and Applications from Space* (NRC 2007) recommended a global wind mission, and the NRC Weather Panel, in the same report, determined that a DWL in low-Earth orbit (LEO) could make a *transformational* impact on global tropospheric and stratospheric analyses. More recently, a WMO (2012b) workshop found the current global observing systems to be heavily skewed toward measuring atmospheric mass rather than wind, especially for the satellite instruments, even though the average influence of wind observations is higher, on both an individual instrument and a "per observation" basis. The workshop final report further stated, "There is a need to invest in enhanced wind observations in the tropics and over the oceans especially. . . . Development of satellite-based wind-profiling systems remains a priority for the future global observing system" (WMO 2012b, p. 9) In addition, the WMO Rolling Review of Requirements, updated in May 2012, states that "wind profiles at all levels outside the main populated areas" is the highest measurement priority (WMO 2012a, p. 8).

Accurate measurements of the global wind field will also support major advances in the understanding of several key climate change issues. Several studies have suggested that the general circulation of the atmosphere varies considerably on decadal time scales and that some of this variation may be due to greenhouse gas forcing (Chen et al. 2002; Mitas and Clement 2005, 2006; Vecchi et al. 2006). Each of these studies, however, relies on climate models and datasets that provide an incomplete picture of large-scale circulation changes.

Moreover, there is an urgent need to improve the accuracy of horizontal and vertical transport estimates for climate applications. For example, recent studies (Graversen 2006; Graversen et al. 2008) indicate that the dramatic reduction in sea ice extent observed in the Arctic may be partly due to systematic changes to heat transport into the Arctic. In addition, Yang et al. (2010) found that about 50% of the recent Arctic warming in the free troposphere is due to increased poleward energy transport. However, these findings are based on reanalysis wind data with large uncertainties in the Arctic for the zonally averaged, meridional wind component.

Large areas of the tropical atmosphere are devoid of measured wind profiles. This suggests the potential for a large improvement in forecast skill for a variety of tropical phenomena, including tropical cyclones, monsoonal circulations, and the African easterly jet, especially given the dominance of the wind field in the mass–motion balance relationship (Baker et al. 1995; Žagar et al. 2008).

The scientific evidence thus supports the notion of a clear imbalance in the current global observing system as noted above (WMO 2012b). A comparison of atmospheric mass field measurements coverage by satellites in LEO versus the coverage of the radiosonde network is striking. The radiosonde

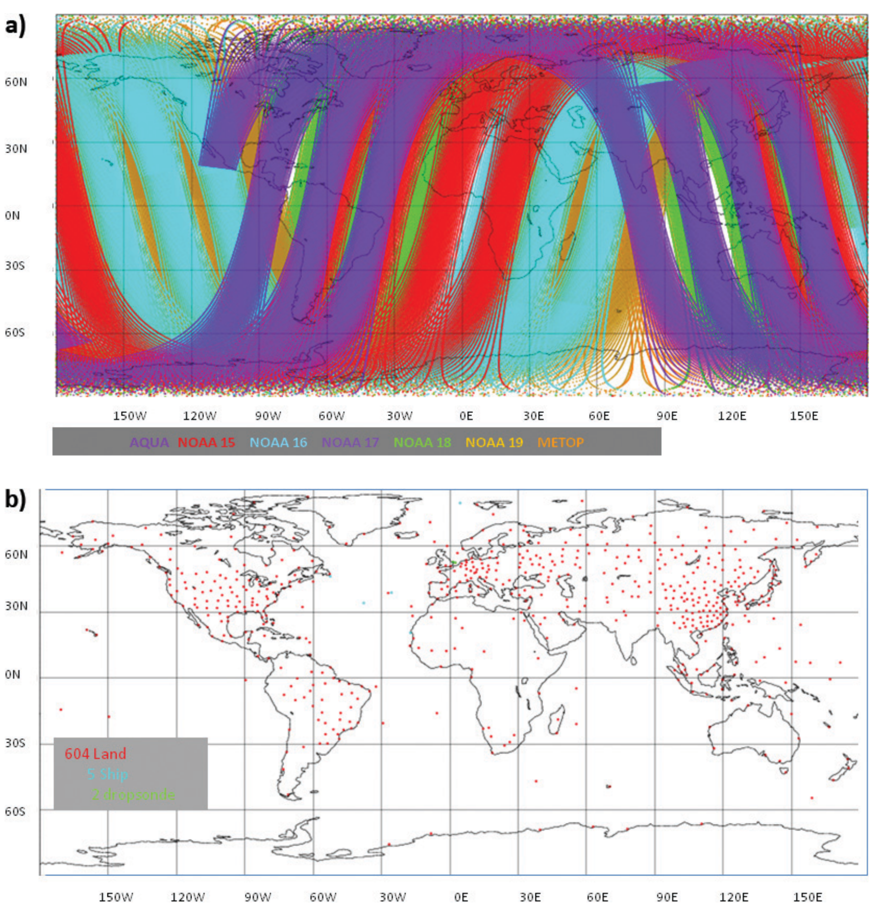

Fig. 1. Depicted is (a) the current upper-air AMSU-measured mass and (b) the 1200 UTC radiosonde-measured wind observational coverage. Maps provided by ECMWF.

network, which is primarily land based, remains the primary source of global wind profiles. While single-level wind measurements obtained from aircraft, by tracking cloud or water vapor features from scatterometers, etc., are important components of the global observing system, additional wind profiles are needed, especially over the oceans and remote land areas to depict vertical wind shear structures as noted above (Houchi et al. 2010).

Figure 1 illustrates the measurement imbalance between the mass and wind fields by comparing the coverage of seven Advanced Microwave Sounding Units (AMSUs) and the 1200 UTC radiosonde locations where wind profiles are provided, typically twice per day (once per day over some parts of South America and Australia). In addition to AMSU coverage, global mass data are also provided by three hyperspectral sounders [the National Aeronautics and Space Administration (NASA) Atmospheric Infrared Sounder (AIRS), the European Organisation for the Exploitation of Meteorological Satellites (EUMETSAT) Infrared Atmospheric Sounding Interferometer (IASI), and the *Suomi National Polar-Orbiting Partnership* (*NPP*) satellite Cross-Track Infrared Sounder (CrIS)]. Satellite temperature profiles are also obtained via the Taiwan–United States Constellation Observing System for Meteorology, Ionosphere and Climate (COSMIC; Anthes et al. 2008).

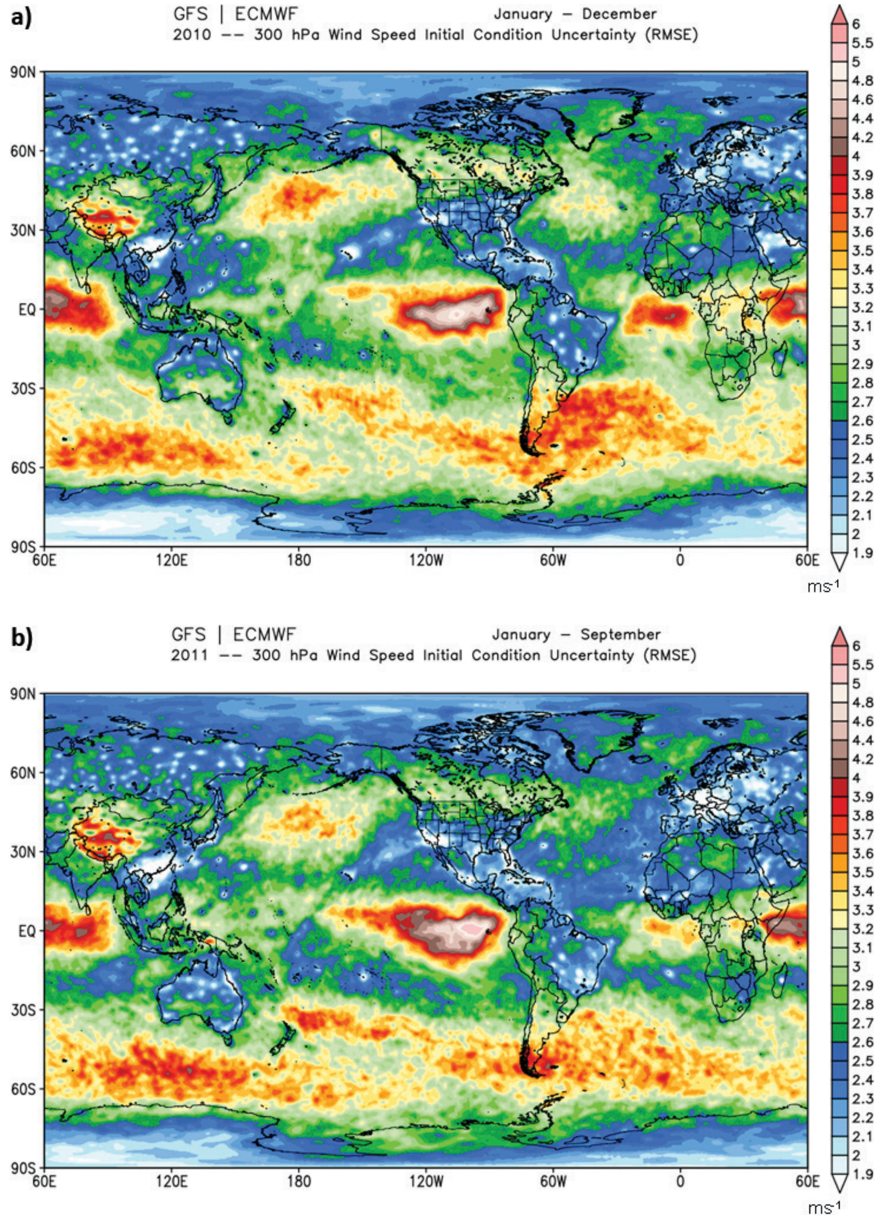

Fig. 2. Depicted are the RMS differences (m s^{-1}) in 300-hPa wind speed analyses produced by ECMWF and the NCEP GFS: (a) Jan–Dec 2010 and (b) Jan–Sep 2011. Includes all daily analyses provided at 0000 and 1200 UTC. This quantity is a proxy for actual analysis error, which cannot be directly quantified. Note that the influence of individual radiosonde stations appears in many areas (Russia, Australia, Brazil, and oceanic islands) as localized regions of reduced analysis difference. Effect of aircraft observations can also be seen [e.g., along the flight corridor between Hawaii and the West Coast (Langland and Maue 2012)].

One measure of the uncertainty of atmospheric analyses is the difference between analyses produced by various operational data assimilation systems, such as those at the European Centre for Medium-Range Weather Forecasts (ECMWF) and National Centers for Environmental Prediction (NCEP). These analysis differences are estimates of actual analysis error, which cannot be directly quantified because the true atmospheric state at any given time is unknown. We show results obtained as multimonth averages during 2010 (Fig. 2a) and 2011 (Fig. 2b) in o rder to demonstrate that the basic pattern of these differences is quite robust from year to year, which implies a strong dependence of analysis error on the components and quality of the global observing system. The basic global pattern of analysis differences can be modulated to some extent by year-to-year and seasonal variability in atmospheric circulation, as seen by comparing Figs. 2a,b.

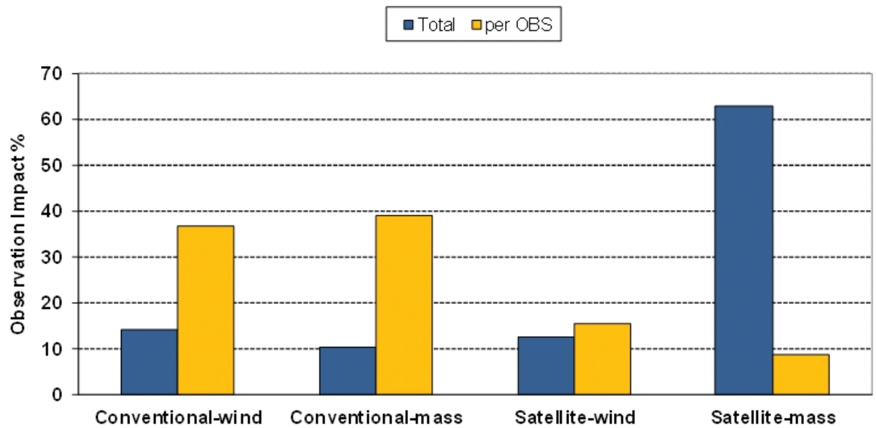

Fig. 3. The contribution of mass vs wind observations in reducing the 24-h forecast error, expressed as observation impact (%), in terms of the total number of observations and on a per-observation basis for the ECMWF data assimilation system.

In regions such as Europe, the United States, and East Asia that are well covered by radiosonde, aircraft, and land surface observations, the differences between ECMWF and NCEP analyses of upper-tropospheric winds (Figs. 2a,b) are relatively small, with correspondingly small analysis uncertainty. Similar patterns exist in the lower troposphere for variables such as temperature and geopotential height (Langland et al. 2008). In contrast, in regions where atmospheric analyses rely primarily on satellite radiance data, there tend to be larger differences between the various analyses of wind, temperature, and height, indicative of larger analysis uncertainties. For example, in Figs. 2a,b there is larger uncertainty in the analyzed 300-hPa wind speed over much of the tropics, southern midlatitudes, and North Pacific basin. Wind observations from geostationary satellite imagery reduce analysis uncertainty but not to the same extent as do observations from radiosondes. Note that analysis uncertainty is smaller over the North Atlantic than over the North Pacific due to more numerous aircraft observations. Analysis differences in polar regions are also generally somewhat smaller due to the prevailing wind–mass balance and the availability of Moderate Resolution Imaging Spectroradiometer (MODIS) and Advanced Very High Resolution Radiometer (AVHRR) wind observations (Key et al. 2003).

IMPACT OF GLOBAL WIND PROFILES ON WEATHER FORECASTING AND CLIMATE RESEARCH.

NWP. Forecast sensitivity to observations. The relative impact of various types of measurements on the quality of atmospheric analyses can be estimated by the so-called forecast sensitivity to observations (FSO), developed by Baker (2000). The FSO technique has been used extensively to assess the sensitivity of forecast errors to different components of the global observing system (Baker and Langland 2008, 2009; Cardinali 2009; Gelaro et al. 2010; Langland and Baker 2004; Ota et al. 2013). This approach can also be used to assess the relative influence of mass and wind field observations on short-range forecast errors.

In Fig. 3 (Källén et al. 2010), the forecast error impact is given for the total number of observations of each type, as well as the error contribution per observation for the ECMWF data assimilation system. As may be seen in Fig. 3, the conventional observing system is well balanced in terms of mass and wind observations, while the satellite observing system is dominated by mass observations. If, however, the impact factor is divided by the number of observations, the individual space-based wind observations are more influential than the space-based mass observations. This evidence is further confirmation that the space-based observing system is unbalanced in terms of the total number of mass and wind observations, as discussed above, but the available wind observations still have a large impact on forecast quality.

OSSEs. An extensive series of global observing system simulation experiments (OSSEs) has been conducted since the mid-1980s to determine the potential influence of wind profile observations from space and to evaluate trade-offs in the design of a space-based wind lidar. These early experiments showed the great potential for space-based wind profile observations reducing analysis errors and improving numerical

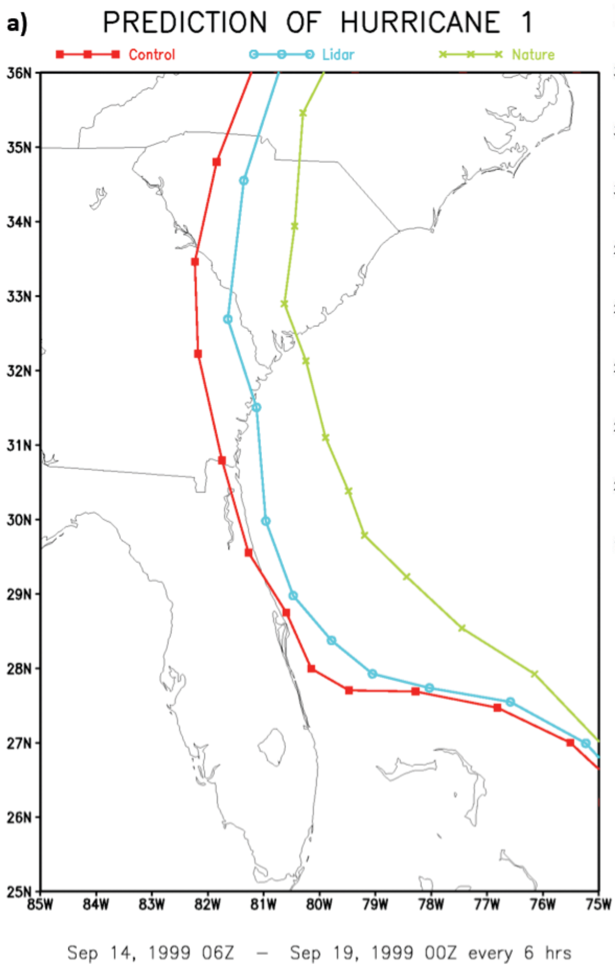

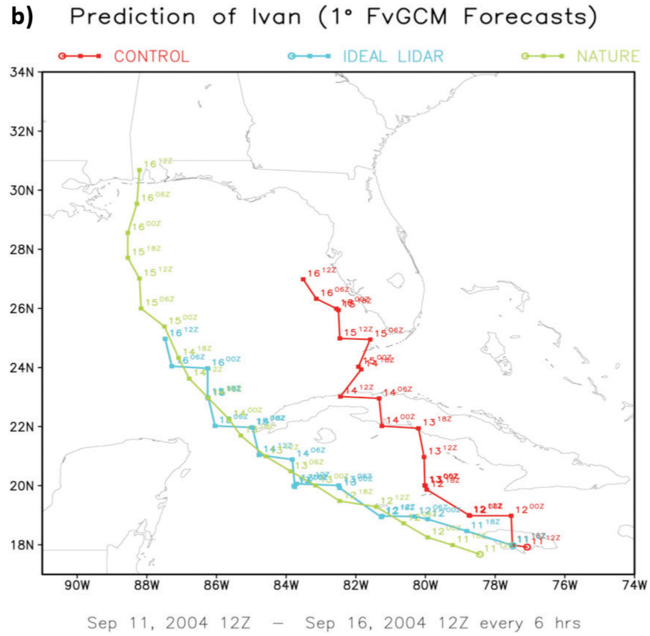

Fig. 4. The potential impact of lidar winds for hurricane-track forecasts. Green denotes the "observed" track from NR, red denotes the forecast with all currently used simulated data, and blue denotes the improved forecast for the same time period with simulated wind lidar data added. (a) A land-falling hurricane simulated in NR and (b) the prediction of Hurricane Ivan.

forecasts. These studies were also used to evaluate trade-offs in lidar design (Atlas et al. 1985a,b; Atlas 1997; Masutani et al. 2010).

OSSEs have also been used to assess the potential impact of DWL on hurricane-track forecasts. For this purpose, a reference atmosphere, referred to as a "nature run" (NR), was generated using an early version of the finite-volume general circulation model (FvGCM) at 0.5° resolution (Atlas et al. 2005b), and the assimilation and forecast system was the 1.0° resolution version of the NASA Goddard Space Flight Center (GSFC) Goddard Earth Observing System (GEOS) version 3 data assimilation system (Atlas et al. 2005a). The NR covered a 3.5-month period and contained interesting and important meteorological features, including tropical cyclones and a very realistic representation of atmospheric fronts and extratropical cyclone evolution. Following a detailed assessment of the realism of the NR and the differences between the NR model and the assimilation–forecasting model, the entire OSSE system was validated through a comparison of parallel real-data and simulated-data impact experiments.

Figure 4a illustrates an improvement in hurricane landfall prediction as a result of assimilating simulated lidar wind data. The predicted landfall position error was improved by approximately 150 miles. Details of these and other OSSEs are summarized by Atlas and Emmitt (2008) and Atlas and Riishojgaard (2008). Marseille et al. (2008) used a modified OSSE concept to illustrate beneficial DWL impact for severe extratropical storms. Pu et al. (2009) and Zhang and Pu (2010) demonstrated DWL data can have a potential impact on improving tropical cyclone intensity forecasts with a regional OSSE.

A second U.S. landfalling storm (Hurricane Ivan) was evaluated from the extremely active 2004 hurricane season. A "QuickOSSE" methodology was conceived in order to answer observational and dynamical questions related to this hurricane. This methodology involved using a 0.25° resolution version of the FvGCM forecast of Hurricane Ivan for the NR. From this NR, all of the standard and special reconnaissance observations that were available in real time, as well as hypothetical lidar wind profiles covering the storm, were simulated. This was followed by the control assimilation and forecast (using all of the standard observations) and an ideal lidar assimilation and forecast (adding simulated lidar winds to the control) generated using a coarse 1.0° × 1.25° resolution version of the FvGCM.

Figure 4b shows a major improvement in the predicted movement of the hurricane resulting from the assimilation of lidar winds. This was due to a significant improvement in the divergence profile associated with the storm (not shown), enabling it to be more accurately steered by the large-scale flow.

More recently, an ECMWF T511 (~40-km horizontal resolution) NR (Andersson and Masutani 2010) was used to create the simulated observations and serve as the "truth" for impact experiment verification. The Joint Center for Satellite Data Assimilation (JCSDA) has conducted a series of OSSEs aimed at assessing the potential impact of the Global Wind Observing System (GWOS) mission concept outlined in the "Technology used in DWL" section (Riishojgaard et al. 2012), using the T511 nature run provided by ECMWF. All experiments were done with the December 2009 version of the NCEP Global Data Assimilation System (Kleist et al. 2009).

The approach taken to simulate the reference observing system for the OSSEs was simple and aimed at capturing the most salient characteristics of the global observing system. For data with existing real-data parallels (i.e., radiosondes, surface observations, aircraft data, existing satellite systems), simulated observations were created at the times and locations for which actual observations were available in the corresponding 2005–06 period, as recorded in the operational data stream used in NCEP operations. The GWOS DWL observations were simulated, using the Doppler Lidar Simulation Model (DLSM) described by Wood et al. (2000). Direct and coherent detection wind lidar returns (see "Technology used in DWL") were simulated separately, and a detailed model of the instrument error propagation onto the final error of the wind product was included. Details on the simulation of non-DWL data were described by Riishojgaard et al. (2012).

First, a control experiment was performed: a cycling data assimilation run extending over a spinup period from 1 through 6 July, followed by an experimental period from 7 July through 15 August. The control experiment used simulated data for all of the observations with a real-data counterpart in the NCEP operational data stream during this time period that also provided a 40-day interval over which

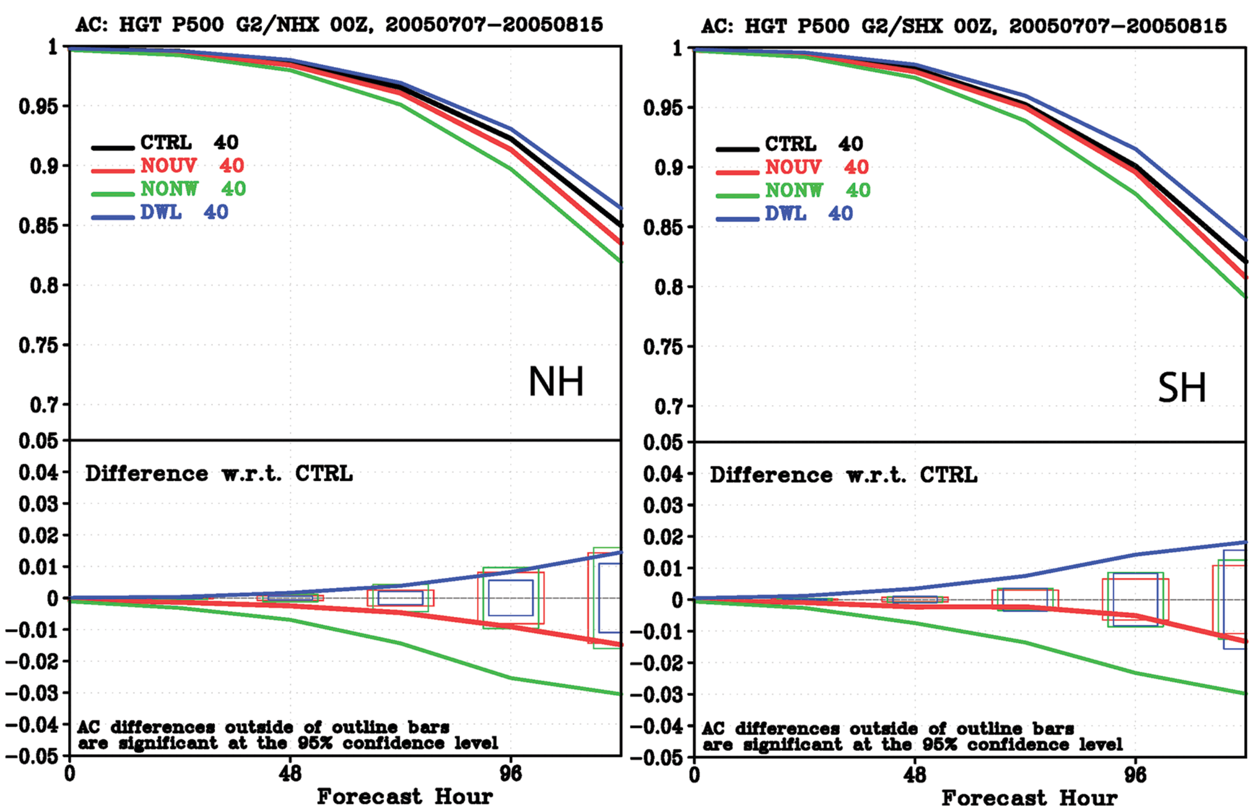

Fig. 5. The impact of various wind observing systems on 500-hPa height forecasts measured by the AC score, averaged over 40 cases. (left) NH and (right) SH results. Error bars represent statistical significance at the 95% level.

diagnostics were calculated. During this period, 5-day forecasts were launched each day at 0000 UTC. Next, a set of three perturbation (assessment) experiments was done: 1) an experiment ("NOUV") from which all radiosonde, pilot balloon, and dropsonde wind observations were removed; 2) an experiment ("NONW") in which all wind observations were withheld (aircraft, scatterometer, winds from feature tracking, etc.) in addition to those withheld from the NOUV experiment (in other words, all wind observations used in the control experiment were withheld.); and 3) an experiment ("DWL") in which the simulated GWOS DWL observations were added to the observations used for the control run. The experimental setup for all runs was consistent with the way the system was used in NCEP operations prior to 22 May 2012. The horizontal resolution was T382, corresponding to a Gaussian grid size of about 45 km.

Figure 5 shows the skill of the 500-hPa-height forecasts as measured by the anomaly correlation coefficient (Miyakoda et al. 1972), referred to here as the anomaly correlation (AC) score, for all four experiments in the Northern Hemisphere (left) and the Southern Hemisphere (right). The AC score can range between 0.0 and 1.0 and is nondimensional. All forecasts were verified using the nature run, and the bottom part of Fig. 5 shows differences in skill with respect to the control run. Differences that exceed the error bars for the respective color are statistically significant at the 95% level. The figure shows that elimination of all wind observations leads to a significant decrease in skill (NOUV and NONW), demonstrating that wind observations have a significant contribution to the skill of the NCEP Global Forecast System (GFS). The addition of the simulated lidar wind observations leads to a statistically significant increase in AC score at day 5 (120 h) of approximately 1.5 and 2 points in the Northern and Southern Hemispheres, respectively. In the Southern Hemisphere, for example, the AC score, is approximately 0.83 versus 0.85 for the control and DWL experiments, respectively.

For comparison purposes, the overall rate of progress of NWP skill over the last 10–20 years has generally ranged from 0.5 to 1 point annually due to a combination of factors: better observations, improvements to model and data assimilation methodology through scientific advances, and increased spatial and temporal resolution due to more powerful computers. Typically, a contribution that can be attributed to a

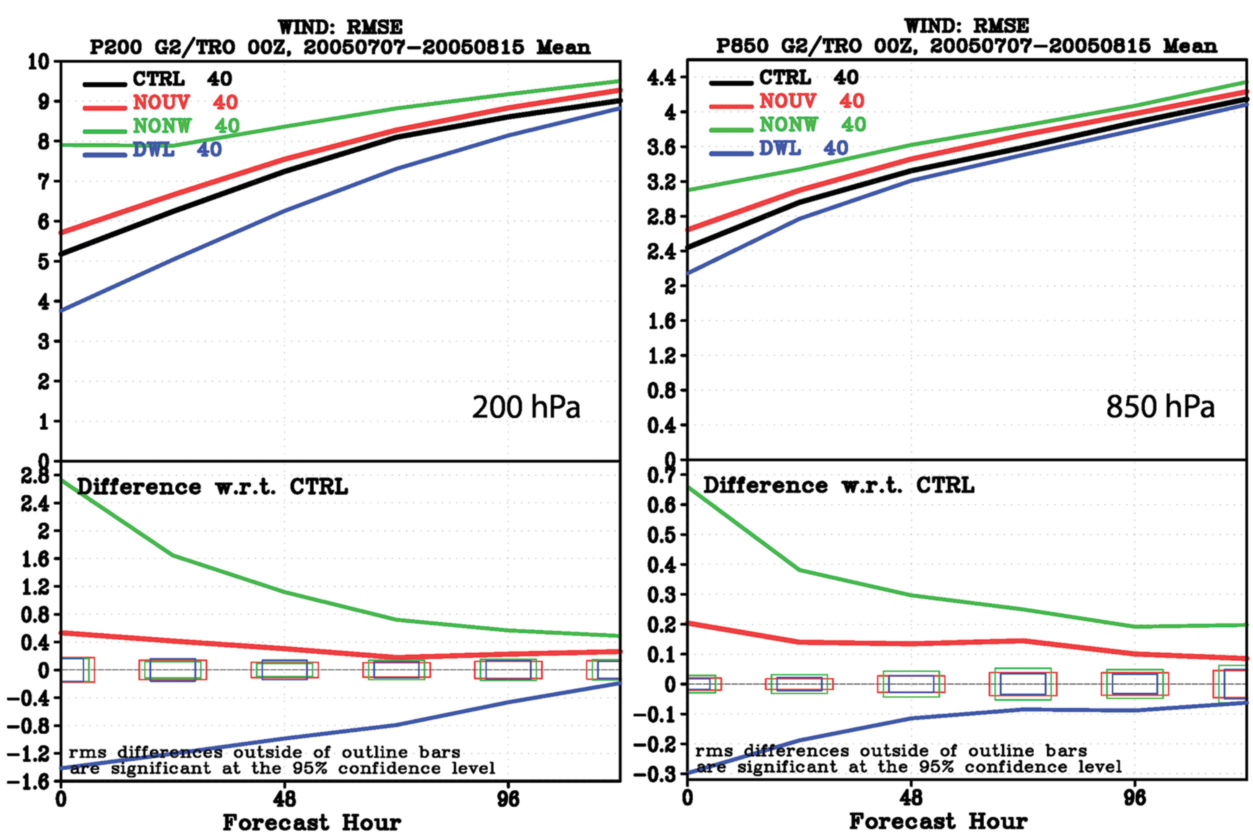

Fig. 6. The impact of various wind-observing systems on 200- and 850-hPa tropical wind forecasts measured by the RMS error (m s^{-1}), averaged over 40 cases. Error bars represent statistical significance at the 95% level.

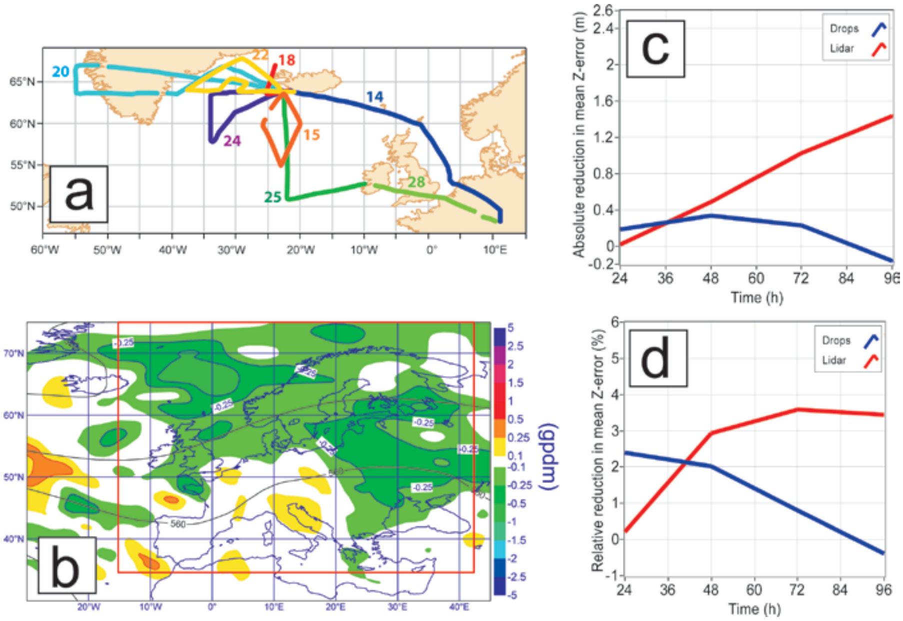

Fig. 7. (a) Flight tracks with lidar observations during the A-TReC. Numbers indicate the day of the flight in Nov 2003. (b) Difference of 500-hPa geopotential height RMS error between an experiment with lidar data and a control run without additional observations. Negative values indicate improvement compared to the control run. (c) Reduction of mean 500-hPa geopotential height errors in an experiment with (red) lidar and (blue) dropsondes compared to the control run. Positive values correspond to lower errors than the control run. (d) As in (c), except normalized with the mean error of the control run.

specific new observing system is generally modest. In that context, the magnitude of the impact of the DWL is exceedingly rare.

Tropical RMS wind errors for the four experiments are shown in Fig. 6. The effect of simulated lidar wind observations in the tropics is initially large, especially at the 200-hPa level. The 850-hPa level is more strongly influenced by the lower boundary conditions and, due to progressive attenuation of the lidar beam at lower levels, fewer wind observations are available at this level. However, the impact tends to decrease rapidly over time at both levels. This behavior is typical for the tropics, and, rather than pointing to problems with the simulated data, it illustrates the challenge of using observations in a dynamically consistent way (Žagar et al. 2004).

Airborne Observing System Experiment over the North Atlantic. A scanning coherent 2-μm Doppler lidar was operated for 28.5 flight hours during the Atlantic "The Observing System Research and Predictability Experiment" (THORPEX) Regional Campaign (A-TReC) in November 2003 onboard the Falcon 20 aircraft of the Deutsches Zentrum für Luft- und Raumfahrt (DLR). The system measured 1612 vertical profiles of wind direction and speed at a resolution of 5–10 km horizontally and 100 m vertically (Fig. 7). Comparison of the lidar observations and collocated dropsondes revealed that the coherent lidar can measure winds with a standard deviation of 0.75–1 m s^{-1} and no significant bias (Weissmann et al. 2005). Although this error is slightly higher than that of conventional dropsonde observations, lidar observations are seen to be more representative of the model wind field because they are computed by averaging over a sampling volume of 5–10 km.

An Observing System Experiment (OSE) was conducted whereby A-TReC lidar observations were assimilated into the operational version of the ECMWF model at that time with a horizontal resolution of about 40 km and 60 levels in the vertical (Weissmann and Cardinali 2007), including the representativeness error. The assumed lidar observation error standard deviation was 1–1.5 m s^{-1}, which is only about half of the assigned error of most conventional observations. Lidar observations were found to have more influence in the analysis than dropsondes. In particular, the mean analysis influence calculated following Cardinali et al. (2004) was 50% higher. The assimilation of lidar wind profiles over the North Atlantic produced an average reduction of 3% in the 48–96-h forecast error for the 500-hPa geopotential height over Europe (Fig. 7). This was a remarkable result given that observations from only eight flights were assimilated in the 17-day period. Consistent with dropsondes having less influence in the analysis, there was less reduction in the forecast error when only dropsonde observations were assimilated (in addition to data from the routine operational observing system).

These findings motivated the deployment of the airborne DWL instruments in the THORPEX Pacific Asian Regional campaign (T-PARC) 2008. Results from this campaign are summarized below.

Airborne OSE over the western Pacific. During the T-PARC field experiment in 2008, airborne DWLs were operated on board the DLR Falcon aircraft and a Naval Research Laboratory (NRL) P-3 aircraft. It was the first time that airborne DWLs were employed for an extended period in the environment of tropical cyclones (TCs). DWL wind measurements were obtained for several TC cases over the western North Pacific. After the field experiment, DLR Falcon DWL observations in the environment of Typhoon Sinlaku were assimilated in the global ECMWF and NRL models. In addition, NRL P-3 DWL observations near Typhoons Nuri and Hagupit were assimilated using the Weather Research and Forecasting Model (WRF).

The DLR Falcon observed over 4000 wind profiles below 9–12 km MSL. About 2500 profiles in an 11-day period covering the life cycle of Typhoon Sinlaku were used in an OSE with the ECMWF and NRL global NWP models. Overall, the DWL observations improved both model forecasts near the observation area (Weissmann et al. 2012). On average, a typhoon track improvement of 9% in the 12–120-h forecast range was obtained with the ECMWF model, with a mean 24–120-h forecast error reduction of 2.5%–5.5% for the 500- and 1000-hPa geopotential height for two verification regions: one area covered the track of Sinlaku and a larger one also included the interaction of Sinlaku with the midlatitudes. In contrast, the NRL experiments did not lead to a significant track improvement likely due to the use of synthetic TC bogus observations that seemed to limit the influence of additional observations near TCs. The mean 24–120-h forecast error of 1000- and 500-hPa geopotential heights, however, was reduced by 1%–3.5% in the same verification areas as with the ECMWF experiments.

Additionally, the DWL observation impact in the ECMWF and NRL models was quantified using FSO diagnostics (Langland and Baker 2004; Cardinali 2009), which confirmed the beneficial impact of DWL observations (Weissmann et al. 2012). The total relative contribution of DWL observations was about twice as high in the NRL system as in the ECMWF system. This is believed to be due to the fewer number of satellite observations assimilated in the NRL system at the time. In the Sinlaku environment and for the NRL system, DWL data had the fourth-largest mean forecast impact per observation, after synthetic TC bogus observations, satellite-derived total precipitable water, and scatterometer surface wind data (Fig. 8a). The impact of DWL measurements in the ECMWF system was similar to that of aircraft observations but smaller than those of drifting buoys, radiosonde and wind profiler observations, atmospheric motion vectors, surface stations, and scatterometer surface winds (Fig. 8b).

A three-dimensional variational data assimilation (3D-Var) WRF system was also used to assimilate the NRL P-3 DWL observations obtained during the early development of Typhoon Nuri, mainly available below 2-km height with 50-m vertical and 1-km horizontal resolution. The P-3 aircraft track and a portion of the path of Nuri in its early development

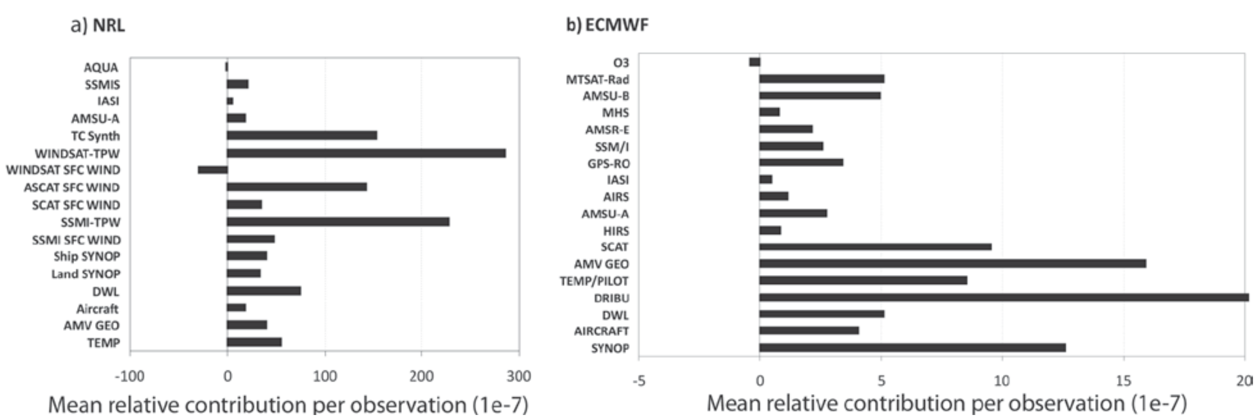

Fig. 8. Mean relative contribution (per observation) of various observation types to the reduction in the 24-h forecast error norm in an area covering Typhoon Sinlaku and its environment (20°–50°N, 120°–160°W) in an experiment with the (a) NRL and (b) ECMWF global models. Scaling is 10^{-7} and positive values represent error reduction. ECMWF results are averaged over all assimilation intervals in the period 11–21 Sep 2008; NRL results only over twelve 6-h assimilation intervals with DWL observations in this period. Contribution of drifting buoy observations in (b) is 63×10^{-7}, which exceeds the scale. Note that the relative magnitude in (a) and (b) should be compared, but not the actual values due to the differences between NRL and ECMWF in the number of observations assimilated, length and number of assimilation intervals, and the "super ob" observation-averaging technique used at NRL. See Weissmann et al. (2012) for more details.

are shown in Fig. 9. Details on the model formulation, the 3D-Var analysis, and initialization procedure can be found in Skamarock et al. (2005), Barker et al. (2004), Pu et al. (2010), and Emmitt et al. (2011a).

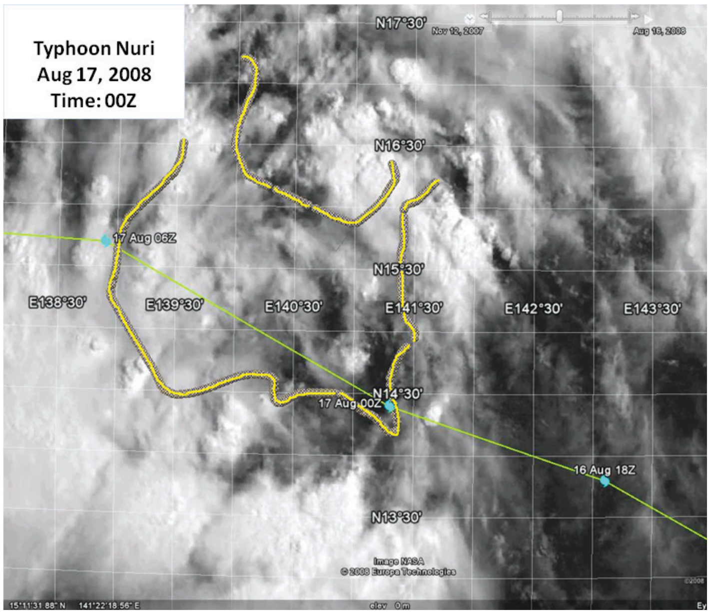

Fig. 9. DWL wind measurements (500 data points collected) at 1500 m above MSL selected from 500 wind profiles around the early stages of Typhoon Nuri (2008) over the western Pacific during 2330 UTC 16 Aug–0200 UTC 17 Aug 2008. NRL P-3 aircraft was flying at 3000 m. Track of Nuri for three 6-h periods is included.

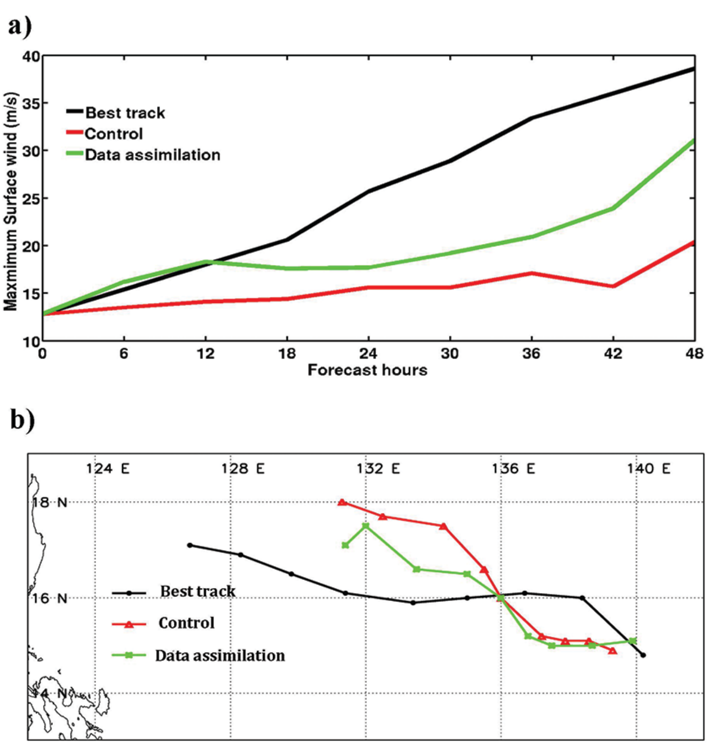

At 2000 UTC 16 August 2008, a tropical easterly wave (TCS-013) was located northwest of Guam with a maximum mean wind of about 12.9 m s^{-1}. During the NRL P-3 mission of 16 August, the system was declared tropical depression 13W and was named Tropical Storm Nuri by 18 August 2008. The impact of airborne DWL measurements on the prediction of the formation of Nuri was evaluated by Pu et al. (2010). Results show that the DWL wind data improved the intensity and track forecast for Nuri compared to the assimilation experiment without DWL observations (control). The experiment using DWL data resulted in a more accurate 12–48-h maximum surface wind forecast (Fig. 10a) when compared to the control and verified against the observed surface wind ("best track"), as determined by the Joint Typhoon Warning Center (JTWC), and in a reduction in the northerly bias in the 24–48-h forecast track of Nuri (Fig. 10b). However, the track of Nuri in both the DWL and control experiments was significantly slower than Nuri's observed track. Compared with the control, assimilation of DWL data reduced the error in the 6–48-h surface maximum wind forecast, on average, by 26% and reduced the track forecast error by 18%. DWL data also reduced the error in both the track and intensity forecast for a second case (Typhoon Hagupit; not shown).

The 2008 T-PARC airborne campaign was the first time that DWL measurements were obtained and assimilated during tropical cyclone development. Because no satellite data were assimilated in the experiments with WRF, the impact of the DWL data in these experiments should be viewed as tentative, but, given the sparse DWL data coverage, very encouraging.

Fig. 10. Impact of actual airborne DWL observations on the numerical simulation of Typhoon Nuri's early rapid intensification. (a) The maximum surface wind and (b) the track from 0000 UTC 17 Aug to 0000 UTC 19 Aug 2008. Forecasts with (green curves) and without (red curves) assimilation of DWL wind are compared with the JTWC best-track data (black curves). DWL data are assimilated for the period 0000–0200 UTC 17 Aug 2008.

Climate change studies. The most comprehensive tool available to analyze climatic trends is the reanalysis technique (Uppala et al. 2005; Simmons et al. 2010). An intercomparison of first-generation reanalyses (Kistler et al. 2001) clearly shows that even such a basic quantity as zonally averaged, time-mean zonal winds are not well constrained by the present observing system. In the tropical upper troposphere and the lower stratosphere, the difference between zonal winds obtained from independent reanalysis efforts are of the same order as the characteristic time variability of this quantity. This does not necessarily imply that the reanalysis technique is inadequate but rather points to the fact that additional wind information is needed to make reanalyses more consistent. Also, more recent reanalysis results show the same features. For example, Fig. 11 shows the zonal wind difference between the most recent reanalysis from ECMWF Re-Analysis (ERA-Interim; see Simmons et al. 2010; Dee et al. 2011) and the second-generation 40-yr ECMWF Re-Analysis (ERA-40; Uppala et al. 2005) for the overlapping time period 1989–2001. The differences are smaller than with Kistler et al. (2001) but the same spatial pattern is found. In addition, as the differences in the stratosphere are emphasized, recent reanalyses have included upper-stratospheric layers. We also find differences in the Arctic and Antarctic regions that are not so apparent in the results from Kistler et al. (2001). The polar area differences are smaller than those found in the tropics, but they point to the need for wind data in the polar atmosphere.

Another aspect of high-latitude wind information is the determination of meridional heat transports. Graversen et al. (2008) have shown that Arctic warming trends in the free troposphere can be, to some extent, explained by an increase in the northward atmospheric heat transport. Graversen et al. (2007) also pointed out that the calculation of meridional heat transports from reanalysis data is restricted by the accuracy of meridional, ageostrophic winds. With the present wind data coverage in the Arctic region, the zonally averaged, meridional wind component is not well constrained. This leads to a spurious mass flux in or out of the Arctic region. Through mass continuity considerations, this mass flux can be adjusted (Trenberth 1997) but improved wind observations are needed to better define the wind field and to make the heat transport calculations more accurate.

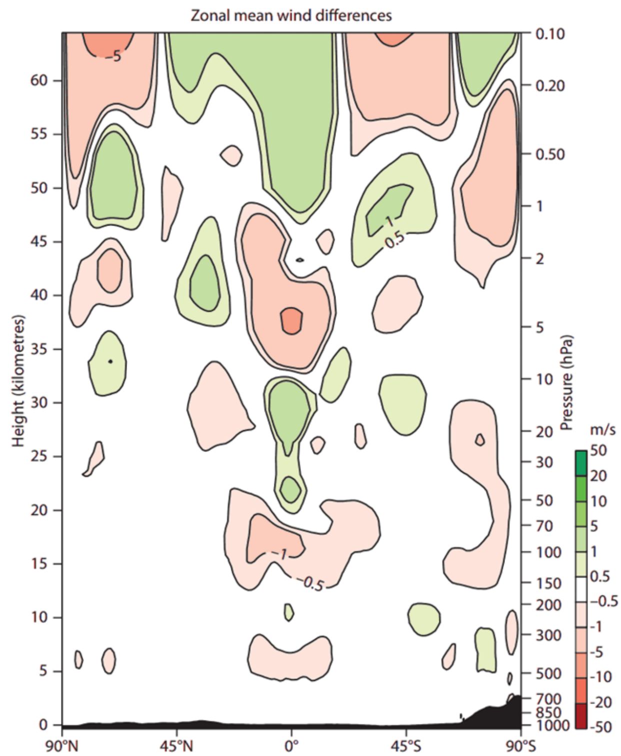

Fig. 11. The zonally averaged latitude–height cross section of zonal mean wind differences (m s^{-1}) between ERA-40 and ERA-Interim for the time period 1989–2001.

Aerosol profiling and pollution transport. Because DWL measurements rely on aerosol backscatter returns to determine line-of-sight velocities, they provide an excellent opportunity to retrieve profiles of aerosol backscatter and derived aerosol extinction (Ansmann et al. 2007; Flamant et al. 2008). Simultaneous measurements of vertically resolved aerosols and winds are critically needed to address a wide range of air quality and climate change issues associated with long-range pollution transport and aerosol direct and indirect effects. The Cloud–Aerosol Lidar with Orthogonal Polarization (CALIOP) instrument (Winker et al. 2003) on the *Cloud–Aerosol Lidar and Infrared Pathfinder Satellite Observations* (*CALIPSO*) satellite has demonstrated the utility of space-based aerosol backscatter measurements in providing long-term continuous profiling of clouds and aerosols. DWL measurements would extend this record of height-resolved aerosol backscatter measurements and add critical information regarding pollution transport.

Global climate models' predictions of the vertical distribution of aerosols vary widely (Kinne et al. 2006) and, consequently, current model-based estimates of long-range aerosol transport are highly uncertain. Quantifying long-range aerosol transport is critical to address outstanding issues at the nexus of air quality and climate change, particularly in the

Arctic. During Northern Hemisphere late winter and early spring, pollution from Europe, Asia, and North America are transported into the Arctic Basin (Shaw 1995). Because of strong temperature inversions, this pollution accumulates in the Arctic boundary layer, leading to "Arctic haze" (Mitchell 1956). Black carbon is a minor but important component of the Arctic haze (Quinn et al. 2007) and contributes to Arctic warming through direct absorption of solar radiation and can change the surface albedo when it is deposited on the snow and ice (Hansen and Nazarenko 2004). Uncertainties in meridional transport of black carbon into the Arctic are even larger than meridional heat transport due to poor constraints on both wind and aerosols.

TECHNOLOGY USED IN DWL. For over 40 years (Siegman 1966; Huffaker et al. 1970, Benedetti-Michelangeli et al. 1972) ground- and aircraft-based wind lidars have been in development to study atmospheric dynamics, to provide context for pollution transport, and to address uncertainties in the model wind fields. Through recent technology advances that include improved structural materials, higher laser efficiency and output power, and more robust optical coatings, the field of Doppler lidar progressed steadily from the fundamental technology demonstrations of the 1970s and has reached a maturity level needed to make the required wind measurements from space. Please refer to the supplemental material (http://dx.doi.org/10.1175/BAMS-D-12-00164.2) and references listed therein for additional background on wind lidar and the recent studies that have been done on the various types of DWL technologies that are considered for the space-based missions described in the following subsections.

Review of DWL systems. Evolution of lidar technology for space-based measurements has focused on Doppler lidar systems compatible with two primary receiver implementations: coherent detection and direct detection. Early Doppler lidars incorporated coherent detection in the thermal infrared to measure winds based on aerosol backscatter. However, more recent advancements in direct detection technology, which has the advantage of being able to measure winds from atmospheric molecules as well as aerosols, have indicated the feasibility of this technique for space. Coherent and direct detection are briefly discussed below; additional information about the different types of DWL systems may be found in Werner (2004), Henderson et al. (2005), and Reitebuch (2012b). A detailed discussion on the physics of measuring atmospheric wind speed with Doppler lidar is provided in the supplemental material.

CD LIDARS. Coherent detection (CD) lidars use heterodyne detection to estimate the frequency shift between the outgoing and backscattered laser pulses. In these systems, a highly stable but low power local oscillator (LO) laser is first used to seed the outgoing laser pulse. The LO is then optically interfered with the aerosol-backscattered, Doppler-shifted return pulse to produce a temporal beat frequency on the face of the detector. This temporal interference requires that the LO have a long temporal coherence length, so that it does not change frequency during the round-trip time of the emitted and atmospheric-backscattered pulse, and that the wavefront of the return light match that of the LO. The center frequency of the remaining signal corresponds to the positive or negative Doppler shift. CD systems can provide better than 1 m s^{-1} precision on the wind speed estimate in high-aerosol loading conditions or clouds.

Multiple references provide additional information on coherent detection systems (Kavaya et al. 1989, 2014; Henderson et al. 1991; Wagener et al. 1995; among others) and their use in atmospheric boundary layer studies (Post and Cupp 1990; Huffaker and Hardesty 1996; Rothermel et al. 1998; Grund et al. 2001; Banta et al. 2002; Koch et al. 2010; Tucker et al. 2009; Bluestein et al. 2011; de Wekker et al. 2012), wind turbine studies (Käsler et al. 2010), and hazard detection and avoidance at airports (Hannon et al. 2005). Coherent airborne DWLs have also been used to explore the potential impact of future space-based lidars and to develop the necessary advanced signal processing and data interpretation algorithms (Emmitt et al. 2010).

DD LIDARS. In direct detection–spatial interference receivers, a spatial copy of the illumination under spectral investigation is interfered with itself and the frequency estimation is performed on both the outgoing pulse and the atmospheric return. Because the illumination intensity and/or frequency are directly measured without the need for a local oscillator, these systems are referred to as "direct detection" wind lidars. In the direct detection case, the interferometer must remain stable over the round-trip return time. Direct detection (DD) systems include Fabry–Perot etalons used in single-edge (Gentry and Korb 1994), double-edge (Korb et al. 1998; Gentry et al. 2000; ESA 2008; Reitebuch et al. 2009; Dong et al. 2010), or multichannel/fringe-imaging [charge-coupled device (CCD)] configurations (McGill et al. 1997a,b);

fringe-imaging Fizeau (Schillinger et al. 2003; ESA 2008; Reitebuch et al. 2009) and fringe-imaging Michelson (Cézard et al. 2009) interferometers; and Mach–Zehnder interferometers (Liu and Kobayashi 1996; Bruneau 2001; Bruneau and Pelon 2003), including the optical autocovariance receiver, a modified Mach–Zehnder interferometer (Schwiesow and Mayor 1995; Grund and Tucker 2011). Each of these systems can be designed to estimate frequency with narrowband (i.e., aerosol scattered) light or with the wings of the spectrally broadened molecular return or both. The 355-nm double-edge technique discussed in the 2007 NRC decadal survey typically has lower precision (~2–4 m s^{-1}) in the molecular scatter velocity estimates, but it is able to make measurements where aerosol loading is very low. Three different approaches for DD wind measurement are discussed below.

Double-edge detection FP. Edge detection systems typically make use of Fabry–Perot (FP) etalon interferometers to estimate the spectral peak of lidar illumination. FP etalon cavities are designed to transmit light at specific frequencies determined by the spacing of two glass plates (or thickness of a single glass plate), the index of refraction of the medium between the plates, the angle of incidence, and the reflectivity of the optical coatings. For a molecular backscatter double-edge system, two FPs are typically used (i.e., separate etalons, or different spacings on sections of the same etalon). The transmission of each etalon is centered on either side or "edge" of the roughly 600 m s^{-1}-wide molecular backscattered spectrum. The transmission of the atmospheric return through both etalons is detected and compared: an imbalance between the detected signal intensities indicates a positive or negative Doppler shift in the return.

The first molecular "double edge" DWL system was demonstrated by Chanin et al. (1989) and Garnier and Chanin (1992). A double-edge receiver was later built at the Goddard Space Flight Center and installed into the NASA Goddard Lidar Observatory for Wind (GLOW; Gentry et al. 2000) mobile Doppler lidar, which continues to make ground-based wind measurements (Vermeesch et al. 2011). The NASA Tropospheric Wind Lidar Technology Experiment (TWiLITE) instrument, also developed at Goddard, uses a double-edge molecular receiver, operating at the 355-nm wavelength. The TWiLiTE system has been developed for operation aboard NASA's high-altitude ER-2 aircraft as part of a path toward a space-based system. A double-edge FP system comprises the molecular channel of the European Space Agency (ESA)'s Atmospheric Dynamics Mission Aeolus (ADM-Aeolus) instrument (ESA 2008; Reitebuch et al. 2009).

Fringe-imaging systems. In a fringe-imaging configuration, Fabry–Perot etalons may also be used for frequency estimation (McKay 1998). A slightly divergent beam of light incident on a plane-parallel Fabry–Perot produces a circular ring pattern of interference fringes. When properly illuminated, these fringes of equal inclination produce a spatial scan of the spectrum of the incoming light where the wavelength is proportional to the radial distance from the center of the ring pattern. The ring pattern may then be imaged on a CCD or focal plane array or modified via special optical components to produce either lines or rings (Hays 1990; Dehring et al. 2005; Irgang et al. 2002) or points (McGill et al. 1997c). The difference between the outgoing pulse fringe pattern and the atmospheric return pattern relates to the Doppler shift/wind measurement. A similar fringe-imaging design using a Mach–Zehnder interferometer has also been investigated (Bruneau 2002). A fringe-imaging Fizeau interferometer system (Schillinger et al. 2003; Reitebuch et al. 2009) is currently being integrated into the aerosol channel of the European ADM-Aeolus mission instrument.

Optical autocovariance. In recent years, Ball Aerospace and Technologies Corporation has developed another type of wind lidar receiver using optical autocovariance techniques (Schwiesow and Mayor 1995). The resulting Optical Autocovariance Wind Lidar (OAWL) is a modified Mach–Zehnder interferometer (Liu and Kobayashi 1996) that uses cat's eye mirrors to increase the interferometer's field of view (Grund and Tucker 2011). The OAWL estimates line-of-sight wind speeds by measuring the Doppler shifts in atmospheric aerosol returns at the 355- and/or 532-nm wavelengths. The OAWL design may be shifted to operate at any wavelength (Grund et al. 2009), or paired with a molecular return channel (i.e., double-edge Fabry–Perot) system operating at 355 nm. The resulting full direct detection system would require only one 355-nm laser to make measurements from both the molecular and aerosol returns in the atmosphere.

Technical readiness and advancements in space-based lidar. Underlying the different design concepts discussed in the following subsections, the level of technical readiness remains one of the most important factors in preparing a wind lidar mission for space. One of the greatest challenges for space-based lidar is building and space qualifying the pulsed laser capable of providing the power, stability, and lifetime required. Specific requirements on the laser including wavelength, power, pulse bandwidth, pulse repetition frequency, and frequency stability depend on the type of system and are driven by performance guidance, an example of which is given in Table ES1 (http://dx.doi.org/10.1175/BAMS-D-12-00164.2).

All DWL systems require a single-longitudinal-mode (single wavelength) laser and all must address challenges in laser lifetime, prevention of laser optical damage, and laser electrical efficiency. Significant effort has been made internationally to space readiness for high-power lasers at the Nd:YAG crystal wavelengths of 1 mm doubled to 532 nm and tripled to 355 nm. These wavelengths apply not only to wind lidar but also to systems such as the laser on NASA's Ice, Cloud, and Land Elevation Satellite-2 (ICESat-2) mission (Sawruk et al. 2013). Likewise, systems using these wavelengths benefit from the experience in laser qualification and laser lifetime gained from the CALIOP system on the *CALIPSO* payload (Weimer et al. 2004; Hovis 2006; Hunt et al. 2009), which, as of this writing, has been operating continuously for over 7 years.

Significant investment has also been made in developing high-power 2-μm wavelength coherent detection systems. Since the mid-1990s NASA's Langley Research Center (LaRC) has worked toward development of a space-based coherent detection lidar, including a 2-μm detector development and a laser development program that has produced a laser with greater than 1-J pulse energies at 10 Hz (Kavaya et al. 2014).

In addition to laser qualification for space, several figures of merit are very important for space missions: reliability, electrical efficiency, cooling requirements, mass, and electrical power needs. NASA tracks the development of technology for space missions using technical readiness levels (TRLs; Mankins 1995), which help to focus risk reduction efforts for future missions. As part of the development of DWL systems for space, airborne demonstrations help to increase a system's TRL by demonstrating operation from a high-altitude platform. The Doppler Aerosol Wind Lidar (DAWN; Braun et al. 2013; Kavaya et al. 2014), TWiLiTE (Gentry et al. 2011), OAWL (Tucker et al. 2012), and ADM-Aeolus airborne demonstrator (Paffrath et al. 2009; Reitebuch et al. 2009) systems have all flown in aircraft, helping to raise the TRLs of the various technologies. These airborne systems may also provide ground- or aircraft-based validation data after a DWL system has been launched.

Profiling wind through the troposphere and lower stratosphere: Full DD and hybrid system concepts. The lidar technologies discussed in the previous section take advantage of laser light backscattered from molecules present throughout the atmospheric column or from aerosols, which are present mainly in the lower troposphere or as thin cirrus at higher altitudes. Some systems operating at high (i.e., ultraviolet) frequencies can take advantage of both aerosol and molecular lidar return. Recent design concepts for space-based wind lidars employ separate receivers to measure Doppler shifts from the aerosols and molecules. In the full direct detection systems, the aerosol and molecular receivers share the same laser and telescope. In the so-called hybrid systems, the two receivers operate at two different laser frequencies but share the same telescope(s). The following subsections describe some recently studied or implemented instrument concepts for measuring atmospheric winds: the ADM-Aeolus system (ESA 2008; LeRille et al. 2012; Reitebuch 2012a), the hybrid system for the U.S. GWOS, and systems for a Winds from the International Space Station for Climate Research (WISSCR) mission.

The ESA ADM-Aeolus single-wavelength full direct detection system. The first spaceborne demonstration of DWL technology will be provided by the ESA's ADM-Aeolus (Stoffelen et al. 2005). ADM-Aeolus features a single 355-nm laser transmitter and two direct detection systems: a double-edge FP etalon for the molecular return and a fringe-imaging Fizeau spectrometer for the aerosol returns (Endemann 2006; LeRille et al. 2012). Subsequent to the 2005 report, several technical modifications have been made to the Aeolus instrument, the most important being changing from burst to continuous operations. The instrument development and expected science capabilities are well documented and highlighted in a special issue of *Tellus A* (2007, Vol. 60, No. 2). Likewise, ESA (2008) discusses the mission objectives, scientific impact studies, and technology, and LeRille et al. (2012) and Reitebuch (2012a) provide the most recent status of ADM-Aeolus.

ADM-Aeolus presently has a planned launch date in 2015 and the expected mission lifetime is 3 years. Line-of-sight (LOS) wind profiles from ADM-Aeolus are expected to give a significant positive impact on NWP analysis quality—in particular, in the tropics at upper levels, where only a limited amount of high-quality wind data is available in the current observing system. Several studies have demonstrated the potential impact of the ADM-Aeolus instrument on NWP forecast quality. Cress and Wergen

(2001) demonstrated the significant impact from withholding existing wind profile information over the North American continent on European forecast quality. Žagar et al. (2004) emphasized the potential impact in the tropics and showed how single line-of-sight wind measurements and mass information can complement each other. As ADM-Aeolus will only measure a single-component wind profile, the full wind information can only be retrieved in a data assimilation system where other observational information is used to complement the ADM-Aeolus winds. Tan et al. (2007) demonstrated the impact of ADM-Aeolus-type wind information on ensemble assimilation systems, while Marseille et al. (2007) and Stoffelen et al. (2006) discussed the ADM-Aeolus impact on OSSE type of experiments. All these studies show that ADM-Aeolus will have a significant impact on NWP quality if the wind observations fulfill the accuracy requirements. Recent experiments confirm that these impact results also hold for the continuous-mode instrument. Furthermore, the ADM-Aeolus instrument can also give information on aerosol concentrations in the atmosphere as discussed by Ansmann et al. (2007) and Flamant et al. (2008).

Studies have been conducted to develop user requirements for an Aeolus follow-on mission. From these studies in the extratropics, wind component profile coverage appears adequate in lieu of obtaining two independent measurement perspectives, while in the tropics both zonal and meridional wind profiles are important. A complement of a side- and back-looking Aeolus-type instrument would fulfill the stated requirements (Stoffelen et al. 2008). If ADM-Aeolus successfully demonstrates the feasibility and utility of space-based Doppler wind lidars, then the period 2016–18 may be unique among the atmospheric data records in providing global wind data coverage and therefore better atmospheric analysis accuracy. Follow-on missions have been considered but future planning awaits the successful demonstration of ADM-Aeolus wind-measuring capabilities. In this respect, ESA's ADM-Aeolus is leading in demonstrating that a DWL can fulfill user requirements on wind profiling and is expected to deliver a well-characterized satellite instrument concept that could be the baseline for follow-on missions.

The NASA GWOS hybrid concept. The GWOS, a mission concept proposed to the NRC decadal survey (NRC 2007), was designed for a winds demonstration mission from a free-flyer satellite in LEO orbit. In addition to component technology advances, important differences from the system concept discussed in Baker et al. (1995) were inclusion of both direct and coherent detection lidar subsystems in a hybrid configuration, and an improved methodology for achieving multiple look angles through telescopes that are shared between the two lidar subsystems. The hybrid concept includes a coherent detection system at the 2-μm wavelength for aerosol return and a double-edge direct detection at the 355-nm wavelength for molecular return. In the GWOS design, scanning is achieved by switching between four fixed conventional telescopes, thus reducing technology risk, angular momentum transients, and power that would be required for scanning a full telescope. Marx et al. (2010) at NASA GSFC have recently completed the build and test of a prototype for the GWOS four-look telescope system. Figure 12 shows the geometry for the GWOS mission concept as an example for an orbiting spacecraft with a DWL; a detailed explanation may be found in the supplemental material, and Fig. 13 illustrates the nominal 24-h GWOS data coverage from sun-synchronous orbit.

The WISSCR concepts. In late 2010/early 2011, an Instrument Design Laboratory (IDL)/Mission Design

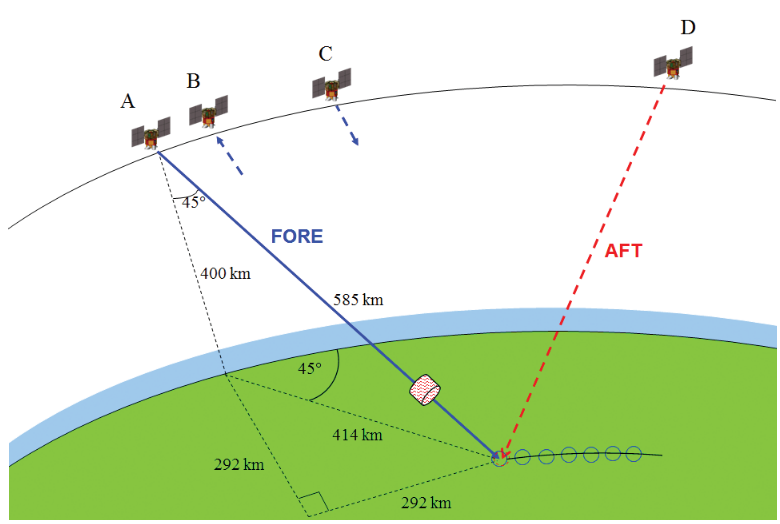

Fig. 12. The orbital geometry for the GWOS mission concept. Points A–D are defined as follows: A is the first forward +45°-azimuth laser shot fired into the atmospheric sample volume; B is the backscattered light from the first shot received from Earth's surface and the conclusion of the atmospheric return from the first shot; C is the second forward +45°-azimuth laser shot fired; and D is the first aft +135°-azimuth laser shot fired into the same atmospheric sample volume about 81 s after position A. Not drawn to scale.

Laboratory (MDL) study was conducted at GSFC to determine the feasibility of using the International Space Station for a DWL mission referred to as the WISSCR concept (Emmitt et al. 2011b). This study and a subsequent WISSCR-like study conducted in 2012 to investigate the feasibility of deploying OAWL on the International Space Station (ISS) are described in the supplemental material.

Comparison of three DWL space-based approaches. Table 1 compares some attributes of the ADM-Aeolus system concept with the GWOS and WISSCR concepts. As a demonstration mission, ADM-Aeolus has a single-perspective view of the target volume and only measures winds along a single line-of-sight from the satellite, whereas GWOS and WISSCR would provide two perspectives into the measurement volume. Horizontal resolution in the table refers to along-track spacing between observations. ADM-Aeolus and WISSCR make measurements along a single track, whereas GWOS makes measurements along two tracks, one on each side of the orbital track. Because ADM-Aeolus will be deployed in sun-synchronous orbit, important science questions can be addressed for both the tropics and the polar regions.

CONCLUDING REMARKS. In recent years, our understanding of the important role that a space-based DWL would have in the global observing system has reached the point where we are confident major advances would result in both NWP applications and climate change research. ESA's ADM-Aeolus DWL, with its single line-of-sight wind measurements, now scheduled for launch in 2015, will be a significant step forward. The two-perspective DWL concepts currently being investigated will build on the initial ESA deployment. Opportunities such as NASA's Earth Venture class of missions in the Earth System Science Pathfinder program (see

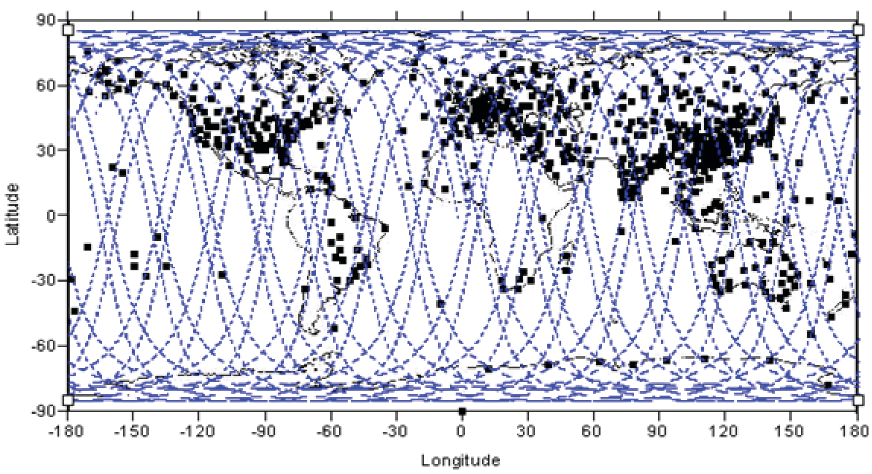

Fig. 13. The 24-h measurement coverage for GWOS, along with the locations of radiosondes collected during a 24-h period. There are two parallel data tracks for GWOS, provided by its four fixed telescopes, with a pair of fore and aft telescopes viewing the atmospheric measurement volume on each side of the spacecraft. Data coverage would be the same for ADM, but with a single data track and a single perspective. Similarly for WIISCR, there would be one data track (with both fore and aft perspectives) but within ±54° of latitude, given the 51.6° ISS orbit.

Table 1. Comparison of some key attributes for ADM-Aeolus, GWOS, and WISSCR.

Attribute	ADM-Aeolus	GWOS	WISSCR
Orbit altitude (km)	400	400	350–400
Orbit inclination	98° sun-synchronous	98° sun-synchronous	51.6°
Number of LOS	1	4	2
Profiles per orbit	~460 single-component profiles	~229 horizontal vectors	~110 vectors (low resolution) ~880 vectors (high resolution)
Horizontal resolution	~100 km between single-component profiles on one side of ground track	350 km with full profile on both sides of ground track	Variable (~30–350 km) with full profiles on one side of ground track
Vertical resolution (km)	PBL: 0.25–0.5 Troposphere: 1 Stratosphere: 2	PBL: 0.25–0.5 Troposphere: 1–2 Stratosphere: 2	PBL: 0.25–0.5 Troposphere: 1–2 Stratosphere: 2

http://science.nasa.gov/about-us/smd-programs/earth-system-science-pathfinder/) are being pursued with the goal of deploying a U.S. space-based DWL as soon as possible.

ACKNOWLEDGMENTS. The authors thank Dr. Ramesh Kakar of the Earth Science Division at NASA headquarters and Dr. George Komar of the NASA Earth Science Technology Office at the Goddard Space Flight Center for supporting research with DWL data, including airborne campaigns, and funding hardware risk reduction studies to advance the readiness of the DWL technology for space. The authors thank Dr. John Cortinas and NOAA's Office of Weather and Air Quality for contributing to the support for DWL OSSEs through NOAA's OSSE Testbed. The expert assistance of Paul Berrisford of ECMWF is sincerely acknowledged. Sidney Wood and Steven Greco of Simpson Weather Associates (SWA) are acknowledged for their dedication to producing simulated space-based DWL observations used in the OSSEs and processing and analyzing data from the U.S. Navy's airborne DWL. Funding for manuscript preparation and submission was provided by SWA. M. Weissmann is part of the Hans-Ertel Centre for Weather Research, a network of universities, research institutes, and Deutscher Wetterdienst funded by the German Federal Ministry of Transport, Building and Urban Development.

The manuscript was significantly improved by addressing the comments of three anonymous reviewers. Prof. Richard Somerville and Dr. Ross Hoffman also provided valuable comments.

REFERENCES

Andersson, E., and M. Masutani, 2010: Collaboration on observing system simulation experiments (Joint OSSE). *ECMWF Newsletter,* No. 123, ECMWF, Reading, United Kingdom, 14–16.

Ansmann, A., U. Wandinger, O. Le Rille, D. Lajas, and A. G. Straume, 2007: Particle backscatter and extinction profiling with the spaceborne high-spectral-resolution Doppler lidar ALADIN: Methodology and simulations. *Appl. Opt.,* **46,** 6606–6622, doi:10.1364/AO.46.006606.

Anthes, R. A., and Coauthors, 2008: The COSMIC/FORMOSAT-3 mission: Early results. *Bull. Amer. Meteor. Soc.,* **89,** 313–333.

Atlas, R., 1997: Atmospheric observations and experiments to assess their usefulness in data assimilation. *J. Meteor. Soc. Japan,* **75,** 111–130.

——, and G. D. Emmitt, 2008: Review of observing system simulation experiments to evaluate the potential impact of lidar winds. *24th International Laser Radar Conference 2008 (ILRC24),* Vol. 2, Curran Associates, 726–729.

——, and L. P. Riishojgaard, 2008: Application of OSSEs to observing system design. *Remote Sensing System Engineering,* P. E. Ardanuy and J. J. Puschell, Eds., International Society for Optical Engineering (SPIE Proceedings, Vol. 7087), 708707, doi:10.1117/12.795344.

——, E. Kalnay, W. E. Baker, J. Susskind, D. Reuter, and M. Halem, 1985a: Simulation studies of the impact of future observing systems on weather prediction. Preprints, *Seventh Conf. on Numerical Weather Prediction,* Montreal, QC, Canada, Amer. Meteor. Soc., 145–151.

——, ——, and M. Halem, 1985b: Impact of satellite temperature sounding and wind data on numerical weather prediction. *Opt. Eng.,* **24,** 341–346.

——, A. Y. Hou, and O. Reale, 2005a: Application of SeaWinds scatterometer and TMI-SSM/I rain rates to hurricane analysis and forecasting. *J. Photogramm. Remote Sens.,* **59,** 233–243.

——, and Coauthors, 2005b: Hurricane forecasting with the high-resolution NASA finite volume general circulation model. *Geophys. Res. Lett.,* **32,** L03807, doi:10.1029/2004GL021513.

Baker, N. L., 2000: Observation adjoint sensitivity and the adaptive observation-targeting problem. Ph.D. dissertation, Naval Postgraduate School, 265 pp.

——, and R. H. Langland, 2008: Diagnostics for evaluating the impact of satellite observations. Recent developments in the use of satellite observations in numerical weather prediction, ECMWF Seminar Proceedings, 309–326.

——, and ——, 2009: Diagnostics for evaluating the impact of satellite observations. *Data Assimilation for Atmospheric, Oceanic and Hydrologic Applications,* S. K. Park and L. Xu, Eds., Springer, 177–196.

Baker, W. E., and Coauthors, 1995: Lidar-measured winds from space: A key component for weather and climate prediction. *Bull. Amer. Meteor. Soc.,* **76,** 869–888.

Banta, R. M., R. K. Newsom, J. K. Lundquist, Y. L. Pichugina, R. L. Coulter, and L. Mahrt, 2002: Nocturnal low-level jet characteristics over Kansas during CASES-99. *Bound.-Layer Meteor.,* **105,** 221–252.

Barker, D. M., W. Huang, Y.-R. Guo, A. J. Bourgeois, and Q. N. Xiao, 2004: A three-dimensional variational data assimilation system for MM5: Implementation and initial results. *Mon. Wea. Rev.,* **132,** 897–914.

Benedetti-Michelangeli, G., F. Congeduti, and G. Fiocco, 1972: Measurement of aerosol motion and wind velocity in the lower troposhere by Doppler optical radar. *J. Atmos. Sci.,* **29,** 906–910.

Bluestein, H. B., G. D. Emmitt, J. Houser, and R. Bluth, 2011: On the use of a mobile Doppler lidar to probe the boundary layer near and in tornadic and non-tornadic supercells. Preprints, *Fifth Symp. on Lidar Atmospheric Applications,* Seattle, WA, Amer. Meteor. Soc., 6.5. [Available online at https://ams.confex.com/ams/91Annual/webprogram/Paper179772.html.]

Braun, S., and Coauthors, 2013: NASA's Genesis and Rapid Intensification Processes (GRIP) Field Experiment. *Bull. Amer. Meteor. Soc.,* **94,** 345–363.

Bruneau, B., and J. Pelon, 2003: Simultaneous measurements of particle backscattering and extinction coefficients and wind velocity by lidar with a Mach-Zehnder interferometer: Principle of operation and performance assessment. *Appl. Opt.,* **42,** 1101–1114.

Bruneau, D., 2001: Mach-Zehnder interferometer as a spectral analyzer for molecular Doppler wind lidar. *Appl. Opt.,* **40,** 391–399.

——, 2002: Fringe-imaging Mach-Zehnder interferometer as a spectral analyzer for molecular Doppler wind lidar. *Appl. Opt.,* **41,** 503–510.

Cardinali, C., 2009: Monitoring the observation impact on the short-range forecast. *Quart. J. Roy. Meteor. Soc.,* **135,** 239–250.

——, S. Pezzulli, and E. Andersson, 2004: Influence-matrix diagnostic of a data assimilation system. *Quart. J. Roy. Meteor. Soc.,* **130,** 2767–2786.

Cézard, N., A. Dolfi-Bouteyre, J.-P. Huignard, and P. H. Flamant, 2009: Performance evaluation of a dual fringe-imaging Michelson interferometer for air parameter measurements with a 355 nm Rayleigh-Mie lidar. *Appl. Opt.,* **48,** 2321–2332.

Chanin, M. L., A. Garnier, A. Hauchecorn, and J. Porteneuve, 1989: A Doppler lidar for measuring winds in the middle atmosphere. *Geophys. Res. Lett.,* **16,** 1273–1276.

Chen, J. Y., B. E. Carlson, and A. D. Del Genio, 2002: Evidence for strengthening of the tropical general circulation in the 1990s. *Science,* **295,** 838–841.

Cress, A., and W. Wergen, 2001: Impact of profile observations on the German Weather Service's NWP system. *Meteor. Z.,* **10,** 91–101.

Dee, D. P., and S. Uppala, 2009: Variational bias correction of satellite radiance data in the ERA-Interim reanalysis. *Quart. J. Roy. Meteor. Soc.,* **135,** 1830–1841.

——, and Coauthors, 2011: The ERA-Interim reanalysis: Configuration and performance of the data assimilation system. *Quart. J. Roy. Meteor. Soc.,* **137,** 553–597.

Dehring, M. T., J. M. Ryan, P. B. Hays, B. Moore III, and J. Wang, 2005: GroundWinds balloon fringe-imaging Doppler lidar mission concept and instrument performance. *Lidar Remote Sensing for Industry and Environmental Monitoring V,* U. N. Singh and K. Mizutani, Eds., International Society for Optical Engineering (SPIE Proceedings, Vol. 5653), doi:10.1117/12.580170.

de Wekker, S. F. J., K. S. Godwin, G. D. Emmitt, and S. Greco, 2012: Airborne Doppler lidar measurements of valley flows in complex coastal terrain. *J. Appl. Meteor. Climatol.,* **51,** 1558–1574.

Dong, J., and Coauthors, 2010: Doppler lidar measurement of wind in the stratosphere. *J. Opt. Soc. Korea,* **14,** 199–203.

Emmitt, G. D., S. Greco, and S. Wood, 2010: Using an airborne Doppler wind lidar to explore the potential impact of a future space-based wind lidar, particularly in the case of tropical cyclones. Preprints, *14th Symp. on Integrated Observing and Assimilation Systems for the Atmosphere, Oceans, and Land Surface (IOAS-AOLS),* Atlanta, GA, Amer. Meteor. Soc., 1.3. [Available online at https://ams.confex.com/ams/90annual/techprogram/paper_165444.htm.]

——, Z. Pu, K. Godwin, and S. Greco, 2011a: Airborne Doppler wind lidar data impacts on tropical cyclone track and intensity forecasting: The data processing, interpretation and assimilation. Preprints, *15th Symp. on Integrated Observing and Assimilation Systems for the Atmosphere, Oceans and Land Surface (IOAS-AOLS),* Seattle, WA, Amer. Meteor. Soc., 9.2. [Available online at https://ams.confex.com/ams/91Annual/webprogram/Paper182343.html.]

——, S. A. Wood, M. J. Kavaya, B. Gentry, and W. Baker, 2011b: Technology and data utility challenges for a Doppler wind lidar on the International Space Station. Preprints, *15th Symp. on Integrated Observing and Assimilation Systems for the Atmosphere, Oceans, and Land Surface (IOAS-AOLS),* Seattle, WA, Amer. Meteor. Soc., 2.2. [Available online at https://ams.confex.com/ams/91Annual/webprogram/Paper182281.html.]

Endemann, M., 2006: ADM-Aeolus: The first spaceborne wind lidar. *Lidar Remote Sensing for Environmental Monitoring VII,* U. N. Singh, T. Itabe, and D. Narayana Rao, Eds., International Society for Optical Engineering (SPIE Proceedings, Vol. 6409), 64090G, doi:10.1117/12.697081.

ESA, 2008: ADM-Aeolus science report. P. Clissold, Ed., European Space Agency Rep. ESA SP-1311, 121 pp.

Flamant, P. H., J. Cuesta, M.-L. Denneulin, A. Dabas, and D. Huber, 2008: ADM-Aeolus retrieval algorithms for aerosol and cloud products. *Tellus,* **60A,** 273–286, doi:10.1111/j.1600-0870.2007.00287.x.

Garnier, A., and M. L. Chanin, 1992: Description of a Doppler Rayleigh lidar for measuring winds in the middle atmosphere. *Appl. Phys.,* **55B,** 35–40.

Gelaro, R., R. H. Langland, S. Pellerin, and R. Todling, 2010: The THORPEX observation impact intercomparison experiment. *Mon. Wea. Rev.,* **138,** 4009–4025.

Gentry, B. M., and C. L. Korb, 1994: Edge technique for high-accuracy Doppler velocimetry. *Appl. Opt.,* **33,** 5770–5777.

——, H. Chen, and S. X. Li, 2000: Wind measurements with 355-nm molecular Doppler lidar. *Opt. Lett.,* **25,** 1231–1233.

——, ——, J. Cervantes, R. Machan, D. Reed, R. Cargo, C. Marx, and P. Jordan, 2011: Airborne testing of the TWiLiTE direct detection Doppler lidar. *16th Coherent Laser Radar Conference 2011 (CLRC XVI),* Curran Associates, 164–167.

Graversen, R. G., 2006: Do changes in the midlatitude circulation have any impact on the Arctic surface temperature trend? *J. Climate,* **19,** 5422–5438.

——, E. Källén, M. Tjernström, and H. Körnich, 2007: Atmospheric mass-transport inconsistencies in the ERA-40 reanalysis. *Quart. J. Roy. Meteor. Soc.,* **133,** 673–680.

——, T. Mauritsen, M. Tjernström, E. Källén, and G. Svensson, 2008: Vertical structure of recent Arctic warming. *Nature,* **451,** 53–56.

Grund, C. J., and S. C. Tucker, 2011: Optical Autocovariance Wind Lidar (OAWL): A new approach to direct-detection Doppler wind profiling. Preprints, *Fifth Symp. on Lidar,* Seattle, WA, Amer. Meteor. Soc., 4.9. [Available online at https://ams.confex.com/ams/91Annual/webprogram/Paper188184.html.]

——, R. M. Banta, J. L. George, J. N. Howell, M. J. Post, R. A. Richter, and A. M. Weickmann, 2001: High-resolution Doppler lidar for boundary layer and cloud research. *J. Atmos. Oceanic Technol.,* **18,** 376–393.

——, J. Howell, R. Pierce, M. Stephens, 2009: Optical autocovariance direct detection lidar for simultaneous wind, aerosol, and chemistry profiling from ground, air, and space platforms. *Advanced Environmental, Chemical, and Biological Sensing Technologies VI.* T. Vo-Dinh, R. A. Lieberman, and G. Gauglitz, Eds., International Society for Optical Engineering (SPIE Proceedings, Vol. 7312), doi:10.1117/12.824204.

Hannon, S. M., K. S. Barr, D. K. Jacob, and M. W. Phillips, 2005: Application of pulsed Doppler lidar in the airport terminal area. *Lidar Remote Sensing for Industry and Environmental Monitoring V,* S. M. Hannon et al., Eds., International Society for Optical Engineering (SPIE Proceedings Vol. 5653), doi:10.1117/12.579037.

Hansen, J., and L. Nazarenko, 2004: Soot climate forcing via snow and ice albedos. *Proc. Natl. Acad. Sci. USA,* **101,** 423–428, doi:10.1073/pnas.2237157100.

Hays, P. B., 1990: Circle to line interferometer optical system. *Appl. Opt.,* **29,** 1482–1489.

Henderson, S. W., P. Gatt, D. Rees, and R. M. Huffaker, 2005: Wind lidar. *Laser Remote Sensing,* T. Fujii and T. Fukuchi, Eds., Optical Science and Engineering Series, Vol. 97, CRC Press, 469–722.

Houchi, K., A. Stoffelen, G. J. Marseille, and J. de Kloe, 2010: Comparison of wind and wind shear climatologies derived from high-resolution radiosondes and the ECMWF model. *J. Geophys. Res.,* **115,** D22123, doi:10.1029/2009JD013196.

Hovis, F. E., 2006: Qualification of the laser transmitter for the CALIPSO aerosol lidar mission. *Solid State Lasers XV: Technology and Devices,* H. J. Hoffman and R. K. Shori, Eds., International Society for Optical Engineering (SPIE Proceedings, Vol. 6100), 61001X, doi:10.1117/12.659748.

Huffaker, R. M., and R. M. Hardesty, 1996: Remote sensing of atmospheric wind velocities using solid-state and CO_2 coherent laser systems. *Proc. IEEE,* **84,** 181–204.

——, A. V. Jelalian, and J. A. L. Thomson, 1970: Laser-Doppler system for detection of aircraft trailing vortices. *Proc. IEEE,* **58,** 322–326.

Hunt, W. H., D. M. Winker, M. A. Vaughan, K. A. Powell, P. L. Lucker, and C. Weimer, 2009: *CALIPSO* lidar description and performance assessment. *J. Atmos. Oceanic Technol.,* **26,** 1214–1228.

Irgang, T. D., P. B. Hays, and W. R. Skinner, 2002: Two-channel direct-detection Doppler lidar employing a charge-coupled device as a detector. *Appl. Opt.*, **41,** 1145–1155.

Källén, E., D. Tan, C. Cardinali, and P. Berrisford, 2010: Spaceborne Doppler wind lidars – Scientific Motivation and Impact Studies for ADM/Aeolus. *33rd Meeting of the Working Group on Space-Based Lidar Winds,* Destin, FL, CIRES. [Available online at http://cires.colorado.edu/events/lidarworkshop/LWG/Feb10/Papers.feb10/Kallen.feb10.ppt.]

Käsler, Y., S. Rahm, R. Simmet, and M. Kühn, 2010: Wake measurements of a multi-MW wind turbine with coherent long-range pulsed Doppler wind lidar. *J. Atmos. Oceanic Technol.,* **27,** 1529–1532.

Kavaya, M. J., S. W. Henderson, J. R. Magee, C. P. Hale, and R. M. Huffaker, 1989: Remote wind profiling with a solid-state Nd:YAG coherent lidar system. *Opt. Lett.,* **14,** 776–778.

——, J. Y. Beyon, G. J. Koch, M. Petros, P. J. Petzar, U. N. Singh, B. C. Trieu, and J. Yu, 2014: The Doppler Aerosol Wind Lidar (DAWN) airborne, wind-profiling, coherent-detection lidar system: Overview and preliminary flight results. *J. Atmos. Oceanic Technol.,* in press.

Key, J., D. Santek, C. S. Velden, N. Bormann, J.-N. Thepaut, L. P. Riishojgaard, Y. Zhu, and W. P. Menzel, 2003: Cloud-drift and water vapor winds in the polar regions from MODIS. *IEEE Trans. Geosci. Remote Sens.,* **41,** 482–492.

Kinne, S., and Coauthors., 2006: An AeroCom initial assessment—Optical properties in aerosol component modules of global models. *Atmos. Chem. Phys.*, **6**, 1815–1834.

Kistler, R., and Coauthors, 2001: The NCEP–NCAR 50–Year Reanalysis: Monthly means CD–ROM and documentation. *Bull. Amer. Meteor. Soc.,* **82,** 247–267.

Kleist, D. T., D. F. Parrish, J. C. Derber, R. Treadon, W.-S. Wu, and S. Lord, 2009: Introduction of the GSI into the NCEP Global Data Assimilation System. *Wea. Forecasting,* **24,** 1691–1705.

Korb, C. L., B. M. Gentry, S. X. Li, and C., 1998: Theory of the double-edge technique for Doppler lidar wind measurement. *Appl. Opt.,* **37,** 3097–3104.

Langland, R. H., and N. L. Baker, 2004: Estimation of observation impact using the NRL atmospheric variational data assimilation adjoint system. *Tellus,* **56A,** 189–201.

——, and R. N. Maue, 2012: Uncertainty in operational atmospheric analyses. *Proc. Fifth WMO Workshop on the Impact of Various Observing Systems on Numerical Weather Prediction,* Sedona, AZ, WMO. [Available online at www.wmo.int/pages/prog/www/OSY/Meetings/NWP5_Sedona2012/1a1_Langland.pdf.]

——, ——, and C. H. Bishop, 2008: Uncertainty in atmospheric temperature analyses. *Tellus,* **60A,** 598–603.

LeRille, O., M. Endemann, A. Culoma, and D. Wernham, 2012: ADM-Aeolus: ESA's high spectral resolution Doppler wind lidar mission: Recent achievements and future prospects. *Proc. 26th Int. Laser Radar Conf.,* Porto Heli, Greece, NASA, S4O-01.

Liu, Z., and T. Kobayashi, 1996: Differential discrimination technique for incoherent Doppler lidar to measure atmospheric wind and backscatter ratio. *Opt. Rev.,* **3,** 47–52.

Mankins, J. C., 1995: Technology readiness levels—A white paper. NASA, 5 pp. [Available online at www.hq.nasa.gov/office/codeq/trl/trl.pdf.]

Marseille, G.-J., A. Stoffelen, and J. Barkmeijer, 2007: Impact assessment of prospective spaceborne Doppler wind lidar observation scenarios. *Tellus,* **60A,** 234–248.

——, ——, and ——, 2008: A cycled sensitivity observing system experiment on simulated Doppler wind lidar data during the 1999 Christmas storm "Martin." *Tellus,* **60A,** 249–260, doi:10.1111/j.1600-0870.2007.00290.x.

Marx, C., B. Gentry, M. Kavaya, P. Jordan, and E. Faust, 2010: Hybrid Doppler Wind Lidar (HDWL) transceiver ACT project. *33rd Meeting of the Working Group on Space-Based Lidar Winds,* Destin, FL, CIRES. [Available online at http://cires.colorado.edu/events/lidarworkshop/LWG/Feb10/Papers.feb10/Marx.feb10.pdf.]

Masutani, M., and Coauthors, 2010: Observing system simulation experiments at the National Centers for Environmental Prediction. *J. Geophys. Res.,* **115,** D07101, doi:10.1029/2009JD012528.

McGill, M. J., W. R. Skinner, and T. D. Irgang, 1997a: Analysis techniques for the recovery of winds and backscatter coefficients from a multiple-channel incoherent Doppler lidar. *Appl. Opt.,* **36,** 1253–1268.

——, ——, and ——, 1997b: Validation of wind profiles measured with incoherent Doppler lidar. *Appl. Opt.,* **36,** 1928–1932.

——, M. Marzouk, V. S. Scott III, and J. D. Spinhirne, 1997c: Holographic circle-to-point converter with particular applications for lidar work. *Opt. Eng.,* **36,** 2171–2175, doi:10.1117/1.601437.

McKay, J. A., 1998: Modeling of direct detection Doppler wind lidar. II. The fringe imaging technique. *Appl. Opt.,* **37,** 6487–6493.

Mitas, C. M., and A. Clement, 2005: Has the Hadley cell been strengthening in recent decades? *Geophys. Res. Lett.,* **32,** L03809, doi:10.1029/2004GL021765.

——, and ——, 2006: Recent behavior of the Hadley cell and tropical thermodynamics in climate models and reanalyses. *Geophys. Res. Lett.,* **33,** L01810, doi:10.1029/2005GL024406.

Mitchell, J. M., 1956: Visual range in the polar regions with particular reference to the Alaskan Arctic. *J. Atmos. Terr. Phys.,* **1** (Suppl.), 195–211.

Miyakoda, K., R. D. Hembree, R. F. Strickler, and I. Shulman, 1972: Cumulative results of extended forecast experiments. I. Model performance for winter cases. *Mon. Wea. Rev.,* **100,** 836–855.

NRC, 2007: *Earth Science and Applications from Space: National Imperatives for the Next Decade and Beyond.* The National Academies Press, 456 pp.

Ota, Y., J. C. Derber, E. Kalnay, and T. Miyoshi, 2013: Ensemble-based observation impact estimates using the NCEP GFS. *Tellus,* **65A,** 20038, doi:10.3402/tellusa.v65i0.20038.

Paffrath, U., C. Lemmerz, O. Reitebuch, B. Witschas, I. Nikolaus, and V. Freudenthaler, 2009: The airborne demonstrator for the direct-detection Doppler wind lidar ALADIN on ADM-Aeolus. Part II: Simulations and Rayleigh receiver radiometric performance. *J. Atmos. Oceanic Technol.,* **26,** 2516–2530.

Petzar, P., and Coauthors, 2010: Field testing of a high-energy 2-mm Doppler lidar. *J. Appl. Remote Sens.,* **4,** 043512, doi:10.1117/1.3368726.

Post, M. J., and R. E. Cupp, 1990: Optimizing a pulsed Doppler lidar. *Appl. Opt.,* **29,** 4145–4158.

Pu, Z., B. Gentry, and B. B. Demoz, 2009: Potential impact of lidar wind measurements on high-impact weather forecasting: A regional OSSEs study. Preprints, *13th Conf. on Integrated Observing Systems for Atmosphere, Ocean, and Land Surface (IOAS-AOLS),* Phoenix, AZ, Amer. Meteor. Soc., 13.5. [Available online at https://ams.confex.com/ams/89annual/techprogram/paper_150417.htm.]

——, L. Zhang, and G. D. Emmitt, 2010: Impact of airborne Doppler wind lidar profiles on numerical simulations of a tropical cyclone. *Geophys. Res. Lett.,* **37,** L05801, doi:10.1029/2009GL041765.

Quinn, P. K., and Coauthors, 2007: Arctic haze: Current trends and knowledge gaps. *Tellus,* **59B,** 99–114.

Reitebuch, O., 2012a: The spaceborne wind lidar mission ADM-Aeolus. *Atmospheric Physics: Background, Methods, Trends,* U. Schumann, Ed., Springer Series on Research Topics in Aerospace, 815–827.

——, 2012b: Wind lidar for atmospheric research. *Atmospheric Physics: Background, Methods, Trends,* U. Schumann, Ed., Springer Series on Research Topics in Aerospace, 487–507.

——, C. Lemmerz, E. Nagel, U. Paffrath, Y. Durand, M. Endemann, F. Fabre, and M. Chaloupy, 2009: The airborne demonstrator for the direct-detection Doppler wind lidar ALADIN on ADM-Aeolus. Part I: Instrument design and comparison to satellite instrument. *J. Atmos. Oceanic Technol.,* **26,** 2501–2515.

Riishojgaard, L. P., Z. Ma, M. Masutani, J. S. Woollen, G. D. Emmitt, S. A. Wood, and S. Greco, 2012: Observation system simulation experiments for a global wind observing sounder. *Geophys. Res. Lett.,* **39,** L17805, doi:10.1029/2012GL051814.

Rothermel, J., and Coauthors, 1998: Remote sensing of multi-level wind fields with high-energy airborne scanning coherent Doppler lidar. *Opt. Express,* **2,** 40–50.

Sawruk, N. W., and Coauthors, 2013: Space qualified laser transmitter for NASA's ICESat-2 mission. *Solid State Lasers XXII: Technology and Devices,* W. A. Clarkson and R. Shori, Eds., International Society for Optical Engineering (SPIE Proceedings, Vol. 8599), 85990O, doi:10.1117/12.2005590.

Schillinger, M., D. Morancais, F. Fabre, and A. Culoma, 2003: ALADIN: The lidar instrument for the Aeolus mission. *Sensors, Systems, and Next-Generation Satellites VI,* H. Fujisada et al., Eds., International Society for Optical Engineering (SPIE Proceedings, Vol. 4881), 40, doi:10.1117/12.463024.

Schwiesow, R. L., and S. D. Mayor, 1995: Coherent optical signal processing for a Doppler lidar using a Michelson interferometer. *Tech. Dig. Ser.–Opt. Soc. Amer.,* **19,** 212–215.

Shaw, G. E., 1995: The Arctic haze phenomenon. *Bull. Amer. Meteor. Soc.,* **76,** 2403–2413.

Siegman, A. E., 1966: The antenna properties of optical heterodyne receivers. *Appl. Opt.,* **5,** 1588–1594.

Simmons, A. J., K. M. Willett, P. D. Jones, P. W. Thorne, and D. P. Dee, 2010: Low-frequency variations in surface atmospheric humidity, temperature, and precipitation: Inferences from reanalyses and monthly gridded observational data sets. *J. Geophys. Res.,* **115,** D01110, doi:10.1029/2009JD012442.

Skamarock, W. C., J. B. Klemp, J. Dudhia, D. O. Gill, D. M. Barker, W. Wang, and J. G. Powers, 2005: A description of the Advanced Research WRF version 2. NCAR Tech. Note NCAR/TN-4681STR, 88 pp.

Stoffelen, A., and Coauthors, 2005: The atmospheric dynamics mission for global wind measurement. *Bull. Amer. Meteor. Soc.,* **86,** 73–87.

——, G.-J. Marseille, F. Bouttier, D. Vasiljevic, S. de Haan, and C. Cardinali, 2006: ADM-Aeolus Doppler wind lidar observation system simulation experiment. *Quart. J. Roy. Meteor. Soc.,* **132,** 1927–1947.

——, ——, J. de Kloe, K. Houchi, H. Körnich, and N. Žagar, 2008: Scientific preparations for Aeolus and Aeolus follow-on. *Ninth Int. Winds Workshop,* Annapolis, MD, EUMETSAT, 8 pp. [Available online at www.knmi.nl/publications/fulltexts/dwl_9iww.pdf.]

Tan, D. G. H., E. Andersson, M. Fisher, and L. Isaksen, 2007: Observing system impact assessment using a data assimilation ensemble technique: Application to the ADM-Aeolus wind profiling mission. *Quart. J. Roy. Meteor. Soc.,* **133,** 381–390.

Trenberth, K. E., 1997: Using atmospheric budgets as a constraint on surface fluxes. *J. Climate,* **10,** 2796–2809.

Tucker, S. C., C. J. Senff, A. M. Weickmann, W. A. Brewer, R. M. Banta, S. P. Sandberg, D. C. Law, and R. M. Hardesty, 2009: Doppler lidar estimation of mixing height using turbulence, shear, and aerosol profiles. *J. Atmos. Oceanic Technol.,* **26,** 673–688.

——, C. Grund, T. Delker, M. Adkins, B. Good, P. Kaptchen, and D. Gleeson, 2012: Wind profiling with the optical autocovariance wind lidar: Results of validation testing. *Second Conf. on Transition of Research to Operations: Successes, Plans, and Challenges,* New Orleans, LA, Amer. Meteor. Soc., TJ10.2. [Available online at https://ams.confex.com/ams/92Annual/webprogram/Paper202733.html.]

Uppala, S. M., and Coauthors, 2005: The ERA-40 Re-Analysis. *Quart. J. Roy. Meteor. Soc.,* **131,** 2961–3012.

Vecchi, G. A., B. J. Soden, A. T. Wittenberg, I. M. Held, A. Leetmaa, and M. J. Harrison, 2006: Weakening of tropical Pacific atmospheric circulation due to anthropogenic forcing. *Nature*, **441**, 73–76.

Vermeesch, K., B. Gentry, G. Koch, M. Boquet, H. Chen, U. Singh, B. Demoz, and T. Bacha, 2011: Comparison of wind measurements at the Howard University Beltsville Research Campus. Preprints, *Fifth Symp. on Lidar Atmospheric Applications,* Seattle, WA, 4.4. [Available online at https://ams.confex.com/ams/91Annual/webprogram/Paper181653.html.]

Wagener, T. J., N. Demma, J. D. Kmetec, and T. S. Kubo, 1995: 2-mm lidar for laser-based remote sensing: Flight demonstration and application survey. *IEEE Aerosp. Electron. Syst. Mag.,* **10,** 23–28.

Weimer, C., R. Schwiesow, and M. LaPole, 2004: CALIPSO: Lidar and Wide-field camera performance. *Earth Observing Systems IX,* W. L. Barnes and J. J. Butler, Eds., International Society for Optical Engineering (SPIE Proceedings, Vol. 5542), 74, doi:10.1117/12.561613.

Weissmann, M., and C. Cardinali, 2007: Impact of airborne Doppler lidar observations on ECMWF forecasts. *Quart. J. Roy. Meteor. Soc.,* **133,** 107–116.

——, R. Busen, A. Dörnbrack, S. Rahm, and O. Reitebuch, 2005: Targeted observations with an airborne wind lidar. *J. Atmos. Oceanic Technol.,* **22,** 1706–1719.

——, R. H. Langland, C. Cardinali, P. M. Pauley, and S. Rahm, 2012: Influence of airborne Doppler wind lidar profiles near Typhoon Sinlaku on ECMWF and NOGAPS forecasts. *Quart. J. Roy. Meteor. Soc.,* **138,** 118–130.

Werner, C., 2004: Doppler wind lidar. *Lidar: Range-Resolved Optical Remote Sensing of the Atmosphere,* C. Weitkamp, Ed., Springer Series in Optical Sciences, Vol. 102, Springer, 325–354.

Winker, D. M., J. Pelon, and M. P. McCormick, 2003: The CALIPSO mission: Spaceborne lidar for obervation of aerosols and clouds. Lidar Remote Sensing for Industry and Environment Monitoring III, U. N. Singh, T. Itabe, and Z. Lui, Eds., International Society for Optical Engineering (SPIE Proceedings, Vol. 4893), 1–11.

——, W. H. Hunt, and M. J. McGill, 2007: Initial performance assessment of CALIOP. *Geophys. Res. Lett.,* **34,** L19803, doi:10.1029/2007GL030135.

Wood, S. A., Jr., G. D. Emmitt, and S. Greco, 2000: DLSM: A coherent and direct detection lidar simulation model for simulating space-based and aircraft-based lidar winds. *Laser Radar Technology and Applications V,* G. W. Kamerman et al., Eds., International Society for Optical Engineering (SPIE Proceedings, Vol. 4035), 2, doi:10.1117/12.397788.

WMO, 1996: Guide to meteorological instruments and methods of observation. 6th ed. WMO-8, 681 pp.

——, cited 2012a: Statement of Guidance for Global Numerical Weather Prediction (NWP). [Available online at www.wmo.int/pages/prog/www/OSY/GOS-RRR.html.]

——, 2012b: WIGOS: WMO Integrated Global Observing System; Final report of the Fifth WMO Workshop on the Impact of Various Observing Systems on Numerical Weather Prediction. WMO Tech. Rep. 2012-1, 23 pp.

Yang, X.-Y., J. C. Fyfe, G. M. Flato, 2010: The role of poleward energy transport in Arctic temperature evolution. *Geophys. Res. Lett.,* **37,** L14803, doi:10.1029/2010GL043934.

Žagar, N., N. Gustafsson, and E. Källén, 2004: Dynamical response of equatorial waves in four-dimensional variational data assimilation. *Tellus,* **56A**, 29–46.

——, A. Stoffelen, G.-J. Marseille, C. Accadia, and P. Schlüssel, 2008: Impact assessment of simulated Doppler wind lidars with a multivariate variational assimilation in the tropics. *Mon. Wea. Rev.,* **136,** 2443–2460.

Zhang, L., and Z. Pu, 2010: An observing system simulation experiment (OSSE) to assess the impact of Doppler wind lidar (DWL) measurements on the numerical simulation of a tropical cyclone. *Adv. Meteor.,* **2010,** 743863, doi:10.1155/2010/743863.

OCEAN WIND SPEED CLIMATOLOGY FROM SPACEBORNE SAR IMAGERY

BY FRANK M. MONALDO, XIAOFENG LI, WILLIAM G. PICHEL, AND CHRISTOPHER R. JACKSON

The authors discuss the potential generation of a >10-yr archive of *Radarsat-1* synthetic aperture radar wind speed data and its use to compute wind speed climatologies.

SAR WIND SPEED RETRIEVAL. The capacity to retrieve high-resolution (<500 m) winds from spaceborne synthetic aperture radar (SAR) imagery has matured significantly over the past decade (Dagestad et al. 2012). The retrieved speeds have been shown to have standard deviations of less than 2 m s^{-1} when compared to buoys and other independent measures (Horstmann et al. 1998; Monaldo et al. 2004; Yang et al. 2011; Thompson et al. 2012). Calibrated SAR radar cross section imagery is being converted to wind speed operationally at the National Oceanic and Atmospheric Administration (NOAA) to aid the National Weather Service (NWS). SAR wind data are also used to aid in offshore wind power siting (Christiansen and Hasager 2005; Christiansen et al. 2006) and applied to study the spatial variability of wind fields, particularly in coastal areas (Loescher et al. 2006).

Microwave measurement of winds from space is not new. The wind archives available from scatterometer satellites such as the Quick Scatterometer (QuikSCAT) and Advanced Scatterometer (ASCAT) provide important global data. However, scatterometer data have resolutions from 12 to 50 km (i.e., one to two orders of magnitude coarser that SAR winds). They are less valuable in coastal areas. SAR winds and conventional scatterometer winds are properly seen as complimentary.

The record of *Radarsat-1* and *Envisat* SAR imagery extends for over a decade and newer satellites [e.g., *Radarsat-2*, COSMO-SkyMed, and *TerraSAR-X*] are beginning to be used for wind speed retrieval. In early 2014, we expect the launch of Sentinel-1 by the European Space Agency, providing imagery on a free and open operational basis.

For over 12 years, NOAA conducted an application demonstration of near real-time SAR wind speed retrieval using *Radarsat-1* data. The software and protocols for this processing, known as the

AFFILIATIONS: MONALDO—The Johns Hopkins University Applied Physics Laboratory, Laurel, Maryland; LI—GST at the National Oceanic and Atmospheric Administration, College Park, Maryland; PICHEL—National Oceanic and Atmospheric Administration, College Park, Maryland; JACKSON—Global Ocean Associates, Alexandria, Virginia
CORRESPONDING AUTHOR: Frank M. Monaldo, The Johns Hopkins University Applied Physics Laboratory, 11100 Johns Hopkins Road, Laurel, MD 20723
E-mail: frank.monaldo@jhuapl.edu

The abstract for this article can be found in this issue, following the table of contents.

DOI:10.1175/BAMS-D-12-00165.1

In final form 27 June 2013

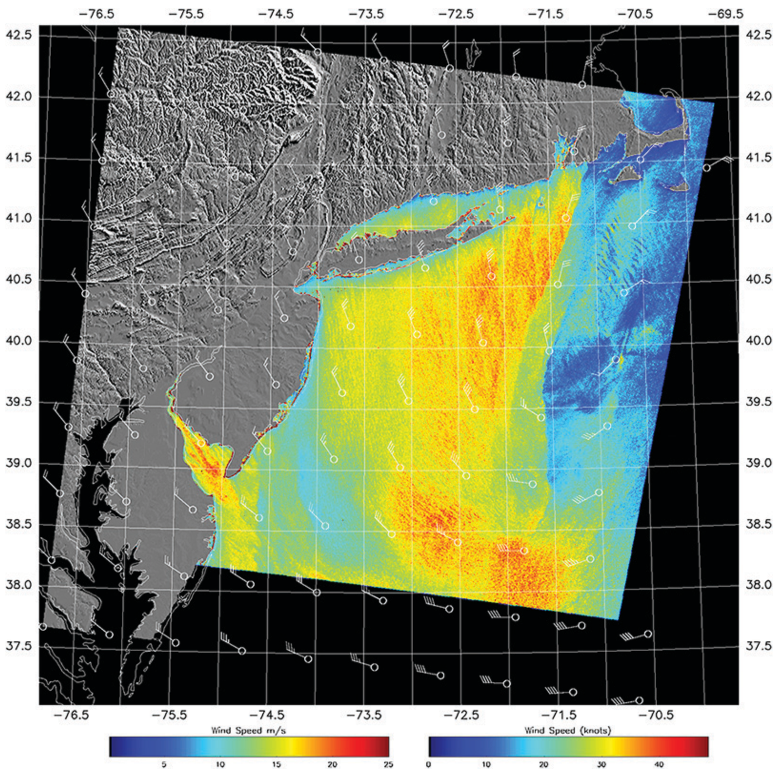

Fig. 1. *Radarsat-1* SAR wind speed retrieval off the U.S. East Coast (including Maryland and Delaware) on 10:58:02 UTC 21 Jan 2001. This image shows winds blowing offshore toward the southeast. The wind barbs represent the National Centers for Environmental Prediction's Climate Forecast Reanalysis wind speed and direction for reference.

Applied Physics Laboratory (APL)/NOAA SAR Wind Retrieval System (ANSWRS), became operational at NOAA on 1 May 2013. At present, the dominant source of data for this system is *Radarsat-2* SAR, but we anticipate that soon Sentinel-1 data will provide the bulk of the data for operational use. Figure 1 is an example of a *Radarsat-1* wind speed image off the coast of Maryland on 21 January 2001 produced by ANSWRS. Wind speed is represented by the color scale shown in the figure.

The multiyear archive of *Radarsat-1* data offers the prospect of generating a high-resolution wind data archive. Now that robust, operational, validated, and well-documented software is available, we intend to generate a SAR wind data archive—particularly useful for wind power assessment. This short paper announces the intention to generate a SAR wind speed database from the *Radarsat-1* record, illustrates the ability to generate a local high-resolution climatology, and introduces issues concerning local climatologies.

The normalized radar cross section (NRCS) for side-looking radars is a function of wind speed and direction, as well as the radar frequency, polarization, and incident angle. However, a single NRCS value can correspond to many wind speed and direction pairs. Given a wind direction, wind speed can be inferred. The ANSWRS software uses wind directions provided by the NOAA NWS Global Forecast System (GFS) model plus the NRCS measurement to perform the inversion to wind speed.

There are a number of available, empirically-derived model functions relating wind speed and direction to NRCS. These functions not only reflect the actual NRCS and marine wind relationship, but also can subtly compensate for small NRCS measurement differences between different satellite SAR instruments. *Radarsat-1* operates at C-band (5-cm wavelength) and HH-polarization. We have found that CMOD4 (for VV-polarization) (Stoffelen and Anderson 1997) and the Thompson et al. (1999) polarization ratio to convert to HH-polarization produce wind speed retrievals most consistent with independent wind speed estimates of 10-m neutral stability winds (Monaldo et al. 2001, 2004). The Thompson polarization ratio function uses a parameter α, which we set to 0.6 to achieve this agreement.

Figure 2 is a comparison of SAR wind speeds retrieved using CMOD4 and the Thompson et al. (1999) polarization ratio with wind speeds estimated by NOAA's Climate Forecast System Reanalysis (CFSR). The area considered is off the coast of Maryland and Delaware (37.75°–39.00°N, 75.30°–74.75°W) covering the years 1996 to 2008 (Monaldo 2010). The data come from 1428 *Radarsat-1* images. There is almost no mean difference between the SAR and CFSR winds, and the probability density functions are similar. Hence, we chose this model function for this work.

SAMPLE WIND POWER CLIMATOLOGY.

The *Radarsat-1* SAR images off the east coast of Maryland and Delaware were processed to wind speed at 500-m averaging to average out any NRCS variations associated with ocean surface waves and alleviate the effects of image speckle noise. These swath data are then resampled onto a regular 500-m sampling grid to generate a mean wind speed field. As an initial effort, we averaged SAR wind retrievals

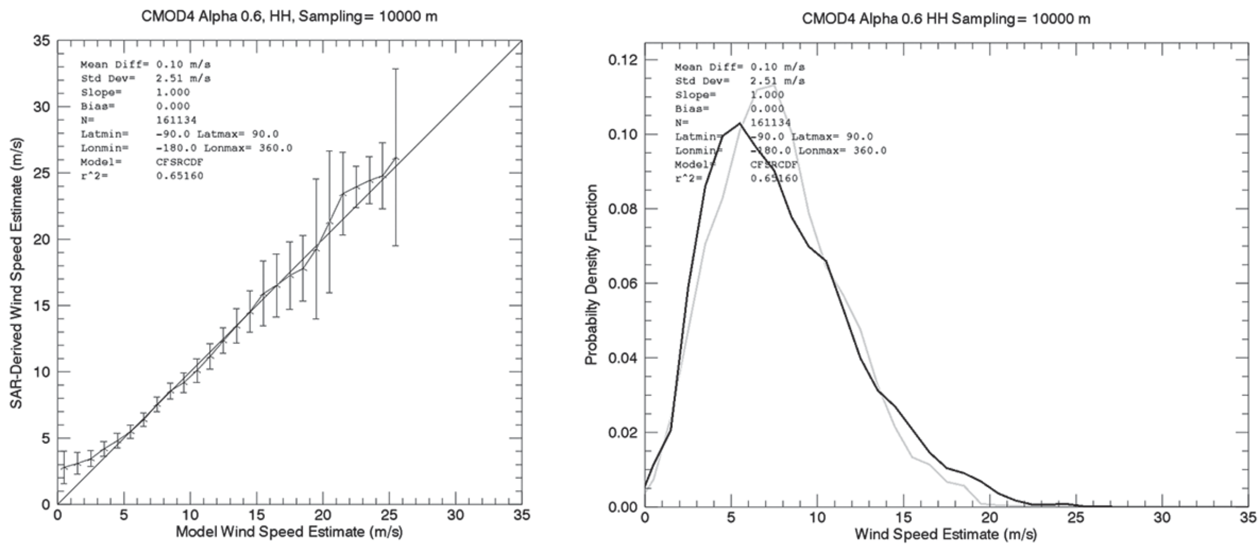

Fig. 2. Comparison of SAR-derived wind speeds with CFSR reanalysis winds normalized to 10 m for a neutral stability atmosphere. The left graph is SAR vs model winds, with 95% limit error bars. The right graph compares the two probability density functions. The thick line represents SAR data and the light-gray line is from the model wind speeds.

into 500 m × 500 m bins, and the mean wind at each sample in the grid was computed by averaging all the data available at any particular grid point from the entire multiyear *Radarsat-1* dataset.

We can relate the SAR-estimated wind speed at 10-m height to wind power at a hub height of 80 m with a standard logarithmic profile (Stull 1988). The potential wind power obtainable—the power flux—is related to wind speed by $P = \rho u^3/2$, where ρ is the air density and u is wind speed. Figure 3 shows the mean wind power density zooming in on a region bounded by 38.35°–39.00°N, 75.30°–74.75°W. Potential wind power clearly increases with distance from shore. The color green at 300 W m^{-2} represents a nominal threshold where harvesting wind power becomes economically feasible. It is interesting to note that wind power estimates are possible even in inland waters such as Rehoboth Bay.

Several factors complicate the use and interpretation of SAR measurement for wind speed climatology. For example, surface roughness can be influenced by factors in addition to wind speed. In Fig. 3 there is an area in the Delaware Bay with apparently high wind power potential. However, we believe the surface roughness in this region is associated with local currents induced by local gradients in bathymetry and not wind speed.

Second, any particular satellite samples the wind field at a place on Earth perhaps twice daily. Given diurnal variability, such sampling could bias the wind speed distribution. Third, wind speed retrievals have been best validated in the regime of 2 to 25 m s^{-1}. Eliminating retrievals beyond these limits

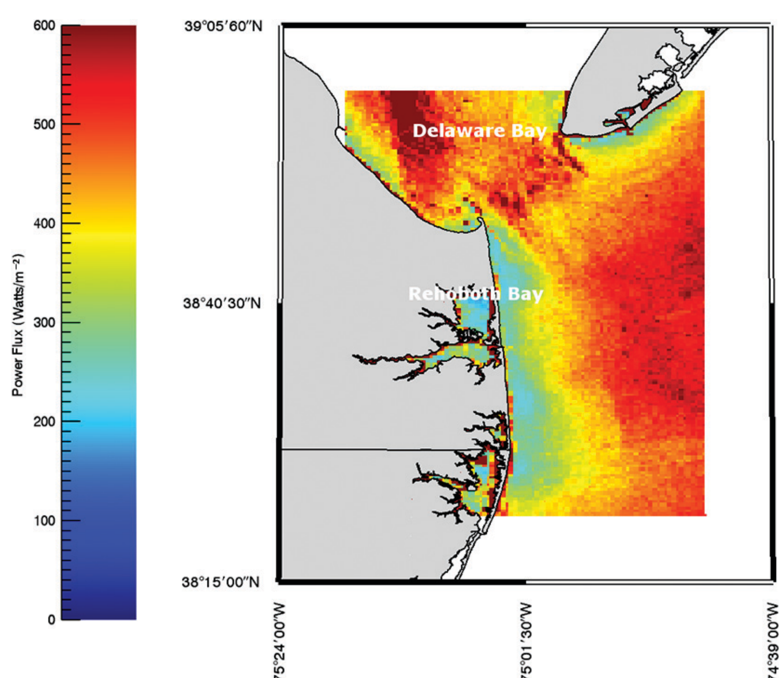

Fig. 3. The mean wind power flux density (W m^{-2}) off the coast of Maryland. Gray represents a land mask and power density is encoded as color. The color red represents 600 W m^{-2}.

could also bias the distribution. Finally, the number of wind speed measurements at a particular point—unlike buoy measurements, which are more continuous—limits the number of independent wind speed measurements.

Barthelmie and Pryor (2003), Pryor et al. (2004), and Barthelmie and Pryor (2006) have addressed these final three issues by analytic means and filtering research-quality buoy anemometer measurements from four different climatic regimes off the coast of North America to match the time and valid range limitations of SAR wind imagery. Within these constraints, they determined how well the moments of the filtered wind speed distribution compared with the moments computed from the entire anemometer database. The data from the filtered and unfiltered anemometer were fit with a Weibull distribution. They found that about 250 independent measurements (or SAR images) are required to fit the parameters of the Weibull wind distribution to the 90% confidence level.

The power flux density associated with wind speed (power/area) increases with the cube of wind speed. Hence, small errors in wind speed grow to fractionally greater errors in wind power. Pryor et al. (2004) performed a similar analysis with power density as with wind speed and found that, given limitations of sampling and limited wind speed range with remote sensors, approximately 1000 measurements (or SAR images) are required to estimate mean wind power flux density at the 90% confidence level.

An additional issue has also been considered. SAR wind retrievals have been tuned to produce wind speed estimates for 10 m above the surface for neutral atmospheric stability. While this is very useful for validation against buoy measurements, applying the results for wind power assessments requires estimating the wind speed at hub height. Badger et al. (2012) has found that combining SAR wind speed retrievals with model-derived wind profiles can, on average, produce accurate hub-height estimates. Even when a particular extrapolation is off, the mean height wind speed adjustment can successfully be made.

FUTURE. On 1 May 2013, NOAA near-real-time wind estimation with SAR became operational, with primary initial reliance on *Radarsat-2* data. Now that the wind speed product is operational, we plan to pursue a wind speed archive with retrospective data. The Alaska Satellite Facility at the University of Alaska, Fairbanks, has an extensive archive of *Radarsat-1* data from 1996 to 2008 (0.5 petabytes). These data were recently reprocessed into SAR imagery, using improved calibration, geolocation, and quality control techniques developed over a decade of processing experience.

The archive of *Radarsat-1* SAR imagery at the Alaska Satellite Facility is available to U.S. investigators. Now that SAR wind products are operational at NOAA, we anticipate the processing of this archive into wind speed data and determining which facility should host these data.

Using the previous research and lessons learned from computing the wind climatology for Maryland and Delaware, we intend to create a *Radarsat-1* wind speed dataset with the following characteristics:

Wind speed data will be stored in the common netCDF format with sufficient information to recompute wind speed as even better wind retrieval algorithms are developed.

High-resolution wind vector data from post-analysis NOAA GFS models will be stored as well, both as part of ongoing calibration/validation and to aid in the interpretation of SAR and model data.

Data from NOAA offshore moored buoys will be collocated and stored in the database.

Data will be posted online so that others may generate climatologies using different atmospheric vertical profile models and different averaging schemes.

ACKNOWLEDGMENTS. The views, opinions, and findings contained here are those of the authors and should not be construed as an official NOAA or U.S. Government position, policy, or decision.

REFERENCES

Badger, M., and Coauthors, 2012: Bringing satellite winds to hub-height. *Proc. EWEA 2012 European Wind Energy Conf.*, Copenhagen, Denmark, European Wind Energy Association. [Available online at http://proceedings.ewea.org/annual2012/allfiles2/979_EWEA2012presentation.pdf.]

Barthelmie, R. J., and S. C. Pryor, 2003: Can satellite sampling of offshore wind speeds realistically represent wind speed distributions? *J. Appl. Meteor.*, **42,** 83–94.

——, and ——, 2006: Challenges in predicting power output from offshore wind farms. *J. Energy Eng.*, **132,** 91–103.

Christiansen, M. B., and C. B. Hasager, 2005: Wake effects of large offshore wind farms identified from satellite SAR. *Remote Sens. Environ.*, **98,** 251–268.

——, ——, and F. M. Monaldo, 2006: Offshore winds observed from space: Issues for planning of offshore wind farms. *Windtech Int.*, **2** (5), 6–9.

Dagestad, K.-F., and Coauthors, 2012: Wind retrieval from synthetic aperture radar: An overview. *Proc. SEASAR 2012 Advances in SAR Oceanography,* Tromsø, Norway, European Space Agency, ESA SP-709.

Horstmann, J., W. Koch, S. Lehner, and W. Rosenthal, 1998: Ocean wind fields and their variability derived from SAR. *Earth Obs. Quart.,* **59,** 8–12.

Loescher, K. A., G. S. Young, B. A. Colle, and N. W. Winstead, 2006: Climatology of barrier jets along the Alaska Coast. Part I: Spatial and temporal distributions. *Mon. Wea. Rev.,* **134,** 437–452.

Monaldo, F. M., 2010: Maryland offshore wind climatology with application to wind power generation. Tech. Rep. SRO-10-10, Johns Hopkins Applied Physics Laboratory, 33 pp.

——, D. R. Thompson, R. C. Beal, W. G. Pichel, and P. Clemente-Colón, 2001: Comparison of SAR-derived wind speed with model predictions and buoy comparisons. *IEEE Trans. Geosci. Remote Sens.,* **39,** 2587–2600.

——, ——, W. G. Pichel, and P. Clemente-Colón, 2004: A systematic comparison of QuikSCAT and SAR ocean surface wind speeds. *IEEE Trans. Geosci. Remote Sens.,* **42,** 283–291.

Pryor, S. C., M. Nielsen, R. J. Barthelmie, and J. Mann, 2004: Can satellite sampling of offshore wind speeds realistically represent wind speed distributions? Part II: Quantifying uncertainties associated with distribution fitting methods. *J. Appl. Meteor.,* **43,** 739–750.

Stoffelen, A. C. M., and D. L. T. Anderson, 1997: Scatterometer data interpretation: Estimation and validation of the transfer function CMOD4. *J. Geophys. Res.,* **102** (C3), 5767–5780.

Stull, R. B., 1988: *An Introduction to Boundary Layer Meteorology.* 1st ed. Kluwer Academic, 666 pp.

Thompson, D. R., T. M. Elfouhaily, and B. Chapron, 1999: Polarization ratio for microwave backscattering from the ocean surface at low to moderate incidence angles. *Proc. 1999 Int. Geoscience and Remote Sensing Symp.,* Seattle, WA, IEEE, 1671–1673.

——, J. Horstmann, A. Mouche, N. S. Winstead, R. Sterner, and F. M. Monaldo, 2012: Comparison of high-resolution wind fields extracted from TerraSAR-X SAR imagery with predictions from the WRF mesoscale model. *J. Geophys. Res.,* **117,** C02035, doi:10.1029/2011JC007526.

Yang, X., X. Li, W. G. Pichel, and Z. Li, 2011: Comparison of ocean surface winds from Envisat ASAR, Metop ASCAT scatterometer, buoy measurements and NOGAPS model. *IEEE Trans. Geosci. Remote Sens.,* **49,** 4743–4750, doi:10.1109/TGRS.2011.2159802.

CMIP5 CLIMATE MODEL ANALYSES

Climate Extremes in the United States

BY DONALD WUEBBLES, GERALD MEEHL, KATHARINE HAYHOE, THOMAS R. KARL, KENNETH KUNKEL, BENJAMIN SANTER, MICHAEL WEHNER, BRIAN COLLE, ERICH M. FISCHER, RONG FU, ALEX GOODMAN, EMILY JANSSEN, VIATCHESLAV KHARIN, HUIKYO LEE, WENHONG LI, LINDSEY N. LONG, SETH C. OLSEN, ZAITAO PAN, ANJI SETH, JUSTIN SHEFFIELD, AND LIQIANG SUN

CMIP5 model simulations of historical and projected climate extremes in the United States are assessed.

This is the fourth in a series of *BAMS* articles on climate extremes in the United States (U.S.). These papers are based on workshops where leading scientists in the field came together to determine how best to assess the state of the science in understanding long-term climate variability and changes in various types of extreme events affecting the United States. The first workshop focused on severe local storms (Kunkel et al. 2013). The second workshop focused on the larger-scale phenomena of heat waves, cold waves, floods, and drought (Peterson et al. 2013). The third workshop examined the current understanding of coastal issues, including observed trends in winds, waves, and extratropical storms (Vose et al. 2014). One of the outcomes of those workshops and the resulting papers was the collective assessment of the state of knowledge regarding changes in various climate extremes (Fig. 1). The

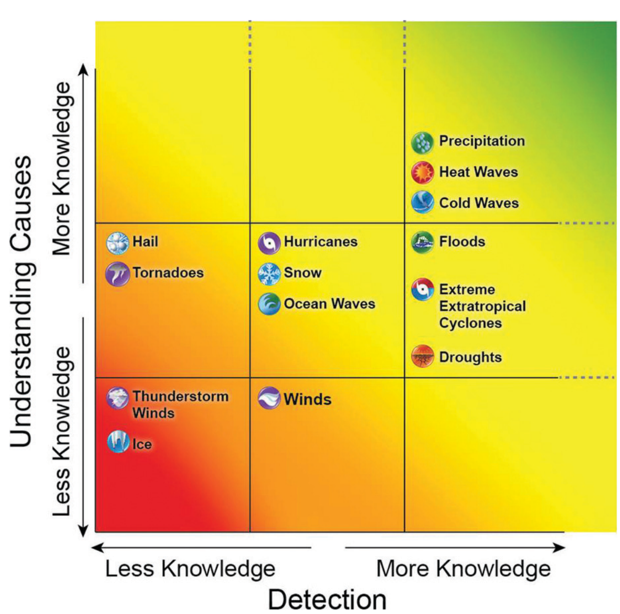

FIG. 1. The collective assessment of the state of knowledge regarding changes in various extreme events from the three earlier climate extremes workshops (Kunkel et al. 2013; Peterson et al. 2013; Vose et al. 2014). This graphic is based on the assumption that detection and attribution of changes in extremes depend on scientists' physical understanding of the factors that cause a particular extreme, as well as on factors that may cause the intensity or frequency of that extreme to change over time and the quality and quantity of the data. The *x* axis refers to the adequacy of data to detect trends while the *y* axis refers to the scientific understanding of what drives those trends—that is, how well the physical processes are understood, and thus how the extremes are expected to change in the future. For each axis, the type of event is assigned to one of three categories of knowledge (from less to more). The dashed lines on the right side and top of the graph imply that the knowledge about the phenomena is not complete.

findings in these workshops also strongly correlate with the global findings in the recent Intergovernmental Panel on Climate Change (IPCC) special report on extreme events (Field et al. 2012; often termed the SREX report).

The previous three workshops focused on the state of current knowledge regarding observed trends in, and drivers of, extreme events. The fourth workshop, the World Climate Research Programme (WCRP) Workshop on phase 5 of the Coupled Model Intercomparison Project (CMIP5) Climate Model Analyses held in March 2012, focused on the ability of the latest generation of climate models to capture observed trends and features of the physical climate system. Our intent in this paper is to assess the latest scientific understanding of CMIP5 model ability to simulate observed and future trends in climate extremes; it is not our intention to provide a complete summary of the entire body of work presented at the WCRP workshop, nor are we able to summarize results from other climate model experiments external to the CMIP5 experiment. For consistency with the previous three workshops, this assessment is limited to those papers presented at that workshop that specifically focused on climate and extreme events relevant to the U.S. With its geographic focus on the U.S., this paper also contributes the ongoing U.S. National Climate Assessment (www.globalchange.gov/what-we-do/assessment).

CMIP EXPERIMENTS. With participation from over 20 modeling groups and more than 40 global models, CMIP5 represents the latest and most ambitious coordinated international climate model intercomparison exercise to date (Taylor et al. 2012). CMIP5 includes a wide range of experiments addressing cloud feedbacks, carbon cycle feedbacks, and paleoclimate. Here, we focus on simulations of the twentieth century based on natural and anthropogenic forcings and the twenty-first century (with extensions to 2300) based on four new scenarios called representative concentration pathways (RCPs; Meehl and Hibbard 2007; Hibbard et al. 2007; Moss et al. 2010; van Vuuren et al. 2011).

Phase 3 of the Coupled Model Intercomparison Project (CMIP3) was the first coordinated international set of climate model experiments to include twentieth- and twenty-first-century experiments (Meehl et al. 2005, 2007). The IPCC's third and fourth Assessment Reports (TAR and AR4) were largely based on CMIP3 simulations. Given the increases in spatial resolution and other improvements in climate modeling capabilities over the last decade since the CMIP3 simulations were completed, CMIP5 provides a unique opportunity to assess scientific understanding of climate variability and change over a range of historical and future conditions.

Despite increases in model resolution and complexity, projected patterns and magnitudes of future temperature and precipitation changes are not substantially different from CMIP3 to CMIP5, both globally and over North America, when differences in forcings are accounted for. Estimates of climate sensitivity (Andrews et al. 2012) and hence the range in future projections due to uncertainty in climate sensitivity is also largely unchanged (Knutti and Sedláček 2012).

To put the new RCP scenarios and CMIP5 models in context, Fig. 2 compares historical simulated and projected future changes in annual-mean surface air temperature averaged over the contiguous United States (CONUS) for the period 1900–2100 as simulated by the CMIP3 model ensemble using the Special Report on Emissions Scenarios (SRES) scenarios (Nakicenovic and Swart 2000) and CMIP5 model ensemble using the RCP scenarios. An ensemble average

AFFILIATIONS: Wuebbles, Goodman, Janssen, Lee, and Olsen—University of Illinois at Urbana–Champaign, Urbana, Illinois; Meehl—National Center for Atmospheric Research, Boulder, Colorado; Hayhoe—Texas Tech University, Lubbock, Texas; Karl—NOAA/National Climatic Data Center, Asheville, North Carolina; Kunkel and Sun—NOAA/Cooperative Institute for Climate and Satellites, Asheville, North Carolina; Santer—Lawrence Livermore National Laboratory, Livermore, California; Wehner—Lawrence Berkeley National Laboratory, Berkeley, California; Colle—Stony Brook University, Stony Brook, New York; Fischer—ETH, Zurich, Switzerland; Fu—The University of Texas at Austin, Austin, Texas; Li—Duke University, Durham, North Carolina; Kharin—Canadian Centre for Climate Modelling and Analysis, Victoria, British Columbia, Canada; Long—NCEP/NWS/NOAA, and Wyle Laboratories, Camp Springs, Maryland; Pan—Saint Louis University, St. Louis, Missouri; Seth—University of Connecticut, Storrs, Connecticut; Sheffield—Princeton University, Princeton, New Jersey

CORRESPONDING AUTHOR: Donald J. Wuebbles, Department of Atmospheric Sciences, University of Illinois, Urbana, IL 61801
E-mail: wuebbles@illinois.edu

The abstract for this article can be found in this issue, following the table of contents.
DOI:10.1175/BAMS-D-12-00172.1

A supplement to this article is available online (10.1175/BAMS-D-12-00172.2)

In final form 14 June 2013

for each model based on all available realizations was calculated prior to the calculation of the equally weighted multimodel averages. At the lower end of the range, the stabilization scenario RCP2.6 reaches its peak change of 2°C above the 1901–60 average around the middle of this century. The higher scenario, RCP8.5, drives end-of-century temperature increases in excess of 6°C, significantly warmer than those projected by SRES A2. SRES B1 and RCP4.5 produce similar but not identical responses over the U.S. at the end of the century, as do SRES A1B and RCP6.0.

The CONUS mean change is similar to that projected for the global mean (land and ocean). An assessment of the total uncertainty for the CONUS projections would be almost certainly larger (Knutti and Sedláček 2012) but is not as straightforward to estimate as previously done for global-mean temperature change in the IPCC AR4 using simple climate models, as there is no way to estimate regional climate sensitivities from those models.

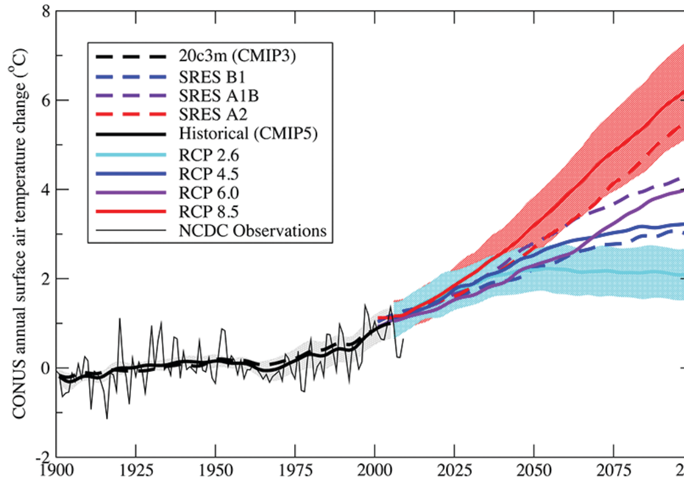

Fig. 2. Projected CMIP3 and CMIP5 annual temperature changes (°C) over CONUS for the multimodel average (lines) and range (shown for RCP8.5 and RCP2.6 only, for illustrative purposes) relative to the 1901–60 average. Shaded regions for the higher RCP8.5 and lower RCP2.6 scenarios represent one standard deviation across the models. The total multimodel range is larger. The standard deviation range in intermediate scenarios (RCP4.5 and RCP6.0) is similar but omitted here for clarity.

Here, we focus on CMIP5-simulated historical and projected future trends in extreme temperature, heavy precipitation, drought, and extratropical cyclones. The CMIP5 models used in the various analyses are listed in Table S1 (i.e., more information can be found online at http://dx.doi.org/10.1175/BAMS-D-12-00172.2).

EXTREME TEMPERATURE. Observations dating back to 1900 show that the temperatures in the twenty-first century have the largest spatial extent of record breaking and much above normal mean monthly maximum and minimum temperatures (Karl et al. 2012). However, the frequency of intense short-duration hot spells is still second to the levels achieved during the hot and dry 1930s (Peterson et al. 2013; hot spells were defined as 4-day periods whose mean temperatures exceeded a threshold for a 1-in-5-yr recurrence). There is also a highly significant decrease in record-breaking cold months including decreases in short-duration cold spells from a maximum in the 1980s to the lowest levels on record in the twenty-first century (Peterson et al. 2013; cold spells were defined as 4-day periods whose mean temperatures were below a threshold for a 1-in-5-yr recurrence). CMIP5-simulated changes in extreme high and low monthly temperatures (defined here as the single hottest and coldest months in a 30-yr period) show that these are expected to grow over time. Projected multimodel mean increases in the temperature of the hottest and coldest months of the year are large across the U.S. under the RCP8.5 scenario (see Fig. ES1 in the supplementary materials). For the contiguous U.S., cold spell temperature increases range from around 3°C in Florida to more than 8°C in the north-central U.S. for 2071–99 compared to 1971–2000. Hot spell temperature increases range from around 5°C in far southern areas and along the west coast to more than 7°C in parts of the Midwest and northern Rockies. Temperature increases in Alaska (Hawaii) are similar (slightly lower) for the hottest month and greater (lower) for Alaska (Hawaii) for the coldest month.

Using metrics for the combined temperature–humidity health effects [e.g., heat index (Steadman 1979), temperature–humidity index (HUMIDEX; Masterson and Richardson 1979), and wet bulb globe temperature (Sherwood and Huber 2010)], both CMIP5 and earlier model simulations consistently project increasing levels of heat stress across the U.S. (e.g., Delworth et al. 1999; Sherwood and Huber 2010; Willett and Sherwood 2012; Fischer et al. 2012). While the projected twenty-first-century changes for the temperature component of heat stress vary substantially across CMIP5 models, there is a clear joint behavior; models that show greater warming also show greater reductions in relative humidity over the continental U.S. This implies that projected increases in combined temperature–humidity measures are substantially more robust than from the two contributing variables independently (Fischer and Knutti 2013). Although most models project somewhat lower relative humidity on the hottest days, the combined effect of temperature and humidity changes is substantial increases in heat stress.

The 20-yr return value of the annual maximum or minimum daily temperature is one measure of changes in rare temperature extremes. In a changing climate, this metric is interpreted as a temperature that has a 5% chance of being exceeded by an annual extreme in any given year. Figure 3 (bottom) shows the projected change in the 20-yr return value of the annual maximum daily surface air temperature over North America at the end of this century (2081–2100) relative to the recent past (1986–2005) for the higher and lower emission RCP scenarios (Kharin et al. 2013). Under the lower RCP2.6 scenario, current annual maximum temperature extreme values are projected to occur between 4 and 10 times more frequently than at the beginning of the twenty-first century. Under the higher RCP8.5 scenario, current annual maximum extremes are projected to occur every year over the entire continent except for parts of Alaska. Figure 3 (top) shows the same for annual minimum daily surface air temperature, which is considerably larger than for the hot extreme temperatures. Under the RCP2.6 scenario, annual minimum temperature extreme values are projected to occur half as often in the southern states and about five times less often in the northern states. Under the RCP8.5 scenario, these minimum extreme values are not projected to recur over most of the continent.

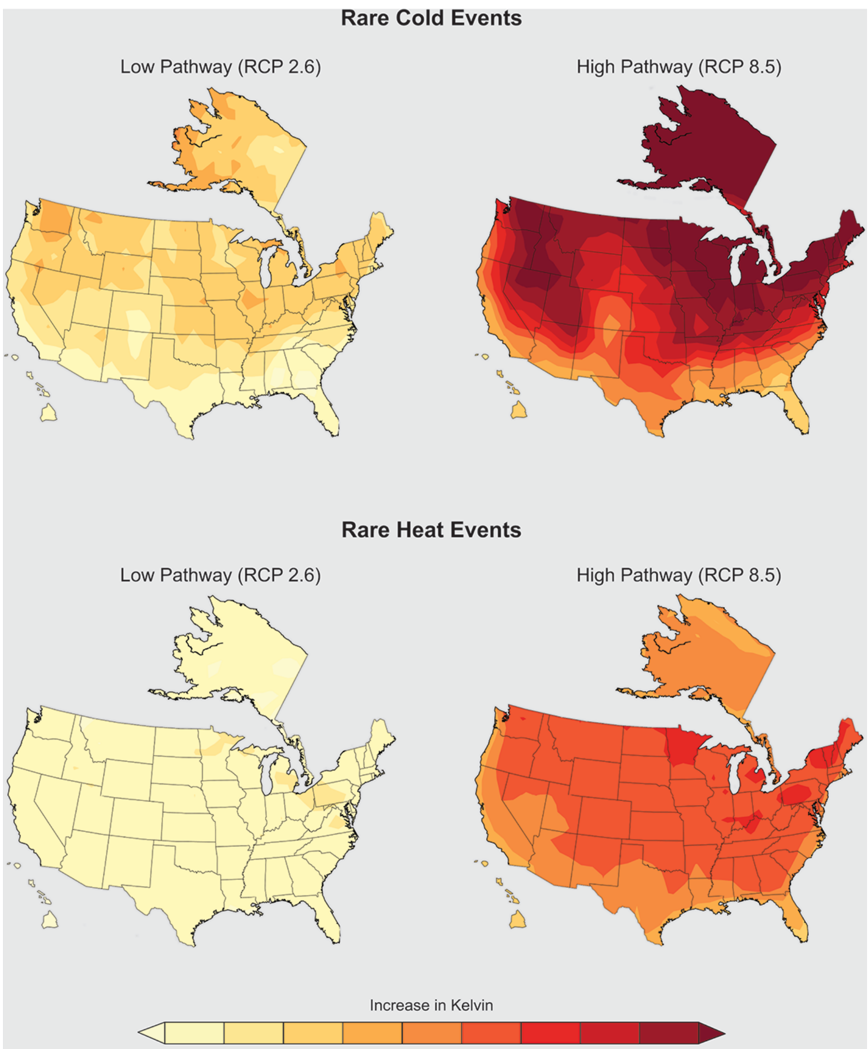

Fig. 3. (top) Projected change (°C) in the 20-yr return value of annual minimum daily surface air temperature at the end of this century (2081–2100) relative to the recent past (1986–2005) for the lower (left) RCP2.6 and higher (right) RCP8.5 scenarios. (bottom) As in (top), but for maximum daily surface air temperature.

Generally the bias in CMIP5 temperature extremes compared to observations follow similar errors to the corresponding seasonal mean. For warm extremes in Fig. 3, the CMIP5 models are 2°–5°C too high in the east half of the U.S. for return values calculated from 1986 to 2005 but lower than 2°C in the western half. For the cold extremes, the CMIP5 models are slightly more than 2°C colder than observed in the western half of the U.S. and less and 2°C colder than observed in the eastern half (Kharin et al. 2013). Multimodel differences in reproducing 1986–2005 observed temperature return values over land areas are slightly larger than the differences in reproducing observed mean seasonal

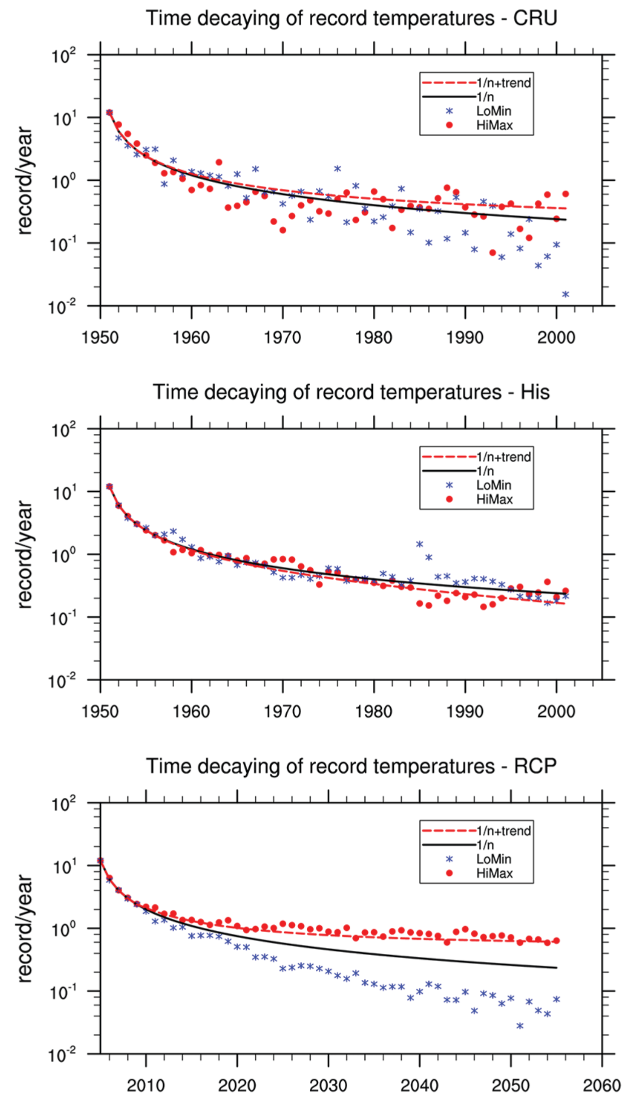

Fig. 4. Temporal decay of yearly frequency of record-breaking monthly-mean temperatures aggregated over the U.S. (30°–50°N, 120°–70°W). (top) Observed data from the Climatic Research Unit (CRU) database (Met Office, www.cru.uea.ac.uk/cru/data/temperature/), (middle) the model ensemble mean of 25 models totaling 100 members for the historical run, and (bottom) model ensemble mean of 22 models totaling 57 members for scenario RCP4.5. For an independently and identically distributed (iid) time series, in the first year (1951 for observation and 2006 for scenario) every month is a record high and low (frequency is 12). In the second year, the chance of record breaking is reduced by half (6), and so on. As the number of years *n* increases, it becomes harder to break a record; the record frequency diminishes according the 1/*n* rate (Meehl et al. 2009). By year 50, the probability is 0.24 (0.02 × 12) month yr^{-1} (black curve). Almost all record highs (red dots) fall below the statistically expected 1/*n* value during 1955–75 and are largely above the 1/*n* curve afterward. The solid black curve represents the theoretically expected 1/*n* curve (for an iid sequence) and the dashed red curve is 1/*n* curve but with warming trend effect on the frequency. The red dots and blue asterisks are the model-simulated frequencies of high and low record temperatures, respectively.

temperatures with an average multimodel standard deviation of about 5°C (Kharin et al. 2013).

The frequency of record-breaking high or low monthly temperatures is another measure of extreme temperature change (Meehl et al. 2009). Figure 4 compares the frequency of high and low record monthly temperatures over a 50-yr period averaged over U.S. During the 1990s the high record frequency was about 0.5 month yr^{-1}, roughly double that expected in an unchanging climate (top panel). An increase in mean temperature itself increases the chance of breaking a record high temperature by about 50%, as reflected by the red dashed curve (Wergen and Krug 2010). Similarly, minimum temperature records were overwhelmingly lower than would be expected in an unchanging climate (about 0.12), producing a high/low record-breaking temperature ratio of 4 during the last 10 yr—a ratio that should be equal to 1 in an unchanging climate. The historical runs capture the general decay trend in record frequency, but the high (low) temperature records recur slightly less (more) frequently than observed during mid-1980s to mid-1990s (middle panel).

Projections using the mid–low RCP4.5 scenario show that the high (low) monthly record temperatures would occur much more (less) frequently in the future (bottom panel) with respect to the 50-yr time frame starting in 2006. By the middle of the century under mid–low emissions (RCP4.5), record high temperatures are projected to be broken at a rate of 0.9 months yr^{-1} and record low temperatures at a rate of 0.07 months yr^{-1}, which gives a high/low temperature record ratio greater than 10 (a value achieved for daily records in July 2012, during the worst U.S. drought in the past five decades). This large ratio cannot be entirely explained by the increase in mean temperature; rather, it suggests a change in the shape of the tails of the daily temperature distribution, consistent with other studies of extreme temperature (Wehner 2005).

EXTREME PRECIPITATION. The extreme precipitation index (EPI; Kunkel et al. 1999, 2003, 2007) has been previously used to provide strong evidence for an upward trend in the frequency and intensity of extreme precipitation events in the U.S. (e.g., Kunkel et al. 2013). Figure 5 (top) compares EPI decadal anomalies based on CMIP5 models to observations for 2-day duration 1-in-5-yr events over the CONUS.

The EPI was calculated annually from 1901 to 2005, and then decadal averages were calculated for the period 1906–2005.

A positive trend in EPI anomalies is evident from observations over the past 4 decades. The multimodel median of CMIP5 simulations also shows an increasing trend in EPI anomalies over the same time period, albeit smaller than observed. The standard deviation between the models is extremely large, often greater than the signal, indicating that there are large differences between extreme precipitation events in the models (see Fig. ES2 in the supplementary materials, which compares the correlation coefficient of observed and modeled decadal average EPI values for the CONUS for each of the 26 CMIP5 models used). Many models have a correlation coefficient with observations greater than 0.50, with the Beijing Climate Center, Climate System Model, version 1.1 (BCC_CSM1.1), for example, approaching 1.00 for a 10-yr return. At the same time, however, seven of the models have a negative correlation, demonstrating the large spread in model ability to capture observed trends in extreme precipitation events. In terms of future projections, Fig. 5 (bottom) shows an increasing trend in EPI values under both the mid–low RCP4.5 and the higher RCP8.5 scenarios. For these projections, the multimodel spread is smaller than the signal, indicating strong agreement of an increase in the EPI across all models. Figure ES3 in the supplementary materials shows that there is a large variation between ensemble individual runs.

An alternate indicator of long-term trends in extreme precipitation is the fraction of the annual total precipitation that falls in the heaviest 1% of daily events. Figure 6 compares simulated historical changes in the top 1% of extreme CONUS precipitation over time with observed data, calculating the 99th percentile for the base period (1900–60), ignoring all days with less than 1 mm of precipitation at each grid point, and summing the data for days above that threshold. The models show an increase

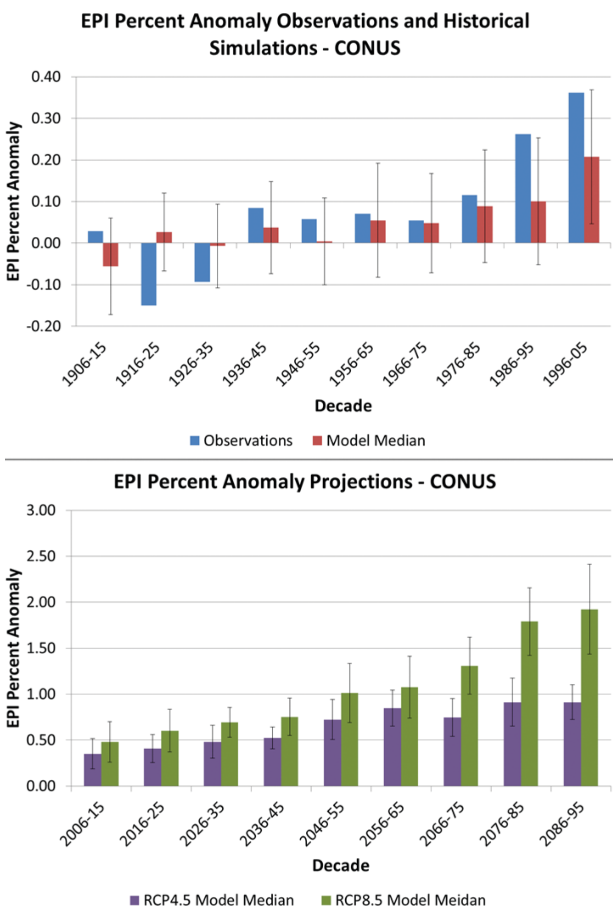

Fig. 5. (top) Observed decadal (blue) and modeled (red) EPI percent anomalies for 2-day duration and 1-in-5-yr events: percent deviation from the long-term mean (1901–60). The red bars are the median of the CMIP5 historical simulations from 1906 to 2005. The error bars represent ±1 standard deviation of the models. (bottom) The model median of EPI percent anomalies for RCP4.5 (purple) and RCP8.5 (green) and historical model simulations for the period 1901–2100 by decade. The long-term mean is 1901–60. Error bars show the spread of the models as ±1 standard deviation.

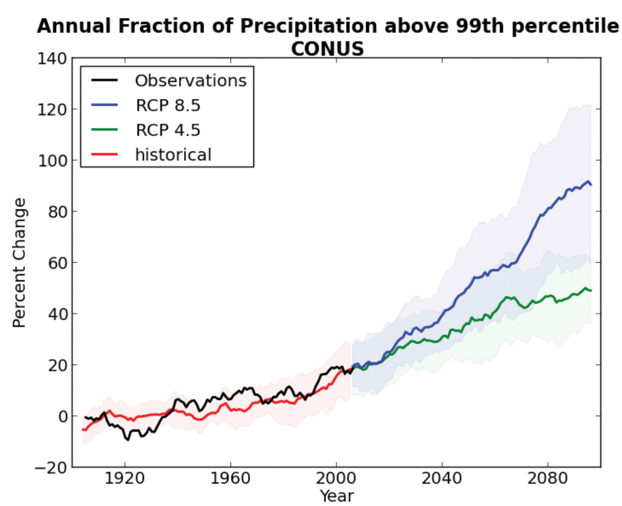

Fig. 6. Percentage of annual precipitation over the contiguous U.S. falling in the heaviest 1% of daily precipitation events, relative to the 1901–60 average, as simulated by the CMIP5 historical simulations (1900–2005) and the RCP4.5 and RCP8.5 simulations (2006–2100). Observational data (1901–2010) are also shown. The solid lines and shaded areas represent the mean and standard deviation of the 9-yr running average.

in the amount of precipitation falling in the largest 1% of events throughout the last century (1901–2000). CMIP5 historical changes in heavy precipitation are broadly consistent with changes in observed heavy precipitation from 1958 to 2007 (Karl et al. 2009). By the end of this century, a 50% increase in the annual fraction of precipitation falling in the heaviest events is projected for the mid–low scenario (RCP4.5), while a 90% increase is projected for the higher scenario (RCP8.5). In general, CMIP5 results suggest that a greater percentage of annual precipitation will fall in the top 1% of events over time and are consistent with the conclusions reached in similar analyses of CMIP3 models (Wehner 2005).

Long period return values represent much rarer extremes than the 99th percentile. Figure 7 (upper) shows that the CMIP5 projection of percent changes in the 20-yr return value of the annual maximum daily precipitation at the end of this century (2081–2100) relative to the recent past (1986–2005) under the higher and lower RCP scenarios increases everywhere in CONUS and Alaska (Kharin et al. 2013). Such rare precipitation events have been increasing (Kunkel et al. 2003; Min et al. 2011; Field et al. 2012) and are also projected to occur more frequently in the future (Fig. 7, lower) but not as often as for warm temperature events of the same current frequency. At the end of this century under the higher RCP8.5 scenario, the current 20-yr event is projected to occur about twice as often in the interior of the U.S., about 3–4 times more frequently along the coasts, and up to 7 times more frequently in parts of Alaska than it does now.

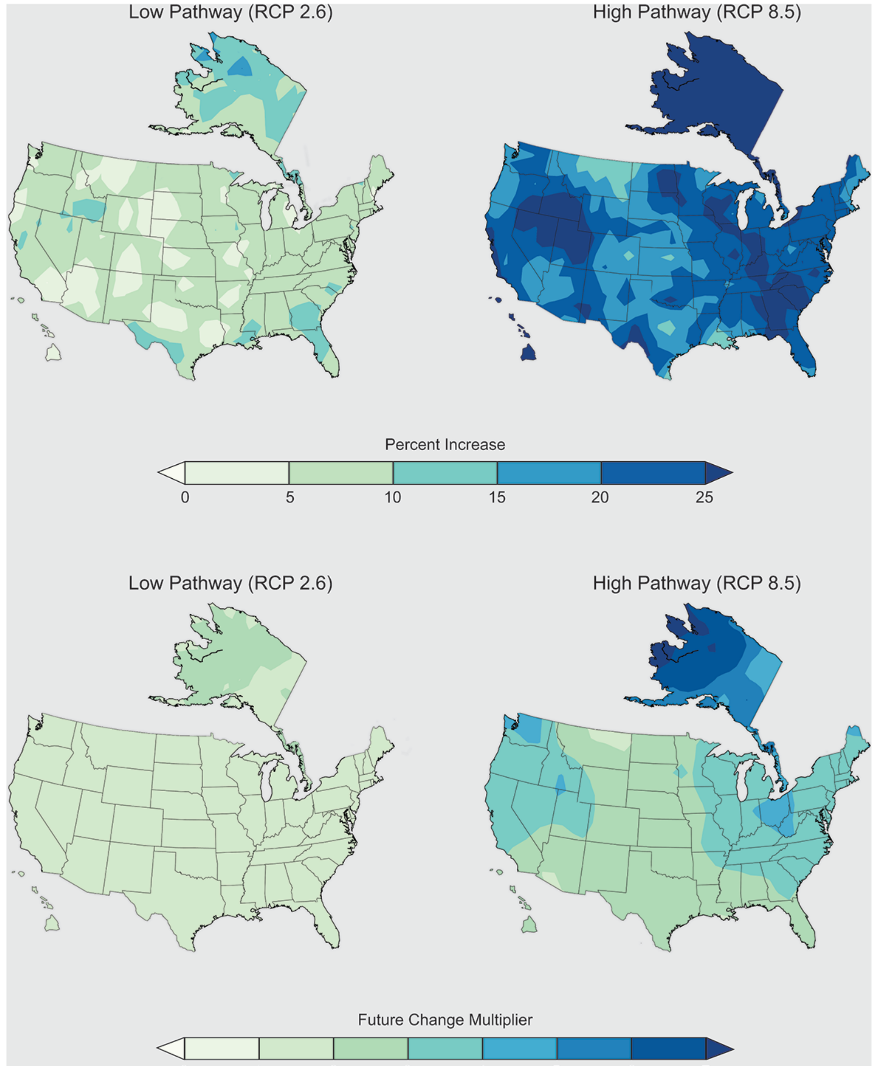

Fig. 7. (top) Projected change (%) in the 20-yr return value of annual maximum daily precipitation at the end of this century (2081–2100) relative to the recent past (1986–2005) for the lower (left) RCP2.6 and higher (right) RCP8.5 scenarios. (bottom) The relative rate at which the 1986–2005 20-yr return value of annual maximum daily precipitation is projected to occur during 2081–2100. A value of two would mean that such an extreme event happens twice as often.

LARGE-SCALE DRIVERS OF PRECIPITATION VARIABILITY AND DROUGHT.

Drought has been a constant challenge for the U.S. Southwest and, in recent years, for the Southeast as well. A sizeable fraction of the precipitation in the arid Southwest derives from the North American monsoon. Past studies using CMIP3 models (e.g., Liang et al. 2008) have shown that climate models do not simulate all aspects of the circulation patterns associated with the monsoon well. The CMIP5 models' simulation of the seasonal cycle of precipitation (Cook and Seager 2013) appears improved over

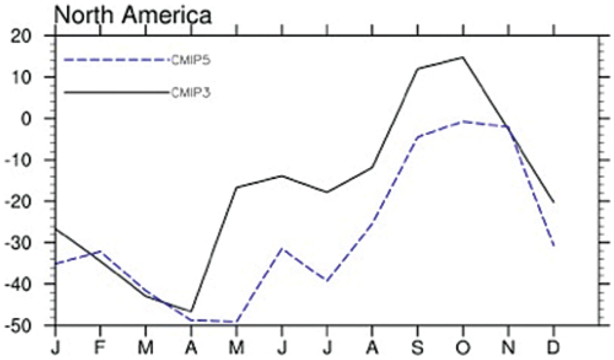

Fig. 8. Percent change in multimodel ensemble-mean monthly precipitation for the North American monsoon region (29°–35°N, 112.5°–120°W) for CMIP3 (2071–2100 SRES mid–high A2 minus 1971–2000 20C3m, and CMIP5 (2076–2100 higher RCP8.5 minus 1981–2005 historical).

CMIP3 (Liang et al. 2008). Observations indicate a decrease in monsoon rainfall over the past two decades, which may partially result from anthropogenically forced warming (Arias et al. 2012). CMIP3 analyses of changes in the annual cycle of precipitation in the North American monsoon region suggested reductions during winter and early summer rainy seasons but indicate increased rainfall later in the rainy season (Seth et al. 2011). CMIP5 simulations (Fig. 8) show a similar response but a stronger reduction in precipitation in the winter and spring, possibly owing to the stronger radiative forcing in the RCP8.5 versus the SRES A2 scenario (also see Seth et al. 2013). A 1979–2005 historical comparison indicates CMIP5 models are drier (by 2–4 mm day^{-1}) than observed through March–September in the core monsoon region, south of 20°N, and slightly wetter (0.5–2 mm day^{-1}) than observed from May to September from 20° to 25°N (Sheffield et al. 2013).

In the Southeast, the seasonal cycle of precipitation is strongly influenced by the position of the western ridge of the North Atlantic subtropical high (NASH). Comparing historical simulated and observed year-to-year variations in summer [June–August (JJA)] precipitation in the Southeast U.S. identified a subgroup of the CMIP5 models that simulate the summer precipitation variability reasonably well owing to their proper representation of the link with the western ridge position. In this subgroup of models, future variability intensifies under the mid–low RCP4.5 scenario due to a pattern shift of the NASH western ridge. The NASH western ridge extends farther westward and leads to more frequent occurrences of *both* the northwestward and southwestward ridge patterns that are respectively related to the dry and wet Southeast U.S. summers—in other words, increasing interannual variability (Li et al. 2011, 2013).

At the global scale, previous evaluations of CMIP3 twenty-first-century projections (Sheffield and Wood 2008) indicated general decreases in soil moisture and a corresponding increase in drought frequency, duration, area, and severity with increasing temperature. CMIP5 models show similar twenty-first-century decreases in soil moisture in most global land areas in summer. There has been a recent increase in the frequency of severe to extreme drought in the western U.S., and the CMIP5 models simulate such an increase for the early twenty-first century (Fig. 9). There is consensus among the models for future summer soil moisture decreases throughout the U.S.. and for winter soil moisture decreases in most of the CONUS (Dirmeyer et al. 2013). Comparisons of CMIP3 and CMIP5 twentieth-century simulations against offline hydrological modeling estimates of global drought variability (Sheffield and Wood 2007) indicate that the models on average capture the regional variation in drought frequency, although there are large intermodel variations and a tendency to overestimate longer-term drought frequency (Fig. 9). The latter is related to differences in modeled variability at interannual to decadal time scales and differing land surface representations.

The south-central U.S. has been prone to drought and floods historically and experienced its worst single year drought in 2011. By the late twenty-first century (2073–99), the CMIP5 models ensemble-mean projections suggest that the net surface water gain over this region, defined as the precipitation minus evapotranspiration (P – ET), will decrease significantly during winter, spring, and fall significantly (~0.2 mm day^{-1} or 20%) under the RCP8.5 scenario relative to that of 1979–2005. Such changes are mainly due to a stronger increase of ET during these seasons, which more than negates a small increase of rainfall during spring. Because soil moisture is recharged during winter and spring in the current climate (1979–2005), the projected reduction of net surface water gain in these seasons would reduce soil moisture and increase the risk of droughts.

EXTRATROPICAL STORMS. Future changes in extratropical cyclones could affect the risk and severity of extreme precipitation over the CONUS, particularly along the eastern seaboard. Recent observational studies have documented a decrease in the frequency of warm season extratropical cyclones over the northeastern U.S. (Leibensperger et al. 2008), while other studies have shown a future decrease in cyclone frequency over the western Atlantic storm track using CMIP3 and other models (Lambert and Fyfe 2006; Bengtsson et al. 2006). Colle et al. (2013) present a more detailed summary of past studies investigating future cyclone changes for this region. Our analysis focuses on eastern North America during the cool season (November–March) using the Hodges (1994, 1995) cyclone tracking scheme to track the cyclones in 15 CMIP5 models (see supplement) using 6-h mean sea level pressure data. Colle et al. (2013) describes the tracking approach and some validation of the tracking procedure for the historical 1979–2004 period during the cool season. They also rank the models and show that six out of the seven top-performing models are the higher-resolution CMIP5 models.

Figure 10a shows the change in cyclone track density over eastern North America and much of the northern Atlantic between the 2039 and 2068 cool seasons and the historical (1979–2004) period, and dotted locations highlight where at least 73% (11 of the 15) of the models predict the same sign of the cyclone changes. Projected changes in cyclone tracks and cyclone deepening, or strengthening, vary substantially from one region to the next. For example, cyclone density is projected to decrease over the western Atlantic but change little or slightly increase over northern New England. Over the smaller U.S. East Coast region, relatively weak cyclones are projected to decrease while stronger cyclones (<980 hPa) are projected to increase (Fig. 10c); however, there is a relatively large standard deviation in the future change of deep cyclones, ranging from a near doubling to no change. Colle et al. (2013) highlights a statistically significant upward trend in the number of relatively strong cyclones along the U.S. East Coast through the mid-twenty-first century using the "best seven" CMIP5 models. In contrast, for the larger Atlantic domain there is a 3%–9% projected reduction in

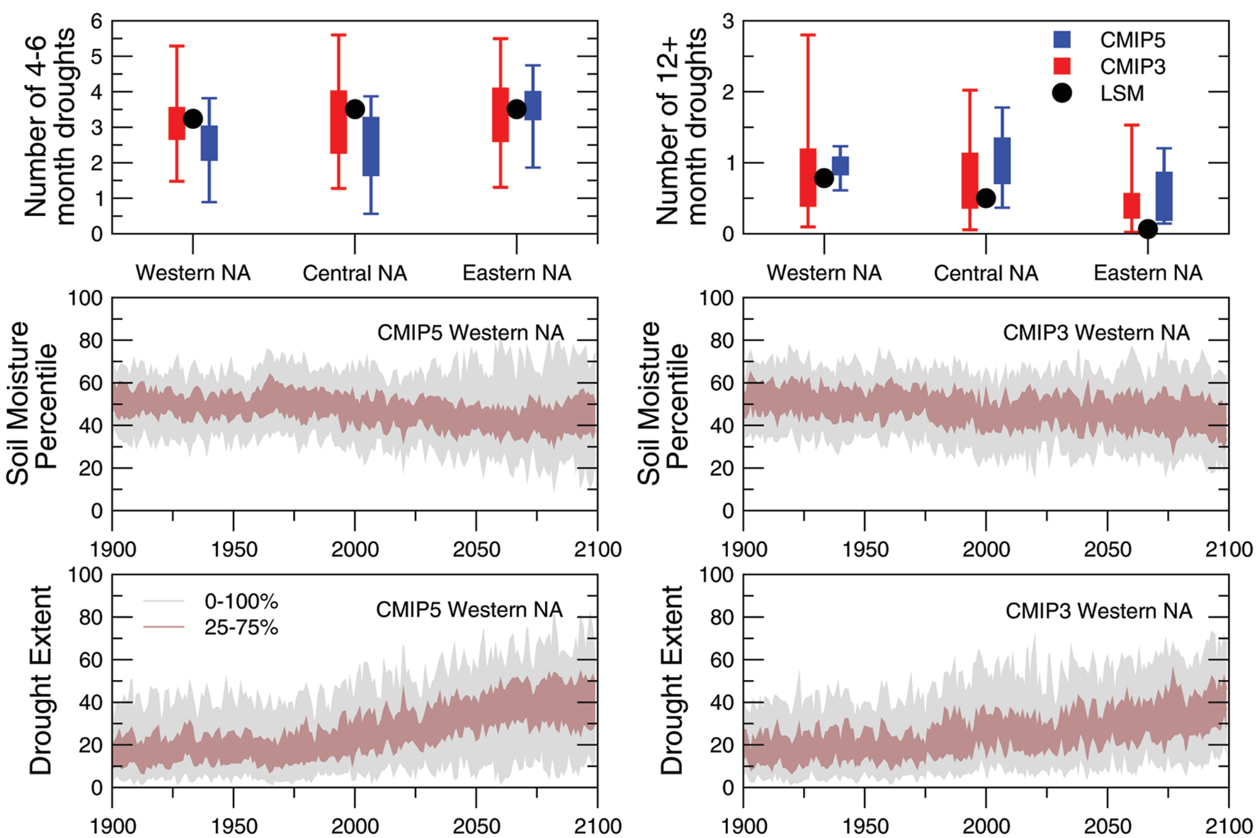

Fig. 9. (top) Evaluation of CMIP5 and CMIP3 models against offline land surface model (LSM) estimates of observed regional drought frequency (number of droughts per 30 yr) for (left) droughts that last for 4–6 months and (right) droughts that last for more than 12 months. (middle) Distribution of projected changes in soil moisture percentile from (left) CMIP5 and (right) CMIP3 models for western North America. (bottom) Distribution of projected changes in drought extent from (left) CMIP5 (higher RCP8.5 scenario) and (right) CMIP3 (mid–high SRES A2 scenario) models for western North America. Drought is defined as soil moisture below the 20th percentile.

the number of relatively strong cyclones (Colle et al. 2013).

The rate at which cyclones strengthen, or deepen, is also projected to change. Over the Northeast, there is a 10%–30% mean increase in the number of CMIP5 cyclones deepening by more than 5 hPa in 6 h (Fig. 10d), with a relatively large spread from a 40% to 60% decrease to a 60% to 90% increase. Meanwhile, the mean CMIP5 weakening rates of more than 2 hPa in 6 h decrease by ~5%, but there is a relatively large uncertainty in this weakening. Just offshore of the U.S. East Coast deepening rates are projected to decrease by 10%–20% by the mid-twenty-first century (Fig. 10b). By the late twenty-first century, a widespread 10%–30% decrease in 5 hPa per 6-h deepening is projected over much of the western and northern Atlantic (not shown). Colle et al. (2013) provide some evidence to suggest this more rapid deepening is the result of increased latent heating. Overall, these results highlight the enormous complexity of projecting the impacts of global change on regional dynamics and storm systems. Additional research is needed using higher-resolution regional models, but overall these CMIP5 results suggest that increasing cyclone intensity may lead to more wind and heavy precipitation extremes along the U.S. East Coast.

SUMMARY. This paper summarizes the results of a series of analyses based on the CMIP5 models

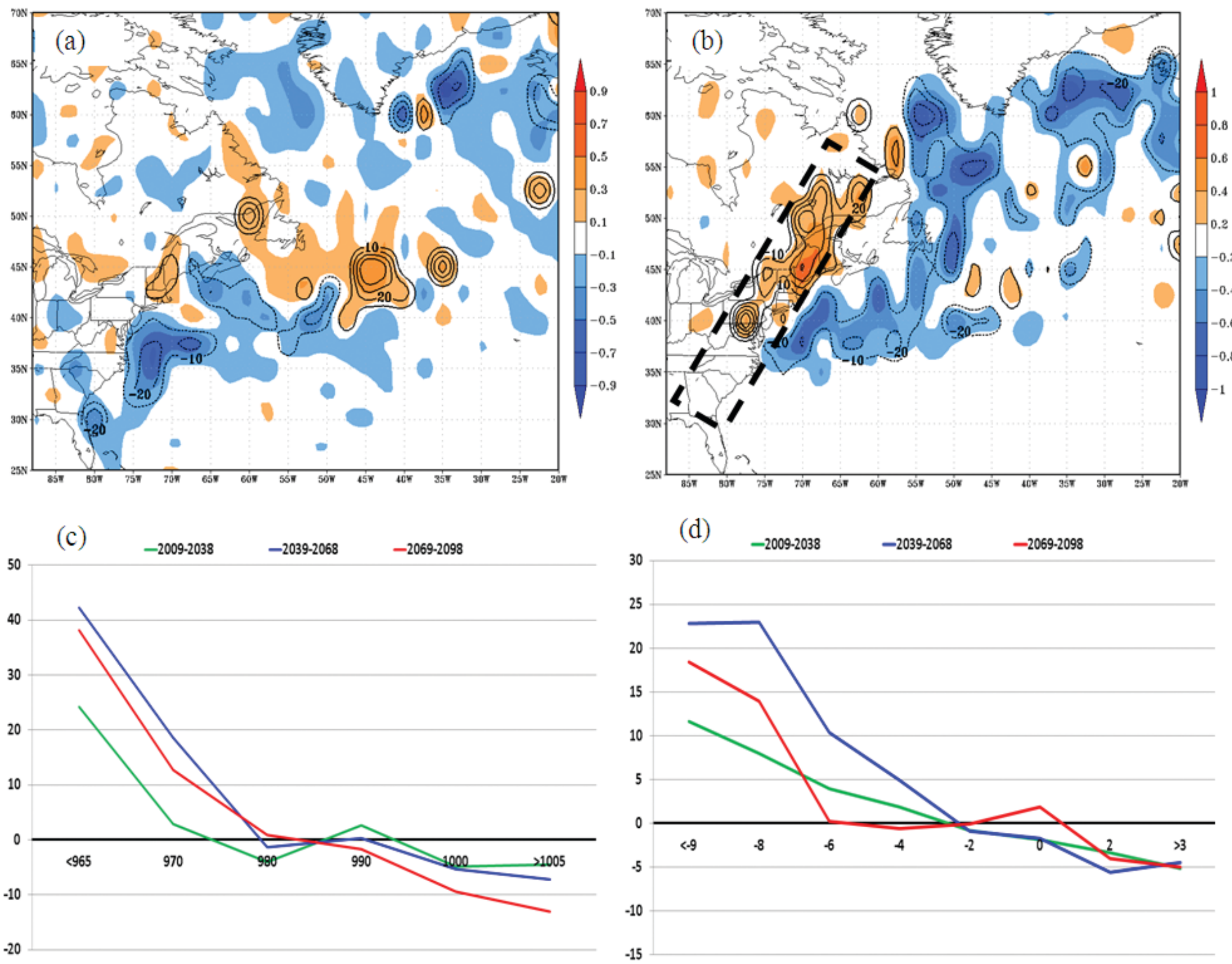

Fig. 10. (a) Difference in cyclone track density per 50,000 km² (shaded every 0.2) and the percent change (contoured every 10%) for the mean of 15 CMIP members between the cool seasons of 2039–68 and the historical (1979–2004) period. (b) As in (a), but for the change in the number of 6-h cyclone deepening rates >5 hPa (shaded as the number of cyclone tracks per 5 cool seasons per 50,000 km²) and the percentage change (contoured every 10% with negative dashed). (c) Percentage difference in the number of cyclone central pressures centered for each 10-hPa bin over the dashed box in (b) between each of the three future periods and 1979–2004 cool seasons. (d) As in (c), but for 6-h deepening rate in hPa, which includes the full evolution of all cyclones within the box in (b).

examining changes in temperature extremes, precipitation extremes, droughts, and atmospheric patterns such as the North American monsoon and the North Atlantic subtropical high that affect extreme temperatures, interannual precipitation, and extratropical cyclones over the continental U.S.. Based on these analyses, including the comparison of the new CMIP5 model experiments with older CMIP3 projections and, where possible, with historical observed trends, we find the following:

- Despite higher model resolution and increased complexity, the spatial patterns, direction of change, and overall magnitudes of projected changes in mean and extreme temperature and precipitation do not differ substantially from CMIP3 to CMIP5, particularly when differences in forcings are accounted for.
- Historical observations, model simulations, and future projections consistently show increases in the frequency of high temperature extremes and decreases in low temperature extremes across different indicators that cover a broad range of return periods, quantiles, or record-breaking frequencies.
- Observations, historical simulations, and future projections also agree on increases in heavy precipitation events consistent across a range of indicators. However, there are large differences between model simulations in the rate of heavy precipitation increase, with many tending to underestimate the historical observed trend. Models do project a further increasing trend in severe precipitation events in the future.
- Projected changes in drought risk based on soil moisture show consistent increases in both summer and winter seasons across the U.S. as a whole. Model ability to simulate large-scale dynamical features such as the North American monsoon (for the Southwest) and the North Atlantic subtropical high (for the Southeast) is critical to simulating trends in long-term summer drought risk for those regions and CMIP5 models vary in the accuracy of their simulations of these features
- Although extratropical cyclones may become weaker and less frequent over much of the western Atlantic storm track, they may become more intense and deepen more rapidly just inland of the U.S. East Coast, especially by the middle of the twenty-first century. The CMIP5 analyses suggest that increasing cyclone intensity may lead to more wind and heavy precipitation extremes along the U.S. East Coast.

The studies presented in this paper provide preliminary analyses of CMIP5 and the comparison with historical trends and with CMIP3 results for extreme events. We believe this is a useful first look at how our confidence in the patterns and direction of change for extreme events has solidified as better and higher-resolution models have become available, particularly as these new model simulations continue to paint the same broad-scale picture of increasing trends in high temperature and precipitation extremes found in earlier studies.

ACKNOWLEDGMENTS. This work was supported in part by NASA Award NNX12AF32G (University of Illinois), from the Regional and Global Climate Modeling Program and the Earth System Modeling Program of the Office of Biological and Environmental Research in the Department of Energy Office of Science under Contract DE-AC02-05CH11231 (LBL), from NSF Grant AGS-1147608 (Duke), and by NOAA Award NA11OAR4310097 (Princeton University). We also acknowledge the support of NOAA Climate Program Office Modeling, Analysis, Predictions and Projections (MAPP) Program as part of the CMIP5 Task Force under Grant NA11OAR4310104 (Stony Brook) and NOAA NESDIS through the Cooperative Institute for Climate and Satellites—North Carolina under Cooperative Agreement NA09NES4400006.

REFERENCES

Andrews, T., J. M. Gregory, M. J. Webb, and K. E. Taylor, 2012: Forcing, feedbacks and climate sensitivity in CMIP5 coupled atmosphere-ocean climate models. *Geophys. Res. Lett.*, **39,** L09712, doi:10.1029/2012GL051607.

Arias, P. A., R. Fu, and K. C. Mo, 2012: Decadal variation of rainfall seasonality in the North American monsoon region and its potential causes. *J. Climate,* **25,** 4258–4274.

Bengtsson, L., K. I. Hodges, and E. Roeckner, 2006: Storm tracks and climate change. *J. Climate,* **19,** 3518–3543.

Colle, B. A., Z. Zhang, K. Lombardo, E. Chang, P. Liu, and M. Zhang, 2013: Historical evaluation and future prediction of eastern North America and western Atlantic extratropical cyclones in the CMIP5 models during the cool season. *J. Climate,* **26,** 6882–6903.

Cook, B. I., and R. Seager, 2013: The response of the North American monsoon to increased greenhouse gas forcing. *J. Geophys. Res.,* **118,** 1690–1699, doi:10.1002/jgrd.50111.

Delworth, T. L., J. D. Mahlman, and T. R. Knutson, 1999: Changes in heat index associated with CO_2-induced global warming. *Climatic Change,* **43,** 369–386.

Dirmeyer, P. A., Y. Jin, B. Singh, and Z. Yan, 2013: Trends in land–atmosphere interactions from CMIP5 simulations. *J. Hydrometeor.,* **14,** 829–849.

Field, C. B., and Coauthors, Eds., 2012: *Managing the Risks of Extreme Events and Disasters to Advance Climate Change Adaptation.* Cambridge University Press, 582 pp.

Fischer, E. M., and R. Knutti, 2013: Robust joint projections for humidity and temperature extremes. *Nat. Climate Change,* **3,** 126–130, doi:10.1038/nclimate1682.

——, K. W. Oleson, and D. M. Lawrence, 2012: Contrasting urban and rural heat stress responses to climate change. *Geophys. Res. Lett.,* **39,** L03705, doi:10.1029/2011GL050576.

Hibbard, K. A., G. A. Meehl, P. Cox, and P. Friedlingstein, 2007: A strategy for climate change stabilization experiments. *Eos, Trans. Amer. Geophys. Union,* **88,** 217–221.

Hodges, K. I., 1994: A general method for tracking analysis and its application to meteorological data. *Mon. Wea. Rev.,* **122,** 2573–2586.

——, 1995: Feature tracking on the unit sphere. *Mon. Wea. Rev.,* **123,** 3458–3465.

Karl, T. R., J. M. Melillo, and T. C. Peterson, Eds., 2009: *Global Climate Change Impacts in the United States.* Cambridge University Press, 188 pp.

——, and Coauthors, 2012: U.S. temperature and drought: Recent anomalies and trends. *Eos, Trans. Amer. Geophys. Union,* **93,** 473–474.

Kharin, V. V., F. W. Zwiers, X. Zhang, and M. Wehner, 2013: Changes in temperature and precipitation extremes in the CMIP5 ensemble. *Climatic Change,* **119,** 345–357.

Knutti, R., and J. Sedláček, 2012: Robustness and uncertainties in the new CMIP5 climate model projections. *Nat. Climate Change,* **3,** 369–373, doi:10.1038/nclimate1716.

Kunkel, K. E., K. Andsager, and D. R. Easterling, 1999: Long-term trends in extreme precipitation events over the conterminous United States and Canada. *J. Climate,* **12,** 2515–2527.

——, D. R. Easterling, K. Redmond, and K. Hubbard, 2003: Temporal variations of extreme precipitation events in the United States: 1895–2000. *Geophys. Res. Lett.,* **30,** 1900, doi:10.1029/2003GL018052.

——, T. R. Karl, and D. R. Easterling, 2007: A Monte Carlo assessment of uncertainties in heavy precipitation frequency variations. *J. Hydrometeor.,* **8,** 1152–1160, doi:10.1175/JHM632.1.

——, and Coauthors, 2013: Monitoring and understanding trends in extreme storms: State of knowledge. *Bull. Amer. Meteor. Soc.,* **94,** 499–514.

Lambert, S. J., and J. C. Fyfe, 2006: Changes in winter cyclone frequencies and strengths simulated in enhanced greenhouse warming experiments: Results from the models participating in the IPCC diagnostic exercise. *Climate Dyn.,* **26,** 713–728.

Leibensperger, M. E., L. J. Mickley, and D. J. Jacob, 2008: Sensitivity of U.S. air quality to mid-latitude cyclone frequency and implications of 1980–2006 climate change. *Atmos. Chem. Phys.,* **8,** 7075–7086.

Li, L., W. Li, and Y. Kushnir, 2011: Variation of North Atlantic subtropical high western ridge and its implications to the southeastern US summer precipitation. *Climate Dyn.,* **39,** 1401–1412, doi:10.1007/s00382-011-1214-y.

——, ——, and Y. Deng, 2013: Summer rainfall variability over the southeastern United States and its intensification in the 21st century as assessed by the CMIP5 models. *J. Geophys. Res. Atmos.,* **118,** 340–354, doi:10.1002/jgrd.50136.

Liang, X.-Z., J. Zhu, K. E. Kunkel, M. Ting, and J. X. L. Wang, 2008: Do CGCMs simulate the North American monsoon precipitation seasonal-interannual variations. *J. Climate,* **21,** 3755–3775.

Masterson, J. M., and F. A. Richardson, 1979: HUMIDEX: A method of quantifying human discomfort due to excessive heat and humidity. Environment Canada Rep., 45 pp.

Meehl, G. A., and K. A. Hibbard, 2007: A strategy for climate change stabilization experiments with AOGCMs and ESMs. WCRP Informal Rep. 3/2007, ICPO Publ. 112, IGBP Rep. 57, 35 pp.

——, C. Covey, B. McAvaney, M. Latif, and R. J. Stouffer, 2005: Overview of the Coupled Model Intercomparison Project. *Bull. Amer. Meteor. Soc.,* **86,** 89–93.

——, ——, T. L. Delworth, M. Latif, B. McAveney, J. F. B. Mitchell, R. J. Stouffer, and K. E. Taylor, 2007: The WCRP CMIP3 multimodel dataset: A new era in climate change research. *Bull. Amer. Meteor. Soc.,* **88,** 1383–1394.

——, C. Tebaldi, G. Walton, D. Easterling, and L. McDaniel, 2009: Relative increase of record high maximum temperatures compared to record low minimum temperatures in the U.S. *Geophys. Res. Lett.,* **36,** L23701, doi:10.1029/2009GL040736.

Min, S.-K., X. Zhang, F. W. Zwiers, and G. C. Hergerl, 2011: Human contribution to more-intense precipitation extremes. *Nature,* **470,** 378–381, doi:10.1038/nature09763.

Moss, R. H., and Coauthors, 2010: The next generation of scenarios for climate change research and assessment. *Nature,* **463,** 747–756, doi:10.1038/nature08823.

Nakicenovic, N., and R. Swart, Ed., 2000: *Special Report on Emissions Scenarios*. Cambridge University Press, 612 pp.

Peterson, T. C., and Coauthors, 2013: Monitoring and understanding changes in heat waves, cold waves, floods and droughts in the United States: State of knowledge. *Bull. Amer. Meteor. Soc.,* **94,** 821–834.

Seth, A., S. A. Rauscher, M. Rojas, S. Camargo, and A. Giannini, 2011: Enhanced spring convective barrier for monsoons in a warmer world? *Climatic Change,* **104,** 403–414, doi:10.1007/s10584-010-9973-8.

——, ——, M. Biasutti, A. Giannini, S. Camargo, and M. Rojas, 2013: CMIP5 projected changes in the annual cycle of precipitation in monsoon regions. *J. Climate,* **26,** 7328–7351.

Sheffield, J., and E. F. Wood, 2007: Characteristics of global and regional drought, 1950–2000: Analysis of soil moisture data from off-line simulation of the terrestrial hydrologic cycle. *J. Geophys. Res.,* **112,** D17115, doi:10.1029/2006JD008288.

——, and ——, 2008: Projected changes in drought occurrence under future global warming from multi-model, multi-scenario, IPCC AR4 simulations. *Climate Dyn.,* **13,** 79–105, doi:10.1007/s00382-007-0340-z.

——, and Coauthors, 2013: North American climate in CMIP5 experiments. Part I: Evaluation of historical simulations of continental and regional climatology. *J. Climate,* **26,** 9209–9245.

Sherwood, S. C., and M. Huber, 2010: An adaptability limit to climate change due to heat stress. *Proc. Natl. Acad. Sci. USA,* **107,** 9552–9555, doi:10.1073/pnas.0913352107.

Steadman, R. G., 1979: The assessment of sultriness. Part I: A temperature-humidity index based on human physiology and clothing science. *J. Appl. Meteor.,* **18,** 861–873.

Taylor, K. E., R. J. Stouffer, and G. A. Meehl, 2012: The CMIP5 experiment design. *Bull. Amer. Meteor. Soc.,* **93,** 485–498.

van Vuuren, D. P., and Coauthors, 2011: The representative concentration pathways: An overview. *Climatic Change,* **109,** 5–31, doi:10.1007/s10584-011-0148-z.

Vose, R. S., and Coauthors, 2014: Monitoring and understanding changes in extremes: Extratropical storms, winds, and waves. *Bull. Amer. Meteor. Soc.,* **95,** 377–386.

Wehner, M., 2005: Changes in daily precipitation and surface air temperature extremes in the IPCC AR4 models. *U.S. CLIVAR Var.,* **3,** 5–9.

Wergen, Q., and J. Krug, 2010: Record-breaking temperatures reveal a warming climate. *Europhys. Lett.,* **92,** 30008, doi:10.1209/0295-5075/92/30008.

Willett, K. M., and S. Sherwood, 2012: Exceedance of heat index thresholds for 15 regions under a warming climate using the wet-bulb globe temperature. *Int. J. Climatol.,* **32,** 161–177, doi:10.1002/joc.2257.

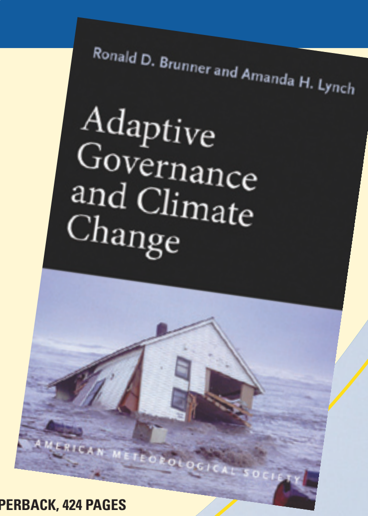

Radar and Atmospheric Science: A Collection of Essays in Honor of David Atlas

Edited by Roger M. Wakimoto and Ramesh Srivastava

This monograph pays tribute to one of the leading scientists in meteorology, Dr. David Atlas. In addition to profiling the life and work of the acknowledged "Father of Radar Meteorology," this collection highlights many of the unique contributions he made to the understanding of the forcing and organization of convective systems, observation and modeling of atmospheric turbulence and waves, and cloud microphysical properties, among many other topics. It is hoped that this text will inspire the next generation of radar meteorologists, provide an excellent resource for scientists and educators, and serve as a historical record of the gathering of scholarly contributions honoring one of the most important meteorologists of our time.

Radar and Atmospheric Science:
A Collection of Essays in Honor of David Atlas

Aug 2003. Meteorological Monograph Series, Vol. 30, No. 52; 270 pp, hardbound; ISBN 1-878220-57-8; AMS code MM52.

Price $100.00 list/$80.00 member

To place an order point your Web browser to www.ametsoc.org/amsbookstore

AMS BOOKS
RESEARCH ◆ APPLICATIONS ◆ HISTORY

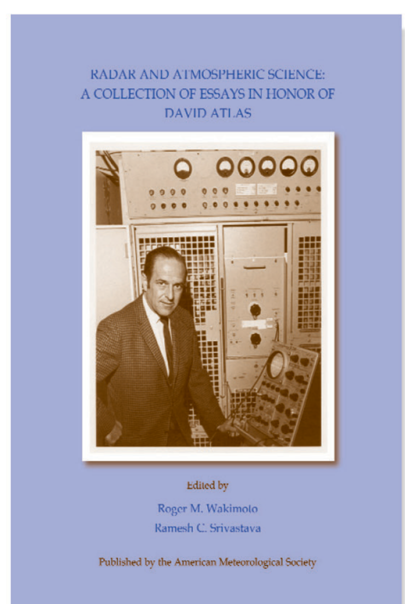

THE NORTH AMERICAN MULTIMODEL ENSEMBLE

Phase-1 Seasonal-to-Interannual Prediction; Phase-2 toward Developing Intraseasonal Prediction

by Ben P. Kirtman, Dughong Min, Johnna M. Infanti, James L. Kinter III, Daniel A. Paolino, Qin Zhang, Huug van den Dool, Suranjana Saha, Malaquias Pena Mendez, Emily Becker, Peitao Peng, Patrick Tripp, Jin Huang, David G. DeWitt, Michael K. Tippett, Anthony G. Barnston, Shuhua Li, Anthony Rosati, Siegfried D. Schubert, Michele Rienecker, Max Suarez, Zhao E. Li, Jelena Marshak, Young-Kwon Lim, Joseph Tribbia, Kathleen Pegion, William J. Merryfield, Bertrand Denis, and Eric F. Wood

The North American Multimodel Ensemble prediction experiment is described, and forecast quality and methods for accessing digital and graphical data from the model are discussed.

After more than three decades of research into the origins of seasonal climate predictability and the development of dynamical model-based seasonal prediction systems, the continuing relatively deliberate pace of progress has inspired two notable changes in prediction strategy, largely based on multi-institutional international collaborations. One change in strategy is the inclusion of quantitative information regarding uncertainty (i.e., probabilistic prediction) in forecasts and probabilistic measures of forecast quality in the verifications (e.g., Palmer et al. 2000; Goddard et al. 2001; Kirtman 2003; Palmer et al. 2004; DeWitt 2005; Hagedorn et al. 2005; Doblas-Reyes et al. 2005; Saha et al. 2006; among many others). The other change is the recognition that a multimodel ensemble strategy is a viable approach for adequately resolving forecast uncertainty (Palmer et al. 2004; Hagedorn et al. 2005; Doblas-Reyes et al. 2005; Palmer et al. 2008), although other techniques such as perturbed physics ensembles (currently in use at the Met Office for their operational system) or stochastic physics (e.g., Berner et al. 2008) have been developed and appear to be quite promising. The first change in prediction strategy naturally follows from the fact that climate variability includes a chaotic or irregular component, and, because of this, forecasts must include a quantitative assessment of this uncertainty. More importantly, the climate prediction community now understands that the potential utility of climate forecasts is based on end-user decision support (Palmer et al. 2000; Morse et al. 2005; Challinor et al. 2005), which requires probabilistic forecasts that include quantitative information regarding forecast uncertainty. The second change in prediction strategy follows from the first, because, given our current modeling capabilities, a multimodel strategy is a practical and relatively simple approach for quantifying forecast uncertainty due to uncertainty in model formulation, although it is likely that the uncertainty is not fully resolved.

More recently, there has been a growing interest in forecast information on time scales beyond 10 days but less than a season. For example, the National Centers for Environmental Prediction Climate Prediction Center (NCEP/CPC) in the United

States currently makes outlook-type forecasts for extended weather forecast ranges (i.e., 2 weeks) such as the NCEP/CPC Global Tropical Hazards/Benefits Assessment provides forecasts of anomalous tropical temperature and precipitation. The U.S. Hazards Assessment product, also issued by NCEP/CPC, includes outlooks of potential hazards in the United States up to 16 days. At present, such outlook-style forecast products are based on a subjective combination of various statistical and dynamical methods, although there is momentum to make the process more objective using real-time dynamic model forecasts. These developments demonstrate the demand for such dynamical forecast information.

This week 2–4 time scale is coupled to the seasonal time scale[1] and is often viewed as a source of predictability for seasonal time scales, yet the mechanisms for predictability on this time scale are less well understood (as compared to, say, ENSO). Despite this, there is substantial evidence for dynamic subseasonal predictions that are of sufficient quality to be useful (e.g., Pegion and Sardeshmukh 2011) and evidence that a multimodel approach will enhance forecast quality on this time scale [see the coordinated Intraseasonal Variability Hindcast Experiment (ISVHE); http://iprc.soest.hawaii.edu/users/jylee/clipas/].

Given the pragmatic utility of the multimodel approach, there is multiagency [National Oceanic and Atmospheric Administration (NOAA), National Science Foundation (NSF), National Aeronautics and Space Administration (NASA), and U.S. Department of Energy (DOE)] support for a North American Multimodel Ensemble (NMME) intraseasonal to seasonal to interannual (ISI) prediction experiment. This experiment leverages an NMME team that has already formed and began producing routine real-time multimodel ensemble ISI predictions since August 2011. The forecasts are provided to the NOAA CPC on an experimental basis for evaluation and consolidation as a multimodel ensemble ISI prediction system. The experimental prediction system developed by this NMME team is as an "NMME of opportunity" in that the seasonal-to-interannual prediction systems are readily available and each team member has independently developed the initialization and prediction protocol. We will refer to the NMME of opportunity as phase-1 NMME (or NMME-1). The NMME-1 focuses on seasonal-to-interannual time scales in that the data that are exchanged monthly.

The newly funded multiagency experiment will develop a more "purposeful NMME" in which the requirements for operational ISI prediction will be used to define the parameters of a rigorous reforecast experiment and evaluation regime. This will be phase-2 NMME (or NMME-2). The NMME team will design and test an operational NMME protocol that will guide future research, development, and implementation of the NMME beyond what can be achieved based on the NMME-1 project.

The NMME-2 experiment will do as follows:

i) Build on existing state-of-the-art U.S. climate prediction models and data assimilation systems that are already in use in NMME-1 (as well as upgraded versions of these forecast systems), introduce a new forecast system, and ensure interoperability so as to easily incorporate future model developments.

[1] Any dynamical seasonal prediction system (e.g., coupled atmosphere–ocean model) must pass through the subseasonal time scale.

AFFILIATIONS: Kirtman, Min, and Infanti—Rosenstiel School for Marine and Atmospheric Science, University of Miami, Miami, Florida; Kinter and Paolino—Center for Ocean–Land–Atmosphere Studies, Calverton, Maryland; Zhang, van den Dool, Saha, Mendez, Becker, Peng, Tripp, and Huang—NOAA/National Centers for Environmental Prediction, Camp Springs, Maryland; Tippett— International Research Institute for Climate and Society, Palisades, New York, and Center of Excellence for Climate Change Research, Department of Meteorology, King Abdulaziz University, Jeddah, Saudi Arabia; DeWitt,* Barnston, and S. Li—International Research Institute for Climate and Society, Palisades, New York; Rosati—NOAA/Geophysical Fluid Dynamics Laboratory, Princeton, New Jersey; Schubert, Rienecker, Suarez, Z. Li, Marshak, and Lim—NASA Goddard Space Flight Center, Greenbelt, Maryland; Tribbia—National Center for Atmospheric Research, Boulder, Colorado; Pegion—CIRES, University of Colorado Boulder, Boulder, Colorado; Merryfield and Denis—Environment Canada, Fredericton, New Brunswick, Canada; Wood—Princeton University, Princeton, New Jersey
***CURRENT AFFILIATION:** NOAA/National Weather Service, Washington, D.C.
CORRESPONDING AUTHOR: Ben Kirtman, Rosenstiel School for Marine and Atmospheric Science, 4600 Rickenbacker Causeway, Miami, FL 33149
E-mail: bkirtman@rsmas.miami.edu

The abstract for this article can be found in this issue, following the table of contents.
DOI:10.1175/BAMS-D-12-00050.1

In final form 6 June 2013

ii) Take into account operational forecast requirements (forecast frequency, lead time, duration, number of ensemble members, etc.) and regional/user-specific needs. A focus of this aspect of the experiment will be the hydrology of various regions in the United States and elsewhere in order to address drought and extreme event prediction. An additional focus of NMME-2 will be to develop and evaluate a protocol for intraseasonal or subseasonal multimodel prediction.
iii) Utilize the NMME system experimentally in a near-operational mode to demonstrate the feasibility and advantages of running such a system as part of NOAA's operations.
iv) Enable rapid sharing of quality-controlled reforecast data among the NMME team members and develop procedures for timely and open access to the data, including documentation of models and forecast procedures, by the broader climate research and applications community.

This paper describes the ongoing NMME-1 project, including a preliminary multimodel forecast quality assessment and our strategy for evaluating how the multimodel approach contributes to the forecast quality. We also describe how NMME-2 will evolve from NMME-1 and the coordinated research activities and data dissemination strategy envisaged.

THE PHASE-1 NMME. Based on two Climate Test bed (CTB) NMME workshops (18 February and 8 April 2011), a collaborative and coordinated implementation strategy for a NMME prediction system (NMME-1) was developed. The strategy included calendar year 2011 (CY2011) experimental real-time ISI forecasting (summarized below) that leveraged existing CTB partner activities.

Hindcast and real-time experimental prediction protocol. The CY2011 NMME experimental predictions have been made in real time since August 2011. As part of the development of the real-time capability, the NMME partners agreed on a hindcast and real-time prediction protocol. Some of the key elements of this protocol include the following:

- Real-time ISI prediction system must be identical to the system used to produce hindcasts. This necessarily includes the procedure for initializing the prediction system. The number of ensemble members per forecast, however, can be larger for the real-time system.
- Hindcast start times must include all 12 calendar months, but the specific day of the month or the ensemble generation strategy is left open to the forecast provider.
- Lead times up to 9 months are required, but longer leads are encouraged.
- The target hindcast period is 30 years (typically 1981–2010).
- The ensemble size is left open to the forecast provider, but larger ensembles are considered better.
- Data distributed must include each ensemble member (not the ensemble mean). Total fields are required [i.e., systematic error corrections to be coordinated by multimodel ensemble (MME) combination lead; NOAA/CPC]. Forecast providers are welcome to also provide bias-corrected forecasts and to develop their own MME combinations.
- Model configurations—resolution, version, physical parameterizations, initialization strategies, and ensemble generation strategies—are left open to forecast providers.
- Required output is monthly means of global grids of SST, 2-m temperature (T2m), and precipitation rate. More fields will be added based on experience and demand. It is also recognized that higher-frequency data are desirable and this will be implemented as feasible.
- Routine real-time forecast data must be available by the eighth of each month.

The NMME-1 activity began in February 2011 and became an experimental real-time system in August 2011. Specifically, on 8 August, NCEP [CPC and the Environmental Modeling Center (EMC)] collected from the respective FTP sites of the NMME partners the real-time seasonal predictions. In the months before August 2011, the hindcast data were collected and climatologies and skill assessments for each model to be applied to subsequent real-time predictions were calculated. Graphical forecast guidance based on the NMME was prepared and given to NOAA operational forecasters in time for the CPC seasonal prediction cycle. The graphical forecast guidance includes North American and global domains and T2m (T), precipitation (P), and SST fields, and the plots are for monthly and seasonal means with and without a skill mask applied. All NMME forecasts are bias corrected (making use of the hindcasts) using cross validation [see Kirtman and Min (2009) for details of how to make the bias correction].

The effort is significant because, although experimental, the NMME protocol adheres to CPC's operational schedule, so the forecasters can use the information for operational guidance. The scripts for the data ingest and graphical outputs are intended to be robust (i.e., any number of models) with any number of ensemble members can be used. A major element of the NMME experiment is to continue this effort for the benefit of operations. Meanwhile, we have built up a live hindcast dataset of about 30 years that is open to anybody and can be used for research. Quite probably, this NMME dataset is now the most extensive multimodel seasonal prediction archive currently available that includes models that are continuing to make real-time predictions. Table 1 summarizes the NMME-1 hindcast datasets and identifies the point of contact for each prediction system.

In addition, NOAA/CPC has agreed to evaluate the hindcasts, combine the forecasts, perform verification, provide an NMME website (www.cpc.ncep.noaa.gov/products/NMME), and make the real-time NMME forecast delivery to NOAA forecasters. CPC is also maintaining an NMME newsletter. The hindcast data and real-time forecast data are also available for download or analysis at the International Research Institute for Climate and Society (IRI) (http://iridl.ldeo.columbia.edu/SOURCES/.Models/.NMME/). The CPC site primarily serves the real-time needs of the project, and the IRI site, along with the analysis tools that are being developed at the IRI (http://iridl.ldeo.columbia.edu/home/.tippett/.NMME/.Verification/), primarily serves research needs in terms of assessing the prediction skill and predictability limits associated with NMME-1 in terms of designing the NMME-2

Table 1. NMME partner models and forecasts.

Model	Hindcast period	Ensemble size	Lead times (months)	Arrangement of ensemble members	Contact and reference
CFSv1	1981–2009	15	0.5–8.5	First 0000 UTC ±2 days, 21st 0000 UTC ±2 days, and 11th 0000 UTC ±2 days	Saha (Saha et al. 2006)
CFSv2	1982–2010	24(28)	0.5–9.5	Four members (0000, 0600, 1200, and 1800 UTC) every fifth day	Saha (Saha et al. 2014)
GFDL Climate Model, version 2.2 (GFDL CM2.2)	1982–2010	10	0.5–11.5	All first of the month 0000 UTC	Rosati (Zhang et al. 2007)
IRI-ECHAM4f*	1982–2010	12	0.5–7.5	All first of the month 0000 UTC	DeWitt (DeWitt 2005)
IRI-ECHAM4a*	1982–2010	12	0.5–7.5	All first of the month 0000 UTC	DeWitt (DeWitt 2005)
CCSM3	1982–2010	6	0.5–11.5	All first of the month 0000 UTC	Kirtman (Kirtman and Min 2009)
Goddard Earth Observing System, version 5 (GEOS5)	1981–2010	11**	0.5–9.5	One member every fifth day	Schubert (G. Vernieres et al. 2011, unpublished manuscript)
Third Generation Canadian Coupled Global Climate Model (CMC1-CanCM3)	1981–2010	10	0.5–11.5	All first of the month 0000 UTC	Merryfield (Merryfield et al. 2013)
Fourth Generation Canadian Coupled Global Climate Model (CMC2-CanCM4)	1981–2010	10	0.5–11.5	All first of the month 0000 UTC	Merryfield (Merryfield et al. 2013)

* Real-time forecasts terminated in Jul 2012.

** The number of forecast and hindcast ensemble members is not constant during the period. It has grown from 6 for the initial Aug 2011 forecasts (and associated hindcasts) to 11 starting with our Jun 2012 forecasts. The additional (beyond 6 initialized every fifth day) ensemble members are based on breeding and other perturbations applied on the day closest to the beginning of the month.

experimental protocol. While the NMME-1 data are limited to monthly-mean data, it is a research tool (or testbed) that is proving extremely useful in supporting the basic prediction and predictability research needs of the project participants. This database also serves as "quick look" easy access data that are the external face of the NMME experiment to the research community.

RESULTS: NMME-1. Here, we show some results from the 28 years of hindcasts that cover a common period (i.e., 1982–2009) for all the models and the real-time experimental forecast from the NMME of opportunity (i.e., NMME-1). The results help provide evidence of the benefit of a multimodel ensemble of predictions, as compared with the ensemble predictions of just one high-performing model. Figure 1 shows the range spanned by the individual ensemble members from each forecast system in NMME-1, for 0.5-month-lead[2] hindcasts for the Niño-3.4 SST index. This presentation of the range assumes that each ensemble member of each model is equally likely to occur. To calculate anomalies, the forecast bias or systematic error has been removed and is calculated separately for each model using all ensemble members for that particular model. See Saha et al. (2006) or Kirtman and Min (2009) for a discussion of how the systematic error is removed. At this short lead time, the hindcasts tend to agree with one another and with the observations, to a great extent, although there is also some disagreement, particularly at certain times (e.g., near the end of 1988 and in the middle of 1998). However, it is worth noting that nowhere do the observations lie noticeably outside the envelope of the predictions.

Figure 2 shows the same results except for 5.5-month-lead predictions, with appropriately greater uncertainties shown by the larger range—often in excess of 2°C. We will show that it is just such dispersion in the individual predictions that best reflects forecast uncertainty, as well as the "best guess" multimodel-mean prediction.

Figure 3 shows the spatial distribution of the anomaly correlation between the 5.5-month lead of the grand ensemble monthly-mean hindcast and observed SST over 1982–2009. Here, the grand ensemble mean is defined as the average of all the hindcasts, assuming that each ensemble member of each model is equally probable. This is distinct from assuming that each model should be weighted equally. High skill is evident in the central and eastern tropical Pacific Ocean, as well as portions of the tropical Atlantic and Indian Oceans and some isolated regions in the extratropics.

One of the important motivating factors for both phases on the NMME project is to understand the complementary sources of skill among the models. Essentially, we seek to understand the "where and why" in how the multimodel approach improves

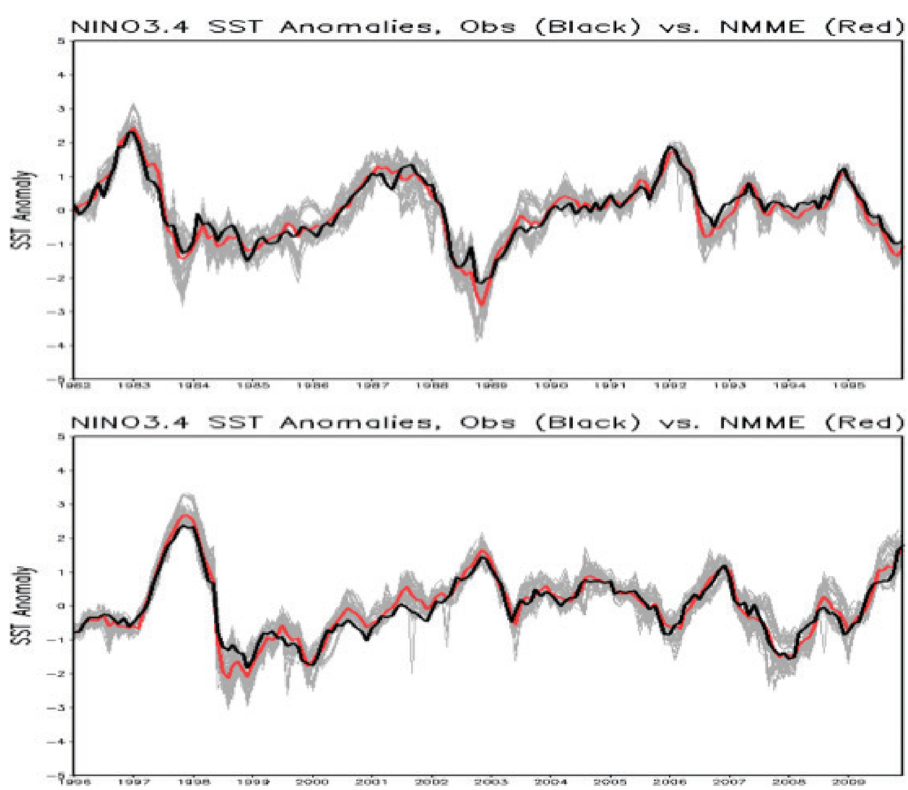

FIG. 1. Niño-3.4 (area-averaged SSTA 5°S–5°N, 170°–120°W) plumes for 0.5-month lead: (top) 1982–95 and (bottom) 1996–2010.

[2] The real-time forecasts are issued on the 15th of the month, so that, for example, a January 2013 monthly-mean forecast issued on 15 January 2013 is the 0.5-month lead, and the February 2013 monthly-mean forecast issued on 15 January 2013 is the 1.5-month lead and so on. The retrospective forecasts also follow this convention.

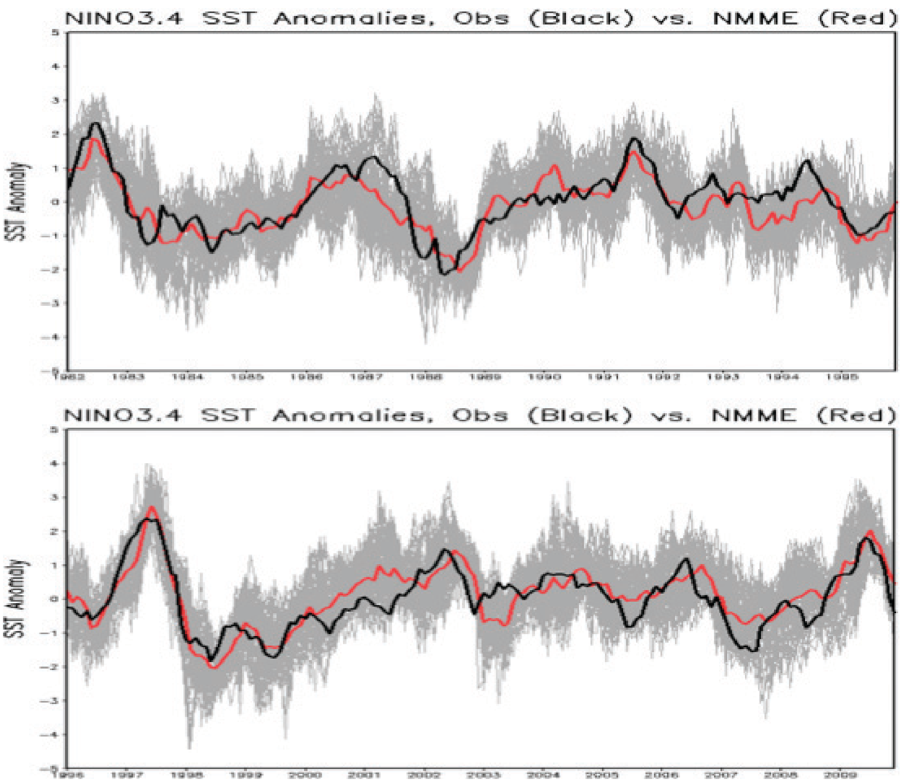

Fig. 2. As in Fig. 1, but for 6.5-month lead.

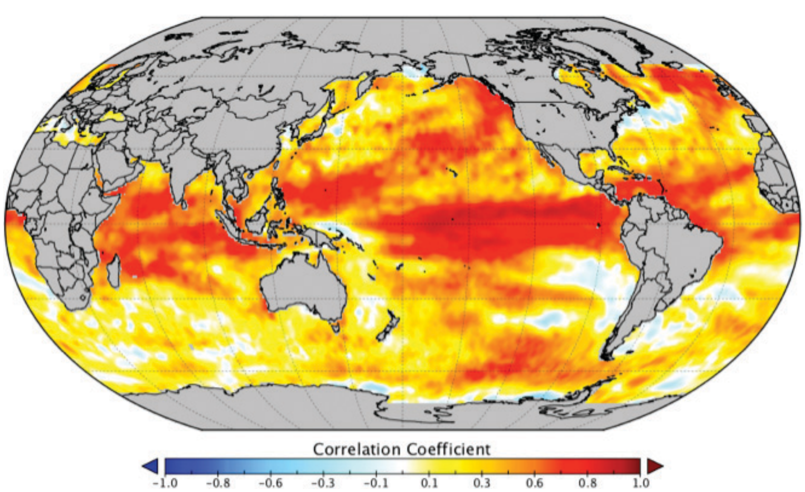

Fig. 3. SSTA correlation coefficient with each ensemble member weighted equally. Retrospective forecasts are initialized in Aug 1982–2009 and verified in the following Feb (i.e., 5.5-month lead).

forecast quality. Here, we show the first step in this process—simply documenting how the multimodel compares to any single model. For example, Fig. 4 shows scatterplots of the root-mean-square error of the SST anomaly (SSTA) for individual models' 0.5- to 5.5-month-lead ensemble-mean hindcasts versus the corresponding multimodel ensemble-mean hindcasts for tropical SST for September starts. The percentage noted in each panel corresponds to the number of points where the individual model beat the multimodel. For every single individual model, most of the points are above the diagonal (i.e., the percentage of points below the diagonal is less than 50%), indicating that the multimodel tends to have smaller errors than the individual models. Generally, the models cluster around 26%–48%. The Community Climate System Model, version 3 (CCSM3), is an outlier and is being replaced with the Community Climate System Model, version 4 (CCSM4) in NMME-2.

Preliminary examination (not shown) has suggested that in general the individual model having the highest anomaly correlation skill is Climate Forecast System, version 2 (CFSv2). However, this identification of the generally best model does not suggest that the other models, when allowed to contribute to the multimodel-mean forecast, do not further enhance the performance. To demonstrate the benefit reaped by using the multimodel ensemble over the single best-performing model, the ranked probability skill score (RPSS)[3] of the multimodel ensemble hindcasts and the CFSv2 hindcasts of SST for December–

[3] RPSS is a probabilistic forecast skill metric [see Weigel et al. (2007) for details]. The RPSS evaluates the hindcasts probabilistically (using tercile-based categories and the equal-odds climatology forecasts as the reference forecast). A good rule of thumb is that an RPSS of 0.08 corresponds to a deterministic correlation of 0.4.

February (DJF) for forecasts initialized in early July are shown in Fig. 5, while those for June–August (JJA) initialized in early January are shown in Fig. 6. In the case of both seasons, the multimodel ensemble produces higher mean skill. There are isolated areas where CFSv2 outperforms the multimodel ensemble, such as in the DJF forecasts (Fig. 5) just south of the equator near 85°, south of Sri Lanka. However, the multimodel ensemble has higher, and more reliably positive, skill over most of the globe than that of any of the individual model forecasts—even the best of them.

The comparatively better RPSS results of the multimodel ensemble hindcasts than those of the CFSv2 forecasts are not limited to SST hindcasts but generalize to predictions for land surface temperature and precipitation as well. Figure 7, for example, shows the spatial distribution of RPSS for land surface temperature for JJA initialized in early January for the multimodel ensemble (top) and CFSv2 (bottom). Again, the multimodel mean has considerably less area with negative skill while maintaining the skill levels at many of the areas where CFSv2 has the highest skill. Multimodel skill at the locations of the most extreme peaks of CFSv2 skill tends to be slightly attenuated (e.g., northeastern Brazil and parts of the Middle East), but mean skill is clearly enhanced.

Figure 8 shows the spatial distribution of RPSS for hindcasts of precipitation for DJF (initialized in July) over North America using the multimodel ensemble (left) and CFSv2 alone (right). Figure 9 is the same as Fig. 8, but for the JJA season (initialized in January). The comparative superiority of the multimodel forecast over CFSv2 alone is noted for both seasons. This is most obvious in the relative lack of negative skill in the multimodel hindcasts but also in the maintenance or even enhancement of areas of peak skill. Additional results for NMME are shown in Yuan and Wood (2012).

It is worth noting that in the case of probabilistic verification, a larger ensemble size has a stronger positive influence on skill than it does for deterministic verification (e.g., using anomaly correlation). This ensemble size effect is described in detail in Richardson (2001), and this greater sensitivity in probability forecasts is due to the larger role of sampling variability in defining tercile probabilities (particularly when done by counting the fraction of ensemble members falling into each category) than in forming an ensemble mean. Indeed, Richardson (2001) shows that a Brier skill score (BSS) of, say, 0.2 for a 100-member ensemble of a single model would be about 0.1 for a 10-member ensemble and 0.17 for a 25-member ensemble. Hence, in addition to the balancing or cancellation of individual model biases,

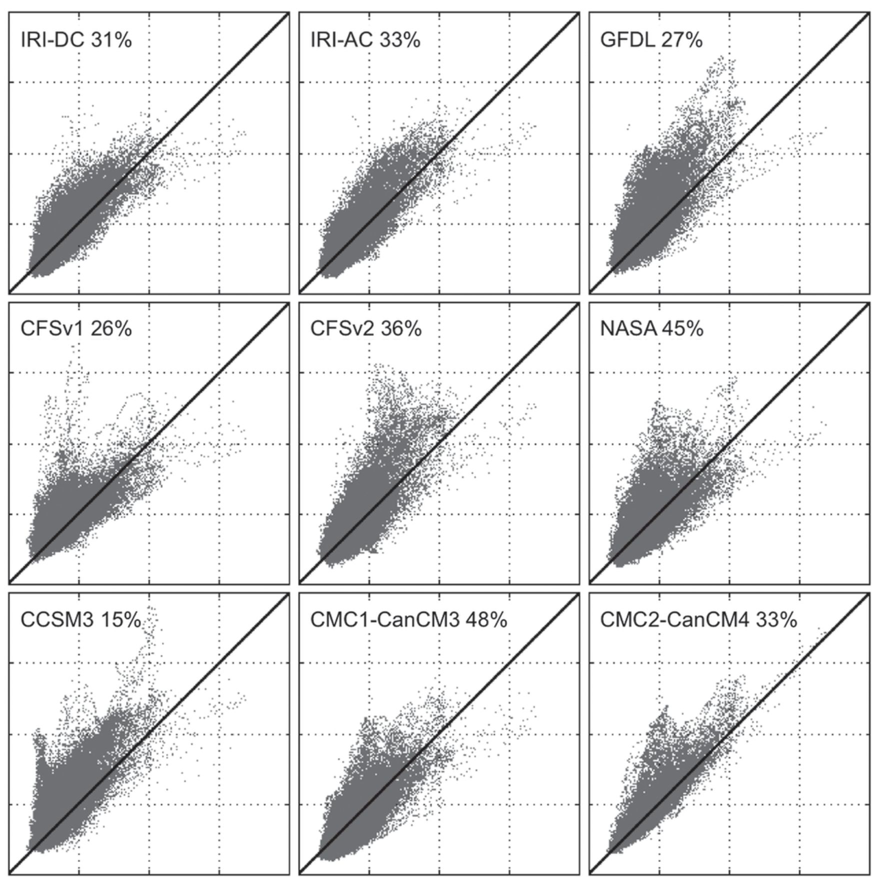

Fig. 4. SSTA RMSE 20°S–20°N for each individual model compared to the multimodel mean; Sep starts 1982–2009, leads 0.5–5.5 months. The *x* axis ranges from 0° to 2°C and corresponds to the NMME RSME, and the *y* axis ranges from 0° to 2°C and corresponds to the individual model RMSE. Dots above the diagonal imply NMME has smaller RMSE. The percentage of points below the diagonal is noted in each panel. IRI-AC corresponds to IRI-ECHAM4a and IRI-DC corresponds to IRI-ECHAM4f in Table 1.

a secondary reason for the relatively better performance of the multimodel hindcasts than CFSv2 is the much larger ensemble size of all the models together than of any single model.

A tool used to diagnose a set of probabilistic forecasts is reliability analysis, which measures the correspondence between the forecast probabilities and their subsequent observed relative frequencies, spanning the full range of issued forecast probabilities for each of the three climatologically equiprobable categories (below, near, or above normal). If one collected all instances of forecasts of 45% probability for "above normal," for example, and that category were actually later observed in 45% of the cases, the forecasts for that particular probability bin would be shown to have perfect reliability. Results of reliability analysis for forecasts initialized in October and verified in the following January–March (JFM) for 2-m temperature anomalies over the globe are shown in Fig. 10 for the multimodel ensemble hindcasts over the 28-yr period for the below-normal and above-normal categories. The light dotted line denotes perfect reliability.

Two aspects of common interest in reliability diagnosis are 1) the overall position of the lines relative to the ideal 45° line and 2) the slope of the lines relative to unity. The general positions of the lines in Fig. 10 are near that of the ideal line, but the line representing above-normal (below normal) forecasts is just slightly higher (lower) than ideal. This indicates a slight tendency to underforecast above-normal and to overforecast below-normal temperature. The observed mean relative frequency of occurrence of the categories, shown as colored dots on the y axis, indicates that above normal occurred in about 39% of cases, while below normal (and near normal) occurred in about 30% of cases. However, this weak shift toward above-normal temperature in the mean

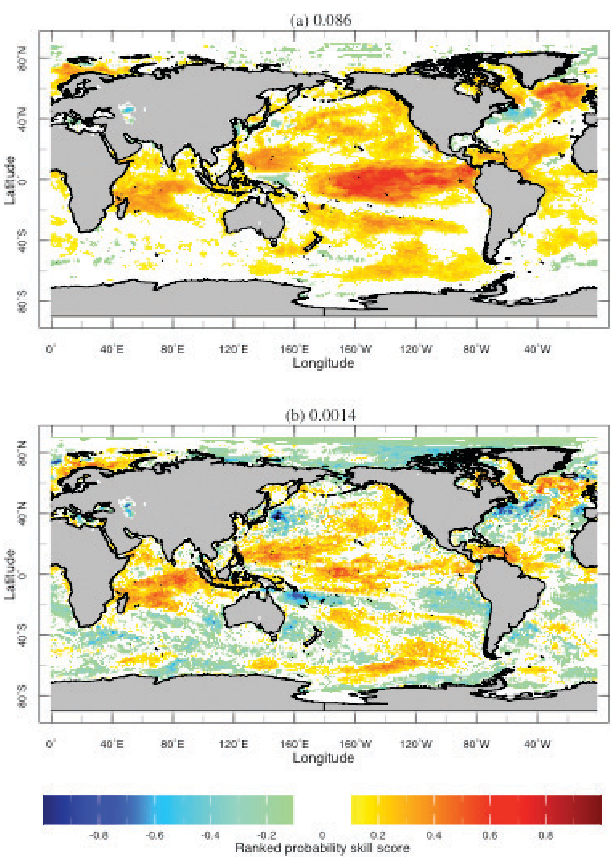

Fig. 5. SSTA RPSS for the (a) grand NMME multimodel ensemble and for (b) CFSv2. The skill is based on hindcasts initialized in Jul 1982–2009 and verified in the following DJF seasonal mean for tercile forecasts. Positive values indicate probabilistic skill that is better than climatology, and negative values indicate probabilistic skill that is worse than a climatological forecast. Global-averaged RPSS is noted in the figure.

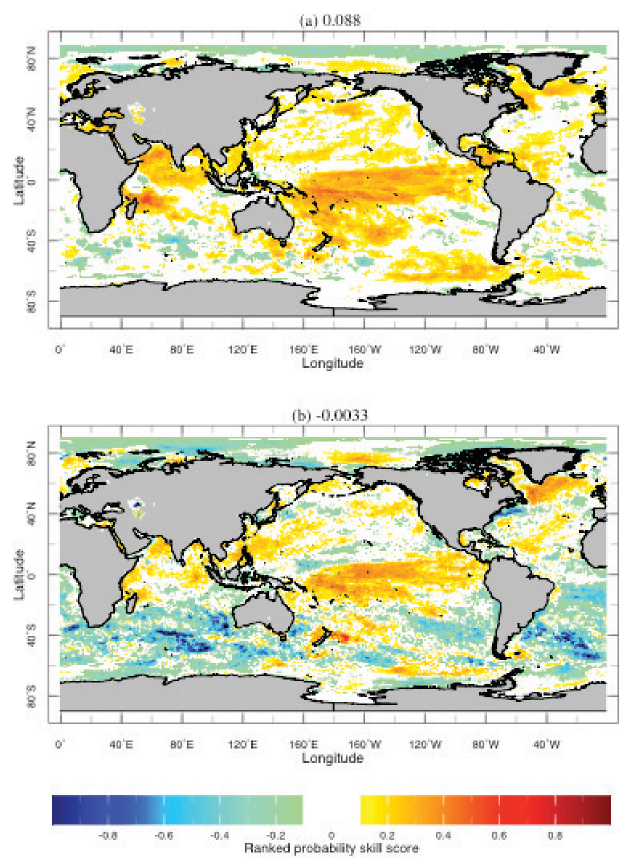

Fig. 6. SSTA RPSS for the (a) grand NMME multimodel ensemble and for (b) CFSv2. The skill is based on hindcasts initialized in Jan 1982–2009 and verified in the following JJA seasonal mean for tercile forecasts. Positive values indicate probabilistic skill that is better than climatology, and negative values indicate probabilistic skill that is worse than a climatological forecast. Global-averaged RPSS is noted in the figure.

climate over the 28-yr period was induced by a slight offset in the base period of the observations and the model hindcasts: for the observations, the period is 1981–2010, while for the model forecasts it is 1982–2009. Thus, the overall position of the reliability curves, while usually indicative of the model bias, is influenced here by the slight model versus observational base period offset.

The slope of the lines is related to the confidence level of the probability forecasts. Lines with slopes of less than 1 indicate forecast overconfidence, with greater relative differences in forecast probability than the corresponding differences in observed frequencies. A bias toward overconfidence has been noted in many individual dynamical models. Figure 10 indicates that this problem, while present, is very mild in the multimodel ensemble hindcasts compared to the individual models shown in Fig. 11. The amelioration of the overconfidence problem is undoubtedly a consequence of partial cancellation of somewhat conflicting signals that are overconfident in many of the individual models, resulting in an appropriately more probabilistically conservative forecast when the models are combined.

The offsetting of potentially overconfident forecasts of individual models when combined into a multimodel ensemble is illustrated by an example of a recent real-time prediction of the Niño-3.4 SST index (Fig. 12). The predictions of the individual ensemble members express the uncertainty distribution within each model, while the overall plume of forecasts express the uncertainty of the full multimodel ensemble. It is noted that the uncertainty distributions of the individual models is smaller than that of the collection of members of all models. The multimodel ensemble is probabilistically less overconfident than the ensembles of most of the individual models, because each individual model is imperfect, but has a higher than realistic confidence level in its "model world." Combining many models serves to offset differing biases, resulting in a more balanced and probabilistically reliable prediction.

One measure of the success of the NMME project is whether it will advance hydrologic applications,

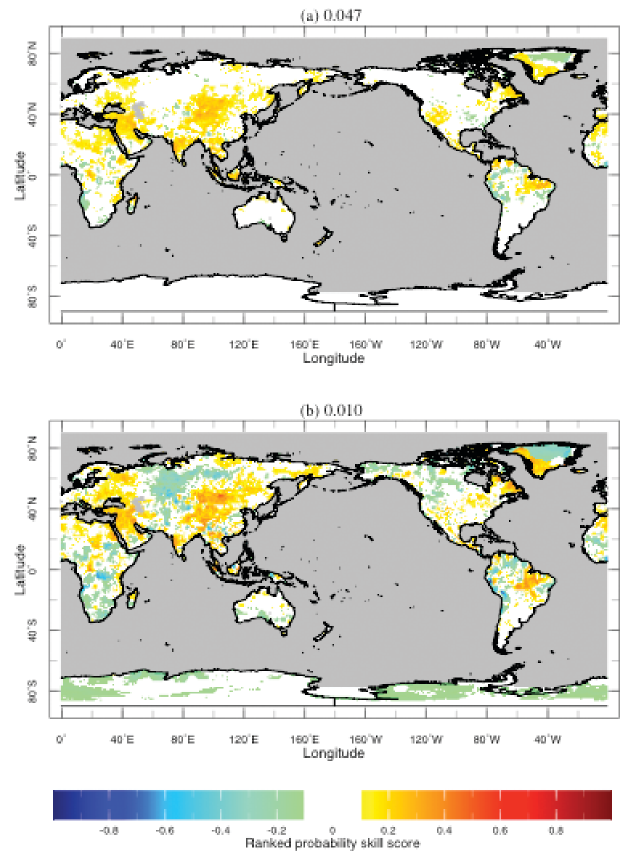

Fig. 7. Surface atmospheric temperature (2 m) RPSS for the (a) grand NMME multimodel ensemble and for (b) CFSv2. The skill is based on hindcasts initialized in Jan 1982–2009 and verified in the following JJA seasonal mean for tercile forecasts. Positive values indicate probabilistic skill that is better than climatology, and negative values indicate probabilistic skill that is worse than a climatological forecast. Global-averaged RPSS is noted in the figure.

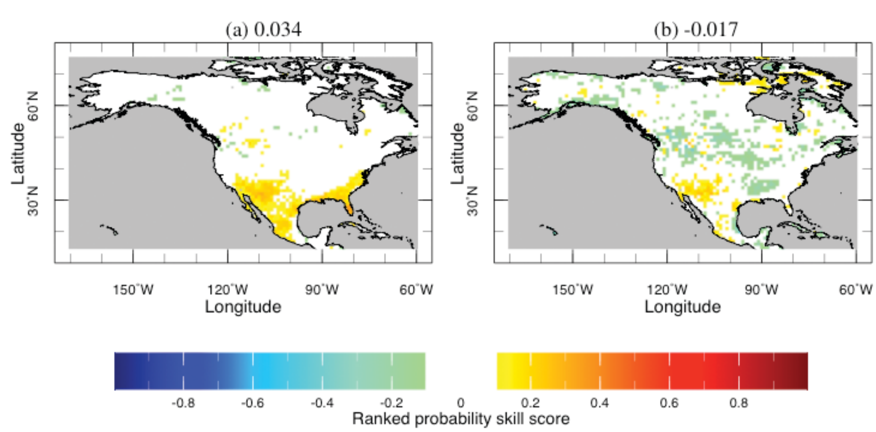

Fig. 8. Precipitation forecast RPSS for the (a) grand NMME multimodel ensemble and for (b) CFSv2. The skill is based on hindcasts initialized in Jul 1982–2009 and verified in the following DJF seasonal mean for tercile forecasts. Positive values indicate probabilistic skill that is better than climatology, and negative values indicate probabilistic skill that is worse than a climatological forecast. Global-averaged RPSS is noted in the figure.

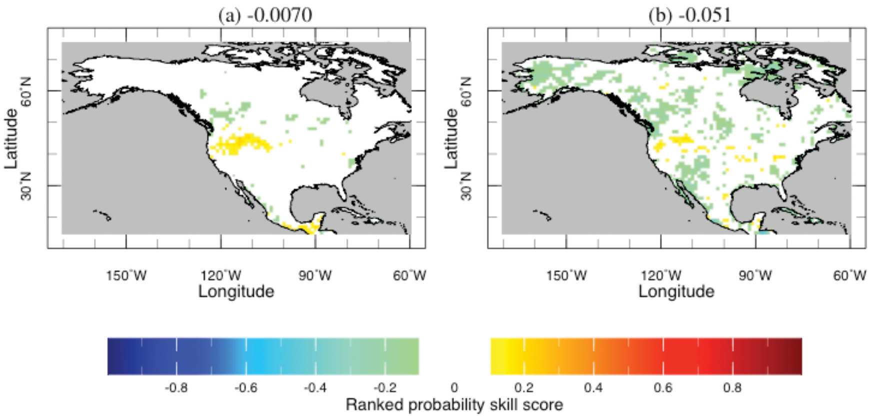

Fig. 9. Precipitation forecast RPSS for the (a) grand NMME multimodel ensemble and for (b) CFSv2. The skill is based on hindcasts initialized in Jan 1982–2009 and verified in the following JJA seasonal mean for tercile forecasts. Positive values indicate probabilistic skill that is better than climatology, and negative values indicate probabilistic skill that is worse than a climatological forecast. Global-averaged RPSS is noted in the figure.

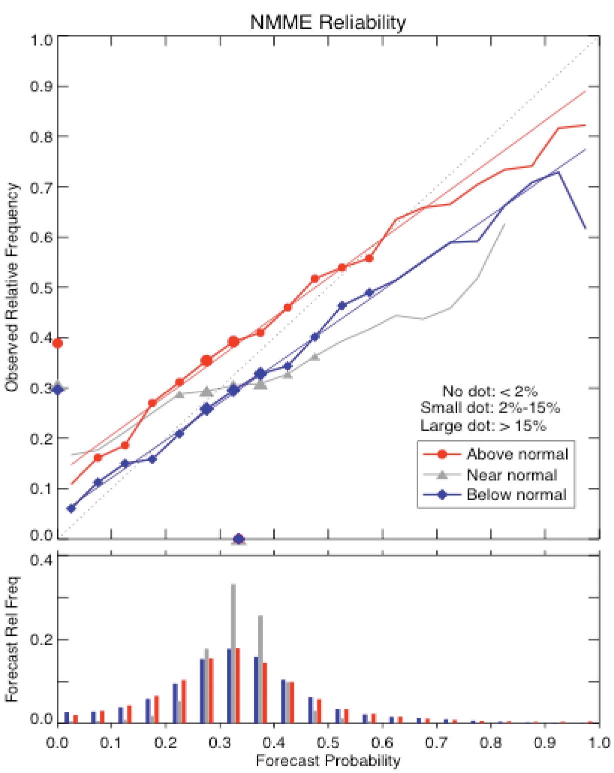

Fig. 10. NMME reliability diagram for T2m anomalies throughout the globe. The reliability corresponds to forecasts initialized in Oct 1982–2009 and verified in following JFM season.

which include streamflow and drought forecasting. Drought forecasting includes not only meteorological drought but also agricultural and hydrological drought. Meteorological drought is assessed through precipitation deficits with indices like the standardized precipitation index (SPI) determined over a window centered on the initial forecast date. Agricultural drought focuses on soil moisture deficits or indices such as their percentiles (Sheffield et al. 2004) and hydrological drought on streamflow. Collectively under the NMME project, seasonal hydrologic forecasting will include drought forecasting as well as related hydrological seasonal forecasting such as persistent wet conditions. Since hydrological applications usually require information at smaller spatial scales than that provided by the seasonal forecast models, the climate forecasts from the multimodel ensemble will be downscaled and bias corrected, using the approach of Luo et al. (2007), and used to drive a calibrated land surface model. The output of the land surface model is then used to for hydrologic forecasts, including drought. This approach has been well developed (Luo and Wood 2007, 2008; Yuan et al. 2013). Figure 13 shows the results for streamflow forecast skill from NMME relative to the skill from the often-used ensemble streamflow prediction (ESP) approach where hydrological model forcings come from historical resampling. The results are presented over the National Integrated Drought Information System (NIDIS) Colorado and southeastern U.S. testbeds. For the Colorado domain, NMME is more skillful than ESP, particularly in the summer with the skill coming primarily from increased precipitation skill. Not shown is the comparison between CFSv2 alone and NMME in which CFSv2 has slightly lower precipitation skill. For the southeast NIDIS domain, ESP is more skillful for 1-month leads due to low NMME precipitation skill, but the situation changes for longer leads when the full resolution is downscaled; bias-corrected forecasts are used in the hydrological model. For both ESP and NMME hydrological forecasts, observed hydrologic initial states are used at the initial forecast time. These can be provided from the North American Land Data Assimilation System (NLDAS) (Mitchell et al. 2004).

For meteorological drought assessed at continental-to-global scales, the 1° NMME model precipitation forecasts can be used. Figure 14 shows the NMME 6-month SPI (SPI6) forecast initiated

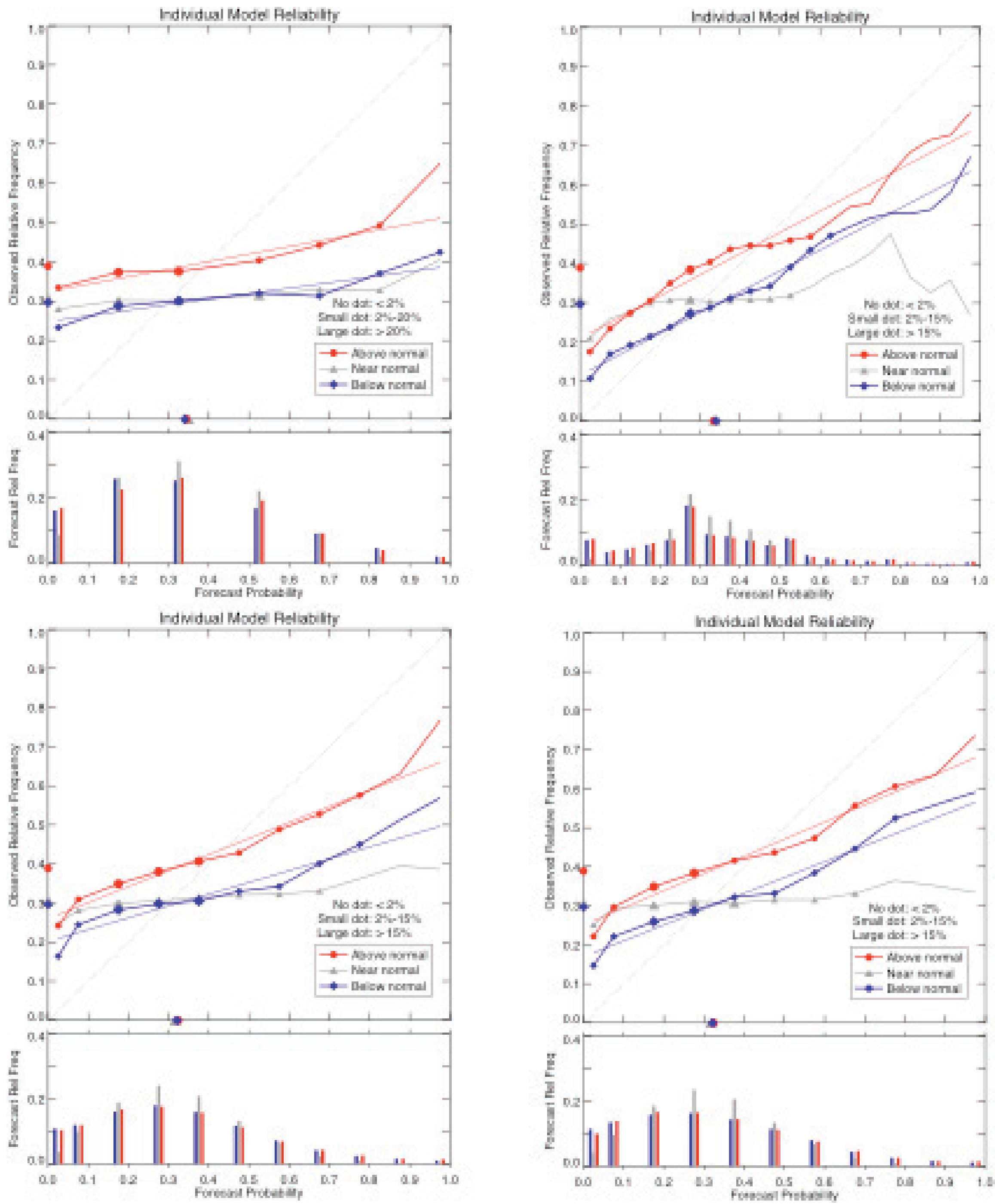

Fig. 11. Reliability diagram for T2m anomalies throughout the globe from a sample of individual models. The reliability corresponds to forecasts initialized in Oct 1982–2009 and verified in following JFM season.

on 1 June 2011 and 2012 for six models (ensemble mean), the equally weighted multimodel mean, and the observed SPI6 from the CPC-merged gauge radar precipitation analysis. As is done with SPI forecasts, observed March–May (MAM) precipitation is combined with JJA-precipitation forecasts to provide the SPI6 forecast. This methodology of combining 50% observational data with 50% forecast data is described in Quan et al. (2012).

THE PHASE-2 NMME. The NMME-2 project was awarded in August 2012 so results to present here are limited. However, there are some specific issues to highlight. In particular, we provide some preliminary results indicating that both modeling system improvements and data assimilation system improvements will contribute to improved NMME-2 forecast quality. We also describe an example of how some lessons learned regarding the retrospective forecast protocol in NMME-1 contribute to the NMME-2 forecast protocol. Finally, we provide some details regarding the data dissemination strategy on NMME-2.

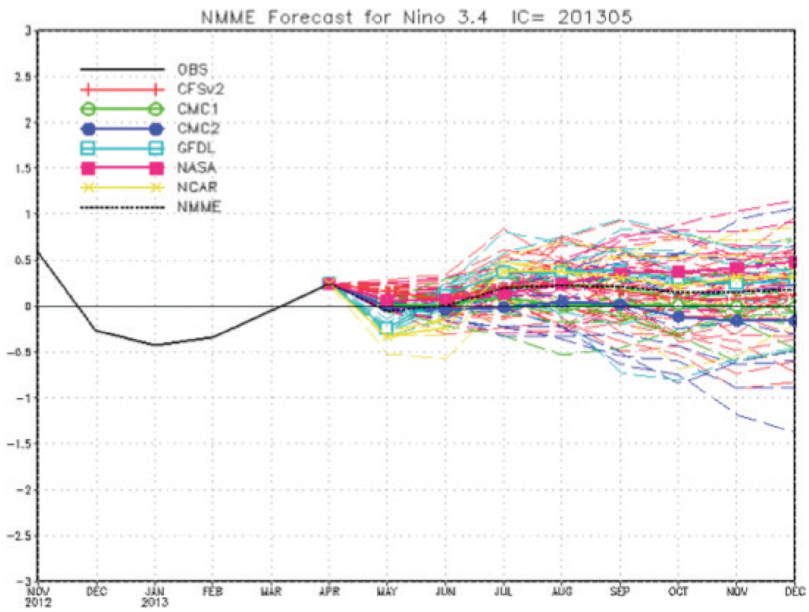

Fig. 12. Real-time Niño-3.4 predictions initialized in May 2013.

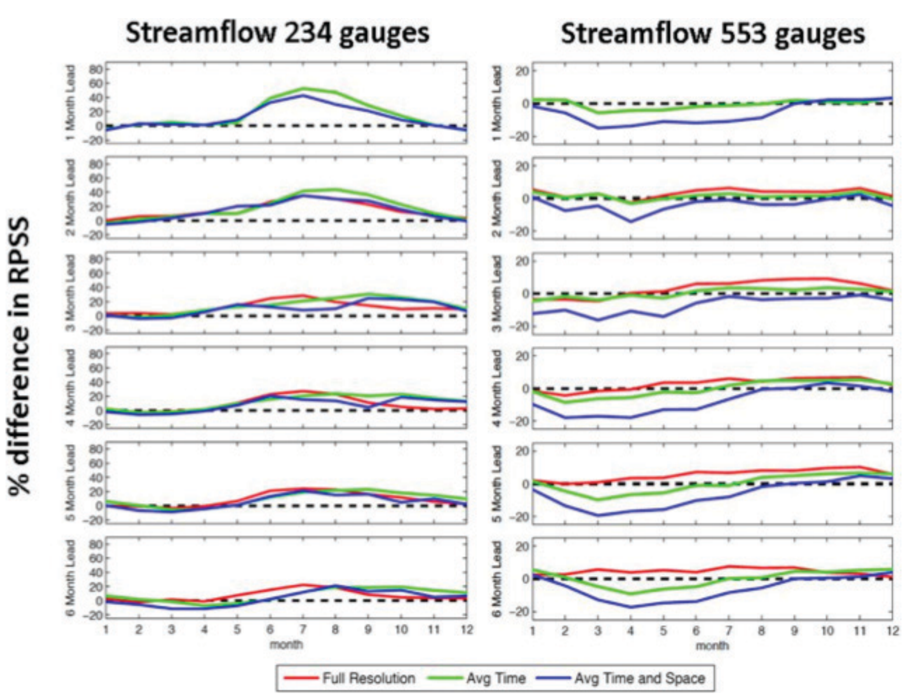

Fig. 13. Percent difference in RPSS skill of streamflow forecasts over the (left) Colorado NIDIS testbed and (right) southeastern U.S. NIDIS testbed with lead times out to 6 months. Skill differences above 0 indicates NMME forecasts are more skillful than ESP. Full resolution indicates using the downscaled 1/8°, daily seasonal climate model variables; Avg Time indicates the forecasts are averaged over the lead time; and Avg Time and Space indicates that the forecasts are averaged over the lead times and domain.

Prediction system improvement. The NMME team will transition from CCSM3 (T85) to CCSM4 (0.9 × 1.25_g1v6 resolution), although if CCSM3 continues to be a useful contributor to the NMME, we will continue the real-time predictions. CCSM4 has significant improvements in the simulation of tropical variability relative to CCSM3 (Neale et al. 2008; Jochum et al. 2008; Gent et al. 2010). The initialization procedure differs from CCSM3 in that we will use the operational Climate Forecast System Reanalysis (CFSR) ocean, land, and atmospheric states to initialize CCSM4 as opposed to ocean-only initialization using optimal interpolation from the Geophysical Fluid Dynamics Laboratory (GFDL) (i.e., Derber and Rosati 1989). We have begun testing the CFSR ocean states in CCSM4 hindcast experiments, and Fig. 15 shows the hindcast SSTA correlation for a parallel set of experiments using CCSM3 with the original GFDL ocean states (bottom panel) and using the CFSR ocean states (top panel). The correlation is notably larger with CCSM4 using CFSR ocean states. We separately examined the impact of the model changes (i.e., CCSM3 vs CCSM4) and the changes associated with the different ocean

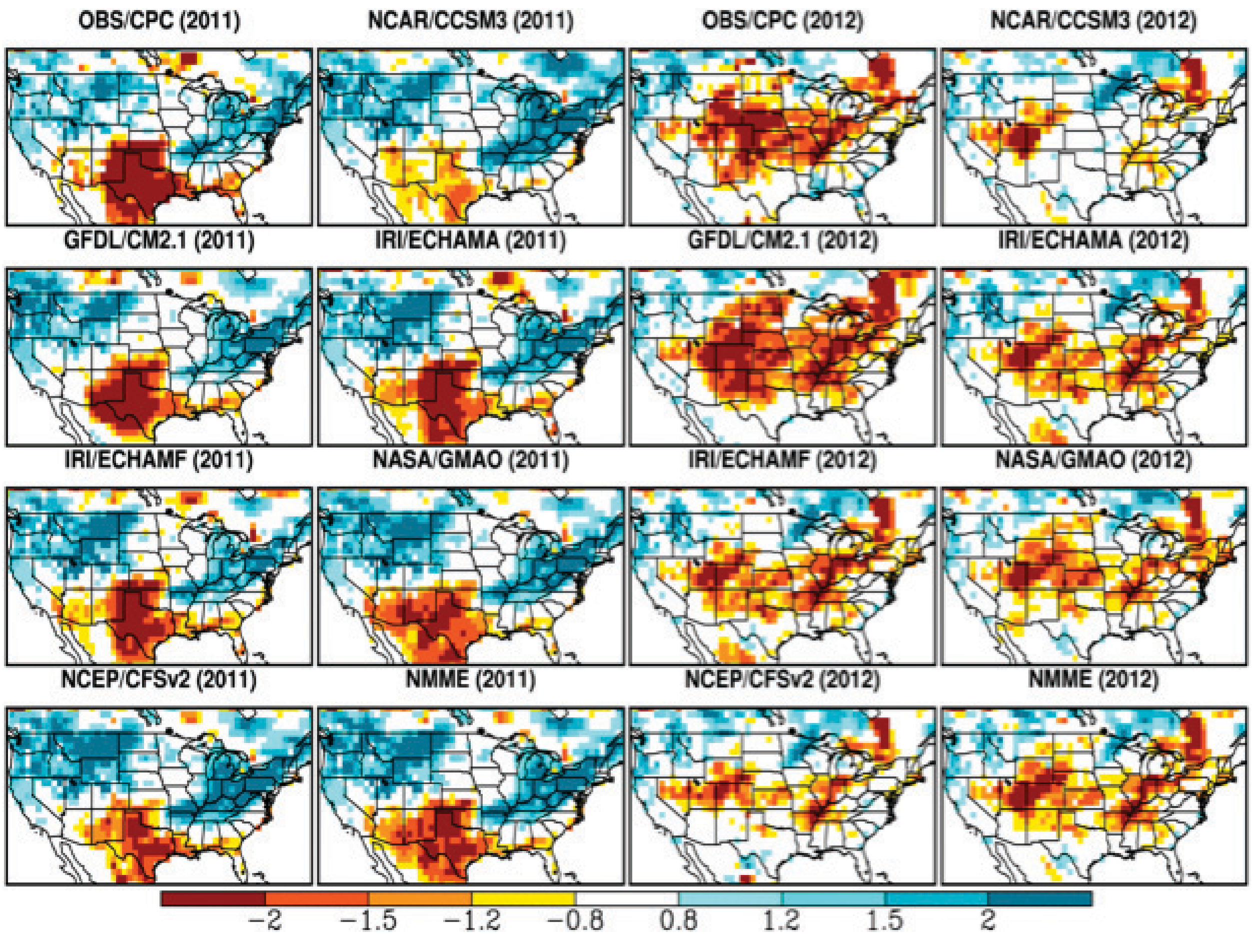

Fig. 14. NMME SPI6 forecasts initialized 1 Jun 2011 and 2012. Observed MAM precipitation is combined with JJA model ensemble-mean forecast. The NMME forecast is the equally weighted ensemble model average.

state. Both changes contribute to the increases in the correlation but are dominated by the model changes. We have also developed procedures for using CFSR data for the atmosphere and land initial states (e.g., Paolino et al. 2012).

The GFDL NMME contribution will transition from the GFDL Climate Model, version 2.1 (CM2.1) to the high-resolution coupled GFDL Climate Model, version 2.5 (CM2.5) (described below). The atmospheric component of CM2.5 is derived from the atmospheric component of the coupled GFDL CM2.1. The horizontal resolution has been refined from roughly 200 km to approximately 50 km. The ocean model is substantially different from that used in CM2.1. The ocean grid is considerably finer, with horizontal spacing varying from 28 km at the equator to 8 km in high latitudes. In addition, the grid boxes maintain an aspect ratio close to one, in contrast to CM2.1 where the aspect ratio can exceed 2 at high latitudes due to the convergence of the meridians. The ocean component uses 50 levels in the vertical as in CM2.1. The land model (Dunne et al. 2013) in CM2.5 is called LM3 and represents a major change from the land model used in CM2.1. LM3 is a new model for land water, energy, and carbon balance. The sea ice component used in CM2.5 is almost identical to that used in CM2.1, called the GFDL Sea Ice Simulator (SIS).

Data dissemination strategy. One of the major challenges for both NMME-1 and NMME-2 is to provide rapid and open access to all the hindcasts and real-time forecasts. The strategy developed includes two major components. First, NOAA/CPC will obtain and store the monthly-mean data (hindcasts and real-time forecasts) for the three [expanding to eight, that is, SST, precipitation, T2m, 500-mb geopotential, maximum temperature (Tmax), minimum temperature (Tmin), and soil moisture and runoff] required variables from all the participating models, and the IRI will maintain a NMME website serving this minimal dataset to the broader research and applications communities in real time. This rapid and open access to the data is a critical element distinguishing the NMME activity.

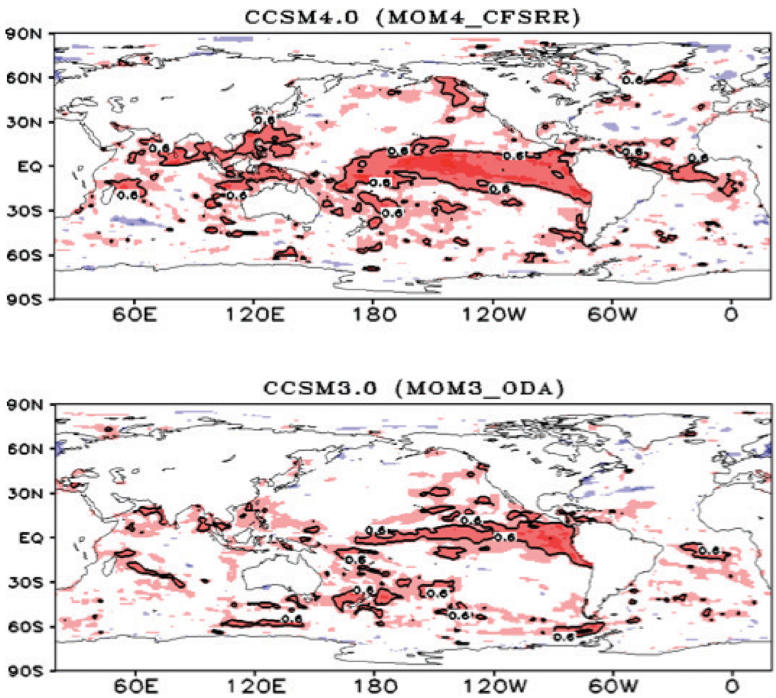

FIG. 15. SSTA correlation coefficient for forecasts initialized in early Jan and verified for May (1982–2000). The top panel shows results using CCSM4 and CFSR initial states for the ocean and the bottom panel shows results for CCSM3 using MOM3 ODA initial states.

The second component of the approach recognizes that the data and possibly the number of participating models will grow; a more robust centralized data strategy is required to meet the needs of the broader research and applications communities. As such, we have developed an NMME-2 data server to be housed at the new National Center for Atmospheric Research (NCAR) Wyoming Supercomputing Center (NWSC). This NMME-2 data server will include high frequency (e.g., 3 hourly and daily) and a much more complete three-dimensional distribution of the data.

NMME-2 RESEARCH. A major challenge to the NMME experiment is to quantitatively document the success of the project. Here, we briefly summarize some elements of our strategy but also welcome the broader research community to rigorously assess and use the data. Indeed, we assert that making the data readily available to all interested parties is the best approach for evaluating the utility of the multimodel approach advocated here. The measures of success envisioned by the NMME-2 team include a spectrum of quantitative metrics such as forecast skill assessment as a function of the number of models and ensemble members to identifying complementary skill among the models to assessing phenomenological skill.

For example, to determine the forecast skill as a function of the number of models and the number of ensemble members, we will assess a hierarchy of methods of varying complexity using a variety of deterministic and probabilistic verification measures. The deterministic verifications will be applied to the multimodel ensemble-mean forecast, while the probabilistic verifications will be applied to the forecast probabilities of tercile-based categories (hereafter called terciles) and of the extreme 15% tails of the climatological distribution. To facilitate this analysis the NMME project is developing an open access "verification map room" (http://iri.columbia.edu/~tippett/NMME/) that will also be easily accessible via smartphone. The reader is also encouraged to visit this website and the developing reliability website (http://iri.columbia.edu/~shuhua/mis-html/Reliability_nmme.html), both of which are already delivering results.

The above forecast skill assessment is applied without any mechanistic or phenomenological perspective. A second important measure of success is the extent to which we provide a better understanding of the mechanisms and sources of predictive skill. In this second category, we confront the forecasts with observations from a mechanistic and phenomenological perspective that also has the advantage of entraining some additional user communities into the skill assessment. We already have in place commitments to use the NMME data for the U.S. drought briefing, to derive standardized drought precipitation indices (K. Mo 2012, personal communication), and for the emerging Global Drought Information System (GDIS). Feedback from these applications will aid in assessing forecast skill from a drought user perspective, and the use of the NMME data in this regard is a clear measure of success.

An NMME, or any combination of forecast methods, begs the question as to how many models and ensemble members we really need for the problem at hand [this question also comes up in the Intergovernmental Panel on Climate Change (IPCC) context]. For example, do the $N + 1$ models always provide more skill than N models? The NMME phase-2 hindcasts provide an excellent opportunity to research this issue for subseasonal-to-seasonal time scales (beyond 2 weeks, excluding the weather prediction portion of each forecast period). Well-known notions with respect to the effective number of degrees of freedom in space and time (often approximated by how many EOFs it takes to explain, say, 90% of the variance of a dataset) can be applied here where an additional dimension "space" is taken to be across all the ensemble members. This way we could find that it takes only *n* models with *k* ensemble members to describe 90% of the information we have generated by *K* members of *N* models. This information content approach can be applied straightforwardly and is directly related to the notion of orthogonality/independence. It will take more originality to combine this with the skill of the forecasts; that is, add the observational dataset (1 single realization) to arrive at those components of a huge forecast dataset that are orthogonal with respect to their ability to add skillful information. These questions and many others can be addressed with the NMME phase-2 data that will be available to researchers beyond the NMME team.

CONCLUDING REMARKS. The purpose of this paper is to introduce the weather and climate research and applications communities to the NMME experiment. Here, we have provided a description of the NMME project and its expected evolution over the next 18–24 months (i.e., NMME-2). Part of the description emphasized both deterministic and probabilistic retrospectives in forecast verification. We chose to compare the NMME system (which includes the NOAA operational CFSv2) to CFSv2 alone. This choice was pragmatic and based on addressing the question of whether the NMME project can enhance the NOAA operational system. Overall, the various skill metrics (correlation, RMSE, RPSS, and reliability) all suggest that the NMME system improves the skill over the CFSv2. Admittedly, we have not clearly shown whether the improvement is due to a larger ensemble size or the use of multiple models (or both); nevertheless, the distribution of the forecast production to a number of different groups and centers is an effective strategy for economically increasing the forecast skill.

The assertion that the use of multiple models is an important aspect of the improved skill is supported by a number of previous efforts [e.g., Climate-System Historical Forecast Project (CHFP; www.wcrp-climate.org/wgsip/chfp/index.shtml), North American Ensemble Forecast System (NAEFS; www.emc.ncep.noaa.gov/gmb/ens/NAEFS.html), The Observing System Research and Predictability Experiment (THORPEX) Interactive Grand Global Ensemble (TIGGE; http://tigge.ecmwf.int/), Development of a European Multimodel Ensemble System for Seasonal-to-Interannual Prediction (DEMETER; www.ecmwf.int/research/demeter/index.html), and Ensemble-Based Predictions of Climate Changes and their Impacts (ENSEMBLES; www.ecmwf.int/research/EU_projects/ENSEMBLES/index.html)]. Indeed, much like the NMME activity, the International Multimodel Ensemble [IMME; the IMME project is an expansion of the European Seasonal to Interannual Prediction (EUROSIP) superensemble to include the CFSv2; see www.ecmwf.int/products/forecasts/d/charts/seasonal/forecast/eurosip/] is motivated by the results of these early studies. The distinction of the NMME project is twofold. First, the previous efforts focus entirely on retrospective forecasts, whereas the NMME project includes both real-time and retrospective forecasts. Second, the NMME project is committed to provide easy access to all the data (in near–real time), whereas the access to data is restricted in the IMME project. There is an important caveat here; namely, while multimodels' approaches are the pragmatic approach, we recognize that they do not adequately resolve the uncertainty due to model formulation.

Finally, we note that the NMME models that are retained as we enter phase-2 of the project are from major national modeling centers [i.e., NOAA–GFDL, NOAA–NCEP, NASA, NCAR, and the Canadian Meteorological Centre (CMC)], and it is our expectation that these efforts have critical mass in terms of human resources for continued evaluation and testing and that participation by the various NMME partners is mutually beneficial. For example, the project leverages all the model, assimilation, and data development activities at the various centers. The various centers, in turn, test their models against other state-of-the-art prediction systems in both retrospective and real-time mode and potentially have a much wider user community examine the predictions in various applications. We also believe that this continual enhanced collaboration among a broad base of researchers will lead to improved specific operational prediction products. Just as important, the core research collaboration that is at the heart of the NMME project will lead to a better understanding of mechanism of and sources for predictability and better estimates of the inherent limits of predictability. Moreover, some of these national efforts have distinct science missions, and the NMME project provides common experimental framework to evaluate model performance. Nevertheless, it remains a challenge to demonstrate that the research results from the NMME experiment feedback to model development, and the success of the project should be evaluated in this regard.

ACKNOWLEDGMENTS. The phase-1 NMME project was supported by the NOAA MAPP program, and the phase-2 NMME project is support by NOAA MAPP, NSF, NASA, and the DOE.

REFERENCES

Berner, J., F. J. Doblas-Reyes, T. N. Palmer, G. Shutts, and A. Weisheimer, 2008: Impact of a quasi-stochastic cellular automaton backscatter scheme on the systematic error and seasonal prediction skill of a global climate model. *Philos. Trans. Roy. Soc. London,* **A366,** 2561–2579, doi:10.1098/rsta.2008.0033.

Challinor, and Coauthors, 2005: Probabilistic simulations of crop yield over western India using the DEMETER seasonal hindcast ensembles. *Tellus,* **57A,** 498–512.

Derber, J., and A. Rosati, 1989: A global oceanic data assimilation system. *J. Phys. Oceanogr.,* **19,** 1333–1347.

DeWitt, D. G., 2005: Retrospective forecasts of interannual sea surface temperature anomalies from 1982 to present using a directly coupled atmosphere–ocean general circulation model. *Mon. Wea. Rev.,* **133,** 2972–2995.

Doblas-Reyes, F. J., R. Hagedorn, and T. N. Palmer, 2005: The rationale behind the success of multi-model ensembles in seasonal forecasting—II. Calibration and combination. *Tellus,* **57A,** 234–252, doi:10.1111/j.1600-0870.2005.00104.x.

Dunne, J. P., and Coauthors, 2013: GFDL's ESM2 global coupled climate–carbon Earth System Models. Part II: Carbon system formulation and baseline simulation characteristics. *J. Climate,* **26,** 2247–2267.

Gent P. R., S. G. Yeager, R. B. Neale, S. Levis, and D. A. Bailey, 2010: Improvements in a half degree atmosphere/land version of the CCSM. *Climate Dyn.,* 34, 819–833.

Goddard, L., S. J. Mason, S. E. Zebiak, C. F. Ropelewski, R. Basher, and M. A. Cane, 2001: Current approaches to seasonal-to-interannual climate predictions. *Int. J. Climatol.,* **21,** 1111–1152.

Hagedorn, R., F. J. Doblas-Reyes, and T. N. Palmer, 2005: The rationale behind the success of multi-model ensembles in seasonal forecasting—I. Basic concept. *Tellus,* **57A,** 219–233, doi:10.1111/j.1600-0870.2005.00103.x.

Jochum M., G. Danabasoglu, M. M. Holland, Y. O. Kwon, and W. G. Large, 2008: Ocean viscosity and climate. *J Geophys Res.,* **113,** C06017, doi:10.1029/2007JC004515.

Kirtman, B. P., 2003: The COLA anomaly coupled model: Ensemble ENSO prediction. *Mon. Wea. Rev.,* **131,** 2324–2341.

——, and D. Min, 2009: Multimodel ensemble ENSO prediction with CCSM and CFS. *Mon. Wea. Rev.,* **137,** 2908–2930.

Luo, L., and E. F. Wood, 2007: Monitoring and predicting the 2007 U.S. drought. *Geophys. Res. Lett.,* **34,** L22702, doi:10.1029/2007GL031673.

——, and ——, 2008: Use of Bayesian merging techniques in a multimodel seasonal hydrologic ensemble prediction system for the eastern United States. *J. Hydrometeor.,* **9,** 866–884.

——, ——, and M. Pan, 2007: Bayesian merging of multiple climate model forecasts for seasonal hydrological predictions. *J. Geophys. Res.,* **112,** D10102, doi:10.1029/2006JD007655.

Merryfield, W. J., and Coauthors, 2013: The Canadian seasonal to interannual prediction system. Part I: Models and initialization. *Mon. Wea. Rev.,* **141,** 2910–2945.

Mitchell, K. E., and Coauthors, 2004: The multi-institution North American Land Data Assimilation System (NLDAS): Utilizing multiple GCIP products and partners in a continental distributed hydrological modeling system. *J. Geophys. Res.,* **109,** D07S90, doi:10.1029/2003JD003823.

Morse, A. P., F. J. Doblas-Reyes, M. B. Hoshen, R. Hagedorn, and T. N. Palmer, 2005: A forecast quality assessment of an end-to-end probabilistic multi-model seasonal forecast system using a malaria model. *Tellus,* **57A,** 464–475, doi:10.1111/j.1600-0870.2005.00124.x.

Neale, R. B., J. H. Richter, and M. Jochum, 2008: The impact of convection on ENSO: From a delayed oscillator to a series of events. *J. Climate,* **21,** 5904–5924, doi:10.1175/2008JCLI2244.1.

Palmer, T. N., and Coauthors, 2004: Development of a European Multimodel Ensemble System for Seasonal-to-Interannual Prediction (DEMETER). *Bull. Amer. Meteor. Soc.,* **85,** 853–872.

——, C. Brankovic, and D. S. Richardson, 2000: A probability and decision-model analysis of PROVOST seasonal multimodel ensemble integrations. *Quart. J. Roy. Meteor. Soc.,* **126,** 2013–2034.

——, F. J. Doblas-Reyes, A. Weisheimer, and M. J. Rodwell, 2008: Toward seamless prediction: Calibration of climate change projections using seasonal forecast. *Bull. Amer. Meteor. Soc.,* **89,** 459–470.

Paolino, D. A., and Coauthors, 2012: The impact of land surface and atmospheric initialization on seasonal forecasts with CCSM. *J. Climate,* **25,** 1007–1021.

Pegion, K., and P. D. Sardeshmukh, 2011: Prospects for Improving Subseasonal Predictions. *Mon. Wea. Rev.,* **139,** 3648–3666, doi:10.1175/MWR-D-11-00004.1.

Quan, X., M. P. Hoerling, B. Lyon, A. Kumar, M. A. Bell, M. K. Tippett, and H. Wang, 2012: Prospects for dynamical prediction of meteorological drought. *J. Appl. Meteor. Climatol.,* **51,** 1238–1252.

Richardson, D. S., 2001: Measures of skill and value of ensemble prediction systems, their interrelationship and the effect of ensemble size. *Quart. J. Roy. Meteor. Soc.,* **127,** 2473–2489, doi:10.1002/qj.49712757715.

Saha, S., and Coauthors, 2006: The NCEP Climate Forecast System. *J. Climate,* **19,** 3483–351.

——, and Coauthors, 2014: The NCEP Climate Forecast System version 2. *J. Climate,* in press.

Sheffield, J., G. Goteti, F. Wen, and E. F. Wood, 2004; A simulated soil moisture based drought analysis for the United States, *J. Geophys. Res.,* **109,** D24108, doi:10.1029/2004JD005182.

Vernieres, G., C. Keppenne, M.M. Rienecker, J. Jacob, and R. Kovach, 2012: The GEOS-ODAS, description and evaluation. NASA Technical Report Series on Global Modeling and Data Assimilation, NASA/TM–2012–104606, Vol. 30.

Weigel, A. P., M. A. Liniger, and C. Appenzeller, 2007: The discrete brier and ranked probability skill scores. *Mon. Wea. Rev.,* **135,** 118–124.

Yuan, X., and E. F. Wood, 2012: On the clustering of climate models in ensemble seasonal forecasting. *Geophys. Res. Lett.,* **39,** L18701, doi:10.1029/2012GL052735.

——, ——, J. K. Roundy, and M. Pan, 2013: CFSv2-based seasonal hydro climatic forecasts over conterminous United States, *J. Climate,* **26,** 4828–4847, doi:10.1175/JCLI-D-12-00683.1.

Zhang, S., M. J. Harrison. A. Rosati, and A. T. Wittenberg, 2007: System design and evaluation of coupled ensemble data assimilation for global oceanic climate studies. *Mon. Wea. Rev.,* **135,** 3541–3564, doi:10.1175/MWR3466.1.

THE SAARC STORM

A Coordinated Field Experiment on Severe Thunderstorm Observations and Regional Modeling over the South Asian Region

BY SOMESHWAR DAS, U. C. MOHANTY, AJIT TYAGI, D. R. SIKKA, P. V. JOSEPH, L. S. RATHORE, ARJUMAND HABIB, SARAJU K. BAIDYA, KINZANG SONAM, AND ABHIJIT SARKAR

South Asian countries have developed a unique program for forecasting severe thunderstorms through field experiments and research on mesoscale modeling.

The Severe Thunderstorm Observations and Regional Modeling (STORM) program was originally conceived for understanding the severe thunderstorms locally known as "kal baisakhi" or nor'westers that affect West Bengal and the northeastern parts of India during the premonsoon season (March–May). In this season, a lot of thunderstorms occur over northeast India, Bangladesh, Nepal, and Bhutan. They are called nor'westers because they usually propagate from the northwest to the southeast. The earliest studies on nor'westers date back from the late 1920s to early 1940s. During the years 1928, 1941, and 1944, the India Meteorological Department (IMD) conducted three field experiments to understand their formation and to facilitate for their better prediction (IMD 1944). Several important features about time of development, movement, and distribution of thunderstorms were determined in these very early campaigns.

The nor'westers cause loss of human lives and damage to properties worth millions of dollars (De et al. 2005). It is now widely believed that severe thunderstorms like nor'westers take their toll quietly but steadily almost every day during the premonsoon season every year, perhaps exceeding the total causalities and damages to properties on a decadal scale compared to cyclones. For example, the severe storm that struck parts of eastern India and Bangladesh on 13 April 2010 (with the most intense portion spanning 30–40 min and winds estimated from 120 to 160 km h^{-1}) killed more than 150 people, completely destroyed over 100,000

AFFILIATIONS: DAS AND SARKAR—National Centre for Medium Range Weather Forecasting, Noida, India; MOHANTY—School of Earth, Ocean and Climate Sciences, Indian Institute of Technology, Bhubaneswar, Odisha, India; TYAGI—Ministry of Earth Sciences, New Delhi, India; SIKKA—Mausam Vihar, New Delhi, India; JOSEPH—Department of Atmospheric Sciences, Cochin University of Science and Technology, Kochi, India; RATHORE—India Meteorological Department, New Delhi, India; HABIB—SAARC Meteorological Research Centre, and Bangladesh Meteorological Department, Dhaka, Bangladesh; BAIDYA—Department of Hydrology and Meteorology, Kathmandu, Nepal; SONAM—Department of Hydro-Meteorological Services, Thimphu, Bhutan
CORRESPONDING AUTHOR: Dr. Someshwar Das, National Centre for Medium Range Weather Forecasting, A-50, Sector-62, Noida 201307, India
E-mail: somesh03@gmail.com

The abstract for this article can be found in this issue, following the table of contents.
DOI:10.1175/BAMS-D-12-00237.1

In final form 20 June 2013

Fig. 1. (a) The South Asian countries in alphabetical order: namely, Afghanistan, Bangladesh, Bhutan, India, Maldives, Nepal, Pakistan, and Sri Lanka under the SAARC. The experimental domains for phase 1 (deep moist convection/nor'westers/severe thunderstorms), phase 2 (dry convection/dust storms/western disturbances), and phase 3 (maritime convection) are outlined in the diagram. (b) Map of India showing state boundaries (source: www.nationsonline.org).

dwellings, partially damaged about 300,000 houses, and left nearly 500,000 people homeless. Widespread damage to crops and livestock including destruction of more than 14,000 ha of maize occurred. The storm uprooted trees, displaced rooftops, and snapped telephone and electricity lines in India, Bangladesh, and Nepal.

Realizing the importance of these extreme weather events and their socioeconomic impact, the India Department of Science and Technology started the nationally coordinated Severe Thunderstorm Observation and Regional Modeling (STORM) program in 2005. It is a comprehensive observational and modeling effort to improve understanding and prediction of severe thunderstorms (STORM 2005). The STORM program is a multiyear exercise and is quite complex in the formulation of its strategy for implementation. It needs different surface-based observational platforms to be organized on a mesonet basis. With gradual organization of desired observational support involving interested academic groups over eastern and northeastern India, two pilot experimental campaigns were conducted during the premonsoon seasons (April–May) of 2006 and 2007 (Mohanty et al. 2006, 2007). However, the weather knows no political boundaries. Since the neighboring South Asian countries are also affected by the nor'westers, the STORM program is expanded to cover the South Asian countries under the South Asian Association for Regional Cooperation (SAARC). The

FIG. 2. The road map of the SAARC STORM program. The field experiments of phase 1, phase 2, and phase 3 are conducted from April to May, from the middle of April to the end of June, and from early March to the middle of May, coinciding with the onset of convection over the three regions.

STORM program covers all the SAARC countries in three phases (Fig. 1a). A road map for the SAARC STORM program is illustrated in Fig. 2. In the first phase, the focus is on nor'westers that form over the eastern and northeastern parts of India, Bangladesh, Nepal, and Bhutan. In the second phase, the dry convective storms/dust storms and deep convection that occur in the western parts of India, Pakistan, and Afghanistan will be investigated. Similarly, in the third phase, the maritime and continental thunderstorms over southern parts of India, Sri Lanka, and Maldives will be investigated. Thus, overall the SAARC STORM program will cover investigations about formation, modeling, and forecasting, including nowcasting of severe convective weather in the premonsoon season over South Asia.

Accordingly, in the first phase, Bangladesh, Bhutan, India, and Nepal started a joint program focusing on nor'westers. Four pilot field experiments have been conducted so far during 1–31 May of 2009–12 jointly with the four countries to collect intensive observations of nor'westers in a coordinated way (Das et al. 2009a, 2011). Considering that the thunderstorms occur at a spatial scale ranging from a few kilometers to a few hundred kilometers, it was decided that a mesonet of automatic weather stations (AWS) would be set up over Bangladesh, Nepal, and Bhutan in a similar way as was done over West Bengal and the northeastern parts of India (Fig. 3). At least one GPS sonde is being set up at an appropriate location in each country (Bangladesh, Bhutan, and Nepal). An additional network of stations including the AWS, GPS sounding system, and Doppler weather radar (DWR) are being set up by the government of India through the Indian Space Research Organization (ISRO). The Doppler weather radars from India, Bangladesh, and Nepal will monitor the entire area covered in Fig. 3.

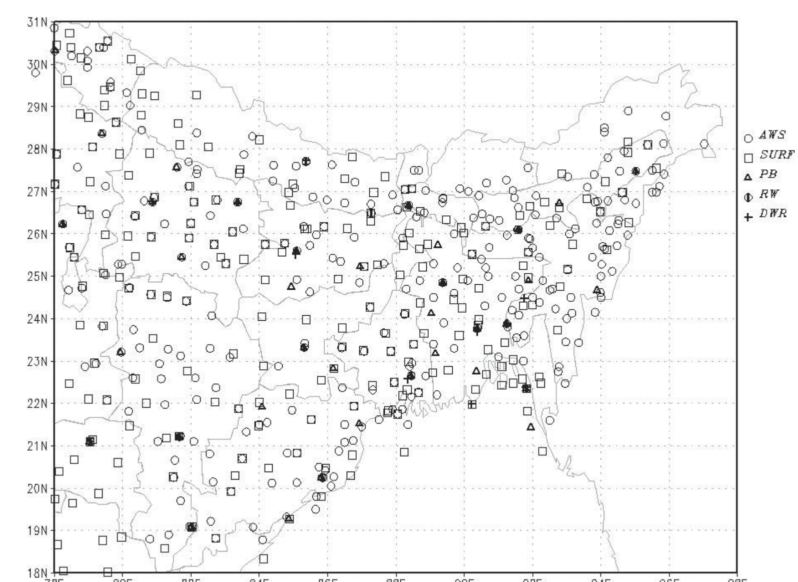

FIG. 3. Network of observatories (AWS, SYNOP, PB, RS/RW, and DWR) for the SAARC STORM pilot field experiment phase 1 covering eastern India, Bangladesh, Bhutan, and Nepal.

SEVERE CONVECTIVE STORMS OF SOUTH ASIA. In this section we briefly describe the severe convective storms affecting the South Asian region.

The nor'westers. The eastern and northeastern parts of India, Bangladesh, Bhutan, and Nepal are affected by severe thunderstorms during the premonsoon months (March–May). There are as many as 30–40 days of thunderstorms in parts of northeast India during this season (STORM 2005; Tyagi 2007; Das 2010; Yamane et al. 2009a,b). Severe thunder clouds (cumulonimbus) are often arranged in long lines of 200–400 km in length and travel with speeds of about 50–60 km h^{-1} (Das et al. 2009b). Figure 4a shows a typical nor'wester (squall line) observed by the DWR of Kolkata (22.57°N, 88.37°E). The highest wind speeds in these squalls are 140–150 km h^{-1}. A few of the nor'westers even reach the intensity of a tornado. Strong heating of the landmass during midday initiates convection, which gets intensified by mixing with the low-level warm moist air mass from the Bay of Bengal, and triggers violent storms (Srinivasan et al. 1973). The realization of instability depends on the large-scale flow and the synoptic systems present. In the lower troposphere, troughs, low pressure areas, and wind convergence lines are important. In the upper troposphere, a trough in westerlies and a jet stream are commonly associated with nor'westers. Superposition of favorable upper- and lower-tropospheric conditions result in generally widespread outbreaks of nor'westers (STORM 2005). Areas of upper-tropospheric positive vorticity advection in association with the troughs in westerlies are of particular importance to provide the large-scale vertical velocity situation favorable for triggering widespread thunderstorm activity (Alvi and Punjabi 1966; Raman and Raghavan 1961; Rao et al. 1971; Koteswaram and Srinivasan 1958; Krishna Rao 1966).

Hailstorms. India is among the countries in the world with the highest frequency of hail. There are about 29 hail days per year of moderate to severe intensity (Nizamuddin 1993). Hail sizes comparable to mangoes, lemons, and tennis balls have been observed. Eliot (1899) found that, out of 597 hailstorms in India, 153 yielded hailstones of 3-cm diameter or greater. India and Bangladesh are different from other Northern Hemisphere tropical stations in that hail is observed in the winter and premonsoon seasons with virtually no events after the onset of the southwest monsoon. Chaudhury and Banerjee (1983) show that the percentage of hailstorm days out of thunderstorm days decreases from 5% to less than 2% from March to May for northeast India and Bangladesh.

Tornadoes. About 72% of the reported tornadoes in South Asia occur in northeast India and Bangladesh. About 76% of the tornadoes in India occur during March–May, with the most favored month being April. More number of tornadoes have occurred in the afternoon and evening (Gupta and Ghosh 1980; Bhattacharya and Banerjee 1980; Mandal and Saha 1983). Asnani (1985), Goldar et al. (2001), and Litta et al. (2010, 2011, 2012b) have studied the tornadoes of India.

Dust storms. The northwest India, Pakistan, and Afghanistan get convective dust storms called "aandhi" locally during the premonsoon season (Joseph et al. 1980). Convective dust storms also occur in the region extending westward across Pakistan and Arabia to the arid regions of Africa like Sudan, Chad, etc. (Barkan et al. 2004, 2005; Hussain et al. 2005; Middleton 1986a,b; Middleton and Goudie 2001). In this season, the lowest atmospheric layers have very high temperature and relatively low moisture content, which makes the thunderstorms have high bases above the ground on the order of 3–4 km. The ground being dry over long periods, there is plenty of loose and fine dust available. These factors enable the severe thunderstorms of northwest India to generate dust storms. They are usually brief but can block out the sun, drastically reduce visibility, and cause property damage and injuries. Joseph et al. (1980) have done pioneering work on dust storms and the variations in horizontal visibility caused by them, studying 40 cases that occurred at the Indira Gandhi International Airport in Delhi. Studies on the climatology of dust storms and thunderstorms over Pakistan have been carried out by Hussain et al. (2005) and Mir et al. (2006). Their results indicate that extreme eastern and western parts of the northwest frontier of Pakistan, all of Jammu and Kashmir, and the north/northeastern parts of Punjab share about 65% of the total tropical storm (TS) frequency (over Pakistan).

Maritime thunderstorms. Studies of convective regimes over the northern Indian Ocean adjoining Sri Lanka and the Maldives Islands have been carried out under special field experiments named the Joint Air–Sea Monsoon Interaction Experiment (JASMINE; Webster et al. 2002) and the *Mirai* Indian Ocean Cruise for the Study of the MJO Onset (MISMO; Yoneyama et al. 2008). While the objective of JASMINE was to understand the physical processes that produce intraseasonal variability in the monsoon, the MISMO observational campaign was conducted to understand atmospheric and oceanic conditions in the central equatorial Indian Ocean when convection in the MJO was initiated. Over southern peninsular India and adjoining regions, the Tropical Rainfall Measuring Mission (TRMM) observations show that wide convective cores and

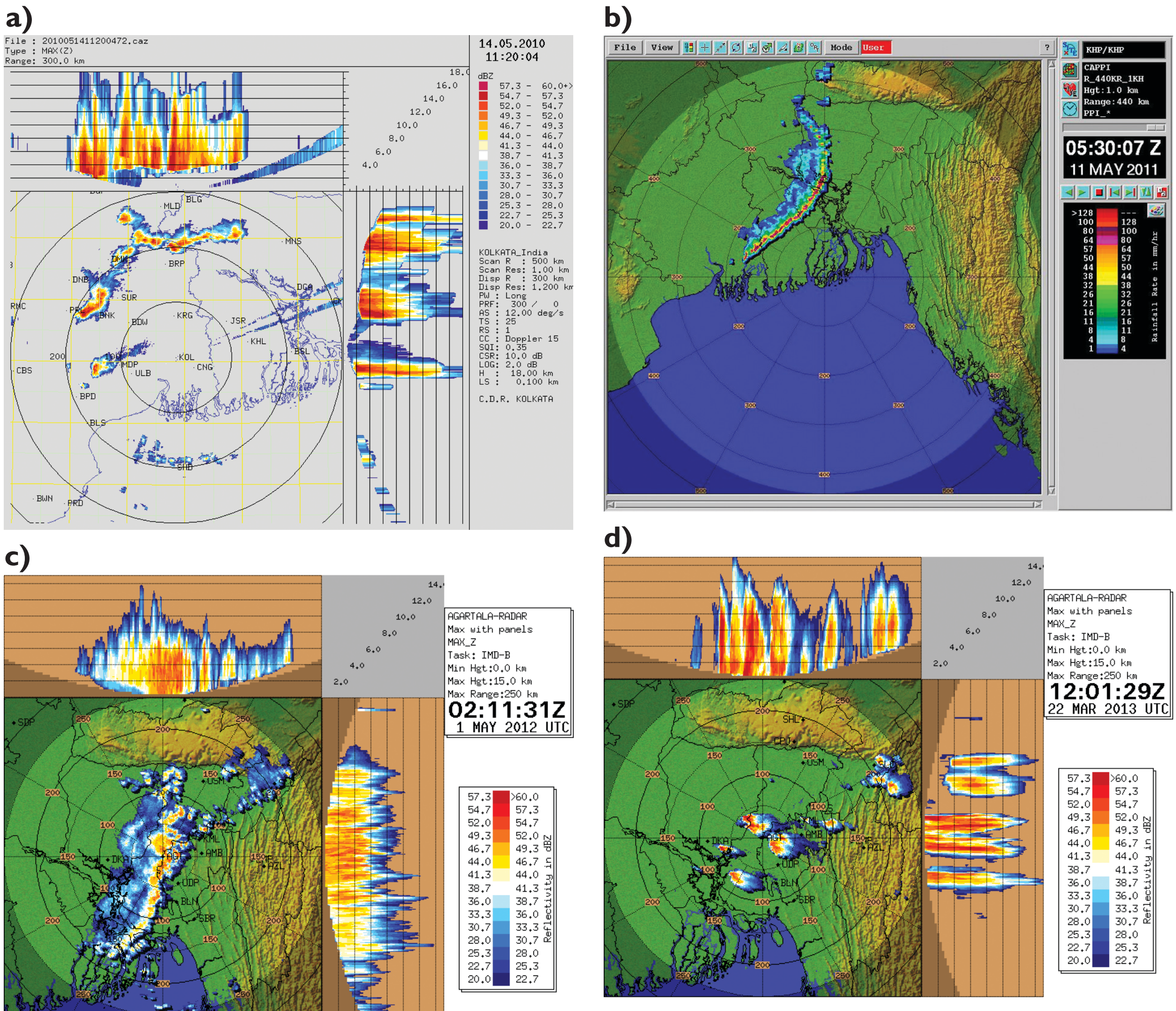

e)

f)

Fig. 4. Squall lines observed by (a) Doppler radar of Kolkata on 14 May 2010; (b) Khepupara radar on 11 May 2011; and Doppler radar images of Agartala on (c) 1 May 2012 and (d) 22 Mar 2013. The last event was (e) a tornado that struck in Brahmanbaria, Bangladesh, on 22 Mar 2013, killing many people and (f) producing hail of large size.

broad stratiform regions dominate over the deep convective cores (Houze et al. 2007; Romatschke et al. 2010). Further, the diurnal variation shows their occurrences mostly in the late evening. In Sri Lanka, the highest frequencies of thunderstorms occur during the two intermonsoons from March to April and from October to November (Das 2010). The potential for thunderstorms is higher over the western and eastern slopes or foot of the central hills and at minimum toward the northern parts of the country. In Maldives, thunderstorms occur more frequently in the central and northern parts of the country. There are two peak seasons of thunderstorms in this region: one extending from April to June and another from October to December, coinciding with the transitional southwest and northeast monsoon seasons.

Although many studies have been conducted in South Asia to understand the dynamical and thermodynamical structures of severe weather phenomena, they are mostly in the form of case studies and are limited because of the lack of observations. The microphysical processes leading to the development of these severe storms are also not well understood because of the lack of mesoscale observations. Improvement in the prediction of these important weather phenomena is also highly handicapped because of a lack of mesoscale observations in the vertical levels of the troposphere and an insufficient understanding of these phenomena. An unavailability of sophisticated instruments is responsible for an incomplete understanding of the burst of severe storms over South Asia.

There are many issues that need to be addressed on the dynamics and thermodynamics of severe thunderstorms over this part of South Asia. For instance, we need to find out the following: (i) What is the threshold value of CAPE for generation of thunderstorms over the South Asian region? (ii) What are the typical magnitudes of updrafts and downdrafts? (iii) What are the typical structures of hydrometeor profiles inside these thunderstorms? (iv) What is the relationship between thunderstorm behavior and synoptic-scale or mesoscale environment? (v) Which convective environments are conducive to thunderstorm genesis? (vi) What are the factors that distinguish genesis and maintenance of daytime and nocturnal (stable boundary layer) thunderstorms? Other questions that might come from midlatitude storm experience would be the roles of shear, capping, low-level jets (if any), and studies of storm rotation; its impacts on cell motion (if any) and tornadogenesis and whether it is associated with supercells; and the predictability of hail or lightning occurrence. We shall also have to (i) characterize system morphology and evolution of severe thunderstorms, (ii) document conditions leading to occurrence of severe weather, (iii) assess thunderstorm predictability, and (iv) determine what severe weather precursors associated with thunderstorms can be identified by radar and with what lead time. These are some of the issues addressed during the STORM program.

OBJECTIVES OF THE FIELD EXPERIMENT.

The SAARC STORM field experiment has the following objectives under its three phases.

Field experiment phase 1 (2009–16). Phase 1 has the following focus:

1) Prepare a well-designed coordinated plan for monitoring the life cycles of nor'westers/severe thunderstorms and their three-dimensional structure over northeastern parts of India (including West Bengal), Bangladesh, Nepal, and Bhutan during the premonsoon season.
2) Evolve strategies for observational systems of large-scale, synoptic-scale, and mesoscale environments; planetary boundary layer processes; convective dynamics; aerosols; cloud microphysics; and electrification for better understanding of atmospheric processes during different stages of convective development.
3) Formulate ideas on modeling mesoscale convection over the region and validate available models with the data to be collected during the pilot phase and the main experiment.
4) Facilitate the participation of universities and other organizations in the region.

Field experiment phase 2 (2012–16). In the second phase, the focus is on the investigation of deep convective storms as well as the dry convective storms/dust storms (aandhis) that occur in the western parts of India and adjoining Pakistan and Afghanistan region.

Field experiment phase 3 (2013–16). In the third phase, the aim is to investigate the tropical maritime as well as continental thunderstorms that occur in the southern peninsular India, Sri Lanka, and Maldives area.

Some of the science plans (monitoring life cycles of nor'westers/severe thunderstorms and their three-dimensional structures) to understand the interrelationship among dynamics, cloud microphysics, and electrical properties in the thunderstorm environment are new to the severe weather research. A summary of the field experiments on convection, clouds, and tropical storms conducted around the world is given in Tyagi et al. (2012).

EXPERIMENTAL DESIGN. Figure 2 illustrates the road map of the SAARC STORM program. The field experiments are conducted during the beginning of April to the end of May in phase 1, during the middle of April to the end of June in phase 2, and during early March to the middle of May in phase 3, coinciding with the onset of deep convection over the three regions. Joint pilot field experiments will be conducted including all three phases in the years 2013–14. The final (main) field experiments of all three phases will be conducted jointly during 2015–16. An extensive mesonetwork of observations with modern instruments/sensors (AWS, GPS sounding system, DWR, wind profilers, etc.) over this region is proposed to be set up to improve the understanding of the physical, dynamical, and thermodynamical characteristics of these thunderstorms. Figure 3 illustrates the distributions of observatories. Table 1 provides a list of equipment being used. The field experiments are being carried out in two stages: pilot phase and main phase. Table 2 provides the list of participating organizations. An operational management committee (OMC) has been set up at New Delhi to provide advisories regarding intensive observation period (IOP), three times a week (Monday, Wednesday, and Friday). An IOP is defined as the period when a severe weather event (nor'westers, squalls, hail, etc.) is expected to take place and predetermined detailed hourly/3-hourly/6-hourly observations at the surface, upper air, weather radar, satellite, etc., are planned to examine the event more closely. Observations are collected from the following network of stations during the pilot field experiments:

1) Large-scale meteorological observations covering the whole region are routinely collected with available network and existing observational schedule.
2) The mesonetwork of synoptic systems (SYNOP) and AWS (Fig. 3).
3) Upper-air observations from radiosonde/radio wind (RS/RW) stations available in the region. On days of IOP, vertical soundings of the atmosphere are made at 0600, 0900, 1200, and 1500 UTC. Pilot balloon observations are taken in the region of interest.
4) Wind profilers are proposed to be installed at strategic locations in the region.
5) The Doppler weather radar at Kolkata (West Bengal), Patna (25°36′N, 85°7′E; Bihar), Mohanbari (27°27′N, 95°2′E; Assam), and Agartala (23°49′N, 91°16′E; Tripura) is operated at 15-min intervals around the clock on IOP days. Other weather radars of India at Ranchi (23°21′N, 85°20′E; Jharkhand), Bhubaneshwar (20°14′N, 85°50′E; Orrisa), Paradeep (20°18′N, 86°30′E; West Bengal), and Guwahati (26°11′N, 91°44′E; Assam) provide 3-hourly data on a regular basis and hourly in IOPs during thunderstorms.
6) A mobile Doppler radar is proposed for the main field experiment.
7) Services of an aircraft with meteorological instrumentation for dropwindsondes and other airborne measurements are proposed for the main experiment.
8) A research ship is proposed to be located at the head Bay of Bengal during the main experiment. Devices for the measurement of sea surface temperature would also be a part of sensors onboard the ship.
9) Towers of 30-m height with six levels of instrumentation for air temperature; dewpoint temperature; and *u*, *v*, and *w* components of wind are set up at different locations in the region.
10) One disdrometer is made available at the location of the Doppler radar and other places of interest.

Table 1. List of equipment used in the field experiment.

	Equipment/type of station	No.
1	Automatic weather stations	299
2	Surface synoptic stations	217
3	Radiosonde/radio wind/GPS sounding systems	19
4	Pilot balloon stations	36
5	DigiCORA	1
6	Doppler weather radars/storm radars	10
7	Mobile Doppler radar (proposed)	1
8	Wind profilers (proposed)	1
9	Reconnaissance aircraft/dropsondes (proposed)	1
10	Meteorological towers (30 m)	2
11	Disdrometer	1
12	Soil moisture/soil temperature stations	10
13	Atmospheric electricity field stations	1
14	CCN counter	1
15	Aerosol sampler (SPMS)/particle sensor	1
16	Polarized lidars (proposed)	1
17	Phased array sodar (proposed)	1
18	Microwave radiometers (proposed)	1
19	Mobile mesonet (proposed)	1
20	Mobile GPS sounding system (proposed)	1
21	Sky radiometers (proposed)	1
22	Lightning detectors (proposed)	4

11) Measurements of soil moisture and soil temperature are made at some of the mesonet stations for land surface process studies.
12) For the study of thunderstorm microphysics and electricity, some stations have atmospheric electric sensors. In addition, one station has two storm trackers, one CCN counter, one aerosol sampler (SPMS), and one aerosol particle sensor.
13) Radiometers for measuring humidity structure of the troposphere at several stations.

During the field experiment, IMD and the National Centre for Medium Range Weather Forecasting (NCMRWF) provide 5-day forecasts of the probability of severe nor'wester outbreaks in and around the field experiment area using their global and mesoscale models. The OMC set up at IMD, Delhi, provides weather advisories for deciding the IOP days and conducting the field experiment.

PILOT FIELD EXPERIMENTS AND RESULTS. Widespread outbreaks of intense thunderstorms occurred on many days affecting India, Bangladesh, Nepal, and Bhutan during the pilot field experiments of 2006–12. Some of the more prominent among them occurred on 11 May 2009, 14 May 2010, 11 May 2011, 1 May 2012, and 22 March 2013, as shown by the radar images in Fig. 4. The last event was a tornado (Fig. 4e) that killed 22 people, injured 300 others, destroyed 500 houses, affected electric lines, and collapsed a road communication system by breaking down numerous trees in the Brahmanbaria district of Bangladesh around 1130 UTC [1730 local standard time (LST)] 22 March 2013 (source: http://reliefweb.int/report/bangladesh/situation-report-tornado-brahmanbaria-24-mar-2013). Many studies have been carried out using the pilot field experiment datasets (Abhilash et al. 2007, 2008; Das et al. 2009b; Litta and Mohanty 2008; Joseph 2009; Rao 2009; Litta et al. 2012a; Gopalakrishnan et al. 2011; A. Tyagi et al. 2011, 2012; B. Tyagi et al. 2013). For brevity, we illustrate here one case study of 11 May 2009 (Fig. 5), which was

Table 2. List of organizations participating in the field experiment.

	Name of the institution
1	Ministry of Earth Sciences, New Delhi, India
2	India Meteorological Department, New Delhi, India
3	National Centre for Medium Range Weather Forecasting, Noida, India
4	Indian Institute of Tropical Meteorology, Pune, India
5	Indian Space Research Organization, Banglore, India
6	Space Application Centre, Ahmedabad, India
7	National Atmospheric Research Laboratory, Gadanki, India
8	North-East Space Application Centre, Mizoram, India
9	Indian Institute of Technology, New Delhi, India
10	Indian Institute of Technology, Kharagpur, India
11	Indian Air Force, New Delhi, India
12	Indian Navy, New Delhi, India
13	Calcutta university and colleges, Calcutta, India
14	Jadavpur University, Kolkata, India
15	State Council for Science and Technology, West Bengal, Kolkata, India
16	State Council for Science and Technology, Meghalaya, Shillong, India
17	Space Physical Laboratory, Tiruvanantapuram, India
18	National Physical Laboratory, New Delhi, India
19	Defense Research and Development Organization, Chandipur, India
20	Indian Institute of Science, Bangalore, India
21	Andhra University, Vishakhapatnam, India
22	University of Pune, Pune, India
23	Cochin University of Science and Technology, Kochi, India
24	Birla Institute of Technology, Mesra, Ranchi, India
25	B.C. Agriculture University, Kalyani, India
26	Burdwan University, Shanti Niketan, India
27	Yogi Baman University, Andhra Pradesh, India
28	Vidyasagar University, Paschim Medinipur, India
29	SAARC Meteorological Research Centre, Dhaka, Bangladesh
30	Bangladesh Meteorological Department, Dhaka, Bangladesh
31	Department of Hydrology and Meteorology, Kathmandu, Nepal
32	Department of Hydro-Meteorological Services (DHMS), Thimphu, Bhutan

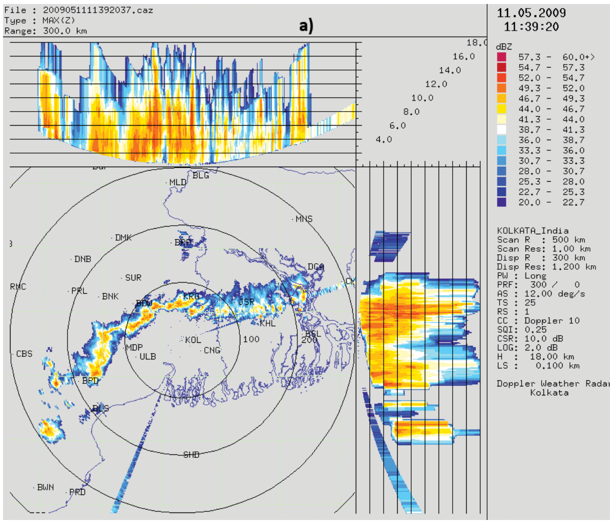

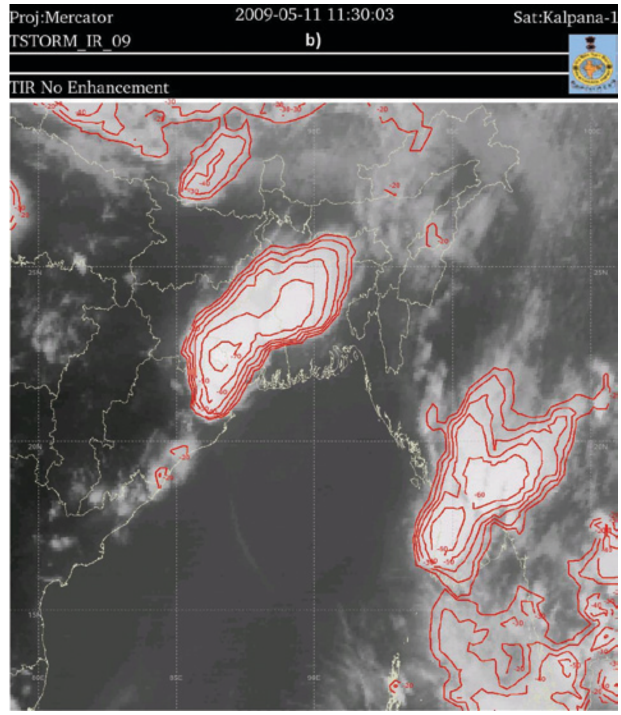

Fig. 5. A typical nor'wester observed by (a) Doppler weather radar of Kolkata and (b) cloud imageries with contours of the cloud-top temperature obtained from the *Kalpana-1* satellite at 1130 UTC (1700 LST) 11 May 2009, which affected parts of east India and Bangladesh.

also declared as an IOP day for east and northeast India, particularly over sub-Himalayan West Bengal, Sikkim, and the northeastern states of India, including Assam. Details of various cases are given in Mohanty et al. (2006, 2007, 2009) and Das et al. (2009a, 2011). The synoptic features, satellite and Doppler radar analysis, and realized weather along with some of the weather charts are described in the following subsections.

Synoptic features (based on 0000/0300 UTC 11 May 2009 weather charts). At mean sea level, a trough was established from east Uttar Pradesh to north Tamilnadu across east Madhya Pradesh and Andhra Pradesh. Please see Fig. 1b for the state boundaries of India. Cyclonic circulation occurred in lower levels over Bihar and its neighborhood. The trough from this extended up to the extreme south peninsula across Chattisgarh, Telangana, and Rayalaseema (Andhra Pradesh). Another cyclonic circulation occurred over Arunachal Pradesh and adjoining Assam and Meghalaya. Moisture incursion took place over the area. A trough from Arunachal Pradesh to the northwest Bay of Bengal was also seen in the middle troposphere. Westerly jet maxima were found over the region.

Realized weather. A squall passed over Agartala at 1830 UTC (0000 LST) from the north with a maximum speed of 28.1 kt (52 km h^{-1}). Another squall passed over Bankura (23°1′N, 87°4′E; West Bengal) at 1019 UTC (1549 LST) from the northwest with a maximum speed of 30.2 kt (56 km h^{-1}). It passed over Alipore (22°30′N, 88°18′E; Kolkata) at 1245 UTC (1815 LST) from the northwest with a maximum speed of 35.1 kt (65 km h^{-1}). Dum Dum (22°35′N, 88°24′E; Kolkata) reported the squall at 1243 UTC (1813 LST) from the northwest with a maximum speed of 46.9 kt (87 km h^{-1}). The Air Force station Barrackpore (22°46′N, 88°22′E; Kolkata) reported the squall at 1240 UTC (1810 LST), with a maximum speed of 50 kt (92.7 km h^{-1}) from the north. The maximum rainfall recorded over the region was 48 mm at Basirhat (22°38′N, 88°52′E; West Bengal). The wind fields at the surface (10 m) and 850-hPa, wind shear between 500 and 850 hPa, vertical velocity, and CAPE along with observed precipitation by TRMM are shown in Figs. 6–8.

Doppler weather radar analysis. A strong echo developed over Ranchi at 0800 UTC (1330 LST; Fig. 5a), and a few more echoes developed near Dumka (24°16′N, 88°15′E; Jharkhand) and between Krishnanagar (23°13′N, 87°33′E; West Bengal) and Mymensingh (24°51′N, 90°40′E; Bangladesh). These echoes intensified into two squall lines, one with northeast–southwest orientation and another with east–west orientation; merging together by 1130 UTC (1700 LST), these squall lines moved southeast and dissipated over the sea by 1600 UTC (2130 LST).

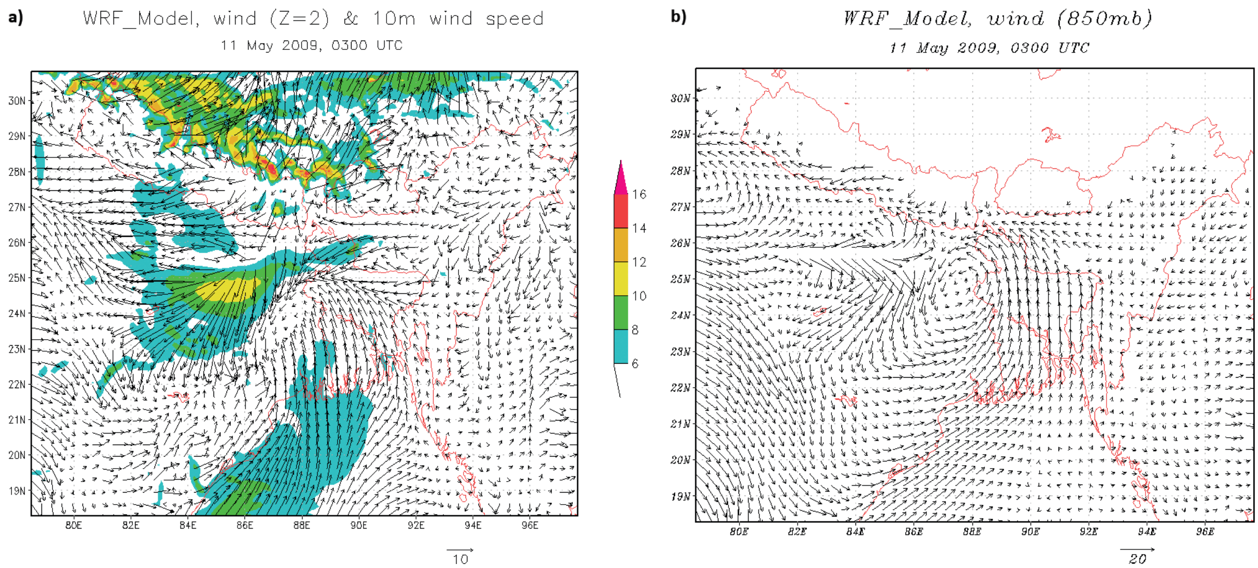

Fig. 6. Vector wind fields at (a) sigma level 2 with shaded wind speed at 10 m above the surface and (b) 850 hPa on 11 May 2009.

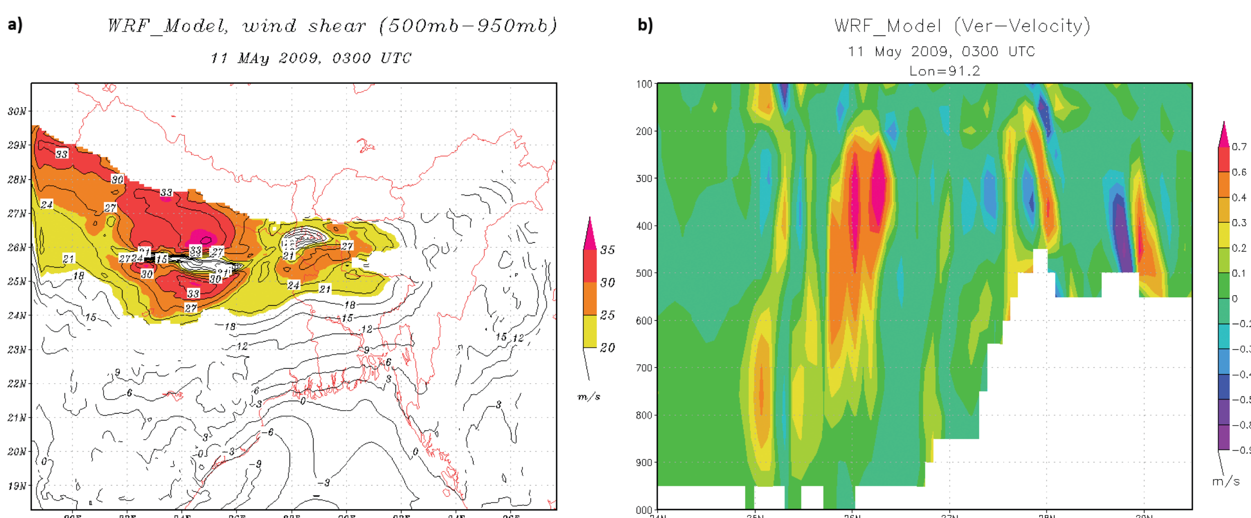

Fig. 7. (a) Wind shear (500–850 hPa) and (b) vertical cross section of the vertical velocity (m s^{-1}) at the location of the storm (91°E).

Kalpana-1 satellite picture analysis. The *Kalpana-1* satellite picture of 1130 UTC (1700 LST) is shown in Fig. 5b. Moderate convection was seen over central Nepal. A cluster of clouds [cloud-top temperature (CTT) = –50°C] moved eastward; expanded into Bangladesh; and merged with convection over Jharkhand, Orissa, and West Bengal (CTT = –70°C). Moving south, it dissipated over the sea after 2330 UTC (0500 LST). Convection persisted over south Orissa and adjoining Andhra Pradesh from 1100 to 1700 UTC (1630 to 2230 LST; minimum CTT = –50°C).

Mesoscale analysis. The Weather Research and Forecasting (WRF) model (version 3.0) analysis products run at 9-km resolution and 28 vertical levels are shown in Figs. 6–8. The model was run with the Kain–Fritsch convection scheme, Yonsei University (YSU) boundary layer parameterization, WRF single-moment 6-class microphysics scheme (WSM6) cloud microphysics, and the National Oceanic and Atmospheric Administration (NOAA) unified land surface model. Figures 4a and 4b present winds at 10 m and 850 hPa, respectively. Moisture incursion is seen over east India at lower levels with southwesterly flow of 10–15 kt over the coastal area. A cyclonic circulation is seen over West Bengal, adjoining Bihar, and Jharkhand (Fig. 6b). The wind fields indicate mesoscale convergence that extended up to 850 hPa.

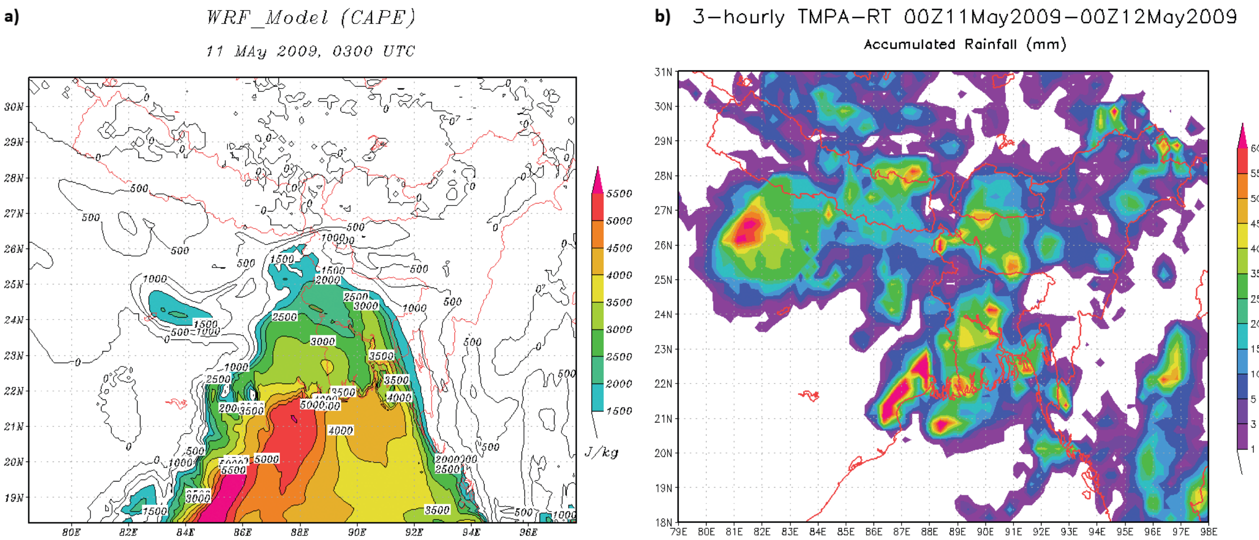

FIG. 8. (a) CAPE (J Kg^{-1}) and (b) TRMM precipitation (mm) accumulated for 24 h.

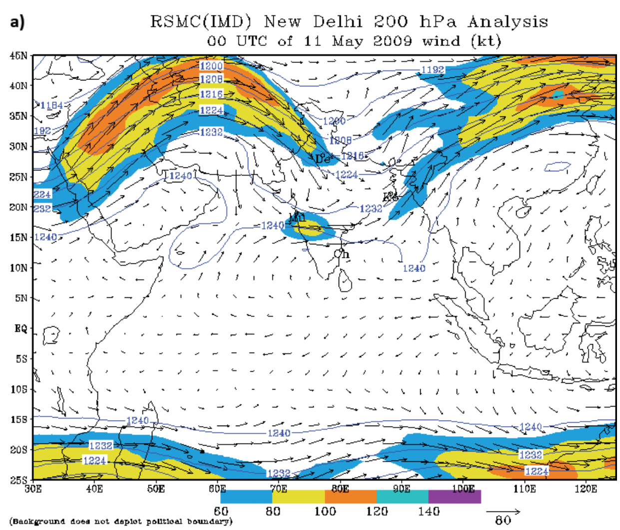

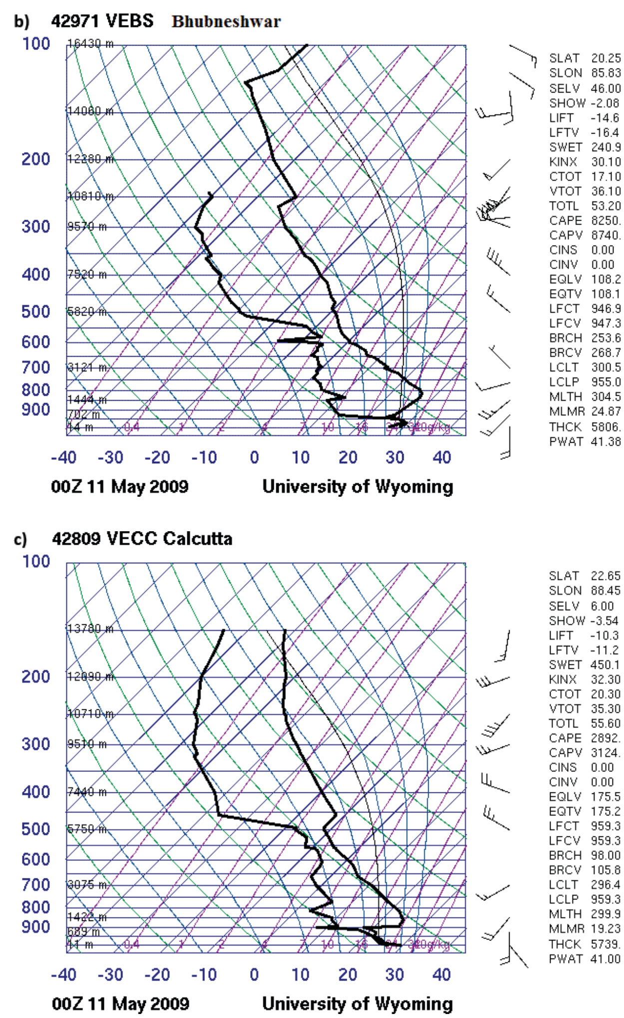

FIG. 9. (a) Vector wind fields at 200 hPa with geopotential contours and skew-*T* diagrams of (b) Bhubneshwar and (c) Kolkata at 0000 UTC 11 May 2009 obtained from the University of Wyoming website.

A significant trough was seen at 200 hPa (Fig. 9a) over north-central India. A belt of strong wind shear (Fig. 6a) was seen extending from Uttaranchal, the southern plains of Nepal, Uttar Pradesh, Bihar, West Bengal, and northwestern Bangladesh. Many pockets of strong rising motion (Fig. 6b) were seen along 91°E. Regions of high CAPE (Fig. 8a) are seen along the east coast of India and off the coasts of Orissa, West Bengal, and Bangladesh. Such high values of CAPE can occur because of confluence of cold air advection from land and warm moist air from the ocean as seen in Figs. 9a and 6b. The superimposition of cold northwesterly air from the Himalayas at upper levels (Fig. 9a) over the warm moist air from the Bay of Bengal (Fig. 6b) produces very high instability (CAPE > 5000 J kg^{-1}) during the premonsoon season as seen in the skew-T diagrams of Bhubneshwar

(CAPE = 8250 J kg^{-1}) and Kolkata (CAPE = 2892 J kg^{-1}) in Figs. 9b and 9c, respectively. All the convective indices of Bhubneshwar [i.e., lifting index = −10.8, severe weather threat (sweat) index = 682.4, and total index = 60.3] indicate very unstable atmosphere and the likelihood of severe thunderstorms with a lifting mechanism. Intense precipitation was observed by TRMM (Fig. 8b) over Uttar Pradesh, eastern Nepal, Orissa, West Bengal, Assam, Bangladesh, and southern parts of Bhutan. The model could not capture the wide-spread rainfall and squalls over east India but has done reasonably well in predicting rainfall over the northeastern states. It shows some fidelity (nearly correct genesis and intensification), but the time of occurrence is still not very good. Detailed model evaluation results based on the pilot data are discussed in Abhilash et al. (2007), Das et al. (2009b), Litta and Mohanty (2008), Litta et al. (2012a), A. Tyagi et al. (2011, 2012), and B. Tyagi et al. (2013).

COMMON SYNOPTIC FEATURES OBSERVED DURING STORM PILOT PHASES.

Severe weather days. Weak surface pressure field associated with weak surface and lower atmospheric wind forcing coupled with strong daytime heating makes the atmosphere potentially unstable in the premonsoon months of April and May. On some of the occasions, the thunderstorms are initially local in nature but develop into squall lines and even extend to mesoscale convective system (MCS) by mergers (Tyagi et al. 2012). Some of them last for 1–3 hours. Others can go even up to 8–12 hours. The possible synoptic systems or features that provide the trigger are as follows (Mohanty et al. 2006, 2007; Das et al. 2009a, 2011):

1) surface or low-level trough in pressure and wind field;
2) strong southerlies or southwesterly winds 10–20 kt along north Andhra, Orissa, and the Gangetic West Bengal coast and backing to easterlies or southeasterlies over West Bengal and its neighborhood form a cyclonic circulation between the surface and 1.5 km that brings moist air from the Bay of Bengal over the eastern Indian region;
3) the atmosphere having latent/potential instability that usually is present on most of the days;
4) a suitably placed trough in the middle and upper atmosphere between 500- and 200-hPa levels in the subtropical westerlies to provide an upper-level divergent field;
5) the accelerating subtropical westerly jet stream with appropriate location of entrance and exit regions of the jet maxima (mostly in April and early May); and
6) wind shear of 40–60 kt between 200 and 850 hPa favoring development of thunderstorms.

Features associated with weak convection. The following features are associated with weak convection:

(i) weak or no surface and lower-tropospheric trough in the wind field;
(ii) dry northwesterly winds prevailing in the lower troposphere over the eastern region; and
(iii) coastal winds (up to a height of 1.5 km) along the Orissa and Gangetic West Bengal coasts that are northwesterly or weak southwesterly.

SUMMARY AND RESEARCH OPPORTUNITIES.

The SAARC STORM is a coordinated effort on understanding severe thunderstorms through observations and regional modeling by eight South Asian countries. It is a multiyear exercise being conducted in three phases (2009–16) using different observational networks (surface, upper-air, satellite, radar, and mobile platforms). The program will investigate the severe storms like nor'westers (which form over the eastern and northeastern parts of India, Bangladesh, Nepal, and Bhutan in the first phase), the dry convective storms/dust storms and deep convection (which occur in the western parts of India, Pakistan, and Afghanistan in the second phase), and the maritime and continental thunderstorms (which occur over southern parts of India, Sri Lanka, and the Maldives in the third phase). Thus, overall the SAARC STORM program will collect massive observations to investigate the life cycle of the storms and utilize them for modeling and forecasting including nowcasting of severe convective weather in the premonsoon season over South Asia. The results based on the pilot experiments conducted so far (which are described in many papers; e.g., Abhilash et al. 2007, 2008; Das et al. 2009b; Litta and Mohanty 2008; Joseph 2009; Rao 2009; Litta et al. 2012a; Gopalakrishnan et al. 2011; A. Tyagi et al. 2011, 2012; B. Tyagi et al. 2013) are summarized below.

The cloud tops usually reached 10–12 km, but in some cases they penetrate the tropopause and even reach 18-km height. The squall lines were usually 150–250 km in length and occasionally more than 300 km in length. The average speed of movement of the squall lines is about 50–60 km h^{-1}. The lifetime of intense squall lines was about 8–10 h. The majority of squalls were from the northwesterly direction. Dominance of northwesterly squalls is observed in this pilot phase, which is a well-noted feature. As found in the previous experiments, more than 85% of the squalls are of moderate intensity with wind speed less than or equal to 40 kt. About 12% of the total numbers were intense ones with wind speed greater than 40 kt. The intense squalls recorded wind speed up to 111.2 and 102 km h^{-1} over Barrackpore and Agartala, respectively. Most squalls occurred during 1230–1830 UTC (1800–0000 LST). More than 80% of the squalls occurred after 0630 UTC (1200 LST), which indicates that the atmospheric conditions are favorable for the occurrence of squalls after 0630 UTC (1200 LST), which is a well-known feature. The cloud-top temperatures varied between –40° and –70°C, and temperatures as low as –80°C have also been observed. The preferred tracks of convection were from northwest to southeast and from west to east. Squall lines forming over Bangladesh and Jharkhand moved and merged over West Bengal, which was a feature observed on severe weather days over east India. Studies show that the assimilation of radar data in the model is crucial for improving the thunderstorm forecast. Use of combined satellite and radar data along with modeling could help in nowcasting and forecasting. Results obtained so far indicate that the mesoscale models provide a promising tool for forecasting genesis and intensification for nearly 50% of the cases based on existing observatories. More dense observational networks with upper-air soundings in the region of genesis are required to increase the forecasting skill.

Severe thunderstorms are among the major high-impact weather phenomena that cause maximum impact on the human lives. Improving the skills of forecasting these phenomena is a challenge. The World Meteorological Organization (WMO) is leading a major campaign called the Severe Weather Forecast Demonstration Project (SWFDP) in different parts of the globe. The SAARC STORM program will complement the WMO SWFDP.

ACKNOWLEDGMENTS. At the outset, the Department of Science and Technology, Government of India is acknowledged for initiating the STORM program in 2005. Subsequently, the Ministry of Earth Sciences of the government of India took over the program in 2008. The program was expanded to cover the whole SAARC region in phases under the coordination of SAARC Meteorological Research Centre (SMRC), Dhaka.

We express our gratitude to the members of the governing board of SMRC and the SAARC program committee for approving the program. The approval of the government of India for providing additional AWS, GPS sounding systems, and Doppler Weather Radar for installations in the data-sparse regions in Bangladesh, Nepal, and Bhutan are gratefully acknowledged. The members of the IPC are acknowledged for steering and guiding the program.

REFERENCES

Abhilash, S., and Coauthors, 2007: Assimilation of Doppler weather radar observations in a mesoscale model for the prediction of intense rainfall events associated with mesoscale convective systems using 3DVAR. *J. Earth Syst. Sci.,* **116,** 275–304.

——, K. Mohankumar, and S. Das, 2008: Simulation of microphysical structure associated with tropical cloud clusters using mesoscale model and comparison with TRMM observations. *Int. J. Remote Sens.,* **29,** 2411–2432.

Alvi, S. M. A., and K. G. Punjabi, 1966: Diurnal and seasonal variations of squalls in India. *Indian J. Meteor. Geophys.,* **7,** 206–216.

Asnani G. C., 1985: Tornadoes–A review. *Vayu Mandal,* 97–133.

Barkan, J., H. Kutiel, and P. Alpert, 2004: Climatology of dust sources in North Africa and the Arabian Peninsula, based on TOMS data. *Indoor Built Environ.,* **13,** 407–419.

——, P. Alpert, H. Kutiel, and P. Kishcha, 2005: Synoptics of dust transportation days from Africa towards Italy and central Europe. *J. Geophys. Res.,* **110,** D07208, doi:10.1029/2004JD005222.

Bhattacharya, P. K., and S. K. Banerjee, 1980: Premonsoon tornadoes over West Bengal during April 1977. *Vayu Mandal,* **10,** 14–18.

Chaudhury, A., and A. K. Banerjee, 1983: A study of hailstorms over northeast India. *Vayu Mandal,* **13,** 91–95.

Das, S., 2010: Climatology of thunderstorms over the SAARC region. SMRC Rep. 35, 75 pp. [Available from SAARC Meteorological Research Centre E-4/C, Agargaon, Dhaka-1207, Bangladesh.]

——, and Coauthors, 2009a: SAARC STORM pilot field experiment 2009. SMRC Rep. 32, 72 pp. [Available from SAARC Meteorological Research Centre E-4/C, Agargaon, Dhaka-1207, Bangladesh.]

——, B. R. S. B. Basnayake, M. K. Das, M. A. R. Akand, M. M. Rahman, M. A. Sarker, and M. N. Islam, 2009b: Composite characteristics of nor'westers observed by TRMM and simulated by WRF model. SMRC Rep. 25, 44 pp. [Available from SAARC Meteorological Research Centre, E-4/C, Agargaon, Dhaka-1207, Bangladesh.]

——, and Coauthors, 2011: SAARC STORM pilot field experiment 2010. SMRC No. 40, 72 pp. [Available from SAARC Meteorological Research Centre E-4/C, Agargaon, Dhaka-1207, Bangladesh.]

De, U. S., R. K. Dube, and G. S. Prakasa Rao, 2005: Extreme weather events over India in the last 100 years. *J. Indian Geophys. Union,* **9,** 173–187.

Eliot, J., 1899: Hailstorm in India during the period 1883–1897 with a discussion on their distribution. *Indian Meteor. Mem.,* **6,** 237–315.

Goldar, R. N., S. K. Banerjee, and G. C. Debnath, 2001: Tornado in India and neighborhood. India Meteorological Department Calcutta Regional Meteorological Centre Scientific Rep. 2/2001, 27 pp.

Gopalakrishnan, V., S. D. Pawar, P. Murugavel, and K. P. Johare, 2011: Electrical characteristics of thunderstorms in the eastern part of India. *J. Atmos. Sol.-Terr. Phys.,* **73,** 1876–1882, doi:10.1016/j.jastp.2011.04.022.

Gupta, H. N., and S. K. Ghosh, 1980: North Delhi tornado of 17 March 1978. *Mausam,* **31,** 93–100.

Houze, R. A., Jr., D. C. Wilton, and B. F. Smull, 2007: Monsoon convection in the Himalayan region as seen by the TRMM Precipitation Radar. *Quart. J. Roy. Meteor. Soc.,* **133,** 1389–1411.

Hussain, A., H. Mir, and M. Afzal, 2005: Analysis of dust storms frequency over Pakistan during 1961–2000. *Pak. J. Meteor.,* **2,** 49–68.

IMD, 1944: Nor'wester of Bengal. India Meteorological Department Tech. Note 10. 17 pp.

Joseph, P. V., 2009: Local severe storms. *Mausam,* **60,** 139–154.

——, D. K. Raipal, and S. N. Deka, 1980: ANDHI, the convective dust storm of northwest India. *Mausam,* **31,** 431–442.

Koteswaram, P., and V. Srinivasan, 1958: Thunderstorm over Gangetic West Bengal in the pre-monsoon season and the synoptic factors favourable for their formation. *Indian J. Meteor. Geophys.,* **9,** 301–312.

Krishna Rao, P. R., 1966: Thunderstorm studies in India—A review. *Indian J. Meteor. Geophys.,* **12,** 3–13.

Litta, A. J., and U. C. Mohanty, 2008: Simulation of a severe thunderstorm event during the STORM field experiment of 2006 using WRF-NMM model. *Curr. Sci.,* **95,** 204–215.

——, ——, and S. C. Bhan, 2010: Numerical simulation of tornado over Ludhiana (India) using WRF NMM model. *Meteor. Appl.,* **17,** 64–75.

——, ——, ——, and M. Mohapatra, 2011: Simulation of tornadoes over India using WRF-NMM model. *Challenges and Opportunities in Agrometeorology,* S. D. Attri et al., Eds., Springer, 173–187.

——, ——, S. Das, and S. M. Idicula, 2012a: Numerical simulation of severe local storms over east India using WRF-NMM mesoscale model. *Atmos. Res.,* **116,** 161–184.

——, ——, S. K. Prasad, M. Mohapatra, A. Tyagi, and S. C. Sahu, 2012b: Simulation of a tornado over Orissa (India) on 31 March 2009 using WRF-NMM model. *Nat. Hazards,* **61,** 1219–1242.

Mandal, G. S., and S. K. Saha, 1983: Characteristics of some recent north Indian tornadoes. *Vayu Mandal,* **13,** 74–80.

Middleton, N. J., 1986a: Dust storms in the Middle East. *J. Arid Environ.,* **10,** 83–96.

——, 1986b: A geography of dust storms in south-west Asia. *J. Climatol.,* **6,** 183–196.

——, and A. S. Goudie, 2001: Saharan dust: Sources and trajectories. *Trans. Inst. Br. Geogr.,* **26,** 165–181.

Mir, H., A. Hussain, and Z. A. Babar, 2006: Analysis of thunderstorms activity over Pakistan during (1961–2000). *Pak. J. Meteor.,* **3,** 13–32.

Mohanty, U. C., and Coauthors, 2006: Weather summary during pilot experiment of Severe Thunderstorms Observations and Regional Modeling (STORM) programme. India Department of Science and Technology Rep., 177 pp.

——, and Coauthors, 2007: Weather summary during pilot experiment of Severe Thunderstorms Observations and Regional Modeling (STORM) programme. India Department of Science and Technology Rep., 179 pp.

——, and Coauthors, 2009: Weather summary during pilot experiment of Severe Thunderstorms Observations and Regional Modeling (STORM) programme. India Department of Science and Technology Rep., 158 pp.

Nizamuddin, S., 1993: Hail occurrences in India. *Weather,* **48,** 90–92.

Raman, P. K., and K. Raghavan, 1961: Diurnal variations of thunderstorms in India during different seasons. *Indian J. Meteor. Geophys.,* **12,** 115–130.

Rao, K. N., C. E. J. Daniel, and L. V. Balasubramanian, 1971: Thunderstorms over India. India Meteorological Department Scientific Rep. 153, 21 pp.

Rao, P. S., 2009: Field experimental studies on land-ocean-atmosphere interactions over the Indian region during 1999–2009. *Mausam,* **60,** 239–252.

Romatschke, U., S. Medina, and R. A. Houze Jr., 2010: Regional, seasonal, and diurnal variations of extreme convection in the South Asian region. *J. Climate,* **23,** 419–439.

Srinivasan, V., K. Ramamurthy, and Y. R. Nene, 1973: Summer nor'wester and Andhi and large scale convective activity over peninsula and central parts of the country. India Meteorological Department Forecasting Manual Part 3, 137 pp.

STORM, 2005: STORM science plan. India Department of Science and Technology Rep., 118 pp. [Available online at www.imd.gov.in/SciencePlanofFDPs/STORM%20Science%20Plan.pdf.]

Tyagi, A., 2007: Thunderstorm climatology over Indian region. *Mausam,* **58,** 189–212.
——, D. R. Sikka, S. Goyal, and M. Bhowmick, 2012: A satellite based study of pre-monsoon thunderstorms (nor'westers) over eastern India and their organization into mesoscale convective complexes. *Mausam,* **63,** 29–54.
Tyagi, B., V. Naresh Krishna, and A. N. V. Satyanarayana, 2011: Study of thermodynamic indices for forecasting pre-monsoon thunderstorms over Kolkata during STORM pilot phase 2006–2008. *Nat. Hazards,* **56,** 681–698, doi:10.1007/s11069-010-9582-x.
——, A. N. V. Satyanarayana, and V. Naresh Krishna, 2013 Thermodynamical structure of atmosphere during pre-monsoon thunderstorm season over Kharagpur as revealed by STORM data. *Pure Appl. Geophys.,* **170,** 675–687, doi:10.1007/s00024-012-0566-5.
Webster, P. J., and Coauthors, 2002: The JASMINE pilot study. *Bull. Amer. Meteor. Soc.,* **83,** 1603–1630.
Yamane, Y., T. Hayashi, A. M. Dewan, and F. Akter, 2009a: Severe local convective storms in Bangladesh: Part I. Climatology. *J. Atmos. Res.,* **95,** 400–406, doi:10.1016/j.atmosres.2009.11.004.
——, ——, ——, and ——, 2009b: Severe local convective storms in Bangladesh: Part II. Environmental conditions. *J. Atmos. Res.,* **95,** 407–418, doi:10.1016/j.atmosres.2009.11.003.
Yoneyama, K., and Coauthors, 2008: MISMO field experiment in the equatorial Indian Ocean. *Bull. Amer. Meteor. Soc.,* **89,** 1889–1903.

SEVERE CONVECTIVE STORMS

Meteorological Monograph No. 50

Edited by Charles Doswell III

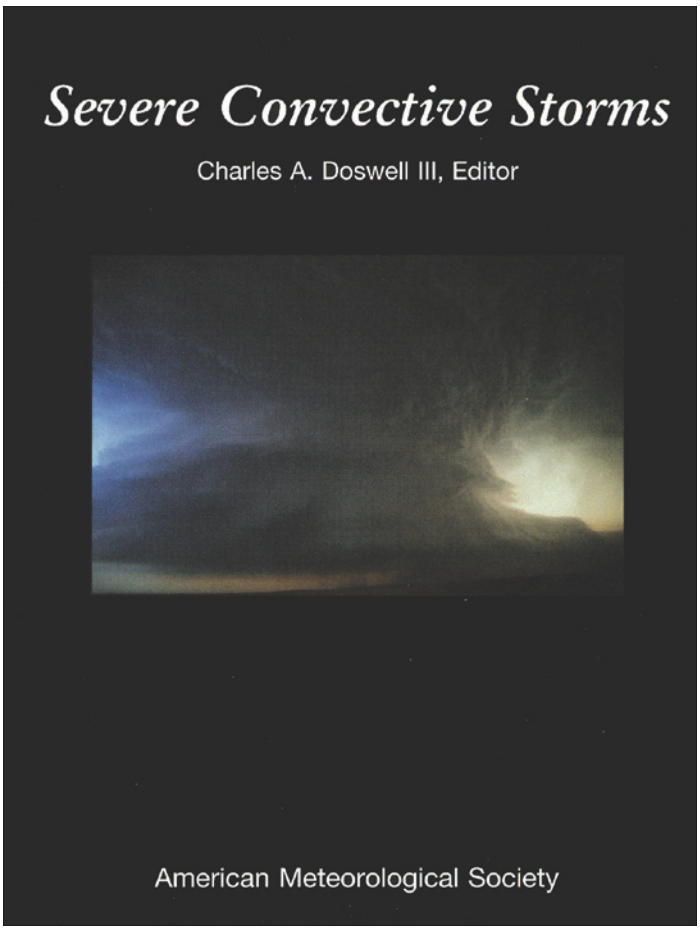

This volume is a collection of 13 review papers by a distinguished group of scientists, providing a summary of the current scientific understanding of convective storms and the weather they produce, as well as showing how that understanding works in forecasting practice. The volume is loaded with outstanding illustrations, and is destined to become one of the most widely referred-to books on convection and convective processes.

SEVERE CONVECTIVE STORMS, Meteorological Monograph No. 50

ISBN 1-878220-41-1, 576 pp., hardbound, $110 list/$90 member, student member price: $75.

ORDER ONLINE

www.ametsoc.org/amsbookstore

or see the order form in the back of this issue.

GENERALIZATION, CONSISTENCY, AND UNIFICATION IN THE PARAMETERIZATION PROBLEM

BY J.-I. YANO, M. VLAD, S. H. DERBYSHIRE, J.-F. GELEYN, AND K. KOBER

The purpose of the workshop series called "Concepts for Convective Parameterizations in Large-Scale Models" has been to encourage small numbers of European scientists to discuss the fundamental theoretical issues of convection parameterization. The workshop series has been funded by European Cooperation in the Field of Scientific and Technical Research (COST) Action ES0905. The sixth workshop in the series discussed the issues of generalization, consistency, and unification of parameterizations in atmospheric modeling with a focus on convection.

The workshop may be best summarized from the round table discussion organized on the last day, which began by asking for a starting point for such development of parameterizations. Key presentations during the workshop are also highlighted from this discussion.

WORKSHOP ON CONCEPTS FOR CONVECTIVE PARAMETERIZATIONS IN LARGE-SCALE MODELS VI: "GENERALIZATION, CONSISTENCY, UNIFICATION"

WHAT: Forty-one scientists from 16 European countries and Israel met to discuss how to construct parameterizations correctly.
WHEN: 19–21 March 2013
WHERE: Palma, Spain

ULTIMATELY TURBULENT. Subgrid-scale atmospheric processes are ultimately turbulent (considering their extremely high Reynolds number associated with the flow). Thus, at least in the ultimate sense, turbulence theories are the most robust starting point for parameterization development: a rising convective plume is associated with filamentation of the plume edge air with subsequent dispersions associated with its turbulent behavior. As a result, as it rises, the plume air is gradually replaced by external air and gradually loses its compactness. The plume eventually breaks up into fragments of clouds.

A semi-analytical method based on the Langevin equation can be used to study particle advection by turbulent flows (Vlad and Spineanu 2004, and references therein). A series of studies for two-dimensional turbulence reveals the trapping of the fluid particles inside eddies, which determine nonlinear transport far from Gaussian statistics. Stochastic quasi-coherent structures are generated as a result. An extension of this method to three-dimensional convective cloud turbulent motions also finds trapping: it manifests a very inhomogeneous turbulent diffusion that is associated with the untrapped fluid particles, whereas diffusion is very

AFFILIATIONS: YANO AND GELEYN—GAME-CNRM, CNRS, Météo-France, Toulouse, France; VLAD—National Institute of Laser, Plasma and Radiation Physics, Bucharest, Romania; DERBYSHIRE—Met Office, Exeter, United Kingdom; KOBER—Meteorologisches Institut, Ludwig-Maximilians-Universität München, Munich, Germany
CORRESPONDING AUTHOR: Jun-Ichi Yano, GAME-CNRM, CNRS, Météo-France, 42 Av. Coriolis, Toulouse, France
E-mail: jiy.gfder@gmail.com

DOI:10.1175/BAMS-D-13-00123.1

In final form 30 October 2013

small for the trapped particles. The entrainment process is stochastic. It appears not only at the top and on the boundaries of the cloud, but also inside the cloud.

Trapping, by limiting the dilution only to a part of the buoyant parcel, helps to maintain undiluted kernels of various sizes, stochastically distributed inside the cloud. This line of research may lead to a development of a parameterization based on turbulence physics.

Laboratory experiments are an equally important but long-forgotten tradition for addressing these turbulent questions. The entrainment-plume hypothesis, which was subsequently adopted by Arakawa and Schubert's (1974) mass-flux parameterization, was originally proposed based on a water tank experiment by Morton et al. (1956). During the discussion, a participant showed an impressive experiment of thermal plume evolution by simply using a humidifier as a plume source. Thanks to contemporary laser technology, extensive measurements of the velocity field are possible in much higher resolution than conventional large-eddy simulations (LESs) can achieve. Verifications of the entrainment/detrainment hypothesis must, rather, be based on those high-resolution laboratory experiments, if these direct measurements are ever to be relevant for a parameterization verification.

PHENOMENOLOGICAL. A view opposing the ultimate turbulence perspective is to remain with the phenomenological observational information available from the synoptic scales. This is a classical approach originally established by Yanai et al. (1973). From this latter point of view, the ultimate goal of parameterizations is to predict correctly the apparent source terms, which can be diagnosed by a conventional sounding network. A clever exploitation of such a sounding network can even provide some subgrid-scale information such as mass flux profiles, which must be specified under a mass-flux-based parameterization. The vast information potentially contained in these sounding network datasets should not be forgotten.

The basic working principle under this framework is quasi-equilibrium. In the course of the presentations, the need to go beyond this traditional assumption is much emphasized. However, the actual precipitation time series generated by an operational convection parameterization under quasi-equilibrium is often highly noisy, suggesting that the system does not stay on a slow process as the hypothesis indicates. This is a more basic issue to be addressed before moving to more sophisticated approaches.

INTERMEDIATE VIEWS. An intermediate view between these two perspectives is to try to exploit information from finescale numerical modeling by cloud-resolving models (CRMs) as well as LESs, but without getting into full turbulence details. This is a direction strongly promoted under a leadership of the Global Energy and Water Cycle Experiment (GEWEX) Cloud System Study (GCSS; presently Global Atmospheric System Studies) over the last decades. The vast information provided for the subgrid-scale processes by this modeling is hardly disputed. For example, extensive diagnoses of entrainment and detrainment rates are available from these modeling results.

However, these models are far from perfect. For example, reproduction of observed tendencies in deep convective momentum transport by CRMs, as one of the presenters points out, is not quite easy. Moreover, such information may not be as directly useful as it seems at first glance. Parameterizations cannot be considered simple approximations of CRMs and LESs: the associated assumptions are so drastic that information from CRMs and LESs may not be directly relevant for verifications of a parameterization formulation. More emphatically stated, parameterization is more like a sketch or schematic diagram of reality represented by CRMs and LESs. In general, where curve fitting is used to construct a parameterization, it should be accompanied by analysis of causal mechanisms.

Another perspective for bridging the gap between the turbulence and the phenomenological views is to argue that for various reasons, not all the details of subgrid-scale turbulent processes may be relevant for constructing a parameterization for large-scale flow simulations. This perspective is analogous to the concept of a slow manifold, which is constructed by filtering out fast time scale processes such as gravity waves as originally formulated for an idealized dry large-scale atmospheric circulation. Although this perception is appealing, it is less likely that such an analogy with a slow manifold can be established with the atmospheric subgrid-scale processes: that many of these processes tend to be associated with coherencies and spatiotemporal organizations suggests that they should not be naively linked with the notion of a slow manifold.

Nevertheless, the analogy with a slow manifold is, at a very conceptual level, a potentially helpful perspective: intuitively not all the physics matter for developing parameterizations. We may also equally ask this: How many of the turbulence features must correctly be reproduced in weather forecast models? For example, from the point of view of turbulence studies, reproduction of an inertial subrange spectrum would be of critical importance. However, it does not follow automatically that its reproduction is also critically important for, say, a successful seasonal forecast.

MORAL AND WISDOM. As a whole, the workshop identified multiple pathways for constructing parameterizations in a general, consistent, and unified manner. Once a basic strategy is defined, doing it from there is more of a matter of morality: proceeding carefully and diligently (i.e., without cheating).

The moist thermodynamic description of the atmosphere is a good example that helps make this point. The extension of dry thermodynamics to its moist counterpart is straightforward at the most conceptual level. However, the actual procedure tends to be rather involved, and for simplification's sake, various approximations are introduced in many of the derivations found in the literature. A good lesson that can be learned here is that a much simpler expression for the moist adiabatic lapse rate can be obtained when the whole derivation is performed without any approximations (Geleyn and Marquet 2012).

An important general wisdom is to never go backward. It is often tempting to simply add an extra term for representing something missing in the original formulation. For example, downdraft is added to mass-flux convection parameterization in such a manner that the implementation of downdraft effects in the whole formulation remains somehow ad hoc. Recall that the basic idea of mass-flux formulation is based on a dichotomy of updrafts and environment. Consistently adding a new component on top of them requires more careful considerations.

Efforts for recovering such internal consistencies in operational contexts should be well emphasized. Especially emphasized are the importance of achieving "seamlessness" from one version of a model to another (e.g., from a climate to a forecast version), as well as achieving a "traceability" of physical effects identified in more explicit studies by LES and CRM into a parameterization.

Unfortunately, pursuing generality, consistency, and unification in parameterizations is not simply a moral matter but also an ontological task: it is difficult for us to see the problem as a whole. Our situation may be compared to the famous Indian allegory of the blind scholars touching parts of an elephant in order to conceive the whole picture of this animal. Each scholar only perceives a part of the animal (the trunk, a leg, the nose, etc.), and they dispute vigorously with each other over the true nature of the elephant. By this analogy, scientists contest priorities in parameterization development because each of us sees only a part of the whole problem.

A way to avoid such myopic tendencies in our parameterization research is to make a parameterization formulation simple and compact so that we can see the formulation as a whole more easily. For example, the workshop featured a few presentations on the introduction of stochasticity into parameterizations. However, looking at the issue from a wider perspective of parameterization strategy, this idea is a mixed blessing. It is hard to beat the intuitive appeal of introducing stochasticity for representing subgrid-scale variabilities and for enhancing ensemble forecast spread. However, stochasticity adds extra complexity on top of the entrainment/detrainment and closure problems that we have to deal with operationally.

Another example, equally emphasized during the workshop, is the coupling of convection with boundary layer processes. Triggering convection by various boundary layer processes such as cold pools is, again, an attractive possibility to pursue in parameterizations. The fundamental importance of such investigations is hardly debatable. However, operational implementations of such processes tend to make convection parameterization less reliable due to complexity of the boundary layer processes.

Establishing generality, consistency, and unification of physical parameterizations in operational forecast models is becoming increasingly urgent with an accelerated increase in model resolutions. A solid commitment of the operational research centers is definitely required, but that is not enough. The pathway is not unique, nor is the choice of pathway even obvious, given the ontological reasons above. The problem must be seen as a whole before a right choice can be made. The facets of the problem will not all be put together into a single whole except through true interdisciplinarity: that is going to be the theme of the next workshop in the series.

REFERENCES

Arakawa, A., and W. H. Schubert, 1974: Interaction of a cumulus cloud ensemble with the large-scale environment, Part I. *J. Atmos. Sci.,* **31,** 674–701, doi:10.1175/1520-0469(1974)031<0674:IOACCE>2.0.CO;2.

Geleyn, J.-F., and P. Marquet, 2012: Moist-entropic vertical adiabatic lapse rates: The standard cases and some lead towards inhomogeneous conditions. The CAS/JSC Working Group on Numerical Experimentation (WGNE) Blue Book, section 4, 3–4.

Morton, B. R., G. Taylor, and J. S. Turner, 1956: Turbulent gravitational convection from maintained and instantaneous sources. *Proc. Roy. Soc. London,* **234A,** 1–23, doi:10.1098/rspa.1956.0011.

Vlad, M., and F. Spineanu, 2004: Trajectory structures and transport. *Phys. Rev. E,* **70,** 056304, doi:10.1103/PhysRevE.70.056304.

Yanai, M., S. Esbensen, and J.-H. Chu, 1973: Determination of bulk properties of tropical cloud clusters from large-scale heat and moisture budgets. *J. Atmos. Sci.,* **30,** 611–627, doi:10.1175/1520-0469(1973)030<0611:DOBPOT>2.0.CO;2.

GLOBAL CLIMATE CHANGE: FACT OR FICTION?

BY PAUL MARK TAG

For those of you who jumped here after reading the title expecting a sophisticated scientific treatise concerning global warming, I apologize for such a cheap trick. I am a writer, and I write fiction.

Six years ago I explained in another *BAMS* article why I retired from my job with the Naval Research Laboratory to start a new career, writing fiction. I had been a research meteorologist for 30-some years prior. At that time, I had just completed *Category 5*, my first thriller. That story revolves around hurricanes, obviously. I then switched to genetics and the genome as the basis for my second thriller, *Prophecy*. With *White Thaw: The Helheim Conspiracy*, I wanted to return to my area of science and chose a topically relevant subject these days, global climate change. But first, I had to decide how to approach such a sensitive issue in a work of fiction.

For the serious student of climate change, there are abundant quantities of data and research to be waded through, and questions to be addressed. If glaciers are receding, is this occurrence part of a cycle that repeats itself over the centuries? Is the planet warming permanently or is there a long-term cycle? Is the seemingly increasing degree of severe weather related to global warming? But, ultimately, most of us want to know to what degree we humans are impacting our environment. Because of the complexities of these issues, I decided that I could not fashion an exciting thriller around such subtlety and nuance. I needed something more definitive.

Accordingly, I chose to create a fictional scenario that I could control, one that was both plausible but also one for which I could give an accurate scientific description. Thriller writers often refer to a premise as being "*incredible but plausible*." Remember Michael Crichton's *Jurassic Park*, where DNA encased in amber is used to recreate a dinosaur? In *Category 5*, my antagonists launch a laser into space to heat water surrounding hurricanes. Both concepts are incredible but plausible.

For *White Thaw*, I needed a potential environmental disaster. Robin Brody—a meteorologist and esteemed colleague who regularly critiques my writing—and I had a hint of an idea but needed to flesh it out. Our concept involved the Gulf Stream. Most of us know that the reason Western Europe is warm compared to Alaska (at approximately the same latitudes) is because of this river of warm water flowing north from the tropics. So we consulted an oceanographer friend, Kevin Rabe, who expanded our knowledge about the workings of the Gulf Stream. He also told us of the concern that as Greenland's ice melts, the resulting less dense fresh water flooding the North Atlantic might alter the Gulf Stream's northward flow.

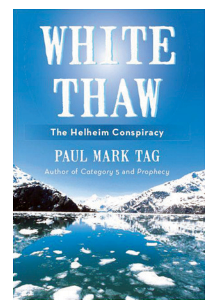

Following this discussion, Robin and I knew that we had a scientifically sound premise for my story: the bad guys, for their own nefarious purposes, would plan an ecological disaster by releasing into the northern Atlantic several glaciers on the eastern side of Greenland. The name "Helheim" in the book's title refers to Greenland's Helheim Glacier. (A recent *BAMS* article by Straneo et al. mentioned this glacier in its exploration of the response of "marine terminating glaciers" to oceanic and atmospheric forcing.)

We then came up with an idea by which the antagonists could accomplish this deed. I'll not spoil the premise by explaining that here. Although our concept for doing so made sense to us, I had to make sure. For this reason, I contacted one of the foremost glacier experts in the world, Konrad Steffen, who at the time was working at the Cooperative Institute for

Research in Environmental Sciences (CIRES) at the University of Colorado. (He's currently the director of the Swiss Federal Institute for Forest, Snow and Landscape Research.) He was most gracious and agreed to help.

In addition to explaining to him the premise behind my thriller, I needed a lot of advice. For example, my initial inclination was to focus on the Jakobshavn Glacier on the west side of Greenland. For purposes of my diabolical deed, Steffen said that a glacier on the eastern side of Greenland was a better choice, and suggested the area near Kulusuk on the southeastern corner of Greenland. That recommendation led to the Helheim Glacier.

As I developed my story, I had numerous questions about Greenland itself. Following our initial e-mails, Steffen and I talked on the telephone. Because he has spent considerable time on the ice in Greenland, there was no question too trivial that he could not answer. Is the surface of Greenland smooth enough to operate a snowmobile? How deep must one go, and what concerns would there be in building an under-ice structure? Which months in Greenland are best to camp on the ice and to do research? What physical dangers lurk there, particularly during the warm half of the year? How does a researcher get transported to his ice camp? Steffen answered these questions and more, all of which were important to the technical development of my story. Further, he provided necessary geographic and physical data. Most important, at the end of our discussions, he gave his blessing to our idea concerning the release of the Helheim Glacier. Incredible but plausible.

Once I had all of the scientific details in place, it was then a matter of identifying a suitable villain and developing an exciting plot to pull the story together. It took me two-and-a-half years. Steffen read my initial draft and offered suggestions, as well as correcting scientific errors I had made.

The result was *White Thaw: The Helheim Conspiracy*. I have focused above on my environmental consultants, but I had others, related to medical matters, weapons, aircraft, and aviation, for example. As I always say in my acknowledgements, if there are errors left in the finished product, it's my own fault. I couldn't have gotten better support from all of the experts who helped me develop this book. Please visit me at www.paulmarktag.com.

FOR FURTHER READING

Straneo, F., and Coauthors, 2013: Challenges to understanding the dynamic response of Greenland's marine terminating glaciers to oceanic and atmospheric forcing. *Bull. Amer. Meteor. Soc.*, **94**, 1131–1144.

Tag, P. M., 2007: A meteorological fiction. *Bull. Amer. Meteor. Soc.*, **88**, 1986–1987.

NEW PUBLICATIONS

PALEOCLIMATE

M. Bender, 2013, 306 pp., $27.95, paperbound, Princeton University Press, ISBN 978-0-691-14555-6

In this title, the author provides a concise, comprehensive introduction to the subject. After briefly describing the major periods in Earth history to provide geologic context, he discusses controls on climate and how the record of past climate is determined. The book then proceeds chronologically, introducing the history of climate changes over millions of years—its patterns and major transitions and why average global temperature has varied so much. The book ends with a discussion of the past 10,000 years and how anthropogenic climate change fits into the context of paleoclimate.

DELUGE: TROPICAL STORM IRENE, VERMONT'S FLASH FLOODS, AND HOW ONE SMALL STATE SAVED ITSELF

P. Shinn, 2013, 216 pp., $27.95, hardbound, University Press of New England, ISBN 978-1-61168-318-9

On 28 August 2011, Hurricane Irene made landfall in New Jersey. It was downgraded to a tropical storm as it headed into New England, but as Irene's eye drifted north, its bands of heavy rains traveled westward over Vermont's Green Mountains. Streams and rivers overflowed, and for weeks, mountain towns were isolated. In the immediate aftermath of the disaster, it fell on the shoulders of ordinary Vermonters to help victims and rebuild the state. This book is the complete story of the floods, the rescue, and the recovery, as told by the people who lived through it.

MANAGING OCEAN ENVIRONMENTS IN A CHANGING CLIMATE

K. Noone, U. Sumaila, and R. Diaz, 2013, 359 pp., $119.95, hardbound, Elsevier, ISBN 978-0-12-407668-6

This book summarizes the current state of several threats to the global oceans. The text begins with a global-scale focus for the first several chapters and then provides an example of how this approach can be applied on a regional scale for the Pacific area. The book links environmental and economic aspects of ocean threats and provides an economic analysis of action versus inaction. It also gives recommendations for stakeholders to stimulate the development of policies that would help move toward sustainable use of marine resources and services.

ANTARCTICA: GLOBAL SCIENCE FROM A FROZEN CONTINENT

David W. H. Walton, Ed., 2013, 342 pp., $55.00, hardbound, Cambridge University Press, ISBN 978-1-107-00392-7

In this engaging, colorfully illustrated compendium, we are presented with an alluring introduction to the past, present, and future of Antarctic science. The contributors, all leading experts in their various scientific fields, reflect the international and interdisciplinary nature of this subject matter. Throughout this book the importance of Antarctic science is made evident, as is its position in fostering international cooperation, thus enabling humans to investigate and understand one of the most hostile and remote—yet globally significant—climates on Earth.

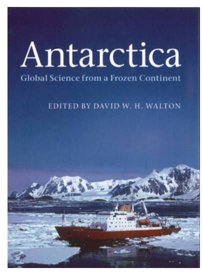

This book stands alone in offering an overview of Antarctic science pertinent to both scientists and nonscientists alike. Indeed, there is something for everyone in this book. For those not involved in scientific research, the presentation is inviting and accessible. The lure of Antarctica is evident in every chapter and from every discipline, from its first scientific discoveries to its hidden geologic secrets, from its extreme climate to its central role in ocean and atmospheric circulation, and from its ecological wonders to its importance in space science.

The book opens with a chapter on the history of Antarctic scientific exploration, storied and revealing of our insatiable thirst for knowledge in a place most inhospitable and unlike any other place on Earth. In the next six chapters we learn about the key discoveries and functions of each of Antarctica's Earth system components (e.g., geology, cryosphere, atmosphere, ocean, ecosystem, space). The next three chapters address the challenges and successes of conducting science in one of the coldest, driest, and windiest places on Earth, the required physical and human logistics to access and inhabit those remote locations, and the need for international collaboration and cooperation for exploring its vastness. Although these three chapters are outside traditional scientific disciplines, they are integral and fascinating keys to conducting, and therefore understanding, Antarctic science. The last chapter appropriately ends with an overview of current climate and ecosystem change in Antarctica, its sensitivity and vulnerability to change, and its future.

METEOROLOGY OF CLOUDS

L. Downing, 2013, 142 pp., $3.99, e-book, AuthorHouse, ISBN 978-4918-0432-2

This publication is a presentation of cloud meteorology as experienced by an aviation meteorologist. According to the author, clouds are visual indicators of the atmosphere's dynamics and related weather phenomena, and, to some extent, predictors of coming weather conditions. He notes that while clouds are icons of nature, they are also a complicated subject studied in meteorology. The book presents explanations of cloud formation, cloud types, and cloud dynamics, as well as the atmospheric forces internal and external to cloud existence. It also discusses the chaotic nature of the Earth's atmosphere and its impact on clouds and cloud systems.

EXPLORING CLIMATE CHANGE THROUGH SCIENCE AND IN SOCIETY

M. Hulme, 2013, 330 pp., $48.95, paperbound, Routledge, ISBN 978-0-415-81163-7

This book gathers together a collection of Mike Hulme's most popular, prominent, and controversial works since the late 1980s. The argument the author has made is that climate change has to be understood as much as an idea situated in different cultural contexts as it is as a physical phenomenon to be studied through universal scientific practices. The 55 short items are grouped together in seven themes—science, researching, culture, policy, communicating, controversy, futures—and it also includes three new essays written specifically for the book.

OXYGEN: A FOUR BILLION YEAR HISTORY

D. Canfield, 2014, 224 pp., $27.95, hardbound, Princeton University Press, ISBN 978-0-691-14502-0

This book is an account of the history of atmospheric oxygen on Earth. It emphasizes the relationship of oxygen to the evolution of life and the evolving chemistry of the Earth. With a first-person narrative, the author draws from a variety of fields to explain why our oxygenated Earth became the ideal place for life. Describing which processes act to control oxygen levels in the atmosphere, he traces the records of oxygen concentration through time. He guides readers through the various lines of scientific evidence and highlights the scientists and researchers who have made key discoveries in the field.

For those involved in polar science, whether research, teaching, outreach, or management, this will be a valued resource for attaining and disseminating an interdisciplinary and international view of Antarctic science. However, this is not meant to be an exhaustive scientific description of any one subject matter, but an enticing and well-integrated overview. For those eager to delve deeper and learn more, there is a list of suggested (and freely accessible) readings at the end of the book. One may also want to have a well-labeled map of Antarctica on hand for general reference—a feature found missing in this book. (Indeed, one or two reference maps showing geographic, historic, and scientific landmarks would have made nice inner covers; the chapters themselves do contain various maps, but alas, none serve as a complete reference for the book as a whole.)

While there are many books about the history and exploration of Antarctica, about personal accounts of harrowing expeditions or of first encounters, about the fantastical beauty of its icy landscapes and amazing wildlife (or more recently about travel guides for tourists), none succinctly capture the global importance of Antarctic science and its central role in understanding our world from most every discipline. In fact, the one aspect most appreciated about this book is its clear message that what happens in Antarctica affects us all. The more we learn about Antarctica, the more we realize it is both the record keeper and climate moderator of planet Earth.

Considering the weight of that statement, it is amazing that Antarctica is also a leading example of international collaboration, cooperation, and stewardship. This book is unique in conveying that message and shares also the challenges, successes, and failures of investigating and managing "the frozen commons." Indeed, the last three chapters of this book should be required reading for all citizens to show we have, and can, act responsibly, but it requires diligence and perseverance. As conveyed in this book, the oceans and coastal regions of Antarctica in particular are forever feeling the effects of increased fishing, tourism, pollutants, and other (sanctioned and nonsanctioned) commercial activities. Thus, there are, and always will be, geopolitical challenges, but the last 50-plus years have shown that international cooperation and stewardship are possible and necessary.

—Sharon Stammerjohn

Sharon Stammerjohn is a senior research associate at the Institute of Arctic and Alpine Research at the University of Colorado Boulder. Her specialties are polar oceanography and climate, with a focus on interdisciplinary approaches to understanding environmental and ecosystem response to climate variability.

REANALYSIS

Looking back at the Bulletin of May 1956:

Thunderstorm Charts and Climatic Maps among Projects of WMO

A three-year project of charting the course of thunderstorms over the world has recently been completed by the World Meteorological Organization, according to a United Nations announcement. The data, collected through thunder and lightning observations on land and at sea, are being published in a series of seventeen world maps giving the average number of thunderstorm days for each month, for the quarters, and for the whole year.

As a basis for the maps, ships made observations of thunderstorms on several million punch cards provided by the British and German meteorological services. From these records, the mean number of thunderstorm days for a given area could be calculated. The ships' data were augmented by land observations.

In a broader field of map-making, the World Meteorological Organization has been considering methods of establishing a climatological atlas of the world. At its second Congress, held last May in Geneva, the need for an up-to-date atlas of this type was recognized. Delegates also stressed the desirability of having a certain degree of uniformity and regional atlases.

As a step in this direction, WMO set up a working group to study the questions involved. This group, which met last December in the Laboratory of Climatology, Centerton, New Jersey, decided that WMO work should lead to coverage of the world in a series of loose-leaf sheets based upon national, subregional, and regional maps on a uniform basis. Specifications for the maps were also laid down.

Such climatic maps would summarize the knowledge of the climate of a region in a form suitable for a wide variety of users, including meteorologists, farmers, hydrologists, civil engineers, biologists, and those engaged in public transport. . . .

—*Bull. Amer. Meteor. Soc.,* **37,** 240

45 BEACON

LETTER FROM HEADQUARTERS

HAVE YOU LOOKED AT AMS BOOKS LATELY?

In past columns, I have occasionally recommended books from other publishers that I thought AMS members would enjoy or benefit from. This month I would like to remind readers of the excellent books produced by the AMS—all of which are now available through a new bookstore interface on the AMS website.

The AMS books program has been building over the past decade, slowly ramping up the number of books published each year, on average, and working to create books that reach beyond our narrowly focused community into a broader audience. A benchmark in this expanded scope was the publication of the *AMS Weather Book: The Ultimate Guide to America's Weather* in 2009, which has achieved broad distribution through bookstores and online book retailers. It continues to represent a terrific book for a general audience and one that I routinely recommend to precollege students, teachers, and weather enthusiasts.

Books released in recent years have spanned a broad spectrum of topics. All have a core centered in our disciplines that cover weather, water, and climate, but several have been scholarly works that reach across disciplinary boundaries in ways that bridge the divide between the physical sciences and the social sciences. Examples of this are *Adaptive Governance and Climate Change* and *Economic and Societal Impacts of Tornadoes* (as well as the follow-up book *Deadly Season: Analyzing the 2011 Tornado Outbreaks*, which deals with the devastating 2011 tornado season). Another great example is *Taken by Storm, 1938: A Social and Meteorological History of the Great New England Hurricane*, which was presented with the "ASLI's Choice—History" award earlier this year by Atmospheric Science Librarians International.

A couple of recent additions to the AMS book list are likely to be especially appealing to both members of our community and a broader audience. Bill Hooke has authored a book titled *Living on the Real World: How Thinking and Acting Like Meteorologists Will Help Save the Planet*, which is based on his blog "Living on the Real World" (www.livingontherealworld.org; if you are not already regular readers of this insightful blog, you should be). I very strongly encourage you to obtain and read a copy of this terrific book, and then pass it on to a colleague or friend who is not part of our community so that they can gain a deeper understanding of all that our community has to offer the world. On a much lighter note, another book that makes a great gift (including to yourself) is the joke book compiled by Jon Malay, *Partly to Mostly Funny: The Ultimate Weather Joke Book*. I gave this to my mother for Christmas and she thoroughly enjoyed it!

I hope this brief highlight of a few AMS books sparks enough curiosity for you to visit the new AMS Bookstore site at https://secure.ametsoc.org/amsbookstore/ and check out the array of titles there. I think you will be glad you did. I would be surprised if you did not find at least one book you would like to add to your own collection or give to someone you know—and, of course, all AMS members are eligible for great discounts on these books.

KEITH L. SEITTER, CCM
EXECUTIVE DIRECTOR

*[Editor's Note: The following post is adapted from William Hooke's blog, Living on the Real World (*www.livingon-therealworld.org/*). Hooke is the former director of the AMS Policy Program and currently a senior policy fellow.]*

Three (Simultaneous) Real-World Challenges
(Originally posted 7 December 2013)
. . .that we face locally, everywhere . . . and globally. In a nutshell, here's the unending task of living on the real world. We must simultaneously, everywhere, at every moment, and for extended periods, master the threefold job of 1) sipping from Earth's resources, while 2) protecting Earth's habitat, diversity, and environment, and 3) building resilience to Earth's extremes. How are we faring? Three stories, in this week's news:

Britain struggles with a fierce cold-season storm. *The Daily Mail* reported that:

- *The worst tidal surge for more than 60 years battered coastal towns along the east coast of Britain last night.*
- *Sea walls were breached more than two hours before high tide last night after thousands of people had been evacuated from their homes.*
- *The North Sea surge hit the north Norfolk coast early yesterday evening and headed south throughout the night. Chaotic scenes in the seaside town of Scarborough offered a glimpse into the floods which were set to swamp the east coast of Britain just a few hours later.*
- *The fierce Atlantic storm—which has already claimed two lives—caused widespread disruption yesterday, but some agencies this morning said that the expected flooding overnight was less severe than expected.*
- *Seaside towns across the region were braced for the worst floods in 60 years as 140-mph winds battered the nation in a hurricane-force storm.*
- *More than 15,000 homes in Norfolk, Suffolk and Essex were evacuated, while residents were also rescued in Rhyl, North Wales, and Merseyside.*

- *A lorry driver died in Scotland and a man riding a mobility scooter in King's Park in Retford, Nottinghamshire, was also killed when hit by a falling tree.*
- *More than 120,000 homes were left without power as the most serious tidal surge for 60 years was predicted to hit the east coast last night. As they were taken away from their homes in dinghies, forecasters feared the worst was yet to come during last night's high tide at around 10 pm.*

In London, the Thames Barrier was closed twice in two consecutive days to protect the city from the surge.

In Shanghai, smog hit extremely hazardous levels. Many news outlets covered this story. Here's part of what The Weather Channel had to say: *Shanghai authorities ordered school children indoors and halted all construction Friday as China's financial hub suffered one of its worst bouts of air pollution, bringing visibility down to a few dozen meters, delaying flights and obscuring the city's spectacular skyline.*

The financial district was shrouded in a yellow haze, and noticeably fewer people walked the city's streets. Vehicle traffic also was thinner, as authorities pulled 30 percent of government vehicles from the roads. They also banned fireworks and public sporting events.

"I feel like I'm living in clouds of smog," said Zheng Qiaoyun, a local resident who kept her 6-month-old son at home. "I have a headache, I'm coughing, and it's hard to breathe on my way to my office."

Shanghai's concentration of tiny, harmful PM 2.5 particles reached 602.5 micrograms per cubic meter Friday afternoon, an extremely hazardous level that was the highest since the city began recording such data last December. That compares with the World Health Organization's safety guideline of 25 micrograms.

The dirty air that has gripped Shanghai and its neighboring provinces for days is attributed to coal burning, car exhaust, factory pollution and weather patterns, and is a stark reminder that pollution is a serious challenge in China. Beijing, the capital, has seen extremely heavy smog several times over the past year. In the far northeastern city of Harbin, some monitoring sites reported PM 2.5 rates up to 1,000 micrograms per cubic meter in October, when the winter heating season kicked off.

Meanwhile, here in the United States, water shortages loom. This according to a paper published in *Environmental Research Letters* by scientists at CIRES (the Cooperative Institute for Research in Environmental Sciences; run jointly by NOAA and the University of Colorado) and another study published by researchers at Columbia University. *The Huffington Post* provides its own synthesis:

For decades scientists have been saying that the United States' lakes, rivers and aquifers are going to have a hard time quenching the thirst of a growing population in a warming world.

A recent report from NOAA's Cooperative Institute for Research in Environmental Sciences does not alleviate those fears. It showed that nearly one in 10 watersheds in the U.S. is "stressed," with demand for water exceeding natural supply—a trend that, researchers say, appears likely to become the new normal.

"By midcentury, we expect to see less reliable surface water supplies in several regions of the United States," said Kristen Averyt, associate director for science at CIRES and one of the authors of the study. "This is likely to create growing challenges for agriculture, electrical suppliers and municipalities, as there may be more demand for water and less to go around."

And a recent Columbia University Water Center study on water scarcity in the U.S. showed that it's not just climate change that is putting stress on water supply, it's also a surging population. Since 1950 there has been a 99 percent increase in population in the U.S. combined with a 127 percent increase in water usage.

"All cities and all businesses require water, yet in many regions, they need more water than is actually available—and that demand is growing," Upmanu Lall, director, Columbia Water Center said to Business Insider. "The new study reveals that certain areas face exposure to drought, which will magnify existing problems of water supply and demand."

The Huffington Post goes on to offer a notional list of 11 major U.S. cities that might experience future water shortages.

Some observations:

These stories aren't exhaustive or necessarily the most telling of events underway as of this writing. They're just three of thousands of active news stories, from three locations: Britain, China, and the U.S. Pick any other three nations, and it would be easy to find dozens of similar stories. Pick the same three nations tomorrow, and the action will have shifted to other issues.

Pervasive. Unrelenting. Constantly evolving. That's the challenge facing seven billion people living on the real world.

There's no reason or room for despair. Instead we should be motivated to up our game. We need to get better at seeing these events coming and predicting their impacts. We need policies that help us forestall the Earth's more serious threats. We need to harness social networking to the task of sharing and learning from experience. And we need leadership and a public that shoulders responsibility for outcomes at a local level rather than depending on top-down, command-and-control response from a distance.

Here's a thought exercise you might want to try: identify three (or so) of the real-world challenges closest to you geographically and professionally and most salient at the moment. Picture the next step you plan to take to meet in part one or more of those challenges . . . or how your ongoing work is already making a contribution. Then say to the world:

Bring it on.

THE HIGHLIGHT

ADVICE TO EARLY-CAREER PROFESSIONALS
with Falguni Patadia

- *Where do you currently work and what is your position?* I work in the Climate and Radiation Branch of NASA Goddard Space Flight Center (GSFC) as a research associate under the NASA Goddard Earth Sciences Technology & Research (GESTAR) cooperative agreement with Morgan State University. I came here in 2011 as a postdoctoral fellow. I work on retrieving information about atmospheric aerosols from satellite measurements. Specifically, I work with the MODIS aerosol retrieval team. We are responsible for maintaining, evaluating, and improving the aerosol product. I am leading the effort of characterizing the uncertainty in our retrievals. However, I also handle smaller projects within the group. Part of my job also involves publishing my research and presenting it at meetings and conferences. There is also opportunity for me to mentor undergraduate students during the summer.

Falguni Patadia

- *How did you find this job?* During my Ph.D., I worked on satellite remote sensing of aerosols and their effects on the Earth's radiation budget. NASA GSFC hosts some of the world leaders in satellite remote sensing of aerosols, and therefore I was very familiar with the work being done at GSFC and research opportunities there. I knew that scientists at this institution did cutting-edge research in my field of interest. NASA also has the reputation of being one of the best places to work. These things attracted me to Goddard. When I was ready to graduate, I started looking for job opportunities at GSFC, and I applied for a couple of positions there. My advisor, who had some collaboration with scientists at GSFC, recommended me for this job.

- *To get to this point in your career, what role did mentors and advisors play?* My advisor, Sundar Christopher, who was also my mentor during my Ph.D., played a key role in getting me to this point in my career. I was fortunate to have an advisor who was interested in my career. He pushed me to be at the top of the research work in my field. He made sure that I had a challenging and high-quality scientific project to work on during my Ph.D. He was very encouraging and always showed a lot of trust in me. I matured exponentially as a scientist and published quality work during my Ph.D. He also introduced me to various job opportunities and educated me about how, where, and when to apply for a job. These attributes helped me to get my current position.

- *Is there anything you would have done differently in college knowing what you know now about your job?* Yes, one thing: In my last two years or so working on my Ph.D., I would have tried to participate in summer internships at either NASA centers or in an industry to get short-term, real-life working experience. That also helps the community know you, your work, and your caliber.

- *What do you want to be doing in five years? Why?* I would be very fortunate to continue working with the MODIS aerosol team and be leading some of the projects of my interest. Within the MODIS team there are great opportunities to write proposals. So, five years from now I see myself transforming from an associate researcher to an independent scientist. I also envision working with and mentoring students.

- *Whom do you admire in our profession? Why do you feel that way?* I really admire the professors and scientists in the universities. I think they do great research but, more importantly, they play a very vital role in training and preparing the next generation of scientists.

- *Who do you seek out for advice and why? To whom do you routinely provide advice, if anyone?* I seek out both my senior and fellow colleagues. Senior colleagues have years of invaluable experience, and their advice helps me a great deal both on the professional and personal front. My fellow colleagues' advice is unique to me because we share similar concerns, experiences, and outlooks. I do not provide advice to anyone on a routine basis as of now. My fellow and junior colleagues seek my advice occasionally.

- *What advice would you give to an early-career professional starting in this field?* 1) Seek a mentor, 2) aim to publish at least one high-quality journal article per year, 3) attend meetings and present your work, 4) keep up with your network and build it further, and 5) take a professional development course if there is one available. AMS meetings provide this opportunity with the student conference.

- *Do you have any helpful tips for someone going through the job search right now?* Apply for all jobs you find. You will learn the interview patterns if not anything else. E-mail scientists in your field and ask them if they or anyone else are looking to hire people with your expertise. Do not shy away from following up. Everybody is busy and the lack of a response might just be an overlook. So be persistent, because nobody minds that. In fact, they like it because it shows that you're serious. Also, look at the authors of research articles you have been reading, referencing, etc., for your work and reach out to them. Networking is definitely important, and being proactive is yet another asset.

- *What is it like to be an early-career professional and work for the government/private sector/academia?* You have to be ready to be on your own with minimal guidance. You have to be very creative, show ownership, and demonstrate leadership qualities. NASA has a postdoctoral program and hence there are many early-career professionals around you. I found out that it really increases your enthusiasm and provides the ground for developing collaborations between young professionals.

- *What was the most difficult part of the job search process?* I think the most difficult part of a job search is to find out what you really want to do—that is, work in a private sector or academia. The next challenge is to find that job of your interest. I was fortunate to find an advisor who helped and guided me to figure this out before I graduated. The other part of the job search process we all find challenging is to find a scientific position that pays decently. Usually the postdoctoral positions, mostly at universities, are low-paying jobs.

- *How do you feel the field has changed?* I think that the field now requires a lot more experience with computer programming. That being said, programming skills in FORTRAN, familiarity with some visualization software (GrADS, Matlab, IDL, etc.), and working on Unix/Linux platforms suffices our needs. The other thing that has changed is the demand to multitask, perform interdisciplinary research, and at the same time be able to communicate your work effectively.

- *What are some of the challenges facing early-career professionals?* In academia, both at research institutes and universities, the "temporariness" or short-term funding situation is a very big challenge. Before you can concentrate on your work and establish yourself as a professional, you have to start worrying about securing funding. I think that this competition to win proposals and bring funding is a big challenge facing early-career professionals, especially in the current economic situation.

Sometimes, early-career professionals also have to learn to juggle work and parenting simultaneously, and you could be out of competition if you're not prudent enough. If you're not overly ambitious and happy with what you do, it might not be a problem. However, I see many talented colleagues lose confidence in the early stages of their career and I think that's why finding a mentor at the onset is really important.

POLICY PROGRAM NOTES

THE ROLE OF SCIENCE IN POLICY

Scientists who contribute to policy are most effective when they have clear goals and a strategy for achieving them. Developing those goals and strategies starts, in my view, with thinking carefully about the role of science in policymaking.

In broad terms, there are two possible goals for engaging the policy process and two primary strategies for achieving those goals. The goals are either to improve policies that affect science (policy for science) or to improve policies that can benefit from scientific understanding (science for policy). Scientists attempt to achieve their goals by either providing information (i.e., educating policymakers about science) or by championing particular policy outcomes (e.g., by using persuasive arguments, political pressure, or positive incentives to achieve particular policy goals).

These goals and strategies for policy engagement can be combined in different ways, and they aren't necessarily exclusive: some combine both goals and strategies simultaneously. However, the different goals and strategies confer different risks and opportunities, and tensions can arise among those whose goals and strategies differ.

Most scientists recognize that the pursuit of objectivity in research, though perhaps impossible for any human to fully achieve, is a cornerstone of science. Science generates knowledge and understanding by attempting to eliminate potential sources of bias, often through controlled experiments. This pursuit of objectivity increases the credibility of scientific advances and expands society's willingness to take up and use the new knowledge and understanding science provides.

However, societal choices necessarily involve both objective information (e.g., what the potential response options are, what benefits and risks may be associated with those options, and how benefits and risks may be distributed among different groups or individuals) and subjective value judgments (what are the most desirable outcomes, how do we balance competing interests, or what we "should" do). This means that people can agree on a common set of facts relating to a societal challenge but disagree on appropriate policy responses.

The need for societal decision making to go beyond objective information contributes to a long-running and often contentious disagreement within the scientific community on the appropriate role of scientists in civic discussions. Some argue that scientists should maintain their objectivity by avoiding civic engagement altogether or by focusing exclusively on providing information relevant to civic discussions. This helps, the argument goes, to ensure that scientific insights are as free from external influences as possible and are perceived as unbiased, accurate, and legitimate.

Other scientists argue that membership in society confers a right or even a responsibility to engage more actively in civic discussions. Scientists possess specialized knowledge relating to societally relevant topics and best understand how to integrate that knowledge into decision making, this argument goes. Direct participation increases the likelihood that society will make choices that help manage risks and realize opportunities.

Even among scientists disposed to civic engagement, differences arise based on the range of ways that scientists can choose to participate in policy discussions. The difference between scientific debates and courtroom advocacy is particularly illustrative.

In the courtroom, advocates make the strongest case on behalf of their client that they possibly can. It isn't the lawyer's job to make the counter case.

That falls on the other side. This can be a powerful approach for winning a public debate or influencing a decision. Science, in contrast, relies on a full and objective assessment of the evidence. Scientists have an obligation to identify conflicting evidence, expose weaknesses in their analysis, and offer plausible alternative interpretations. This is a powerful approach for expanding knowledge and understanding and for building credibility as a source of information.

The policy process includes elements of both courtroom advocacy (e.g., the two-party system in the United States) and scientific assessments of information (e.g., the role of scientific advisory boards, or the Congressional Budget Office and the Congressional Research Service). Scientists who engage with the policy process must decide whether to engage in a manner that is consistent with science but that is sometimes at odds with the norms of the policy process, or vice versa.

Notably, the difference between those who favor one approach or another is based on value judgments. It is a philosophical difference of opinion relating to the appropriate role of scientists in society for which there is no clear scientific answer. However, the different approaches do have potentially significant implications for how effectively science can contribute to the broader society and how others in society will view science. There are opportunities and risks associated with each approach.

A focus on providing information, which is the approach the AMS takes, increases credibility and helps open doors, particularly over time as trust builds with policymakers. For institutions, a focus on information also makes it possible for people with divergent views and interests to come together and coexist. However, providing information isn't always the most effective approach to achieving a specific policy objective or outcome.

One partial and imperfect solution, that in my view can work well, is to explicitly and assiduously differentiate scientific information from personal opinions when engaging in civic discussions. With this approach, a scientist can say what policy choices (s)he thinks are best as long as it is clear to the policymaker that the conversation has moved beyond scientific questions.

Of course, no single approach to issues as complex as these will apply in all cases or for all members of our community, but there is great value in understanding what the options are and the risks and opportunities associated with each. This helps insure that individuals and organizations that choose to engage the policy process will be cognizant of the potential implications of their choices for the broader scientific community. As a result, careful consideration of the role of science in policy is a critical first step for anyone interested in contributing to the policy process.

—Paul Higgins, AMS Policy Program Director

FOR FURTHER READING

Higgins, P. A. T., K. M. A. Chan, and S. Porder, 2006: Bridge over a philosophical divide. *Evidence & Policy*, **2**, 251–257.

ABOUT OUR MEMBERS

Warren M. Washington has been chosen by the Association of American Geographers (AAG) to receive the 2014 AAG Honorary Geographer Award. He is being recognized for his contributions as a pioneer in the development of coupled climate models as well as a leading scientist in the area of climate variability and change. Inaugurated in 1997, the AAG bestows its Honorary Geographer Award each year on an individual to recognize excellence in the arts, research, teaching, and writing on geographic topics by nongeographers.

The AAG also acknowledges Washington's leadership role as an advocate for science in general, particularly his service as chair of the National Science Board. This award recognizes his many contributions as a role model and mentor for young scientists, including members of the geography community, and his commitment to advancing diversity.

Born in Portland, Oregon, Washington developed an interest in science at an early age. His interest led him to pursue a bachelor's degree in physics and a master's in meteorology from Oregon State University. He then went on to earn a doctorate in meteorology from Pennsylvania State University. Washington joined the National Center for Atmospheric Research (NCAR) in 1963 as a research scientist.

He is now a senior scientist at NCAR, where he also serves as chief scientist of the DOE/UCAR Cooperative Agreement in the Climate Change Research Section in the center's Climate and Global Dynamics Division.

MAKE PURCHASES AT OUR NEW ONLINE BOOKSTORE!

CLIMATE CHANGE

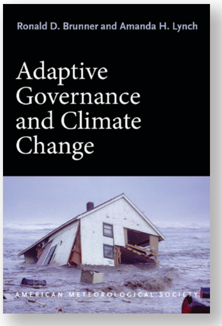

Adaptive Governance and Climate Change

RONALD D. BRUNNER AND AMANDA H. LYNCH

©2010, PAPERBACK, 424 PAGES, ISBN 978-1-878220-97-4

LIST $35 MEMBER $22

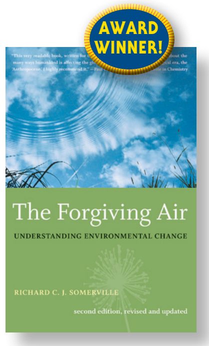

The Forgiving Air: Understanding Environmental Change, 2nd ed.

RICHARD C. J. SOMERVILLE

©2008, PAPERBACK, 224 PAGES, ISBN 978-1-878220-85-1

LIST $22 MEMBER $16

ASK ABOUT THE HISTORIC ARCHIVE OF CALLENDAR'S PAPERS AVAILABLE ON DVD.

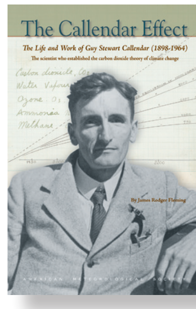

The Callendar Effect: The Life and Work of Guy Stewart Callendar (1898–1964)

JAMES RODGER FLEMING

© 2007, HARDCOVER, 176 PAGES HM, ISBN 978-1-878220-76-9

LIST $34.95 MEMBER $24.95

MIDLATITUDE WEATHER SYSTEMS

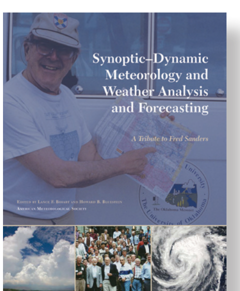

Synoptic–Dynamic Meteorology and Weather Analysis and Forecasting: A Tribute to Fred Sanders

EDITED BY LANCE F. BOSART AND HOWARD B. BLUESTEIN

© 2008, HARDCOVER, 440 PAGES, MM VOL. 33, NO. 55, ISBN 978-1-878220-84-4

LIST $120 MEMBER $80
STUDENT MEM. $60

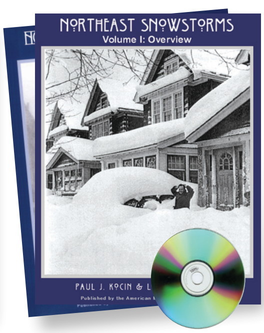

Northeast Snowstorms (Volume I: Overview, Volume II: The Cases)

PAUL J. KOCIN AND LOUIS W. UCCELLINI

© 2004, TWO HARDCOVER VOLS, PLUS DVD, MM VOL. 32, NO. 54, ISBN 978-1-878220-64-6

LIST $100 MEMBER $80
STUDENT MEM. $60

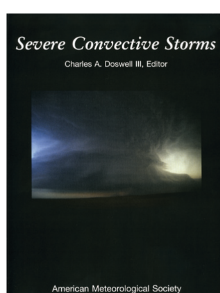

Severe Convective Storms

EDITED BY CHARLES A. DOSWELL III

© 2001, HARDCOVER, 570 PAGES, MM VOL. 28, NO. 50, ISBN 978-1-878220-41-7

LIST $110 MEMBER $90
STUDENT MEM. $75

MM = METEOROLOGICAL MONOGRAPH SERIES
HM = HISTORICAL MONOGRAPH SERIES

HISTORY

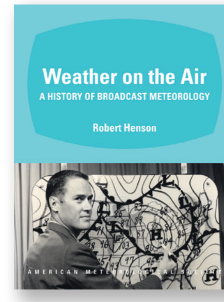

Weather on the Air: A History of Broadcast Meteorology

ROBERT HENSON

Weather on the Air documents the evolution of weathercasts—the people, technology, science, and show business that combine to deliver the weather to the public each day. An invaluable tool for students of broadcast meteorology, this book will entertain anyone fascinated by the public face of weather. Includes more than 100 photographs!

©2010, HARDCOVER, 264 PAGES, ISBN 978-1-878220-98-1

LIST $35 MEMBER $25

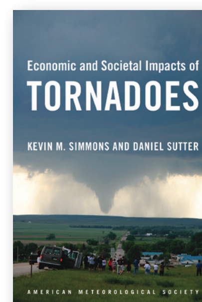

Economic and Societal Impacts of Tornadoes

KEVIN M. SIMMONS AND DANIEL SUTTER

Two economists' unique database has enabled a fascinating and game-changing study of tornado impacts and how factors such as storm timing and warning lead time affect impacts; whether Doppler radar and shelters are worth the investment; and more. For meteorologists, social scientists, and emergency managers.

©2011, PAPERBACK, 296 PAGES, ISBN 978-1-878220-99-8

LIST $30 MEMBER $22

Deadly Season: Analyzing the 2011 Tornado Outbreaks

KEVIN M. SIMMONS AND DANIEL SUTTER

Examine the factors that contributed to the outcomes of the 2011 tornadoes, identifying both patterns and anomalies. Their conclusions, and assessment of early recovery efforts, are aimed at helping community leaders and policymakers keep vulnerable populations safer in the future.

© 2012 , PAPERBACK, ISBN 978-1-878220-25-7
LIST $25 MEMBER $20

www.ametsoc.org/amsbookstore 617-226-3998 or use the order form in this magazine

NEW MEMBERS

The Council has approved the election of the following candidates to the grade of **Full Member:**

Muhamad Shah Alam
Lisa S. Alexander
Fred A. Allen Jr.
Julie M. Arblaster
Sadibou Ba
Joseph L. Bailey
Noel C. Baker
John M. Balbus
Simone Balog
Neil P. Barton
Erik H. Becker
Elizabeth J. Bentley
Bernard Blair
Jim Blatchford
Jeffrey A. Boeckl
Andrew T. Bohrer
Anne C.B. Borgstroem
Brandon M. Bouche
John H. Brooks Jr.
Christopher C. Burt
Kathleen F. Bush
Cassandra P. Calderella
Aditya Choukulkar
Alisha M. Christian
Francis Codron
Andrew J. Condon
Jessica Conley
Brian A. Crandall
Edward D. Creegan
Holly Dail
Nikolay N. Damyanov
Christopher M. Davis
Jason Davis
Elise D. Dolinar
Aaron Donohoe
Adrian Dozier
Caroline Draxl
Tyler H. Eliasen
Ryan M. Erb
Peter E. Fearon
Richard Fitzgerald
Jacob M. Gajewski
Jan T. Galkowski
Ari B. Gerstman
Alexander R. Gibbs
Justin Gibbs
Donald J. Giuliano
Kevin P. Good II
Ian Grooms
Markus S. Gross
Jianping Guo
Ashok R. Gupta
Martin Hagen
Christine L. Haman
Amanda E. Hansen
Ryan J. Harris
Adam Hartman
Bryan Hartzell
Jon Haverfield
Alison J. Hayes
Brian M. Hays
Stephanie Hedstrom
Jonathan J. Helmus
Rob E. Hodges
Daniel Holdaway
Michael Hollan
Kenta Hood
Jana B. Houser
Gwo-Jong Huang
Chelsea R. Humphrey
Kyle F. Itterly
Diane J. Ivy
David Jackson
Justyn Jackson
Michael P. Joyce
Martin Jucker
Joerg A. Kachelmann
Andre Kamga Foamouhoue
Manabu Kanda
Despina S. Karras
Michael J. Kavaya
Matthew Kelsch
Claire Kennedy
David W. Kenny
Thomas J. Kilpatrick
Pierre-Emmanuel Kirstetter
Robert Knapp
Roman S. Kowch
Matthew R. Kumjian
Emil Robert Kursinski
Sandra G. LaCorte
Vladimir Lapin
Shao-Yi Lee
Melissa L. LeFevre
Katharina Lengfeld
Kenneth D. Leppert II

The Executive Committee has approved the election of the following candidates to the grade of **Student Member:**

Brian E. Adams
Kyle K. Ahern
Christian F. Akerley
Carina R. Alden
Bryan Allen
Tyler Allender
Jhonatan J. Alvizurez Sr.
Dillon J. Amaya
Alexander E. Anderson
Brittny Andreola
Tawana Andrew
Ernest C. Andrews III
Dominic J. Antonacci
Dicky L. Armstrong Jr.
Coral Arroyo
Craig Arsedo
Daniel A. Arteaga
Sarah Ash
Michael J. Austerberry
Emily Ayscue
Abbigale N. Bailey
Jonah Balla
Kelly A. Balmes
Christian R. Barriera
Mackenzie Bart
Rory Barton-Grimley
Samantha Basile
Colin Baxter
Kelley J. Bayern
Paul E. Beam
Molly L. Becker
Joshua Benson
Samantha Berkseth
David A. Bishop
Ian G. Boatman
Levi Boggs
Jillian Bohenek
Benjamin M. Bonner
Stephanie A. Bonney
Alexander Boothe
Evemarie Y. Bracetti
Allison L. Brannan
Melissa Breeden
Haley Brink
Leyton Briol
Matthew Brothers
Mary R. Brown
Todd E. Brown
Joseph J. Brum
Kelcy N. Brunner-Miller
Zoe P. Buccella
Gaje Buchanan
Bryan Burlingame
Kristin N. Butt
Lei Cai
Henry H. Cantrell
Samantha S. Carr
Vincent A. Carretti
Jose R. Cartagena
Nicole A. Casamassina
Ian Cassette
Hanser Castro
Alexandra M. Catena
Jessica Caubre
Laura A. Caudle
Erik T. Chan
Kirsten M. Chaney
Xi Chen
Xiaomin Chen
Caleb C. Chevalier
William L. Churchill
Juliana Ciccarelli
Joseph Cleveland
Jorge Clouthier-Lopez
Kaitlyn Colna
Amanda Conaway
Kevin J. Conrath
Martin P. Coolidge
John W. Cooney
Jillian N. Coughlin
Katherine M. Coughlin
Zachary E. Covey
Renee Cox
Dakota A. Crane

NEW MEMBERS

Ray Leuning
Jing Li
Shuangcai Li
Ying Li
Robert Light
John C. Lin
Pu Lin
Junjun Liu
Keith L. Lynch
Matthew MacDonald
Megan S. Mallard
Thomas G. Mara
Timothy C. Martin
Joseph Martucci
Matthew S. Mayernik
William R. McCarty
Timothy P. McGeehan
Gerald E. Meier
Travis Miguez
Luis F. Millan Valle
Neha Mirchandani
Joseph J. Moore
Michael J. Mueller
VSN Murty
Bibi S. Naz
Dianna N. Nelson
Nathan New
Craig Nikkel
Hajime Nishigaki
Christopher Nowotarski
Leonard A. Nurse
Kaitlyn E. O'Brien
Marita O'Brien
Scott O'Donnell
Robert D. Ottmann
Michael D. Page
Luca Panziera
Seoyeon Park
Matthew J. Payne
Jonathon Pelissero
Melissa Peterson
Andrew Pineiro
Raul E. Pineiro
Franco Prodi
Ajaya Mohan Ravindran
Ann M. Reiser
Isha M. Renta
Antonio G. Riggi
Emily M. Riley
Jacob M. Rissberger
Joshua A. Roberti
Kristina Rohrbach
Charles E. Roop
Benjamin V. Root
Paul Rubio
Roop K. Saini
Jared S. Scharmett
Michael J. Schwartz
ManishKumar Shrivastava
Hallie L. Shulman
Amanda J. Silver
Florin Spineanu
Justin P. Stachnik
Jennifer E. Stanonis
Paul Staten
Andrew Stewart
Kara J. Sulia
Petteri Survo
Farahnaz Taghavi
Samantha S. Thomas
Danielle C. Thorne
Anna M. Trevino
Frederic Tridon
Chia-Lun Tsai
Vladimir Tsirkunov
Paul A. Ullrich
Jessica Van Meter
Jean Vieux
Katy M. Vincent
Katrina S. Virts
Jessica J. Voveris
Brian T. Walder
Peng Wang
Nathaniel A. Wardle
Jean-Philippe Wasselin
John L. Williams III
Kate M. Wilson
Ariel J. Winstanley
Barbara Winter
Sean D. Wolinsky
Josh Wurster
Pengfei Xue
Qiong Yang
Jiacan Yuan

Mileidy Crespo-Jones
Erika L. Cropp
Antonio D. Cruz
Travis C. Cruz
Connor Dacey
Farrah Daham
Aika Y. Davis
Gabriela De La Cruz Tello
Lucia De Rosa
Brett F. Dean
Neil Debbage
Eleanor G. Delap
Stephen Demetry
Connor A. Dennhardt
Thomas R. Dewberry II
Benjamin D. Dillahunt
Yifeng Ding
Andrew L. Dipaolo
Chloe Doberstein
Benjamin L. Dominguez
Andrew M. Dotson
William A. Doubleday-Potts
Erin Dougherty
Samuel P. Douglass Jr.
Alexandria Downs
Cameron B. Duck
Jason A. Ducker
Rebecca Duell
Chad A. Dumas
Justin Dumas
Kimberly Duong
Nicholas Easter
Jacob P. Edman
Alex Edwards
Jonathan Edwards-Opperman
Elke Eichelmann
Bret Edward Eilertson
ShoShoni J. Elbe
Meredyth A. Ellington
Ashley M. Ellis
Geneva M. Ely
Adrianne J. Engel
Robert Englund
Jackeline M. Fain
James Fallon
David Farnham
Nicholas Farruggio
Ashley Feaster
Eric Federico
Janet Feezor
Bradley Fehnel
Sabrina Fehr
Kelsie M. Ferin
Aaron C. Findley
Volkan H. Firat
Michael A. Flanigan
Clare Marie Flynn
Josephine Fong
Ivan Leonel Fontanez
Ashley Fortin
Catherine A. Foster
Felicia M. Francis
Mara Freilich
Brian M. Freitag
Rebecca L. Fuller
Sara L. Fults
Csilla V. Gal
Jared M. Gallegos
Christian I. Garcia
Omar C. Gates
Sean P. Gay
Gillian P. Gelinas
Christopher A. M. Gerlach
Michael S. Gernert
Mohamed Ghonima
Joseph Giacomelli
Thomas C. Giebel
Daphne Y. Girisgen
Megan Godfrey
Chad A. Goergens

Continued

NEW MEMBERS

The Executive Committee has approved the election of the following candidates to the grade of **Student Member:**

Joseph N. Gollotto Jr.
Robert A. Gould
David M. Grace
Benjamin Green
Ryann A. Green
Ethan P. Greene
Arden Gregory
Matthew Gropp
Caleb T. Grunzke
Bradford P. Guay
Nigel Haarstad
Liana Haddad
Alexander Hahne
Brittany Hailey
Jeremy Hall
Catherine C. Halverson
Tori Hampton
Tyler Hansen
Gregory W. Hanson
Ty J.A. Hardy
Derek R. Harrington
Kelly D. Harris
Sara E. Harrison
Justin J. Hartnett
Samuel K. Hartwick
Shelby Hays
Kaitlyn N. Heinlein
Gabriel D. Henderson
Brittany N. Henley
Alex Herbst
Alexandria J. Herdt
Jeff Herrera
Sean Heslin
Tracy Hinson
Martin S. Hoecker-Martinez
John W. Holland
Kylie Holmes
Matthew R. Hook
Kacie E. Hoover
John Hottenstein
Xiangting Hou
Macy E. Howarth
Jiaxi Hu
Emily C. Huang
Wan Ting Katty Huang
James Jacob Huff
Jensen L. Hufnagel
Amber T. Hughes
Carter B. Hulsey
Ranya Ilayian
Tyler James Jankoski
Sabrina T. Jauernic
Raymond Jefferson Jr.
Dylan P. Jeffrey
Valerian Jewtoukoff
Wang Jiajia
Joshua E. Johns
Da'Vel Johnson
Zach Johnson
Catherine Jones
Griffin W. Jones
Megan E. Jones
Benjamin J. Joseph
Casey Joseph
Oscar E. Jurado
Nathan M. Jurgensen
Andrew Kalin
Christian R. Kamrath
Joseph Karel
Branden T. Katona
Amanpreet Kaur
David Keellings
Jake M. Keiser
Thomas F. Kelleher
William Kenny
James A. Kessler
Peeyush Khare
Sanghoon Kim
Jessica L. Klosterman
Stevy C. Knight III
William S. Koerner
Christopher Koh
Monika Kohn
Zachary L. Kornse
Margarita V. Korobkov
Erik M. Kostrzewa
Kyle Koval
Emily L. Kreyenhagen
Stephanie E. Kroese
Joseph A. Krystyniak
Michelle Kuyper
Samantha A. Kvartunas
Katherine E. Kyzer
Austin M. Lacey
Matthew K. Laffin
Allison T. LaFleur
Andrew Lammers
Yang Lang
Jaret Lansford
Shelby Latino
Matthew Lauridsen
Corey D. Lea
Zack T. Leasor
Mark Leberfinger
Michael B. Ledermann
Stephanie R. Lein
Elizabeth M. Lennartson
Katherine B. Lenninger
Shirley W. Leung
Emily G. Lewis
Wyndam R. Lewis
Xiaoqiong Li
Colton R. Lindsey
Brendan A. Linton
Yang Liu
Nathaniel Loeb
Scott Loeffler
Elimay M. Lopez
Hiriagnny A. Lorenzo Paulino
Devin H. Low
YinLin Lu
Mallory M. Lumpe
Qianwen Luo
Drew Lyon
Ding Ma
Anthony Macari III
James C. Maciag
Nicole Madden
Christopher M. Maderia
Emily Madison
Maria M. Madsen
Kathleen Magee
Ryan Mahoney
Andrew Mahre
Taylor S. Mandelbaum
Alexander Manion
Zachary N. Manyak
Joseph P. Markiewicz III
Erin M. Markovich
Jesse C. Marks
Gustavo M. Marques
Joanna Marrufo
Dominique J. Marshall
Michael L. Marston Jr.
Jonathan Martinez
Ashley M. Maupin
Tiffany A. Maupin
Kelsey D. McCallister
James L. McCoy
Justin T. McCoy
Kathleen McCracken
Joshua J. McDanel
Brandon McGill
Robert J. McGinnis
Colleen E. McHugh
Francis P. McInerney
Megan McKeown
Victoria S. McKinney
Talmor Meir
David Melecio-Vazquez
Catherine A. Menke
Christian J. Mercado
Lauren Merritt
Brian D. Mette
John Meyer
Adrian Mitchell
Valerie Morel
David Morgan
Matthew T. Morris
Alex Morrison
Lacey Morrow
Amanda M. Murphy
David Myers
Bappaditya Nag
Jonathan Napora
Michael B. Natoli
Isidro Navarro
Lawrence A. Nelson
Mark Nissenbaum
Kyle Noel
Thomas C. Noelcke
Navideh Noori
Dustin J. Norman
Evan Ntonados
Jonathan O'Brien
Katherine A. O'Brien

NEW MEMBERS

Dan O'Sullivan Jr.
Curt Olson
Jose J. Orengo
Luis E. Ortiz
Berenice Oseguera
Craig Oswald
Brandon M. Owen
Christopher Pace
Emily G. Parker
Scot Parker
Shane N. Pendleton
Jeremy G. Pendley
Caitlin A. Pennington
Kyle S. Pennington
William T. Peyton
Charles Phillips
Simone M. Phillips
Daniela M. Pirraglia
Corallys Plasencia
Christian Plaud
Cassandra Plotkin
Cody Poche
Shaina E. Poore
Anna Possner
Trisha L. Prins
Jessica M. Ptashenchuk
Anna Ptasznik
Brendan M. Pucel
Alex R. Puckett
Christopher A. Quick
Mitchell Raeck
Elisa Raffa
John H. Ramer
Yentil M. Ramirez Lopez
Eva M. Ratcliffe
Malori A. Redman
Isaac W. Renfrow
Lauren Replogle
Christina M. Reuille
Mehdi Rezaeianzadeh
Chelsy Richley
Damian M. Rickard
Zachary J. Riel
Joshua Rivas
Nayrobie L. Rivera
Joseph P. Robinson
Geoffrey S. Roest
Andrew L. Rogers
Benjamin D. Roob Jr.
Renautha Rose
Brett Charles Rossio
Juan J. Ruberte Rodriguez
Stephanie S. Rushley
Alexis Santos
Robert R. Santucci
Davanna G. Saunders
Kathryn Sauter
Amanda M. Sava
Ajda Savarin
Mekensie E. Schell
Kathleen A. Schiro
Michael L. Schmidt
Timothy M. Schmidt
Tori Schow
Andrea Schrepfer
Zoe M. Schroder
Sophia Sciotto
Samuel A. Scoleri
Josh P. Searles
Lauren E. Seidensticke
Austin J. Sellman
Pedro E. Sequera
Ahmed A. Shaaban
Julia Shates
Elliot Shiben
John M. Simmons
Kevin A. Sinwell
Klint T. Skelly
Amanda M. Sleinkofer
Joseph Slezak
Alan Smith
Andrew W. Smith
Claire F. Smith
Erik T. Smith
Jessica R. Smith
Oliver C.C. Smith
Ryan Smithies
Christopher Soelle
Awolou S. Sossa
Michael Spagnolo
Kent H. Sparrow
Kayla E. St. Germain
Katie Starr
Nick Stasiak
Andrew C. Stein
Michael J. Stewart
Abigail E. Stimach
Alexandra Stinner
Victoria Strait
Allison M. Streeter
Samantha I. Strong-Henninger
Ed Sullivan
Sierra B. Sult
Travis S. Swaggerty
Alyssa Sweeney
Shannon M. Sweeney
Jordan T. Swift
Joanna E. Szewczyk
Jon Taylor
Brian Tennant
Bonnie M. Thompson
Preston A. Thornton
Ryan P. Thorp
Yang Tian
Katelyn L. Tisch
Matthew Toadvine
Stella E. Todzo
Javier O. Tomas
Jessica M. Tomaszewski
Anthony D. Torres
Jean C. Torres
Jorel Torres
Tyler Tracksell
Anna T. Trugmsn
Szu-Ting Tseng
Adrienne K. Tucker
Kristofer S. Tuftedal
Axel J. Ufarry Alvarado
Atiba Upchurch
Hans J. VanBenschoten
Gibril Momodu Vandy
Rosa M. Vargas Martes
Nelson A. Velazquez Jr.
Cameron D. Venable
Michael C. Veres
Daniel Vidal
Maximilian A. Vido
Peter T. Vonich
Gretchen Wachenheim
Lori Wachowicz
Courtney A. Wagel
Kevin M. Wagner
Tara C. Wagoner
XiuQuan Wang
Aaron Ward
AJ Waterman
Kirsten R. Watkins
Nicholas Weber
Stephen Weber
Eric M. Weglarz
Kaylee A. Wendt
Morgan A. Wentling
Daniel Wesloh
Jeff Wetter
Andrew J. White
Arielle D. Whooley
Rebecca Wiegand
Matthew Wiesner
Eddie Wildermuth
Jacob Wilkins
Skylar Williams
William N. Wilson
Jacey N. Wipf
Matthew Woelfle
Christopher A. Wolfe
Owen G. Wolfe
Marisa Woloszyn
Falicia L. Woody
Chao Wu
Qiusheng Wu
Wei Wu
Weiyi Xu
Yangyang Xu
Huang Yang
John Xun Yang
Matthew D. Yannetti
Keith P. Yaple
Cameron Young
Jordan D. Young
Mark Young
Nicholas Zelasko
Zhenhai Zhang
Qing Zhu

NEW MEMBERS

The Council has approved the election of the following candidate to the grade of **Full Member with Student Privileges:**

David S. Bonnette	Brett Fulton	Katherine A. Long	Zachary Suriano
Benjamin E. Brown-Steiner	Hesham A. Hassan	Erin M. Lynch	Adam Troxell
Christopher Buttaro	Josh Henry	Laren Mahoney	William Watson
Chapin Cofod	Souichiro Hioki	Michael J. McClellan	Chen Wei
Zhoe V. Comas	Samy M. Kamal	Daniel Moser	Ho-Hsuan Wei
Chelsea O. Cooper	Argyro G. Kavvada	Omar Nava	Melissa Weiss
Maged Mohamed El Soury	Sahiba Khan	Amy E. Pack	Kyle R. Wodzicki
Kyle A. Elliott	Dylan S. Ladner	Gino F. Recchia	GuanNian Zeng
Nicholas R. Esposito	Robert William Lee	Chana D. Seitz	Chen Zhou
Caitlin M. Fine	Erik A. Lindgren	Jason A. Sulskis	

The Executive Committee has approved the election of the following candidates to the grade of **Associate Member:**

Joe Bilecki	Bernard Hohman II	Larry A. Lovering	Richard Rennolds II
Anthony Grimes	Joe D. Ikerd	Christopher Mangle	Jordan A. Stillman
Matthew W. Hacker	Robert Jubenville	John T. Murphy	Martin W. Turner
Jeff Hahn	Latif Kalin	Morgan Radford	Charles Weir
Max A. Hartwig	Brian Kennedy		

The Executive Committee has approved the election of the following candidates to the grade of **Associate Member—Precollege Student:**

Nathan R. Anthony	Alex F. Forbes	Jillian Olson	Caleb B. Smith
Joshua Barnett	Madeline Greenberg	Ryan Peterson	Zane A. Smith
Ethan Becker	Erin Jones	Vishal Ravi	Jacob Soule
Nicholas E. Butler	Ketzel Levens	Violet Scibior	Rani Wiggins
Forrest Eppler	Tyler P. Meluch		

The Executive Committee has approved the election of the following candidates to the grade of **Associate Member/K–12 Teacher:**

Victoria Gorman	Faye Landsman	Steven Marshall	Alycia Obernuefemann

CALENDAR OF MEETINGS

The Call for Papers and Calendar sections list conferences, symposia, and workshops that are of potential interest to AMS members. **Complete information about events listed in the calendar can be found on the meetings page of the AMS website, www.ametsoc.org.** New additions to the calendar are highlighted.

To list an event in the calendar, please submit the event name, dates, location, and deadlines for abstracts, manuscripts, and preregistration to amsmtgs@ametsoc.org. For a submission to appear in a given issue, it must be submitted at least eight weeks prior to the month of publication (that is, to appear in the March *Bulletin,* the submission must be received by 1 January).

AMS MEETINGS

2014

APRIL

31st Conference on Hurricanes and Tropical Meteorology, 31 March–4 April, San Diego, California
Abstract deadline: 22 November 2013
Preregistration deadline: 18 February 2014
Manuscript deadline: 5 May 2014
Initial announcement published: Sept. 2013

MAY

31th Conference on Agricultural and Forest Meteorology, 12–15 May, Portland, Oregon
Abstract deadline: 13 January 2014
Preregistration deadline: 21 March 2014
Manuscript deadline: 13 June 2014
Initial announcement published: Nov. 2013

Second Conference on Atmospheric Biogeosciences, 12–15 May, Portland, Oregon
Abstract deadline: 13 January 2014
Preregistration deadline: 21 March 2014
Manuscript deadline: 13 June 2014
Initial announcement published: Nov. 2013

JUNE

21st Conference on Applied Climatology, 10–12 June, Westminster, Colorado
Abstract deadline: 27 January 2014
Preregistration deadline: 5 May 2014
Manuscript deadline: 15 July 2014
Initial announcement published: Sept. 2013

17th Symposium on Meteorological Observations and Instrumentation, 10–12 June, Westminster, Colorado
Abstract deadline: 27 January 2013
Preregistration deadline: 5 May 2014
Manuscript deadline: 15 July 2014
Initial announcement published: Sept. 2013

42nd Conference on Broadcast Meteorology, 17–20 June, Olympic Valley, California
Abstract deadline: 27 January 2014
Preregistration deadline: 5 May 2014
Initial announcement published: Nov. 2013

JULY

14th Conference on Atmospheric Radiation, 7–11 July, Boston, Massachusetts
Abstract deadline: 7 March 2014
Preregistration deadline: 21 April 2014
Manuscript deadline: 11 August 2014
Initial announcement published: Nov. 2013

14th Conference on Cloud Physics, 7–11 July, Boston, Massachusetts
Abstract deadline: 7 March 2014
Preregistration deadline: 21 April 2014
Manuscript deadline: 11 August 2014
Initial announcement Published: Nov. 2013

Anthony Slingo Symposium, 7–11 July, Boston, Massachusetts
Abstract deadline: 7 March 2014
Preregistration deadline: 21 April 2014
Manuscript deadline: 11 August 2014
Initial announcement published: Dec. 2013

AUGUST

16th Conference on Mountain Meteorology, 18–22 August, San Diego, California
Abstract deadline: 18 April 2014
Preregistration deadline: 7 July 2014
Manuscript deadline: 22 September 2014
Initial announcement Published: Mar. 2014

NOVEMBER

27th Conference on Severe Local Storms, 3–7 November, Madison, Wisconsin
Abstract deadline: 1 July 2014
Preregistration deadline: 9 September 2014
Manuscript deadline: 7 December 2014
Initial announcement published: Feb. 2014

AMS MEETINGS

2015

JANUARY

14th Annual AMS Student Conference, 3–4 January, Phoenix, Arizona

31st Conference on Environmental Information Processing Technologies, 4–8 January, Phoenix, Arizona
Abstract deadline: 1 August 2014
Preregistration deadline: 1 December 2014
Manuscript deadline: 5 February 2015
Initial announcement published: Mar. 2014

*An exhibit program will be held at this meeting.

29th Conference on Hydrology, 4–8 January, Phoenix, Arizona
Abstract deadline: 1 August 2014
Preregistration deadline: 1 December 2014
Manuscript deadline: 5 February 2015
Initial announcement published: Mar. 2014

27th Conference on Climate Variability and Change, 4–8 January, Phoenix, Arizona
Abstract deadline: 1 August 2014
Preregistration deadline: 1 December 2014
Manuscript deadline: 5 February 2015
Initial announcement published: Mar. 2014

24th Symposium on Education, 4–8 January, Phoenix, Arizona
Abstract deadline: 1 August 2014
Preregistration deadline: 1 December 2014
Manuscript Deadline: 5 February 2015
Initial announcement published: April 2014

20th Conference on Satellite Meteorology and Oceanography, 11th Symposium on New Generation Operational Environmental Satellite Systems, and Third AMS Symposium on the Joint Center for Satellite Data Assimilation (JCSDA), 4–8 January, Phoenix, Arizona
Abstract deadline: 1 August 2014
Preregistration deadline: 1 December 2014
Manuscript deadline: 5 February 2015
Initial announcement published: Mar. 2014

19th Conference on Air–Sea Interaction, 4–8 January, Phoenix, Arizona
Abstract deadline: 1 August 2014
Preregistration deadline: 1 December 2014
Manuscript deadline: 5 February 2015
Initial announcement published: Mar. 2014

19th Conference on Integrated Observing and Assimilation Systems for Atmosphere, Oceans, and Land Surface (IOAS-AOLS), 4–8 January, Phoenix, Arizona
Abstract deadline: 1 August 2014
Preregistration deadline: 1 December 2014
Manuscript deadline: 5 February 2015
Initial announcement published: Mar. 2014

18th Conference on the Middle Atmosphere, 4–8 January, Phoenix, Arizona
Abstract deadline: 1 August 2014
Preregistration deadline: 1 December 2014
Manuscript deadline: 5 February 2015
Initial announcement published: Mar. 2014

17th Conference on Conference on Atmospheric Chemistry, 4–8 January, Phoenix, Arizona
Abstract deadline: 1 August 2014
Preregistration deadline: 1 December 2014
Manuscript deadline: 5 February 2015
Initial announcement published: Mar. 2014

17th Conference on Aviation, Range and Aerospace Meteorology (ARAM), 4–8 January, Phoenix, Arizona
Abstract deadline: 1 August 2014
Preregistration deadline: 1 December 2014
Manuscript deadline: 5 February 2015
Initial announcement published: Mar. 2014

13th Conference on Artificial and Computational Intelligence and its Applications to the Environmental Sciences, 4–8 January, Phoenix, Arizona
Abstract deadline: 1 August 2014
Preregistration deadline: 1 December 2014
Manuscript deadline: 5 February 2015
Initial announcement published: Mar. 2014

13th Symposium on the Coastal Environment, 4–8 January, Phoenix, Arizona
Abstract deadline: 1 August 2014
Preregistration deadline: 1 December 2014
Manuscript deadline: 5 February 2015
Initial announcement published: Mar. 2014

12th Conference on Space Weather, 4–8 January, Phoenix, Arizona
Abstract deadline: 1 August 2014
Preregistration deadline: 1 December 2014
Manuscript deadline: 5 February 2015
Initial announcement published: Mar. 2014

11IMPACTS: Major Weather Events and Societal Impacts of 2014, 6 January, Phoenix, Arizona
Abstract deadline: 1 August 2014
Preregistration deadline: 1 December 2014
Manuscript deadline: 5 February 2015
Initial announcement published: Mar. 2014

Tenth Symposium on Societal Applications: Policy, Research and Practice, 4–8 January, Phoenix, Arizona
Abstract deadline: 1 August 2014
Preregistration deadline: 1 December 2014
Manuscript deadline: 5 February 2015
Initial announcement published: Mar. 2014

Seventh Symposium on Lidar Atmospheric Applications, 4–8 January, Phoenix, Arizona
Abstract deadline: 1 August 2014
Preregistration deadline: 1 December 2014
Manuscript deadline: 5 February 2015
Initial announcement published: Mar. 2014

Seventh Symposium on Aerosol–Cloud–Climate Interactions, 4–8 January, Phoenix, Arizona
Abstract deadline: 1 August 2014
Preregistration deadline: 1 December 2014
Manuscript deadline: 5 February 2015
Initial announcement published: Mar. 2014

Seventh Conference on the Meteorological Applications of Lightning Data, 4–8 January, Phoenix, Arizona
Abstract deadline: 1 August 2014
Preregistration deadline: 1 December 2014
Manuscript deadline: 5 February 2015
Initial announcement published: Mar. 2014

Sixth Conference on Environment and Health, 4–8 January, Phoenix, Arizona
Abstract deadline: 1 August 2014
Preregistration deadline: 1 December 2014
Manuscript deadline: 5 February 2015
Initial announcement published: Mar. 2014

Fifth Conference on Transition of Research to Operations, 4–8 January, Phoenix, Arizona
Abstract deadline: 1 August 2014
Preregistration deadline: 1 December 2014
Manuscript deadline: 5 February 2015
Initial announcement published: Mar. 2014

---

* An exhibit program will be held at this meeting.

Fifth Symposium on Advances in Modeling and Analysis Using Python, 4–8 January, Phoenix, Arizona
Abstract deadline: 1 August 2014
Preregistration deadline: 1 December 2014
Manuscript deadline: 5 February 2015
Initial announcement published: Mar. 2014

Third Annual Symposium on the Weather and Climate Enterprise, 4–8 January, Phoenix, Arizona
Abstract deadline: 1 August 2014
Preregistration deadline: 1 December 2014
Manuscript deadline: 5 February 2015
Initial announcement published: Mar. 2014

Third Symposium on Building a Weather-Ready Nation: Enhancing Our Nation's Readiness, Responsiveness, and Resilience to High Impact Weather Events, 4–8 January, Phoenix, Arizona
Abstract deadline: 1 August 2014
Preregistration deadline: 1 December 2014
Manuscript deadline: 5 February 2015
Initial announcement published: Mar. 2014

Third Symposium on Prediction of the Madden–Julian Oscillation: Processes, Prediction, and Impact, 4–8 January, Phoenix, Arizona
Abstract deadline: 1 August 2014
Preregistration deadline: 1 December 2014
Manuscript deadline: 5 February 2015
Initial announcement published: April 2014

First Symposium on High Performance Computing for Weather, Water, and Climate, 8 January, Phoenix, Arizona
Abstract deadline: 1 August 2014
Preregistration deadline: 1 December 2014
Manuscript Deadline: 5 February 2015
Initial announcement published: April 2014

Special Symposium on Model Postprocessing and Downscaling, 4–8 January, Phoenix, Arizona
Abstract deadline: 1 August 2014
Preregistration deadline: 1 December 2014
Manuscript deadline: 5 February 2015
Initial announcement published: Mar. 2014

MEETINGS OF INTEREST

2014

MARCH

Ninth International Conference on Air Quality: Science and Application, 24–28 March, Garmisch-Partenkirchen, Germany

APRIL

12th Annual Southeast Severe Storms Symposium, 4–5 April, Starkville, Mississippi

Ninth Weather Radar and Hydrology (WRaH) International Symposium, 7–9 April, Washington, D.C.

MAY

12th Annual Climate Prediction Applications Science Workshop (CPASW), 6–8 May, Fairfax, Virginia

Northern Plains Convective Storms Symposium, 19–20 May, Grand Forks, North Dakota

First International Summit on Tornadoes and Climate Change, 25–30 May, Chania, Crete, Greece

JUNE

71st Eastern Snow Conference, 3–5 June, Boone, North Carolina

15th International Conference on Atmospheric Electricity (ICAE 2014), 14–19 June, Norman, Oklahoma

The Latsis Symposium 2014: Atmosphere and Climate Dynamics: From Clouds to Global Circulations 18–21 June, Zürich, Switzerland

2014 A&WMA Annual Conference & Exhibition "Navigating Environmental Crossroads", 24–27 June, Long Beach, California

1st European Hail Workshop, 25–27 June, Bern, Switzerland

JULY

Trending Now—Water: 7th International Scientific Conference on the Global Water and Energy Cycle, 4–17 July, The Hague, the Netherlands

AUGUST

International Conference on Business Strategy and Social Sciences, 16–17 August, Kuala Lumpur Malaysia

First World Weather Open Science Conference, 16–21 August, Montreal, Quebec, Canada

SEPTEMBER

Eighth European Conference on Radar in Meteorology and Hydrology, 1–5 September, Garmisch-Partenkirchen, Germany

20th International Congress of Biometeorology, 28 September–2 October, Cleveland, Ohio

OCTOBER

14th Annual Meeting of the European Meteorological Society (EMS) and the 10th European Conference on Applied Climatology (ECAC), 6–10 October, Prague, Czech Republic

Climate Research and Earth Observations from Space: Climate Information for Decision Making, 13–17 October, Darmstadt, Germany

NOAA's 39th Climate Diagnostics and Prediction Workshop, 20–23 October, St. Louis, Missouri

* An exhibit program will be held at this meeting.

CALL FOR PAPERS

CALL FOR PAPERS

16th Annual High Plains Conference, 6–7 August 2014, Hastings, Nebraska

The 16th Annual High Plains Conference, sponsored by the High Plains Chapter of the American Meteorological Society and the National Weather Association, will be held 6–7 August 2014 on the campus of Hastings College in Hastings, Nebraska. The conference will feature daytime oral presentations and invited speakers.

Oral and poster presentations are solicited on all topics related to weather that affects the Central and High Plains regions of the United States. In addition, presentations on decision support services, weather-related sociology, and the use of geographic information systems and social media are also welcomed. Please note if you have a preference for an oral or poster presentation.

Abstracts are now being accepted and may be sent to jeffrey.halblaub@noaa.gov. The abstract deadline is *4 July 2014*. The abstract should be in MS Word format and no more than one page in length. National Weather Service employees are reminded to have their science and operations officer review the abstract in accordance with NWSPD-100 (Clearance for NWS Employee Papers). Authors of accepted abstracts will be notified via e-mail no later than 11 July 2014.

University students are encouraged to submit abstracts. The registration fee is waived by the chapter for students who present at the conference, and up to $1000 has been set aside for the top student presentations.

Preliminary program, registration, hotel, and general information will be forthcoming on the High Plains Chapter website (www.highplains-amsnwa.org) and on the chapter Facebook page (High Plains Chapter of the AMS and NWA). Please contact Jeff Halblaub (e-mail: jeffrey.halblaub@noaa.gov) or Joe Guerrero (e-mail: joseph.guerrero@noaa.gov) with any questions. (4/14)

CALL FOR PAPERS

14th Annual Meeting of the European Meteorological Society (EMS) and the 10th European Conference on Applied Climatology (ECAC), 6–10 October 2014, Prague, Czech Republic

The EMS & ECAC 2014 will be held 6–10 October 2014 in Prague, Czech Repbulic. The conference theme will be "Creating Climate Services through Partnerships".

The session program consists of the following program groups: Monitoring climate and climate change (MC); Understanding processes and climate change (UC); Research and services for socio-economic sectors (SE); Communication and education (CE); Numerical weather prediction (NWP); and The atmospheric system and its interactions (ASI).

Facilities will be available for groups wishing to hold side meetings. Please use the request form at the conference site: www.ems2014.eu/side_meeting_request.html.

The scientific program and abstract submission are now accessible at http://meetingorganizer.copernicus.org/ems2014/sessionprogramme. The deadline for abstract submissions is *15 April 2014*. The deadline for abstract submission with application for young scientist travel award or waiver is *12 March 2014*. (4/14)

CALL FOR PAPERS

24th Symposium on Education, 4–8 January 2015, Phoenix, Arizona

The 24th Symposium on Education, sponsored by the American Meteorological Society, will be held 4–8 January 2015, as part of the 95th AMS Annual Meeting in Phoenix, Arizona. Preliminary programs, registration, hotel, and general information will be posted on the AMS website (www.ametsoc.org/meet/annual/) in late September 2014.

The theme for the 2015 AMS Annual Meeting is "Fulfilling the Vision of Weather, Water, and Climate Information for Every Need, Time, and Place." People, businesses, and governments depend increasingly on weather, water, and climate information to address their specific needs, as well as on the tools to understand and interpret this information. We are converging on a day when such information is integrated into peoples' daily decisions and actions. This revolution in highly targeted customized information—delivered when and where it is most useful—will make our lives safer, more productive, and more enjoyable. The challenge for our community is this: collaborate and innovate to develop—and ultimately deliver—actionable, user-specific weather, water, and climate information across all spatial and temporal scales in support of our nation's safety, health, and prosperity. The AMS meeting will explore the many topics required for our community to implement this vision. The Symposium on Education is specifically looking to share educational materials, outreach strategies, and effective programs for informing stakeholders, students, and the community about weather, water, and climate.

Please contact the program chairpersons (contact information noted below) by *1 May 2014* if you would like to propose a session topic for this conference.

The $95 abstract fee includes the submission of your abstract, the posting of your extended abstract, and the uploading and recording of your presentation, which will be archived on the AMS website.

Please submit your abstract electronically via the Web by *1 August 2014* (refer to the AMS Web page at www.ametsoc.org/meet/online_submit.html). An abstract fee of $95 (payable by credit card or purchase order) is charged at the time of submission (refundable only if abstract is not accepted).

Authors of accepted presentations will be notified via e-mail by late September 2014. All extended abstracts are to be submitted electronically and will be available online via the web. Instructions for formatting extended abstracts will be posted on the AMS website. Authors have the option to submit manuscripts (up to 10 MB) electronically by *5 February 2015*. All abstracts, extended abstracts, and presentations will be available on the AMS website at no cost.

For additional information please contact the program chairpersons, Donna Charlevoix (e-mail: donnac@unavco.org; tel: 303-381-7483); or Diane Stanitski (e-mail: diane.stanitski@noaa.gov; tel: 301-427-2465). (4/14)

CALL FOR PAPERS

Joint 20th American Meteorological Society (AMS) Satellite Conference, 11th AMS Annual Symposium on New Generation Operational Environmental Satellite Systems, and 3rd AMS Symposium on the Joint Center for Satellite Data Assimilation (JCSDA), 4–8 January 2015, Phoenix, Arizona

The Joint 20th AMS Satellite Conference, 11th AMS Annual Symposium on New Generation Operational Environmental Satellite Systems, and 3rd AMS JCSDA Symposium, organized by the AMS Committee on Satellite Meteorology, Oceanography and Climatology, Joint Polar Satellite System (JPSS) and Geostationary Operational Environmental Satellite R-Series (GOES-R) Symposium Committee, and JCSDA, will be held 4–8 January 2015, as part of the 95th AMS Annual Meeting in Phoenix, Arizona. Preliminary programs, registration, hotel, and general information will be posted on the AMS website (www.ametsoc.org/meet/annual/) in late-September 2014.

The theme for the 2015 AMS Annual Meeting is "Fulfilling the Vision of Weather, Water, and Climate Information for Every Need, Time, and Place." People, businesses, and governments depend increasingly on weather, water, and climate information matched to their specific needs. We are converging on a day when such information is integrated into nearly every decision or action people take. This revolution in highly targeted, customized information—delivered when and where it is most useful—will make our lives safer, more productive, and more enjoyable. The challenge for our community is this: *collaborate and innovate to develop—and ultimately deliver—actionable, user-specific weather, water, and climate information across all spatial and temporal scales in support of our nation's safety, health, and prosperity.* The meeting will explore the many topics required for our community to implement this vision.

A joint program committee is soliciting papers describing new concepts, research, operations, and practical application of satellite measurements to meteorological, oceanographic, climatological, and other environmental problems. The organizers are particularly interested in papers focused on improved use of satellite data for analyzing and predicting the weather, the ocean, the climate, and the environment. This includes research and progress on current and next-generation passive and active systems, including geostationary microwave imagers, geostationary hyperspectral IR sounders, Doppler wind lidar, soil moisture and ocean salinity, and outcomes of various missions aimed at trace/greenhouse gases or more detailed aerosol information. Major areas of interest include

- factors influencing the design and operation of satellites and satellite instrumentation for observing the atmosphere, oceans, and the Earth;
- research/studies that assess the impact of satellite data on forecast skill;
- the potential of satellite systems to provide stable, accurate, and systematic observations of all components of the climate system;
- display and use of satellite data for both research and operational purposes, including weather, ocean, and climate monitoring and forecasting;
- how satellite data are being used to advance our understanding of fundamental weather and climate processes in the atmosphere, oceans, land surface, and cryosphere, and will continue to improve our ability to observe, analyze, predict, and communicate weather and climate data at a new level of fidelity and timeliness;
- design of next generation retrieval, data assimilation, and data fusion algorithms, especially as pertains to an integrated view of the Earth system;
- development of innovative methods of processing, combining, assimilating and analyzing the observations from satellites, and the development of applications such as those related to energy security, and land and ocean remote sensing applications (e.g., soil moisture, ocean color).

Please contact the joint program cochairs (contact information noted below) by *1 May 2014* if you would like to propose a session topic for this conference.

Presenters are requested to please submit abstracts electronically via the web by *1 August 2014* (refer to the AMS web page at www.ametsoc.org/meet/online_submit.html). An abstract fee of $95 (payable by credit card or purchase order) is charged at the time of submission (refundable only if abstract is not accepted). This fee covers the submission of your abstract, the posting of your extended abstract, and the uploading and recording of your presentation, which will be archived on the AMS website.

Authors of accepted presentations will be notified via e-mail by late-September 2014. All extended abstracts are to be submitted electronically and will be available online via the web. Instructions for formatting extended abstracts will be posted on the AMS website. Authors have the option to submit manuscripts (up to 10 MB) electronically by *5 February 2015*. All abstracts, extended abstracts, and presentations will be available on the AMS website at no cost.

For additional information please contact one of the cochairs of the joint program committee: Derek Possett, University of Michigan (tel: 734-936-0502; e-mail: dposselt@umich.edu), Ken Carey, ERT, Inc. (tel: 703-980-0500; e-mail: ken.carey@ertcorp.com), Gary McWilliams, Goddard Space Flight Center, JPSS Program Office (tel: 240-684-0597; e-mail: Gary.Mcwilliams@noaa.gov); Pat Kablick, University of Maryland (e-mail: pkablick@atmos.umd.edu), and Jim Yoe, JCSDA (tel: 301-683-3515; e-mail: James.G.Yoe@noaa.gov). (3/14; r4/14)

CALL FOR PAPERS

Third Symposium on Prediction of the Madden–Julian Oscillation: Processes, Prediction, and Impact, 4–8 January 2015, Phoenix, Arizona

Third Symposium on Prediction of the Madden–Julian Oscillation: Processes, Prediction, and Impact, sponsored by the American Meteorological Society, and organized by the AMS Committee on Tropical Meteorology, will be held 4–8 January 2015, as part of the 95th AMS Annual Meeting in Phoenix, Arizona. Preliminary programs, registration, hotel, and general information will be posted on the AMS website (www.ametsoc.org/meet/annual/) in late-September 2014.

The Madden–Julian oscillation (MJO) is the dominant mode of tropical intraseasonal variability in the Earth system. It connects weather and climate and influences high-impact events around the globe including monsoons, tropical cyclones, tornados, cold surges, floods, and wildfires. The MJO affects many sectors of the society at mid- and high latitudes as well as in the tropics. Basic research in modeling, analysis, and real time monitoring of the MJO will likely pay a significant economic dividend through potential improvement of intraseasonal prediction of probabilities of extreme events. Such research naturally fits the theme for the 2015 AMS Annual Meeting: "Fulfilling the Vision of Weather, Water, and Climate Information for Every Need, Time, and Place." This symposium solicits papers on all aspects of the MJO, particularly theoretical, observational, modeling, and prediction studies on

- MJO interaction with and impacts on high-impact weather and climate events, including monsoons, tropical cyclones and hurricanes, extratropical storms and blocking, atmospheric rivers, flood, fire, lightening, ENSO, NAO, and polar ice, among others;
- Advances in MJO modeling and forecasting by dynamical and statistical models, sensitivities of numerical simulations and forecast of the MJO to parameterization of convection, radiation, surface and boundary layer processes, cloud microphysics, and air–sea interaction;
- Applications of MJO forecasts.

The Third Symposium on Prediction of the Madden–Julian Oscillation will bring together scientists, forecasters, and end-users from the academic, operational, and private sectors worldwide to improve our understanding and forecasting of the MJO and their applications to benefiting the society. Joint sessions are planned with the Sixth Conference on Weather, Climate, and the New Energy Economy

Please contact the program chairpersons (contact information noted below) by *1 May 2014* if you would like to propose a session topic for this conference.

Please submit your abstract electronically via the Web by *1 August 2014* (refer to the AMS Web page at www.ametsoc.org/meet/online_submit.html). An abstract fee of $95 (payable by credit card or purchase order) is charged at the time of submission (refundable only if abstract is not accepted). The abstract fee includes the submission of your abstract, the posting of your extended abstract, and the uploading and recording of your presentation, which will be archived on the AMS website.

Authors of accepted presentations will be notified via e-mail by late-September 2014. All extended abstracts are to be submitted electronically and will be available online via the web. Instructions for formatting extended abstracts will be posted on the AMS website. Authors have the option to submit manuscripts (up to 10 MB) electronically by 5 February 2015. All abstracts, extended abstracts, and presentations will be available on the AMS website at no cost.

For additional information please contact the program chairpersons, Samson Hagos (e-mail: samson.hagos@pnnl.gov) and Carl Schreck (e-mail: cjschrec@ncsu.edu). (4/14)

CALL FOR PAPERS

First Symposium on High Performance Computing for Weather, Water, and Climate, 8 January 2015, Phoenix, Arizona

First Symposium on High Performance Computing for Weather, Water, and Climate, sponsored by the American Meteorological Society, and organized by the AMS Committee on Probability and Statistics, will be held 4–8 January 2015, as part of the 95th AMS Annual Meeting in Phoenix, Arizona. Preliminary programs, registration, hotel, and general information will be posted on the AMS website (www.ametsoc.org/meet/annual/) in late-September 2014.

The theme for the 2015 AMS Annual Meeting is "Fulfilling the Vision of Weather, Water, and Climate Information for Every Need, Time, and Place," People, businesses, and governments depend increasingly on weather, water, and climate information matched to their specific needs. We are converging on a day when such information is integrated into nearly every decision or action people take. This revolution in highly targeted, customized information—delivered when and where it is most useful—will make our lives safer, more productive, and more enjoyable. The challenge for our community is this: collaborate and innovate to develop—and ultimately deliver—actionable, user-specific weather, water, and climate information across all spatial and temporal scales in support of our nation's safety, health, and prosperity. The meeting will explore the many topics required for our community to implement this vision.

For this symposium, we seek papers focused on computational science aspects of HPC use to deliver more accurate information on weather, water, and climate to users. Topics such as tuning codes for HPC improvement, conversion of code to take full advantage of Phi or GPGPU capabilities, and visualization/access of large data volumes are encouraged.

Please contact the program chairpersons (contact information noted below) by *1 May 2014* if you would like to propose a session topic for this conference.

Please submit your abstract electronically via the Web by *1 August 2014* (refer to the AMS Web page at www.ametsoc.org/meet/online_submit.html). An abstract fee of $95 (payable by credit card or purchase order) is charged at the time of submission (refundable only if abstract is not accepted). The abstract fee includes the submission of your abstract, the posting of your extended abstract, and the uploading and recording of your presentation, which will be archived on the AMS website.

Authors of accepted presentations will be notified via e-mail by late-September 2014. All extended abstracts are to be submitted electronically and will be available online via the web. Instructions for formatting extended abstracts will be posted on the AMS website. Authors have the option to submit manuscripts (up to 10 MB) electronically by *5 February 2015*. All abstracts, extended abstracts, and presentations will be available on the AMS website at no cost.

For additional information please contact the program chairperson(s), Brian Etherton (e-mail: Brian.Etherton@noaa.gov) and Gerry Creager (e-mail: Gerry.Creager@noaa.gov). (4/14)

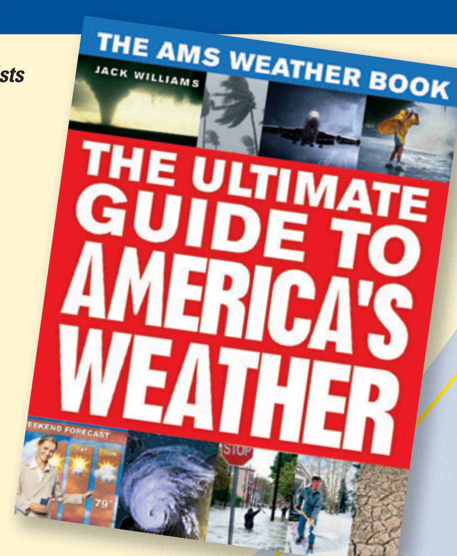

NOMINATION SUBMISSIONS

The Council of the American Meteorological Society invites members of the AMS to submit nominations for the Society Awards, Lecturers, Named Symposia, Fellows, Honorary members, and nominees for elective Officers and Councilors of the Society.

Information regarding awards, including award descriptions, listings of previous recipients, and the process for submitting nominations are on the AMS website www.ametsoc.org/awards.

Note: Deadlines differ and some nominations must be submitted on a specific form vs. electronic submission which is available on the AMS website or by request from Headquarters.

2014 AWARDS COMMITTEES

Each committee or commission listed below has the responsibility to select and submit to the Council the names of individuals nominated for the Society's awards listed. The name(s) of individual(s) nominated, a two-page cv, a bibliography of no more than three pages, and three supporting letters should be electronically submitted before **1 May 2014** for the awards that follow, unless stated otherwise. The nominees for awards remain on the committee's active list for three years.

ATMOSPHERIC RESEARCH AWARDS COMMITTEE

The Carl-Gustaf Rossby Research Medal
The Jule G. Charney Award
The Verner E. Suomi Award*
The Remote Sensing Prize (biennial)
The Clarence Leroy Meisinger Award
The Henry G. Houghton Award

OCEANOGRAPHIC RESEARCH AWARDS COMMITTEE

The Sverdrup Gold Medal
The Henry Stommel Research Award
The Verner E. Suomi Award*
The Nicholas P. Fofonoff Award

AWARDS OVERSIGHT COMMITTEE

The Charles Franklin Brooks Award for Outstanding Services to the Society
The Cleveland Abbe Award for Distinguished Service to the Atmospheric Sciences by an Individual
The Joanne Simpson Mentorship Award
The Award for Outstanding Services to Meteorology by a Corporation
Special Awards

EDUCATION AND HUMAN RESOURCES COMMISSION

The Louis J. Battan Author's Award (Adult and K–12)
The Charles E. Anderson Award
The Teaching Excellence Award
Distinguished Science Journalism in the Atmospheric and Related Sciences

PROFESSIONAL AFFAIRS COMMISSION

Outstanding Contribution to the Advance of Applied Meteorology
Award for Broadcast Meteorology
Award for Excellence in Science Reporting by a Broadcast Meteorologist
The Henry T. Harrison Award for Outstanding Contributions by a Consulting Meteorologist

WEATHER AND CLIMATE ENTERPRISE COMMISSION

The Kenneth C. Spengler Award

LOCAL CHAPTER AFFAIRS COMMITTEE

Local Chapter of the Year Award
(nomination form available online at www.ametsoc.org/amschaps/index.html.)

* Recommended by the Atmospheric Research Awards Committee in even-numbered years and by the Oceanographic Research Awards Committee in odd-numbered years.

2014 AWARDS COMMITTEES

SCIENTIFIC AND TECHNOLOGICAL ACTIVITIES COMMISSION

The Charles L. Mitchell Award
The Award for Exceptional Specific Prediction
The Francis W. Reichelderfer Award
The Helmut E. Landsberg Award
The Award for Outstanding Achievement in Biometeorology

- **LECTURERS** *(Deadline: 1 October 2014)*
  Robert E. Horton Lecturer in Hydrology
  Bernhard Haurwitz Memorial Lecturer
  Walter Orr Roberts Lecturer

- **PAPER**
  Banner I. Miller

- **STUDENT PAPERS**
  Robert Leviton Student Prize
  Max A. Eaton Student Prize
  Spiros G. Geotis Student Prize
  Peter V. Hobbs Student Prize

- **NAMED SYMPOSIA**
  Section E, of the Policy, Guidelines, and Procedures for Awards and Lectureships provides the Policy on Named Conferences/Symposia and Special Issues of AMS Journals *(full policy description available at www.ametsoc.org/awards):*

  > Recognition of scientists in the fields served by the AMS, living or deceased, in the form of a named conference or symposium or a named special issue of one of the Society's journals is an honor reserved for only the most outstanding of our colleagues. It should be awarded only to those individuals who are completing a career, or who have recently died having completed a career, of significant achievements in their field and whose contributions would make them worthy of consideration for Honorary Member of the AMS…

2014 FELLOWS COMMITTEE

The Committee's function is to submit to the Council the names of individuals for election to Fellow.

> Article III, Section 6, of the AMS Constitution provides that those eligible for election to Fellow shall have made outstanding contributions to the atmospheric or related oceanic or hydrologic sciences or their applications during a substantial period of years. The nominees for Fellow must be a member of the Society and remain on the committee's active list for three years.

A nomination letter and three supporting letters should be electronically submitted before 1 May 2014. A list of Fellows and the process for submitting nominations are on the AMS website (www.ametsoc.org/awards).

2015 NOMINATING COMMITTEE

The Committee's function is to submit to the Council the names of individuals for 1) the office of President-Elect for a term of one-year starting at the close of the 96th Annual Meeting (January 2016) and 2) four positions on the Council for a term of three-years starting at the close of the Annual Meeting. Nominations must be submitted prior to 1 April 2015 to the Nominating Committee.

HONORARY MEMBERS

Article III, Section 5, of the AMS Constitution provides that Honorary Members shall be persons of acknowledged preeminence in the atmospheric or related oceanic or hydrologic sciences, either through their own contributions to the sciences or their application or through furtherance of the advance of those sciences in some other way. They shall be exempt from all dues and assessments. The nominees for Honorary member remain on an active list for three years.

Deadline: 1 June 2014; a form and list of Honorary Members is available at www.ametsoc.org/awards.

CORPORATION AND INSTITUTIONAL MEMBERS

Membership in the American Meteorological Society does not imply AMS endorsement of an organization's products or services.

SUSTAINING MEMBERS

Ball Aerospace & Technologies Corporation
Baron Services, Inc.
Exelis
Lockheed Martin Corporation
Northrop Grumman Corporation
The Boeing Company
University Corporation for Atmospheric Research
Vaisala, Inc.

REGULAR MEMBERS

3TIER Environmental Forecast Group, Inc.
AccuWeather, Inc.
ADNET Systems, Inc.
Aerospace & Marine International Corporation
Atmospheric and Environmental Research, Inc.
Atmospheric Technology Services Company, LLC
Belfort Instrument Company
Botswana Meteorological Services
Campbell Scientific, Inc.
CLS America, Inc.
Coastal Environmental Systems
CSIRO Marine and Atmospheric Research
CSSI, Inc.
Davis Instruments Corporation
DeTect, Inc.
Earth Networks
EKO Instruments Company, Ltd.
Enterprise Electronics Corporation
Environmental Systems Research, Inc.
EWR Weather Radar Systems
Finnish Meteorological Institute
Global Hydrology and Climate Center
Global Weather Corporation
Johns Hopkins University, Applied Physics Laboratory
Kipp & Zonen USA Inc.
MeteoSwiss
Murray & Trettel, Inc.
National Centre for Medium Range Weather Forecasting
Orbital Sciences Corporation
Panasonic Weather Solutions
Pelmorex Media Inc.
R. M. Young Company
Raytheon Company
Riverside Technology, inc.
Royal Netherlands Meteorological Institute
Schneider Electric Weather
Science Applications International Corporation
Scintec AG
SeaSpace Corporation
SGT, Inc.
Sonalysts, Inc.
SpectraSensors, Inc.
Sutron Corporation
The Weather Channel
U.S Department of Energy, Office of Science
Unisys Corporation
University of Alabama in Huntsville,Earth System Science Ctr
University of Wisconsin - Madison, SSEC
Vieux, Inc.
Weather Analytics
Weather Decision Technologies
Weather Modification, Inc.
Weather Services International, Inc.
WindLogics, Inc.

SMALL BUSINESS MEMBERS

Climadata Corporation
Geonor, Inc.
National Council of Industrial Meteorologists
National Weather Service Employees Organization
Remtech, Inc.
www.WeatherVideoHD.TV

PUBLICATIONS MEMBERS

Abdus Salam International Centre for Theoretical Physics
Bureau of Meteorology
Civil Aeronautics Administration, MOTC
Colorado State University Libraries
Columbia University, Lahmont-Doherty Geological Observatory
Dartmouth College Baker Library
Desert Research Institute
Deutscher Wetterdienst
Embry Riddle Aeronautical University
Environment Canada Library, Downsview
EUMETSAT Library
Florida International University Library
Geophysical Institute/International Arctic Research Center
Harvard University, Gordon McKay and Blue Hill Libraries
Hong Kong Observatory Library
Illinois State Water Survey
Indian Institute of Tropical Meteorology
Indiana University Library
Institute of Global Environment and Society Library

For questions relating to corporation and institutional membership, please contact Gary Rasmussen at AMS Headquarters—telephone: 617-227-2426, x3981; fax: 617-742-8718; e-mail: grasmussen@ametsoc.org; or write to American Meteorological Society, Attn: Dr. R. Gary Rasmussen, 45 Beacon St., Boston, MA 02108-3693.

CORPORATION AND INSTITUTIONAL MEMBERS

Irish Meteorological Service
Japan Weather Association
Los Alamos National Laboratory
Lyndon State College, Samuel Read Hall Library
MBL/WHOI Library
Meteo-France
Meteorological Service of New Zealand Ltd.
Millersville University, Department of Earth Sciences
MIT, Lincoln Laboratory
National Weather Center Library
New York University
Niedersachsische Staats
NIWA Wellington Library
NOAA - GLERL Library
NOAA AOML Library
NOAA Central Library
NOAA National Climatic Data Center
NOAA Seattle Library
North Carolina State University Hunt Library
Pennsylvania State University, Paterno Library
Purdue University Libraries
Republic of Korea Air Force, Headquarters
South African Weather Service
St. Louis University, Dept. of Earth & Atmospheric Sciences
Swedish Meteorological & Hydrological Institute
U.K. National Meteorological Library
U.S Air Force, 335 TRS/UOAA
U.S. Department of Commerce, Boulder Labs Library
U.S. EPA Main Library
U.S. Naval Maritime Forecast Center
Universitatsbibliothek Innsbruck
Universitatsbibliothek Trier
University of Colorado Libraries
University of Copenhagen, Niels Bohr Institute Library
University of Delaware Library
University of Frankfurt Library
University of Hawaii at Manoa, Library
University of Maryland, McKeldin Library
University of Melbourne, Baillieu Library
University of New South Wales Library
University of North Carolina, Ramsey Library
University of Northern Colorado, Michener Library
University of North Dakota, Chester Fritz Library
University of Oklahoma, School of Meteorology
University of Rhode Island, Pell Marine Science Library
University of Washington Libraries
WeatherPredict Consulting Inc.
Weizmann Institute of Science
Yale University, Geology Library
Zentralanstalt fur Meteorologie und Geodynamik

Color indicates new or reinstated member

FELLOWSHIP AND SCHOLARSHIP SPONSORS

FELLOWSHIPS
AMS 21st Century Campaign
DOE, Atmospheric System Research
Lockheed Martin Corporation*
NASA's Earth Science
NOAA's Climate Program Office
NOAA's National Weather Service

FRESHMAN AND UNDERGRADUATE SCHOLARSHIPS
Baron Integrated Weather Solutions
Baron Services Inc.
Earth Networks
CLS America, Inc.
Harris Corporation
Lockheed Martin MS2
Naval Weather Service Association
Raytheon Company
Riverside Technologies Inc.
R. M. Young Company
Science and Technology Corporation
Stinger Ghaffarian
Vaisala, Inc.
Jerome Namias Memorial Endowed Scholarship
Edgar J. Saltsman Endowed Scholarship
Bernard Vonnegut and Vincent Schaefer Endowed Scholarship
Percival D. Wark and Clara B. (Mackey) Wark Endowed Scholarship

MINORITY SCHOLARSHIPS
AMS 21st Century Campaign
Baron Services Inc.
ERT

SENIOR SCHOLARSHIPS
AMS 75th Anniversary Endowed Scholarship
Bhanwar Lal Bahethi Scholarship
Om and Saraswati Bahethi Scholarship
Saraswati (Sara) Bahethi Scholarship
Werner A. Baum Undergraduate Endowed Scholarship
Loren W. Crow Memorial Scholarship
Karen Hauschild Friday Endowed Scholarship
Bob Glahn Endowed Scholarship in Statistical Meteorology
Dr. Pedro Grau Undergraduate Scholarship
Richard and Helen Hagemeyer Scholarship
John R. Hope Endowed Scholarship in Atmospheric Sciences
David S. Johnson Endowed Scholarship
Larry R. Johnson Scholarship
Dr. Yoram Kaufman Scholarship
Carl W. Kreitzberg Endowed Scholarship
Ethan and Allan Murphy Endowed Memorial Scholarship
K. Vic Ooyama Endowed Scholarship
The Orville Family Endowed Scholarship in Meteorology
Guillermo Salazar Rodriguez Undergraduate Scholarship
Mark J. Schroeder Endowed Scholarship in Meteorology
The Dr. Robert Fraser Scholarship
Michael J. Roberts, Jr. Scholarship
The Naval Weather Service Association Scholarship Award
The Ken Reeves Scholarship

*Corporate Patron

SPACE RESERVED FOR CERTIFIED CONSULTING METEOROLOGISTS

MURRAY AND TRETTEL, INCORPORATED

THOMAS R. PIAZZA

Certified Consulting Meteorologist

Operational Forecasting • Media • Air Quality/Meteorological/PSD Monitoring/Wind Assessment/Studies • Forensic Research • Dispersion Modeling • Nuclear Emergency Support

600 First Bank Drive, Suite A
Palatine, IL 60067
847-934-8230
FAX: 847-963-0199
E-mail: Thomas.Piazza@WeatherCommand.com

NORTH AMERICAN WEATHER CONSULTANTS

DON A. GRIFFITH, PRESIDENT

Certified Consulting Meteorologist

Weather Modification • Air Quality Surveys & Field Studies • Applied Research • Forensic Meteorology

8180 South Highland Dr., Suite B-2
Sandy, UT 84093
801-942-9005
FAX 801-942-9007
E-mail: nawc@nawcinc.com

WEATHER RESEARCH CENTER JOHN C. FREEMAN WEATHER MUSEUM

JILL F. HASLING, DIRECTOR

Certified Consulting Meteorologist

Worldwide Weather & Oceanographic Forecasting • Climatology • Training • Expert Testimony • Research in Meteorology & Oceanography • Wave Spectra • Software Development • The WRC Weather Museum

5104 Caroline St.
Houston, TX 77004
Website: www.wxresearch.com
Phone: 713-529-3076
Fax: 713-528-3538
E-mail: WRC@wxresearch.org

TRC ENVIRONMENTAL CORP.

GALE F. HOFFNAGLE
DOUGLAS R. MURRAY
PIETRO A. CATIZONE
DAVID FOX
ELIZABETH STANKO

Certified Consulting Meteorologists

Environmental Consulting & Research • Applied Meteorology • Air Quality and Meteorological Monitoring • Diffusion Modeling • Tracer Studies • Air Toxics Monitoring • Expert Testimony

1-800-TRC-5601
Offices in major industrial centers throughout the United States

McVEHIL-MONNETT ASSOCIATES, INC.

GEORGE E. McVEHIL, Ph.D.
KENDALL C. NECKER

Certified Consulting Meteorologists

Air Quality Analysis and Monitoring • Permitting • Dispersion Modeling • Air Toxics • Meteorological Analysis • Industrial Meteorology • Litigation Support • Expert Testimony

44 Inverness Drive East
Building C
Englewood, CO 80112
303-790-1332
FAX 303-790-7820
www.mcvehil-monnett.com

APPLIED METEOROLOGY, INC.

JOHN W. HATHORN

Certified Consulting Meteorologist

Meteorological Consulting & Analysis • Air Quality Modeling & Monitoring • Site Selection & Permitting • Environmental Data Acquisition Systems & Network with Remote-Control

9110 Weymouth Dr.
Houston, TX 77031-3034
713-995-5004
E-mail: hathorn.ami@gmail.com

SIMPSON WEATHER ASSOCIATES, INC.

M. GARSTANG, Ph.D.
G. D. EMMITT, Ph.D.
R.H. SIMPSON, Ph.D. (retired)

Certified Consulting Meteorologists

Environmental Risk Assessment • Air Quality Modeling/Monitoring • Instrumentation Development/Deployment • Lidar simulation/application

809 E. Jefferson St.
Charlottesville, VA 22902
434-979-3571
FAX: 434-979-5599

CLIMATOLOGICAL CONSULTING CORPORATION

LEE E. BRANSCOME, Ph.D., President
DOUGLAS A. STEWART, Ph.D.

Certified Consulting Meteorologists

Forensic Meteorology • Weather Risk Analysis • Climate Studies • Computer Modeling of the Atmosphere

7338 155th Place North
Palm Beach Gardens, FL 33418
www.ccc-weather.com
561-744-4889
FAX: 561-744-5098
lbranscome@ccc-weather.com

AEROCOMP

JOSEPH A. CATALANO

Certified Consulting Meteorologist

Expert Testimony • Climatological Analysis • Industrial Meteorology & Air Impact • Atmospheric Modeling • Wind & Ice Loading • Data Management Software & Services

P.O. Box 26109
Santa Ana, CA 92799-6109
714-964-3672
FAX: 714-964-1357
E-mail: ccm299@aerocomp.com

ACCUWEATHER ENTERPRISE SOLUTIONS, INC.

MICHAEL R. SMITH, SENIOR VICE PRESIDENT AND CHIEF INNOVATION EXECUTIVE
STEPHEN P. PRYOR, EXPERT SENIOR FORENSIC METEOROLOGIST

Certified Consulting Meteorologists

• Premier Meteorological Consultants Serving All Industries
• Forensic Services • Forecast Services • Expert Testimony
• Exclusive Technology • Extensive Database • Comprehensive Studies

100 North Broadway, Suite 750
Wichita, KS 67202
www.accuweather.com/enterprisesolutions
Phone: 316-266-8000
Fax: 316-366-4934
sales@accuweather.com

Certified Consulting Meteorologist: The certification program of the American Meteorological Society is aimed at fostering the establishment and maintenance of a high level of professional competency, and mature and ethical counsel, in the field of consulting meteorology. Requirements of knowledge, experience, and character are determined by a five-person board. Objectives of the program and application procedures are described in full detail in the August 2001 *Bulletin* (pp. 1689–1694).

PROFESSIONAL DIRECTORY

SPACE RESERVED FOR CERTIFIED CONSULTING METEOROLOGISTS

METEOROLOGICAL EVALUATION SERVICES, CO. INC. (MES)

PATRICK T. BRENNAN, PRESIDENT

Certified Consulting Meteorologist

Air-Quality Consulting • Expert Testimony • Industrial Meteorology • Nuclear Licensing Studies • Weather Investigations for Legal and Insurance Firms

165 Broadway
Amityville, NY 11701
631-691-3395
E-mail: info@mesamity.com

ACCUWEATHER, INC.

ELLIOT ABRAMS, SENIOR VICE PRESIDENT
STEPHAN M. WISTAR, SENIOR METEOROLOGIST

Certified Consulting Meteorologists

Meteorological Consultants Serving Industry, Government and the Media • Forensic Services • Forecast Services • Expert Testimony • Complete Database • Applied Information Technologies

385 Science Park Road
State College, PA 16803
www.AccuWeather.com
814-235-8626
Fax: 814-235-8769
E-mail: forensics@accuweather.com

Superior Accuracy™

TRINITY CONSULTANTS

GEORGE J. SCHEWE, PRINCIPAL CONSULTANT
ANTHONY J. SCHROEDER, MANAGING CONSULTANT

Certified Consulting Meteorologists

Air Quality Consulting • Regulatory Modeling • Meteorology/Climatology • Dispersion Modeling Courses Worldwide • BREEZE® Dispersion Modeling Software • Litigation Support

Covington, KY 859-341-8100 gschewe@trinityconsultants.com
Indianapolis, IN 317-451-8100 tschroeder@trinityconsultants.com

www.trinityconsultants.com
Offices Nationwide 800-229-6655

ANTHONY (ANDY) JOHNSON

Certified Consulting Meteorologist

Expert Testimony • Weather Investigations for Legal and Insurance Firms • Forensic Meteorology • Consultant since 1979

3912 West Dale Ave.
Tampa, FL 33609
Phone: 813-310-3865
Alt: 813-878-2929
FAX: 813-878-2939
E-mail: AJohnsonWX@gmail.com

METEOROLOGICAL SOLUTIONS INC.

GEORGE W. WILKERSON
DAN A. RISCH

Certified Consulting Meteorologists

AERMOD & CALPUFF Modeling • Permitting • Ambient Monitoring • Meteorological Towers • Calibrations & Audits • Meteorological Data Management • Applied Meteorology • Forecasting • Forensic Meteorology • Hydrometeorological Studies • Field Studies

4525 Wasatch Blvd., Suite 200
Salt Lake City, Utah 84124
Website: www.metsolution.com
801-272-3000
801-272-3040
info@metsolution.com

HOW THE WEATHERWORKS

H. MICHAEL MOGIL, PRESIDENT

Certified Consulting Meteorologist

Specializing in forensic meteorology, expert testimony, and data analysis for legal and insurance matters; also educational design and weather-based training and educational courses, science writing and weather photography.

7765 Preserve Lane - Suite #5
Naples, FL 34119
www.weatherworks.com
hmmogil@weatherworks.com
Phone: 239-591-2468
Cell: 240-426-2900
Fax: 202-742-2806

AIR WEATHER & SEA CONDITIONS, INC.

JAY ROSENTHAL, PRESIDENT

Certified Consulting Meteorologist

Expert testimony and data analysis for legal and insurance matters • Accident weather reconstruction • Satellite Interpretation • Air Pollution Transport • Excellent Client References • Emergency Response

P. O. Box 512
Pacific Palisades, CA 90272
Phone: 818-645-8632
310-454-7549
FAX: 310-454-7569
Website: www.weatherman.org
E-mail: AirWeather@aol.com

MAYACAMAS WEATHER CONSULTANTS

JOHN P. MONTEVERDI, Ph.D., DIRECTOR

Certified Consulting Meteorologist

Forensic Meteorology • Climate Studies • Litigation Support • Expert Testimony • Operational Forecasts and Nowcasts

4425 View Street
Oakland, CA 94611
415-882-9898
Fax: 510-653-4320

E-mail: montever@comcast.net
Website: www.mayacamaswx.com

CLIMATE PHYSICS, LLC

EDWIN X BERRY, Ph.D.

Certified Consulting Meteorologist

In a world of climate delusions
We bring you valid conclusions

439 Grand Ave., #147
Bigfork, MT 59911
406-471-1464
ed@climatephysics.com

WEATHER DECISION TECHNOLOGIES, INC.

RICHARD L. CARPENTER, JR., Ph.D.
E. DeWAYNE MITCHELL
J. WILLIAM CONWAY
BRENT L. SHAW

Certified Consulting Meteorologists

Radar Meteorology • Severe Weather Nowcasting and Analysis • Mesoscale and Microscale Numerical Modeling • Aviation Weather • Forensic Meteorology • Expert Testimony

201 David L. Boren Blvd., Ste. 270
Norman, OK 73072
405-579-7675
www.wdtinc.com
info@wdtinc.com

For professional card rates, please apply to:
Executive Director, American Meteorological Society, 45 Beacon St., Boston, MA 02108-3693

SPACE RESERVED FOR CERTIFIED CONSULTING METEOROLOGISTS

AECOM

HOWARD BALENTINE

Certified Consulting Meteorologists

Air Quality Modeling • Air Pollution and Meteorological Studies • Air Toxic Risk Assessment • Clean Air Act Regulatory Analysis • Climate Change Analyses • Emission Inventory Development • Expert Testimony • Greenhouse Gas Footprint • Risk Management and Process Safety • Toxic and Flammable Hazards Assessment • Weather and Air Quality Forecasting

1220 Avenida Acaso
Camarillo, CA 93012 (805) 388–3775

AECOM

PATRICK MCKEAN VINCE SCHEETZ
PETER P. MILLER II JASON REED

Certified Consulting Meteorologists

Ambient Air Quality/Meteorology Monitoring • Air Pollution Dispersion Modeling • Air Pollution Studies • Air Toxics Health Risk Assessment • Computer Programming • Data Analysis • Environment Impact and Site Surveys • Expert Testimony • Regulatory Guidance and Emission Inventories • Visibility Studies • Weather and Air Quality Forecasting

1601 Prospect Parkway
Fort Collins, CO 80525 (970) 493–8878

AECOM

DAVE HEINOLD BOB PAINE
ROBERT IWANCHUK BILL GROOT

Certified Consulting Meteorologists

Air Quality Modeling • Air Pollution Studies • Ambient Measurements • Air Permitting/Compliance • Clean Air Act Regulatory Analysis • Dispersion Analysis • Expert Testimony • Risk Assessment • Risk Management and Process Safety • Toxic and Flammable Hazards Assessment • Wind Energy Analysis • Weather and Air Quality Forecasting

250 Apollo Drive
Chelmsford, MA 01824 (978) 905–2100

OFFSHORE WEATHER SERVICES PTY LTD

PETER WELLBY

Certified Consulting Meteorologist

Marine, Aviation and Tropical Cyclone forecasting for the offshore and alternative energy industries • Ensemble wind and wave forecasts • Mesoscale wave modelling • Meteorological Consultants • Regional Meteorological/Oceanographic Studies • On site weather forecasters for critical operations • 25 years experience in the offshore industry

277 Blackburn Road Tel: +61 3 98878613
Mount Waverley e-mail: ows@offshoreweather.com.au
Victoria 3149 Australia www.offshoreweather.com.au

THE FLEETWEATHER GROUP

43 Years of Meteorological Consulting - Since 1969

TORE JAKOBSEN, PRESIDENT
STEVEN ROBERTS, CCM, CHIEF FORENSIC METEOROLOGIST

Certified Consulting Meteorologist

FleetWeather Ocean Services • CompuWeather • FleetWeather Forecasting

• Professional Weather Services for the Commercial Shipping Industry
• Past Weather/Forensic Consulting for the Insurance and Legal Industries
• Forecasting Services for Land-Based Weather Sensitive Clients

2566 Route 52
Hopewell Junction, NY 12533 Phone: +1.845.226.8300
fleetweathergroup.com info@fleetweather.com

WeatherExtreme Ltd.

ELIZABETH J. AUSTIN, Ph.D., PRESIDENT

Certified Consulting Meteorologist

Forensic Meteorology • Weather Forecasting • Climate Studies • Atmospheric Modeling • GIS • Weather Risk Analysis • Specialized Graphics & Animations

1119 S. Mission Road, Suite 331 Phone: 775-636-8553
Fallbrook, CA 92028 Fax: 775-636-8430

Website: www.weatherextreme.com
email: elizabeth@weatherextreme.com

Certified Consulting Meteorologist: The certification program of the American Meteorological Society is aimed at fostering the establishment and maintenance of a high level of professional competency, and mature and ethical counsel, in the field of consulting meteorology. Requirements of knowledge, experience, and character are determined by a five-person board. Objectives of the program and application procedures are described in full detail in the August 2001 *Bulletin* (pp. 1689–1694).

PROFESSIONAL DIRECTORY

SPACE RESERVED FOR MEMBERS

INDEX TO ADVERTISERS

AMS Publications, Preprints, etc.

ONLINE CAREER CENTER

The AMS Online Career Center may be accessed through the AMS Web site at www.ametsoc.org/careercenter/index.html. In addition to posting positions, advertisers may search and view job seekers' résumés.

Job Posting Rates:
$375 (30-day posting)

$1593.75 (5 pack of jobs) Usable for 30-day job postings. Buy 5 job posting credits at a 15% discounted rate. These credits may be used at anytime during the next 12 months.

$3000 (10 pack of jobs) Usable for 30-day job postings. Buy 10 job-posting credits at a 20% discounted rate. These credits may be used at anytime during the next 12 months.

$3375 (12 pack of jobs) Usable for 30-day job postings or a continual 12-month posting. Buy 12 job-posting credits at a 25% discounted rate. These credits may be used at anytime during the next 12 months.

Advertisers may upload a company logo free of charge.

Résumés: View complete resumes for free! If you find any candidates you are interested in, submit your interest to them. If the candidate is interested in your opportunity, we connect you for just $20.00. If the candidate is not interested, you pay nothing!

AMS Corporation Member Discounts: Active AMS Corporation Members (small business, regular, or sustaining) receive a 25% discount when posting a position. Contact Kelly G. Savoie (ksavoie@ametsoc.org) to receive a coupon code. To receive the discount, the code must be entered when you post a position. The discount code is non-transferable.

AMS Member Benefit: AMS Members will be given 14-days advance access to a job listing. A member-only symbol will appear next to the posting. After 14 days, the job posting is open to all.

Submission of Ads: Advertisers must create an online account and submit ad text through the AMS Career Center site. Ad text may be entered at any time.

Payment Information: Prepayment is required by credit card or valid purchase order.

Contact Information: If you have questions, please contact Customer Service at 888-575-WORK (9675) (inside U.S.) or 860-440-0635 (outside U.S.).

ADVERTISING POLICY

The AMS will accept tasteful and accurate advertisements for products and services of professional interest to AMS members from organizations that are actively involved in the atmospheric and related sciences. The AMS also accepts advertising from organizations that have an interest in the atmospheric and related sciences and services, but are not actively involved in them. These organizations may promote their contributions to AMS activities and other good works, but may not directly promote products or services. The AMS reserves the right to refuse advertising that does not meet these criteria. Acceptance of advertising does not constitute the Society's endorsement of the product or service being advertised.

ORDER FORM

FOR AMS PUBLICATIONS ADVERTISED IN THIS ISSUE

Name: ______________________________

Address: ______________________________

City, State: ____________________ ZIP: __________

Province: ______________ Country: ______________

☐ Member (# __________)

☐ Nonmember

	Qty.	Member Price* (Please circle appropriate price)	Nonmember Price* (Please circle appropriate price)	Total
Adaptive Governance and Climate Change (p. 583)		$22.00	$35.00	
The AMS Weather Book: The Ultimate Guide				
to America's Weather (p. 648)		$25.00	$35.00	
Deadly Season: Analysis of the 2011 Tornado Outbreaks (p. 569)		$20.00	$25.00	
Economic and Societal Impacts of Tornadoes (p. 601)		$22.00	$30.00	
A Half Century of Progress in Meteorology:				
A Tribute to Richard Reed, MM No. 53 (p. 542)		$60.00	$80.00	
Lewis and Clark: Weather and Climate Data				
from the Expedition Journals (p. 646)		$70.00	$90.00	
The Life Cycles of Extratropical Cyclones (p. 617)		$55.00	$75.00	
Living on the Real World: How Thinking and Acting				
Like Meteorologists Will Help Save the Planet (p. 628)		$22.00	$30.00	
Partly to Mostly Funny: The Ultimate Weather Joke Book (p. 503)		$25.00	$35.00	
Radar and Atmospheric Science: A Collection of Essays				
in Honor of David Atlas (p. 584)		$80.00	$100.00	
Severe Convective Storms, MM No. 50 (p. 618)		$90.00	$110.00	
Student member price:		$75.00		
Taken by Storm, 1938: A Societal and Meteorological History				
of the Great New England Hurricane (p. 622)		$30.00	$40.00	
**** Shipping and handling: Please add $8 PER ORDER for delivery within the U.S. and $15 PER ITEM for deliveries outside the U.S. There is no shipping and handling charge on DVDs or CD-ROMs for either U.S. or foreign orders. Shipping prices subject to change.***		**SHIPPING**		
		TOTAL		

I am paying by: ☐ Check/money order ☐ Credit Card No. ____________________ Exp. date:______

☐ Visa ☐ Mastercard ☐ American Express

Name on Card:____________________ Billing address: ____________________

Signature: ____________________ ____________________

☐ Please include an AMS membership application with my order. ____________________

Please send prepaid orders to: Order Department, American Meteorological Society, 45 Beacon St., Boston, MA 02108-3693